Terms and Conditions of Use of Digitised Theses from Trinity College Library Dublin

Copyright statement

All material supplied by Trinity College Library is protected by copyright (under the Copyright and Related Rights Act, 2000 as amended) and other relevant Intellectual Property Rights. By accessing and using a Digitised Thesis from Trinity College Library you acknowledge that all Intellectual Property Rights in any Works supplied are the sole and exclusive property of the copyright and/or other IPR holder. Specific copyright holders may not be explicitly identified. Use of materials from other sources within a thesis should not be construed as a claim over them.

A non-exclusive, non-transferable licence is hereby granted to those using or reproducing, in whole or in part, the material for valid purposes, providing the copyright owners are acknowledged using the normal conventions. Where specific permission to use material is required, this is identified and such permission must be sought from the copyright holder or agency cited.

Liability statement

By using a Digitised Thesis, I accept that Trinity College Dublin bears no legal responsibility for the accuracy, legality or comprehensiveness of materials contained within the thesis, and that Trinity College Dublin accepts no liability for indirect, consequential, or incidental, damages or losses arising from use of the thesis for whatever reason. Information located in a thesis may be subject to specific use constraints, details of which may not be explicitly described. It is the responsibility of potential and actual users to be aware of such constraints and to abide by them. By making use of material from a digitised thesis, you accept these copyright and disclaimer provisions. Where it is brought to the attention of Trinity College Library that there may be a breach of copyright or other restraint, it is the policy to withdraw or take down access to a thesis while the issue is being resolved.

Access Agreement

By using a Digitised Thesis from Trinity College Library you are bound by the following Terms & Conditions. Please read them carefully.

I have read and I understand the following statement: All material supplied via a Digitised Thesis from Trinity College Library is protected by copyright and other intellectual property rights, and duplication or sale of all or part of any of a thesis is not permitted, except that material may be duplicated by you for your research use or for educational purposes in electronic or print form providing the copyright owners are acknowledged using the normal conventions. You must obtain permission for any other use. Electronic or print copies may not be offered, whether for sale or otherwise to anyone. This copy has been supplied on the understanding that it is copyright material and that no quotation from the thesis may be published without proper acknowledgement.

THE EFFICACY OF IRRADIATION PROTOCOL AND IRRADIATION DISTANCE ON RESIN-BASED COMPOSITE PERFORMANCE

A thesis submitted to the University of Dublin in fulfillment of the requirements for

The degree of Doctor of Philosophy by

Gurcharn Singh Bhamra

May 2008

Materials Science Unit,

Division of Oral Biosciences,

Dublin Dental School and Hospital,

Trinity College,

University of Dublin.

DECLARATION

I hereby declare that the thesis has not been submitted as an exercise for a degree at this or any University, is entirely my own work and I agree that the Library may lend or copy the thesis on request.

Gurcharn S Bhamra

SUMMARY

The objective of the current study was to investigate the efficiency of the overlapping irradiation regime for resin-based composites (RBCs) in ISO 4049 by modifying the irradiation protocol. To exacerbate the potential for uncontrolled initiation on polymerisation and decrease the homogeneity of polymerisation along the length of the specimen, the exit window was moved by three-quarters (not half) the diameter along the top surface only so that some areas received twice the irradiation of adjacent areas. It was proposed that increasing the number of irradiations, with decreasing tip diameter from 13 to 11 and 8mm, would progressively decrease the efficiency of the polymerisation process compared with a 'one-hit' irradiation using a 25mm custom made fibre optic light guide. Additionally, the influence of light irradiation variables (tip diameter, irradiance, irradiation protocol and LCU) on the flexural strength, flexural modulus and the Vickers hardness were assessed. Within the limitations of the experiment tip diameter, irradiance and irradiation protocol had no influence on three-point flexural strength and modulus data. An increase in irradiance for a constant irradiation time resulted in an increase in the Vickers hardness of the bottom surfaces. The study emphasised that the relationship between the development of mechanical properties with energy density is not linear although some clinical implications were highlighted. The objective of Part II of the current study was to investigate RBC placement variables (principally irradiation distance) which has implications for strength and modulus development in clinical practice. In addition, the influence of quartz tungsten halogen LCU irradiation distance on bi-axial flexure strength and short- and long-term *in-vitro* wear resistance were also

assessed. Deviation from the maximum flexure properties from that described in the literature (Musanje and Darvell, 2003) occurred at irradiation distances between 0 and 7mm in three-point flexure and 9 and 11mm in bi-axial flexure. The determination of the mean total volumetric wear was identified to be a more accurate parameter for evaluating material loss due to wear since difficulties with the mean maximum wear depth measurements for data reporting are routinely encountered. Increasing the number of wear cycles to 500,000 results in significant volumetric wear observed over time which is exacerbated with increasing irradiance distances.

ACKNOWLEDGMENTS

I would like to thank my supervisor Dr Garry JP Fleming for his considerable support and patience over the past three years. His positive attitude and willingness to succeed has motivated me in making it possible to complete this PhD. The guidance, encouragement and enthusiasm he has shown is much appreciated.

During this stressful and challenging period Adam Dowling has proved to be a true and loyal friend who has offered his support and assistance continuously throughout my time at the Materials Science Unit.

I would also like to extend my gratitude to Professor Brian Darvell for his useful comments during the latter stages of this thesis which have been invaluable and to Brendan Grufferty for keeping me sane. My wife, Jasdeep, who has made it all worthwhile with her support and encouragement over the three years of this PhD.

I would like to express my appreciation to the Dublin Dental School and Hospital, Trinity College Dublin for the financial support received and for providing me with the opportunity to study at the institution.

Finally I would like to express my gratitude to Drs Andreas Syrek and John Rafelt from 3M ESPE for supplying the RBC materials and answering any relevant questions.

TABLE OF CONTENTS

PART I

THE EFFICACY OF A MODIFIED IRRADIATION PROTOCOL ON RBC PERFORMANCE

PART II

THE INFLUENCE OF IRRADIATION DISTANCE ON RBC PERFORMANCE

LIST OF FIGURES

LIST OF TABLES

PART I

THE EFFICACY OF A MODIFIED IRRADIATION PROTOCOL ON RESIN-BASED COMPOSITE PERFORMANCE

CHAPTER 1 Introduction

1.1 Historical development of resin-based composites

A novel resin-based composite (RBC) was patented in 1958 from the pioneering work carried out by Bowen, the Associate Director of the American Dental Association Research Unit at the National Bureau of Standards, which revolutionised existing dental resin-based technology (Bowen, 1958). Bowen patented the highly viscous dimethacrylate monomer composed of 25wt.% bisphenol-A and glycidyl methacrylate resin and containing 75wt.% quartz or aluminosilicate glass filler which provided the potential for increased physical and mechanical properties and therefore a greater application for dental RBCs. The pale yellow, highly viscous dimethacrylate monomer was given the acronym BisGMA. Initially, the viscosity of BisGMA was identified to be unsuitable for the incorporation of filler particles and manipulation for cavity restoration. Consequently, Bowen (1962) reported the necessity for the admixture of a monomer of lower molecular weight, triethyleneglycol dimethacrylate (TEGDMA), to achieve a suitable viscosity to allow for the incorporation of filler particles which was required for a successful RBC. The glass fillers were coated with a silane coupling agent to provide an adhesive bond between the powdered inorganic filler and the resin matrix (Bowen, 1963). The decreased viscosity of the resin matrix allowed for the addition of an increased wt.% of filler particles and the consequential improvement in mechanical properties compared with monomers of higher viscosity. The mechanical and physical properties of the difunctional BisGMA monomer were reported to be superior to methylmethacrylates because of the larger molecular size and chemical structure, providing decreased

polymerisation shrinkage (Braden, 1974), increased tensile strength (Barker and Setchell, 1972; Vanherle et al., 1985), increased compressive strength and an increased elastic modulus (Vanherle et al., 1985) giving rise to the development of the first generation of commercially available RBCs.

1.2 Traditional RBC technology

The introduction of traditional RBCs based on Bowen's BisGMA resin provided increased clinical success over conventional acrylic materials following placement in anterior teeth (Osborne et al., 1973). Many optimistic clinicians, motivated by the increased aesthetics, decreased polymerisation shrinkage, low thermal conductivity and ease of manipulation, considered these traditional RBCs as a viable alternative to amalgam in posterior restorations (Mack, 1970; Barker and Setchell, 1972). The majority of RBC versus amalgam longevity studies in the early 1970s highlighted similar, if not superior, results for the placement of RBC restorations during the first twelve months following placement (Osborne et al., 1973; Nuckles and Fingar, 1975), which may explain the early enthusiasm for the placement of RBCs in posterior cavities. One of the first commercial RBCs, Adaptic (Johnson & Johnson, Windsor, NJ, US), was reported to have a marginal integrity similar to amalgam after 12 months (Nuckles and Finger, 1975). Osborne et al. (1973) identified that another of the early commercially available RBCs, Concise (3M Dental Products, St Paul, MN, US), had superior marginal adaptation after the first year of service. However, by the second year amalgam was superior with regard to occlusal wear. Further investigations suggested that the occlusal surface of Concise posterior restorations exhibited decreased wear resistance compared with amalgam

following 12 months, which resulted in poor occlusion in posterior restorations and the shifting of the adjacent teeth (Leinfelder et al., 1975). Phillips et al. (1973) investigated RBC versus amalgam longevity studies on Adaptic and an amalgam restorative material, (Velvalloy; S.S. White Dental Products, Philadelphia, PA, USA) and reported a progressive loss of anatomical form on the occlusal surfaces of the RBC restorations over three years. The result compelled the authors to contraindicate the routine use of Adaptic, except where aesthetics were the main concern, or until improvements in the material provided a solution to the inadequate wear characteristics. Furthermore, the first generation of RBCs were identified to possess colour instability and increasing marginal discolouration which was reported to be directly associated with recurrent caries (Nuckles and Fingar, 1975). Despite the major disadvantages of traditional RBCs identified following one or two years placement *in-vivo*, the patient demand for aesthetic restoratives and the possible biocompatibility concerns of potential mercury toxicity from dental amalgam restorations (Fleming et al., 2001) encouraged scientists to examine different filler technologies for improving the properties of traditional RBCs.

The first significant improvement to traditional RBC technology followed the development of P-10 (3M Dental Products, St. Paul, MN, USA) a posterior RBC in the late 1960s. P-10 was designed for the restoration of posterior cavities and was essentially a modification of Concise which had been successfully indicated for use in anterior restorations (Phillips et al., 1973) and contra-indicated for use in posterior restorations (Leinfelder et al., 1975). The wear resistance of P-10 was reported to be significantly increased due to the increased filler content, from 56.8 to 69.1vol.% and decreased mean

filler particle size from 10.0 to 4.4μm for Concise compared with P-10 (Leinfelder and Roberson, 1983; Willems et al., 1993). Commercially available RBC restoratives of the period consisted of a separate base and catalyst component which contained a benzoyl peroxide initiator and a tertiary amine activator (Anusavice, 1996). The components of such two-paste systems were mixed together to produce a chemical reaction that provided a process of self or auto-polymerisation. A major advancement in RBC technology took place in 1970 with the introduction of photo-activated resin formulations and the development of Prisma-Fil (Caulk Dentsply, Milford, DE, USA). Ultra-violet (UV) light was required to polymerise the RBC aided by a photo-chemical initiator within the resin matrix, commonly, benzoin methyl ether (Smith, 1985). The types of UV lamps used for the polymerisation of photo-activated RBCs were reported to emit long wave UV light (340-380nm) with a specific absorption for the benzoin methyl ether initiator of 365nm (Rock, 1974). Powers et al. (1978, 1980) reported increased wear resistance and colour stability of photo-activated RBCs compared with auto-polymerising systems. The increased wear resistance was attributed to a decrease in the incorporation of oxygen that was common with auto-polymerising RBCs, whereby entrapped air incorporated by the mechanical mixing of the base and catalyst created porosity that was responsible, in part for exacerbating the wear process (Leinfelder, 1987). Moreover, a photo-activated system allowed the operator increased working time for more precise manipulation of the material within the oral cavity compared with auto-polymerising RBCs (Lutz and Phillips, 1983). However, a 60s exposure period using UV light to irradiate the RBC specimens was reported to produce a limited depth of cure of 1.5mm (Lee et al., 1976; Murray et al., 1981).

The significantly improved properties and less technique sensitive manipulation of photo-activated compared with auto-polymerised RBCs and concerns that prolonged exposure to UV light may cause damage to the oral mucosa or eyes led to the development of lower energy radiation visible light cured (VLC) RBC materials. The light initiator chemistry of VLC RBCs utilised the absorption of intense visible (blue) light at a wavelength of 470nm for polymerisation of the resin matrix. Dart et al. (1978) patented the first successful VLC RBC composition by irradiation of visible light with a light initiator formulation based on the use of 1,2-diketones, namely benzyl or camphoroquinone (CQ) and an amine activator such as dimethylaminoethylmethacrylate (DMAEMA) which are still utilised in RBC technology today. The visible light-initiating formulation was indicated in the first commercially available VLC RBC (Foto-Fil; Johnson & Johnson, Windsor, NJ, US) which consisted of a BisGMA analogue monomer system, namely urethane dimethacrylate (UDMA). The wavelength of visible light was reported to penetrate RBC materials more efficiently than UV radiation, where increased depths of polymerisation were achieved for shorter irradaition times (Tirtha et al., 1982; Lutz et al., 1983; Watts et al., 1984).

The traditional RBCs of the 1960s contained macrofillers of quartz, glass, borosilicates or ceramics with the size distribution of these ground particles ranging from 1 to 100μm (Anusavice, 1986). The major disadvantages of traditional RBCs were focussed on the weak bond between the fillers and the resin matrix subjecting the material to hydrolysis in function and inherent surface finish and polishing difficulties (Stanford, 1971). RBCs containing macrofillers were reported to be susceptible to fracture, filler particles were

exfoliated from the resin matrix resulting in clinically unacceptable wear resistance, especially under stress bearing situations (Kusy and Leinfelder, 1977). The surface roughness of traditional RBC restorations was also reported to significantly increase shortly after placement (Farah and Dougherty, 1981; Jordan et al., 1982) increasing the susceptibility for plaque formation which resulted in the discolouration of the restoration and the increased formation of secondary caries (Lutz et al., 1983).

1.3 Microfilled RBC technology

Traditionally RBCs contained 65-80wt.% filler particles which was responsible for the increased mechanical strengths and elastic moduli observed compared with their traditional RBC predecessors (Smith, 1985). The wear resistance increased with filler content within the resin matrix (Leinfelder and Roberson, 1983; Lutz et al., 1984; Leinfelder, 1987; Mair et al., 1990), but the wear resistance was dependent on the particle size distribution and the manner in which the particles were packed together (Leinfelder, 1987). Filler technology was improved to include filler particles of less than 1μm diameter and the advent of 'microfilled' RBCs was revolutionised with the development of Isopast (Vivadent, Schaan, Liechtenstein) in 1974 which contained fumed or pyrogenic silica filler particles with a mean size of 0.05μm diameter (Leinfelder, 1995). Since the diameter of incorporated fillers was less than the wavelength of visible light a highly lustrous polish capability and surface finishing resulted (Smith, 1985). The surface area to volume ratio of the filler particles, however, was significantly increased compared with traditional macrofillers which was manifested as an increased difficulty in incorporating

the equivalent weight percentage of filler particles within the resin matrix (Barnes and Kidd, 1980). Unmanageable viscosities resulted from highly filled microfilled resins such that the solution was to decrease the volume fraction of filler. This resulted in decreased strengths and wear resistance and an associated increase in polymerisation shrinkage (Anusavice, 1996). The compromise between a lower volume fraction of filler was overcome by manufacturing the filler particles from a prepolymerised, highly filled microfill RBC ground into particles of approximately 25μm diameter. The filler particles were then incorporated within a low viscosity resin matrix containing a decreased volume fraction of pyrogenic silica and on polymerisation (auto-cured), the uncured resin reacted chemically with the prepolymerised filler particles to form a silica containing matrix of approximately 45-50wt.%. The increased strength and wear resistance and decreased polymerisation shrinkage of the RBC without sacrificing the polishability of the RBC was revolutionary (Barnes and Kidd, 1980).

The commercially available microfilled RBCs of the time included Helioprogress and Heliomolar (Vivadent, Schaan, Liechtenstein), Durafill™ and Dentacolour (Kulzer Inc., Friederichsdorf, Germany) and Silux and Silux Plus™ (3M Dental Products, St. Paul, MN, USA). Microfilled RBCs had one major compromise compared with traditional macrofilled RBC systems namely, the inability to highly load the resin with filler particulates. With fine particles, the liquid demand by the particles to spread out over such a large surface area (within the resin matrix) was so high that only approximate filler loading of 50wt.% could be achieved (Anusavice, 1996). Although the presence of micro-sized fillers resulted in increased polishability and increased colour stability, the wear

resistance remained inadequate in load-bearing situations and the mechanical and physical properties were decreased compared with their macrofilled counterparts (Smith, 1985).

1.4 Hybrid RBC technology

The 'critical diameter' of the abrasive filler particles and the separating distance between the particles within the resin matrix were responsible for the significant improvements in the mechanical and physical properties of the microfilled compared with the traditional RBCs (Jorgensen and Asmussen, 1978). Attempts to combine the advantages of macro- and micro-fine filler particles led to the development of the 'hybrid' RBCs which contained a combination of different particle sizes and particle size distributions. In the early 1980s, the resin matrix of traditional RBCs was reinforced with microfillers to decrease the differences in the mechanical and physical properties of the macrofillers and the matrix (Lutz and Phillips, 1983). When applied commercially to the traditional RBCs of the 1970s (Adaptic and Concise), the use of traditional RBC restoratives amongst dental practitioners for the restoration of posterior dentition was markedly reduced (Lutz et al., 1984).

Traditional hybrid RBCs were filled with filler particle sizes ranging from 1.0 to 5.0μm to approximately 70wt.% with the spaces between the larger particles being filled with particles that were representative of those utilised in microfilled RBCs with particle diameters of 0.05μm and therefore a mean particle diameter of approximately 1μm

(Willems et al., 1993). Traditional macrofillers consisted of directly admixed pyrogenic silica particles, a coupling agent and the organic matrix phase. As a result, these RBCs systems demonstrated a superior wear resistance compared with traditional macrofilled RBCs (Lutz et al., 1984; Leinfelder, 1987; Mair et al., 1990). In contrast to the microfilled systems, larger metal glass fibres (such as barium silicates) could be incorporated as part of the dispersed phase thereby offering an increased radiopacity which was essential for the evaluation of an RBC restoration following placement (Barnes and Kidd, 1980). However, the polishability was not optimised because of the wear patterns inherent in resin systems that contained traditional macrofillers (Heuer et al., 1982). Therefore, hybrid RBCs were not considered optimal for use in anterior restorations although significant improvements in the wear resistance over traditional RBCs increased expectation amongst dental practitioners for application as a posterior filling material. Many variations of filler size, shape and particle size distribution followed in the development of RBCs where traditional RBCs became more hybrid and microfilled systems became more complex and similar to the hybrid RBC types.

The majority of RBC restorations placed by dental practitioners in clinical practice today are similar in formulation to the traditional hybrid RBCs. The only variations were an alteration to the filler loading and morphology whereby modest mechanical and physical improvements were realised. A significant increase in wear resistance and surface polishability of traditional hybrid RBCs was realised with the introduction of filler loadings in excess of 80wt.% with a concomitant decrease in the average particle size to less than lμm. These modern 'micro-hybrid' RBCs (indicated for both anterior and

posterior use) were also termed 'universal' or 'all-purpose' RBCs and included Herculite XRV (Kerr Corporation, Orange, CA, USA), Filtek Z250™ (3M ESPE Dental Products, St Paul, MN, USA), Renew (Bisco, Schaumburg, IL, USA), Virtuoso (Den-Mat Corporation, Santa Maria, CA, USA) and Charisma (Heraeus Kulzer, Dormagen, Germany).

1.5 Nano-filled RBC technology

A 'nano-filled' RBC (Filtek™ Supreme, 3M ESPE Dental Products, St Paul, MN, USA) was marketed in 2003 with claims of translucency, polishability and polish retention similar to microfilled RBCs whilst exhibiting the significantly increased wear resistance and equivalent mechanical properties associated with conventional micro-hybrid RBCs (Mitra et al., 2003). A unique 'nano-filler' technology, formulated with nanomer fillers (ranging from 20 to 75nm diameter) was purported and utilised in conjunction with nano-cluster filler particles (ranging from 0.6 to 1.4μm). Other than the manufacturers 'in-house' reports there is little published research available to date in the dental literature (Mitra et al., 2003). However, it would seem that the loosely bound agglomerates of the nanofillers are not really 'nano' sized as claimed, with cluster particle size ranges from 0.6 to 1.4μm.

1.6 Summary

Since the introduction of RBCs in the mid-1960s (Bowen, 1962; Bowen, 1967) there have been significant developments that continue to improve the mechanical and physical

properties such as strength and wear resistance in attempt to increase the clinical longevity of RBC restorations. However, dental practitioners must select the most appropriate RBC from a wide variety of available materials today and, in some cases, the use of a particular restorative material for a specific application may not be optimal when considering the mechanical and physical characteristics and clinical indications. However, dental RBCs have disadvantages which limit their application, despite improvements which have expanded their indications for clinical use, namely, marginal leakage due to polymerisation shrinkage (Eick and Welch, 1986; Walls et al., 1988; Davidson and Feilzer, 1997; Chen et al., 2001; Ferracane, 2008) and inadequate wear resistance under high masticatory loading in large restorations (Lutz et al., 1984; Mair et al., 1990; Suzuki and Leinfelder, 1993; Hu et al., 1999). These remain the major drawbacks for the acceptance of RBC filling materials as a viable replacement material in the posterior region of the oral cavity.

CHAPTER 2 Light Irradiation and the Associated Pitfalls

2.1 Polymerisation of light-activated RBCs

The first commercially available RBC consisted of a two-paste system composed of a base which contained a benzoyl peroxide initiator and a catalyst, namely a tertiary amine activator (Anusavice, 1996a) that were mixed together to produce a chemical reaction by self or auto-polymerisation. These RBCs had an inherent problem due to incorporation of oxygen during mixing which resulted in poor mechanical properties with the incorporated porosity being responsible for the decreased strength and exacerbated wear rates (Leinfelder, 1987). The introduction of visible light activated RBCs resulted in significant improvements in the clinical performance of these materials in terms of wear resistance, colour stability, strength, radiopacity and degree of conversion (Ferracane, 1995). The first light activated RBC was patented by Dart et al. (1978) which contained CQ and an amine activator which allowed for an increased working time for the operator compared with previously available auto-polymerising systems (Lutz and Philips, 1983). Attempts to improve the properties of RBCs have been made by numerous researchers and many manufacturers by altering the formulations of photo-initiators and amine activators (Yoshida and Greener, 1994; Asmussen and Peutzfeldt, 1996; Venhoven et al., 1996; Park et al., 1999), light curing units (LCUs) (Mills et al., 1999; Jandt et al., 2000; Musanje and Darvell, 2003) and light irradiating methodologies (Watts and Hindi, 1999; Silikas et al., 2000; Sahafi et al., 2001).

2.2 Chemistry of light activation

The light initiator chemistry of the majority of the photo-activated RBCs utilised in modem clinical practice consists of a diketone-amine system which absorbs intense visible (blue) light for the polymerisation of the resin matrix. The most commonly formulated light activation molecules for dental RBCs consist of the light-initiator, CQ and a co-initiator amine activator, DMAEMA. The absorption spectrum of CQ ranges from approximately 430 to 480nm and forms an effective photo-initiator system. However, the irradiation of a photo-activated RBC results primarily in the formation of an excited state photo-sensitiser molecule which after several inefficient steps may result in the formation of a free radical which can initiate a polymerisation chain reaction. Both the photo-sensitiser and the amine must be present at low concentrations for reasons of colour, strength and stiffness, but this makes the rate of free radical production low, and thus the rate of initiation (Yoshida and Greener, 1994; Venhoven et al., 1996). The mobility of the amine free radical species means that mutual annihilation can dominate chain initiation if the concentration rises too high, and likewise the termination of live chains. Mutual reaction of live chains is of low probability because of their relatively low diffusibility, polymerisation relying on the higher mobility of the monomer to permit the reaction to proceed, remembering that continuation of the polymerisation occurs long after irradiation has ceased for this very reason: light only initiates the first stage of the process (Musanje and Darvell, 2006). Hence, too great a rate of amine radical production is counterproductive, leading to loss of polymerisation initiating radicals and the termination of existing chains (Venhoven et al., 1996). This is expected to effect adversely strength, stiffness and hardness (Ferracane and Greener, 1986).

The CQ must first be excited from the ground state, CQ^0, to the so-called excited singlet state, CQ* by the absorption of one quantum of light before it can be converted to the active form, the triplet state, CQ^T. This is an essentially a random and low probability event, but the rate of which is proportional to the concentration of CQ*. The rate of formation of radicals is proportional to both the concentration of CQ^T and the amine. The rate of formation of CQ* depends on the concentration of CQ^0 and the irradiance, but total $CQ = CQ^0 + CQ^* + CQ^T$ ignoring for the moment the consumption of the CQ by the process of radical production. Thus, since the rate of formation of CQ* is proportional to CQ^0 at a given irradiance, this becomes less efficient as the irradiance is raised. Indeed, it leads to an exponentially asymptotic approach to saturation in the absence of any consumption such that it is only at relatively low irradiances that an approach to a simple proportionality between the concentration of CQ* and thus the rate of production of CQ^T can be made. Thus, fundamentally, no such system can show proportionality in any respect to irradiance, although it does, in the limit, approximate this at low irradiance. The CQ supply is limited, and this is indeed consumed by the process of radical production. That is, for a constant irradiation, the rate of production of radicals must fall, and eventually cease, whereupon further irradiation can have no further effect (Tirtha et al., 1982). It follows then that adding in the effect of the mutual annihilation of radicals, when deterioration in mechanical properties must ensue, leads to the conclusion that reciprocity is an impossibility except as the limiting behaviour at low irradiance and low CQ and amine concentrations, that is, doubling irradiance is not equivalent to doubling exposure time. The question of importance, nevertheless, is at what magnitude of irradiance does reciprocity failure become of practical importance. Effectively, as this is a

trade-off between the rates of polymerisation reaction initiation and annihilation of radicals, the expectation is of a peak in the value of the mechanical property of interest as a function of irradiance. This is not the case but an approach to the plateau value with respect to time is evident, as shown by the results of Musanje and Darvell (2003).

Further efforts to improve the properties of the initiating system of RBCs have included the utilisation of alternative photo-initiators and amine activators. Peutzfeldt and Asmussen (1996) reported that the use of diacetyl (2,3-butanedione) and propanal improved the surface hardness and the degree of conversion when formulated with peroxide/amine initiated resins since the diacetyl compounds produced an increased number of free-radicals on absorption of photons with an associated increase in the degree of cross-linking. Park et al. (1999) reported the degree of conversion of a conventional BisGMA/TEGDMA resin consisting of a novel photo-initiator, 1-phenyl-1,2-propanedione (PPD) and CQ. The authors suggested an improved efficiency of polymerisation when PPD and CQ were used in optimum ratios and attributed this to an increased wavelength absorption range of approximately 350 to 480nm in comparison with CQ alone (approximately 430 to 480nm). Moreover, the reduction in the concentration of CQ within the experimental resin compared with the concentration of CQ in the conventional CQ/DMAEMA photo-initiators in RBC materials was suggested to result in improved colour stability.

2.3 Light irradiation devices

The free-radical polymerisation of commercially available RBC systems results in the presence of a significant quantity of residual monomer due to incomplete conversion of the residual monomer (Lovell et al., 1999; Elliot et al., 2001; Orefice et al., 2003). The mechanical and physical properties of the resultant RBC were influenced by the degree of cross-linking and an associated increase in the degree of conversion of the resin matrix following polymerisation (Ferracane et al., 1998; Peutzfeldt and Asmussen, 2000). Consequently, to optimise the degree of conversion of an RBC restorative, many manufacturers have promoted the utilisation of LCUs with differing technologies to maximise the mechanical and physical properties of the resultant RBCs.

2.3.1 Quartz tungsten halogen

The most widely utilised light sources for the photo-activation of RBCs in the dental profession remains the quartz tungsten halogen (QTH) LCUs. The radiation emitted by the QTH bulb generates considerable heat and a broad wavelength of light, of which most is ineffective for the absorption spectrum of CQ. Consequently, band-pass filters are required to reduce the generated heat and limit the output wavelength to approximately 380 to 520nm for QTH LCUs (Cook, 1982). Although the spectral output is reduced and corresponds more effectively with the absorption spectrum of CQ the range of wavelengths remains wide, resulting in a low efficiency of the LCU which is dependent upon the quality of filtration. The practical limitations of band-pass filters and the essential removal of excessive heat restricts the manufacture of conventional QTH LCUs to irradiances less than 1000mW/cm^2. Furthermore, bulbs used in QTH devices have a

limited lifetime of approximately 40 to 100h (Stahl et al., 2000), the dielectric pass-band filter and the reflector degrade over time due to high operating temperatures which results in a significant reduction in efficiency over time (Mills et al., 1999) possibly resulting in inadequately irradiated restorations if the exposure time is not increased to compensate for decreased irradiance (Jandt et al., 2000). Damage to the fibre optic bundle due to poor handling (Pollock et al., 1981) and repeated sterilisation (Ruggeberg et al., 1996) can lead to a reduction in the irradiance over time. Clinical studies on QTH LCUs have shown that 27% of 214 LCUs surveyed in Australia (Martin et al., 1998), 33% of 130 LCUs in Israel (Pilo et al., 1999), 30% of 209 LCUs in Texas (Barghi et al., 1994) and 4.2% of 214 LCUs in Toronto had an irradiance of less than 200mW/cm^2 (El-Mowafy et al., 2005) highlighting that many dental practitioners do not maintain their QTH LCUs to produce the optimal irradiance. The concerns of decreased degree of conversion attributed to irradiance and the dental practitioners desire for decreased chair-side operating times resulted in the introduction of turbo-boosted LCU tip diameters for QTH LCUs and the development of high intensity LCUs. The plasma-arc LCU (Apollo 95E; Dental Medical Diagnostic Systems Inc., Westlake Village, CA, USA) operates at irradiances in excess of 1000mW/cm^2 and claims to polymerise RBCs to a similar depth of cure (compared with QTH LCUs) within a few seconds. However, the use of turbo-boosted LCU tip diameters have been shown to cause increased cuspal deflection compared with conventional LCU tip diameters (Abbas et al., 2003) and the use of high intensity plasma-arc LCUs may not result in adequate polymerisation of the RBC to the 5mm depths at the short irradaition times claimed by the manufacturers (Hofmann et al., 2000; Munksgaard et al., 2000; Peutzfeldt et al., 2000; Abbas et al., 2003). Musanje and Darvell (2003) reported significantly decreased flexural strength and flexural modulus for RBC specimens

irradiated with a plasma-arc LCU when irradiated for less than 5s compared with a conventional QTH LCU. The authors attributed the decreased flexural strength and modulus to the rapid saturation of the photo-sensitiser which decreased the resultant network formation. The authors concluded that a practical maximum irradiance exists for the optimum cure of a particular RBC. Other investigators (Hofmann et al., 2000) have reported a narrower spectral output for the plasma-arc LCU (approximately 440 to 490nm) compared with QTH LCUs (approximately 380 to 520nm). The significant decrease in flexural strength, flexural modulus and Vickers hardness of RBCs containing photo-initiators that absorb light at shorter wavelengths than CQ was attributed to the narrow spectral output of plasma-arc LCU which failed to overlap with the absorbance spectrum of the specific photo-initiator. From a simple rheological perspective, as the rate of polymerisation increases, there exists a decreased potential for stress-relief by pre-gel flow of the material (Davidson and Feilzer, 1997). Clinically, the increased rate of polymerisation from high irradiance LCUs may increase the stresses generated at the tooth and RBC restoration interface and thereby increase the likelihood of marginal leakage (Brackett et al., 2000; Abbas et al., 2003; Hofmann et al., 2003).

2.3.2 Light emitting diode

Light emitting diode (LED) technology was developed over the past 10-15 years to overcome the shortfalls of halogen technology. The idea that LED LCUs would replace QTH LCUs and become commonplace in dental surgeries worldwide within 10 years was boldly proposed in a letter to the British Dental Journal in 1995 by Mills (1995) despite the fact that the technology was not yet available. The transformation of the idea to reality did not come about by accident with many technological challenges having to be

overcome. The low powered blue LEDs available in 1995 were based on silicon carbide technology with an output in excess of the 7μW per LED available (Mills et al., 1999). The problem was overcome in part with the development of an LED based on gallium-nitride technology with over 400 times more output power (3mW per LED) (Nakamura et al., 1995) such that by 2002 prototype LED LCUs with irradiances similar to QTH LCUs (in excess of 500mW/cm^2) were developed. The performance of these prototype LED LCUs is well reported in the dental literature and resulted in polymerised RBCs with reported inferior depth of cure (penetrometer assembly) (Harrington and Wilson, 1993; Uhl et al., 2003), similar depth of cure (Barol hardness) (Mills et al., 2002), similar compressive fracture strengths (Mills et al., 2002) and Knoop hardness values (Uhl et al., 2003). The variously reported data was a combination of the rapid development from 27 blue LEDs to in excess of 63 LEDs per LCU resulting in an increased intensity LED LCU, the curing conditions namely, exposure time and distance (Bennett and Watts, 2004), and the diameter of the LCU light guide tip (Nitta, 2005). The spectral output of the gallium-nitride blue LEDs falls within the spectrum of the commonly used CQ photo-initiator (400-500nm), thereby eliminating the need for the use of filters (Mills, 1995; Mills et al., 1999; Jandt et al., 2000; Mills et al., 2002; Uhl et al., 2003; Uhl et al., 2004a,b). LEDs have an expected lifetime of several thousand hours with little degradation of irradiance over time (Mills, 1995; Mills et al., 1999; Jandt et al., 2000; Mills et al., 2002; Uhl et al., 2004a). The reduced heat generated during use would also be expected to improve the longevity of the LCUs and the light guides (Bennett et al., 2004) together with a reduction in temperature rise of the tooth during irradiation (Uhl et al., 2006). It has been demonstrated that the depth of cure (Mills et al., 1999; Jandt et al.,

2000; Mills et al., 2002), compressive strength (Jandt et al., 2000), flexure strength (Stahl et al., 2000), hardness (Mills et al., 2002; Uhl et al., 2002) and the degree of polymerisation (Yoon et al., 2002) achieved when irradiated with the second generation of LED LCUs were similar or greater to the values achieved with QTH LCUs (Uhl et al., 2002; Aravamydhan et al., 2006).

2.4 How does one assess performance of RBCs?

The International Standard for Dentistry - polymer-based filling, restorative and luting materials (ISO 4049: 2003) is limited in scope as the battery of tests cannot predict how a RBC will perform when placed by dental practitioners in clinical practice. The range of testing methodologies employed to assess RBC performance and stated in ISO 4049 include depth of cure, water sorption, water solubility and three-point flexure strength. It is imperative that there is standardisation and reproducibility of the testing methodologies between test centres when evaluating RBCs using the ISO 4049 standard (ISO 4049, 2000) so that any material tested under standard conditions should produce consistent test results. However, the differences in the three-point flexure strength data reported in the dental literature for the RBCs investigated in the current study varied from 79-184MPa for Z100™ MP Restorative (3M ESPE, St Paul, MN, USA) (Peutzfeld and Asmussen, 2000; Cesar et al., 2001; Yap et al., 2002; Adabo et al., 2003; Palin et al., 2003; Beun et al., 2007), 92-245MPa for Filtek™ Z250 (3M ESPE, St Paul, MN, USA) (Ferracane et al., 2003; Mitra et al., 2003; Yap et al., 2003; Palin et al., 2003, 2005; Calherios et al., 2006), 138-170MPa for Filtek™ P60 (3M ESPE, St Paul, MN, USA) (Adabo et al., 2003;

Ferracane et al., 2003) and 113-153MPa for Filtek™ Supreme (3M ESPE, St Paul, MN, USA) (Mitra et al., 2003; Beun et al., 2007). The variously reported three-point flexure strength data was reported to be indicative of the degree of conversion (Ferracane et al., 2003; Calherios et al., 2006), light intensity (Miyazaki et al., 1996; Calherios et al., 2006), type of mould (Peutzfeld and Asmussen, 2000; Palin et al., 2003; Beun et al., 2007) and LCU (Ferracane et al., 2003; Palin et al., 2003, 2005) employed.

The three-point flexure strength of RBC materials determined using the protocol set out in ISO 4049 (ISO 4049, 2000) involves the fabrication of rectangular bar-shaped specimens with length, width and height dimensions of 25 x 2 x 2mm, respectively. As the length of the rectangular-bar exceeds the LCU tip diameter, an overlapping light irradiation procedure is required. The exit window of the LCU tip diameter is placed at the centre of the specimen, irradiated for the recommended exposure time which can vary depending upon the composition of the RBC. The exit window is then moved by half the diameter of the exit window along the specimen and the adjacent area irradiated, with the procedure repeated until the entire length of the specimen is irradiated on both the top and bottom surfaces (ISO 4049, 2000). The efficiency of the overlapping irradiation regime has been questioned by a number of authors in the dental literature recently in terms of uncontrolled initiation on polymerisation (Mehl et al., 1997; Manhart et al., 2000), non-homogeneously cured specimens (Ferracane et al., 2003) and inconsistent polymerisation along the length of the bar-shaped specimen (Palin et al., 2003, 2005).

A range of LCU tip diameters are currently available to dental practitioners ranging from 8 to 13mm. Consequently 8, 11 and 13mm tip diameters require seven, five and three overlapping irradiations on each side to adequately irradiate the 25mm length of the bar-shaped specimens according to the irradiation protocol. Alternative irradiation methodologies including oven-LCUs (Peutzfeldt and Asmussen, 2000; Ferracane et al., 2003; Palin et al., 2005), the use of a scanning motion with a handheld-LCU along the length of the bar-shaped specimen (Mehl et al., 1997; Manhart et al., 2000) or employing a custom made fibre optic light guide enabling a 'one-hit' irradiation of the entire specimen (Musanje et al., 2001) have been advocated to control initiation on polymerisation and produce homogeneous specimens and consistent polymerisation along the length of the specimen.

2.5 Aims and Objectives

The objective of the current study was to investigate the efficiency of the overlapping irradiation regime by modifying the specimen manufacture protocol in ISO 4049. To exacerbate the potential for uncontrolled initiation on polymerisation and decrease the homogeneity of polymerisation along the length of the specimen, the exit window was moved by three-quarters (not half) the diameter along the specimen so that some areas received twice the irradiation of adjacent areas. It was proposed that increasing the number of irradiations, with decreasing LCU tip diameter from 13 to 11 and 8mm, would progressively decrease the efficiency of the polymerisation process compared with a 'one-hit' irradiation using a custom made fibre optic light guide. In addition, the specimens were irradiated from the top surface only to further exacerbate the

phenomenon investigated. Additionally, the influence of light irradiation variables (tip diameter, irradiance, irradiation protocol and LCU) on the flexural strength, flexural modulus and the Vickers hardness of four RBCs was assessed. The hypothesis tested was that the flexural strength, flexural modulus and the Vickers hardness for the RBCs would be similar regardless of the irradiation variables and the internal control for the investigations were specimens irradiated with was the 25mm custom made fibre optic light guide which enabled a 'one-hit' irradiation.

CHAPTER 3 Materials and Methods

3.1 Materials

The dimethacrylate RBC materials tested in the current study were Z100™, Filtek™ Z250, Filtek™ P60 and Filtek™ Supreme XT (Table 3.1). The materials were manufactured by 3M ESPE Dental Products Division, St. Paul, MN, USA.

Table 3.1: The formulation of the RBC materials used in the current study.

RBC	Filler			Resin
	Type	**Particle size**	**Volume (%)**	
Z100™ (shade A3: batch 20050211)	Zirconia and silica	0.01-3.5 μm	66%	Bis-GMA and TEGDMA
Filtek™ Z250 (shade A3: batch 20050210)	Zirconia and silica	0.01-3.5 μm	61%	Bis-GMA, UDMA, Bis-EMA and TEGDMA
Filtek™ P60 (shade A3; batch 20050329)	Zirconia and silica	0.01-3.5 μm	60%	Bis-GMA, UDMA, Bis-EMA and TEGDMA
Filtek™ Supreme XT (shade A3B; batch 20050106)	Zirconia and silica	0.6-1.4 μm	59.5%	Bis-GMA, UDMA, Bis-EMA and TEGDMA

3.1.1 Dimethacrylate RBC materials

3.1.1.1 Resin chemistry

The dimethacrylate based resin in Z100™ is composed of a monomeric blend of 2,2-bis[4-(2-hydroxy-3-methacryloxypropoxy)phenyl]propane (bisphenol A glycol dimethacrylate; Bis-GMA) and TEGDMA (Figure 3.1). The photo-initiator system within the resin constituent of Z100™ consists of a visible light initiator, namely CQ and a co-initiator, namely DMAEMA which enable light activation and initiation of the polymerisation reaction (Z100™ :Product Report, 1996).

(a)

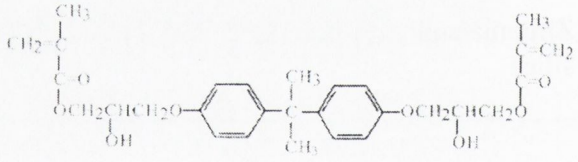

(b)

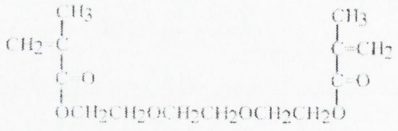

Figure 3.1: The chemical structure of (a) bisphenol A glycol dimethacrylate (Bis-GMA) and (b) triethyleneglycol dimethacrylate (TEGDMA) utilised in the monomer blend of the dimethacrylate RBC, Z100™.

The dimethacrylate based resins in Filtek™ Z250, Filtek™ P60 and Filtek™ Supreme XT are similar to that for Z100™ but the majority of the TEGDMA is replaced with 2,2-bis[4-(2-methacrylyloxyethoxy)phenyl]propane (bisphenol A hexaethoxylated dimethacrylate; Bis-EMA(6) with six ethylene oxide molecules for each bisphenol A group) and 1,6 bis(methacryloxy-2-ethoxycarbonylamino)-2,4,4-trimethylhexane (UDMA) (Figure 3.2). CQ and DMAEMA are the visible light initiator and co-initiator within the resin constituents of Filtek™ Z250, Filtek™ P60 and Filtek™ Supreme XT to enable light activation and initiation of the polymerisation reaction (Filtek™ Z250, Filtek™ P60 and Filtek™ Supreme XT: Product Reports, 1999, 2001 and 2004, respectively).

(a)

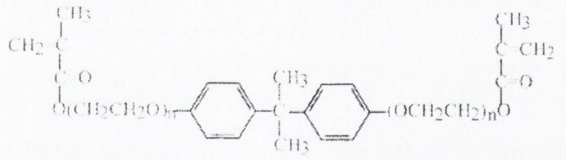

(b)

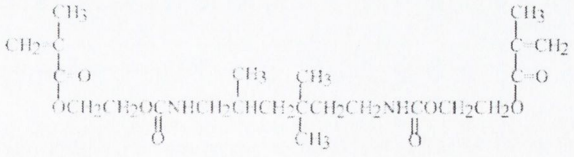

Figure 3.2: The chemical structure of (a) bisphenol A hexaethoxylated dimethacrylate (Bis-EMA) and (b) urethane dimethacrylate (UDMA) utilised in the monomer blend of the dimethacrylate RBCs, Filtek™ Z250, Filtek™ P60 and Filtek™ Supreme XT.

3.1.1.2 Filler morphology

The monomeric resin blend of Z100™ was reinforced to 66vol.% with methacrylate-functional silane coated zirconia-silica filler according to the manufacturer (Table 3.1). In addition, the manufacturer reported a particle size distribution ranging from 0.01-3.5μm with an average particle size of 0.6μm (Z100™: Product Report, 1996).

The filler particles employed by the manufacturers to reinforce the monomeric resin blend of Filtek™ Z250 and Filtek™ P60 were also a methacrylate-functional silane coated zirconia-silica filled to 60 and 61vol.%, respectively (Table 3.1). The manufacturers reported that the employment of optimised sol-gel and milling processes produced an increase in filler consistency and an increase in the number of finer filler particles. However, the particle size distributions reported for Filtek™ Z250 and Filtek™ P60 were similar to Z100™ ranging from 0.01-3.5μm with a primary particle size of 0.6μm (Filtek™ Z250 and Filtek™ P60: Product Reports, 1999 and 2001, respectively).

The monomeric resin blend of Filtek™ Supreme XT was reinforced with a combination of aggregated methacrylate-functional silane coated zirconia-silica clusters with an average cluster particle size of 0.6-1.4μm (primary particle size of 5-20nm) and a non-agglomerated methacrylate-functional silane coated zirconia-silica filler of 20nm resulting in a filler volume of 59.5vol.% (Table 3.1) according to the manufacturer (Filtek™ Supreme XT: Product Report, 2004).

3.1.2 Light curing units

3.1.2.1 Quartz tungsten halogen

The QTH handheld LCU used to irradiate the RBC materials examined in the current study was an Optilux 501 (Kerr Mfg. Co., Orange, CA, USA). The QTH LCU was employed in both standard and boosted modes and the irradiance was measured seven consecutive times using a radiometer incorporated within the Optilux 501 QTH LCU when employed with tip diameters of 13, 11, 8 and 25mm. In addition, an 8mm Turbo tip diameter was also used in standard and boosted modes and the irradiance was also measured consecutively (n=7) using the radiometer.

3.1.2.2 Light emitting diode

A first generation light emitting diode (LED) LCU (Elipar™ Freelight, 3M ESPE Dental Products Division, St. Paul, MN, USA) and a second generation LED LCU (Elipar™ Freelight 2, 3M ESPE Dental Products Division, St. Paul, MN, USA) were used to irradiate the RBC materials under investigation. The irradiance of the Elipar™ Freelight and Elipar™ Freelight 2 LED LCUs were measured consecutively seven times using the radiometer incorporated within the QTH LCU when employed with tip diameters of 13 and 8mm.

3.2 Characterisation techniques: Mechanical properties

The range of testing methodologies employed to assess RBC performance as stated in the most recent ISO specification include depth of cure, water sorption and water solubility and three-point flexure strength. The three-point flexure strength testing methodology involves the fabrication of rectangular bar-shaped specimens with length, width and height dimensions of 25 x 2 x 2mm, respectively. As the length of the rectangular bar exceeds the LCU tip diameter, an overlapping procedure is required. In accordance with ISO 4049, the exit window of the LCU tip is placed at the centre of the specimen and irradiated for the recommended exposure time. The exit window is moved by half the LCU tip diameter and the adjacent area is irradiated by overlapping the previously irradiated section. The procedure is repeated until the entire length of the specimen is irradiated from both the top and bottom surfaces. A range of tip diameters are currently available to GDPs ranging from 8 to 13mm in diameter. Consequently 8, 11 and 13mm tip diameters require seven, five and three overlapping irradiations, respectively to irradiate the 25mm length of the ISO bar-shaped specimens.

3.2.1 Specimen preparation

Twenty rectangular bar-shaped specimens of the four dimethacrylate RBCs investigated (Z100™, Filtek™ Z250, Filtek™ P60 and Filtek™ Supreme XT) were fabricated using a knife-edged split aluminium mould (aluminium alloy 6061) designed to minimise the stresses generated on the specimens upon retrieval following irradiation (Musanje and

Darvell, 2001). In addition, the split-mould allowed the flash of excess material to be easily removed and the diverging end walls allowed easy flow of the material and maximised the expulsion of air (Musanje and Darvell, 2001). A constant excess of uncured resin was placed into the mould, the top surface was covered with a cellulose acetate strip to eliminate oxygen inhibition of the top layer of the RBC. A glass microscope slide and a load of 1kg was applied for 20s to ensure consistent and reproducible packing of the rectangular bar-shaped test specimens. The load and microscope slide were removed and the specimen was irradiated at ambient room temperature (23 ± 1°C) for 40s for Z100™ and 20s for Filtek™ Z250, Filtek™ P60 and Filtek™ Supreme XT.

The entire length of each specimen was irradiated by modifying the ISO 4049 specimen manufacture protocol (ISO 4049, 2000) by placing the tip of the light guide in direct contact with the acetate strip and irradiating from the top surface only. The exit window was moved by three-quarters (not half) the diameter along the specimen so that certain areas received twice the irradiation of adjacent areas to exacerbate the potential for uncontrolled initiation on polymerisation and non-homogeneity of polymerisation along the length of the specimen.

3.2.2 QTH handheld LCU

3.2.2.1 Standard mode ($_s$)

The 13mm tip diameter required three overlapping irradiations to ensure the entire length of each specimen of Z100™ (Group A_s), Filtek™ Z250 (Group B_s), Filtek™ P60 (Group C_s) and Filtek™ Supreme XT (Group D_s) was irradiated using the modified irradiation protocol. The 11mm tip diameter required four overlapping irradiations for Z100™ (Group E_s), Filtek™ Z250 (Group F_s), Filtek™ P60 (Group G_s) and Filtek™ Supreme XT (Group H_s), while the 8mm tip diameter required five overlapping irradiations for each specimen of Z100™ (Group I_s), Filtek™ Z250 (Group J_s), Filtek™ P60 (Group K_s) and Filtek™ Supreme XT (Group L_s). A further four specimen groups of Z100™ (Group M_s), Filtek™ Z250 (Group N_s), Filtek™ P60 (Group O_s) and Filtek™ Supreme XT (Group P_s) were irradiated using a custom made fibre optic light guide (C technologies, Cedar Knolls, NJ, USA) with a rectangular exit window of 3mm wide and 25mm length thus enabling illumination of the entire specimen in 'one-hit' (Table 3.2). The light guide had a 10mm circular collection port with the fibre optics within the bundle randomly arranged to form the exit window (Musanje and Darvell, 2001).

3.2.2.2 Boosted mode ($_b$)

For Z100™ (Group A_b), Filtek™ Z250 (Group B_b), Filtek™ P60 (Group C_b) and Filtek™ Supreme XT (Group D_b), the 13mm tip diameter required three overlapping irradiations

when the modified irradiation protocol was used. The 11mm tip diameter required four overlapping irradiations to ensure the entire length of each specimen of Z100™ (Group E_b), Filtek™ Z250 (Group F_b), Filtek™ P60 (Group G_b) and Filtek™ Supreme XT (Group H_b) was irradiated. In addition, the 8mm tip diameter required five overlapping irradiations for Z100™ (Group I_b), Filtek™ Z250 (Group J_b), Filtek™ P60 (Group K_b) and Filtek™ Supreme XT (Group L_b). Groups of Z100™ (Group M_b), Filtek™ Z250 (Group N_b), Filtek™ P60 (Group O_b) and Filtek™ Supreme XT (Group P_b) were also irradiated using the 25mm custom made fibre optic light guide (Table 3.2).

3.2.2.3 Turbo tip standard ($_{st}$) and boosted mode ($_{bt}$)

The 8mm Turbo tip diameter required five overlapping irradiations to ensure the entire length of each specimen of Z100™ (Group I_{st}), Filtek™ Z250 (Group J_{st}), Filtek™ P60 (Group K_{st}) and Filtek™ Supreme XT (Group L_{st}) was fully irradiated in standard mode. Further specimen groups of Z100™ (Group I_{bt}), Filtek™ Z250 (Group J_{bt}), Filtek™ P60 (Group K_{bt}) and Filtek™ Supreme XT (Group L_{bt}) were irradiated in boosted mode (Table 3.2).

Table 3.2: The specimen groups for each RBC material irradiated when employing the 13, 11, 8, 25 and 8mm 'Turbo' tip diameters with the QTH LCU in standard and boosted modes.

RBC	Operating mode	Tip diameter				
		13mm	11mm	8mm	25mm	8mm 'Turbo'
Z100™	Standard mode	Group A_s	Group E_s	Group I_s	Group M_s	Group I_{st}
	Boosted mode	Group A_b	Group E_b	Group I_b	Group M_b	Group I_{bt}
Filtek™ Z250	Standard mode	Group B_s	Group F_s	Group J_s	Group N_s	Group J_{st}
	Boosted mode	Group B_b	Group F_b	Group J_b	Group N_b	Group J_{bt}
Filtek™ P60	Standard mode	Group C_s	Group G_s	Group K_s	Group O_s	Group K_{st}
	Boosted mode	Group C_b	Group G_b	Group K_b	Group O_b	Group K_{bt}
Filtek™ Supreme XT	Standard mode	Group D_s	Group H_s	Group L_s	Group P_s	Group L_{st}
	Boosted mode	Group D_b	Group H_b	Group L_b	Group P_b	Group L_{bt}

3.2.3 LED handheld LCU

3.2.3.1 Elipar™ Freelight ($_l$)

The 13mm tip diameter required three overlapping irradiations on the top surface for Z100™ (Group Q_l), Filtek™ Z250 (Group R_l), Filtek™ P60 (Group S_l) and Filtek™ Supreme XT (Group T_l) while the 8mm tip diameter required five overlapping irradiations on the top surface for Z100™ (Group U_l), Filtek™ Z250 (Group V_l), Filtek™ P60 (Group W_l) and Filtek™ Supreme XT (Group X_l) to ensure the specimens were irradiated using the modified irradiation protocol with the Elipar™ Freelight LED LCU ($_l$) (Table 3.3).

3.2.3.2 Elipar™ Freelight 2 ($_h$)

Employing the modified irradiation protocol with the Elipar™ Freelight 2 LED LCU ($_h$) required three overlapping irradiations on the top surface for the 13mm LCU tip diameter for Z100™ (Group Q_h), Filtek™ Z250 (Group R_h), Filtek™ P60 (Group S_h) and Filtek™ Supreme XT (Group T_h). In addition, five overlapping irradiations on the top surface for the 8mm LCU tip diameter for Z100™ (Group U_h), Filtek™ Z250 (Group V_h), Filtek™ P60 (Group W_h) and Filtek™ Supreme XT (Group X_h) were required to ensure the specimens were irradiated (Table 3.3).

Table 3.3: The specimen groups for each RBC material irradiated when employing the 13 and 8mm tip diameters with the Elipar™ Freelight and Elipar™ Freelight 2 LED LCUs.

RBC	LED LCU	Tip diameter	
		13mm	8mm
Z100™	Elipar™ Freelight	Group Q_l	Group U_l
	Elipar™ Freelight 2	Group Q_h	Group U_h
Filtek™ Z250	Elipar™ Freelight	Group R_l	Group V_l
	Elipar™ Freelight 2	Group R_h	Group V_h
Filtek™ P60	Elipar™ Freelight	Group S_l	Group W_l
	Elipar™ Freelight 2	Group S_h	Group W_h
Filtek™ Supreme XT	Elipar™ Freelight	Group T_l	Group X_l
	Elipar™ Freelight 2	Group T_h	Group X_h

Following irradiation with the LCU the cellulose acetate strip was discarded, the mould dismantled, the specimen removed and checked for surface imperfections. The specimens with defects were eliminated and the remaining specimens were stored in a light-proof container containing 50ml of deionised water and placed in a climate controlled chamber (Froilabo-Firalabo, SP-260 BVEHF, Meyzieu, France) maintained at 37 ± 1°C at 55% relative humidity for 24h prior to testing and analysis.

3.3 Three-point flexure testing

It is imperative that there is standardisation and reproducibility of the testing methodologies between test centres when evaluating RBCs (ISO 4049, 2000). Therefore, the testing of nominally identical specimens under similar test conditions should produce consistent test results between test centres. However, the variously reported three-point flexure strength data in the dental literature (Miyazaki et al., 1996; Peutzfeldt and Asmussen, 2000; Cesar et al., 2001; Yap et al., 2002; Mitra et al., 2003; Palin et al., 2003; Ferracane et al., 2003; Yap and Teoh, 2003; Palin et al., 2005; Calheiros et al., 2006; Beun et al., 2007) may suggest that the efficacy of the overlapping irradiation regime is flawed in terms of uncontrolled initiation on polymerisation (Mehl et al., 1997; Manhart et al., 2000), non-homogeneously cured specimens (Ferracane et al., 2003) and inconsistent polymerisation along the length of the bar-shaped specimen (Palin et al., 2003, 2005). As a result, the efficacy of ISO 4049: 2000 was examined in terms of the three-point flexure properties and Vickers hardness.

The rectangular bar-shaped specimens with the irradiated side uppermost were centrally loaded with a 0.3mm width knife-edge indenter across a support span of 20mm in accordance with the testing procedure outlined in ISO 4049. The specimens were loaded using a universal tensile testing machine (Instron Model 5565, High Wycombe, Buckinghamshire, UK) at a crosshead speed of 1mm/min and the maximum load to fracture was recorded.

3.3.1 Three-point flexure strength

The three-point flexure strength was calculated using Equation 3.1 (ISO 4049, 2000)

$$\sigma_{max} = \frac{3PL}{2bd^2} \qquad \text{Equation 3.1}$$

where σ_{max} was the maximum flexure stress (MPa), P the measured load at fracture (N), L the support span distance (20mm), b the width and d the thickness of the specimen (mm) measured using a digital micrometer accurate to 100μm (Mitutoyo, Kawasaki, Japan).

3.3.2 Three-point flexure modulus

The three-point flexure modulus was determined using Equation 3.2 (ISO 4049: 2000)

$$E = \left(\frac{\Delta P}{\Delta D}\right)\frac{L^3}{4bd^3} \qquad \text{Equation 3.2}$$

where E was the flexure modulus (GPa), L the support span distance (20mm), b the width and d the thickness of the specimen (mm) and $\left(\frac{\Delta P}{\Delta D}\right)$ the gradient of the steepest linear portion of the load-deflection curve.

3.4 Vickers hardness testing

Vickers hardness measurements were made to investigate the claims of uncontrolled initiation on polymerisation (Mehl et al., 1997; Manhart et al., 2000), non-

homogeneously cured specimens (Ferracane et al., 2003) and inconsistent polymerisation along the length of the bar-shaped specimen (Palin et al., 2003, 2005).

3.4.1 Indentation technique

The Vickers hardness testing methodology employs a downward force, using a diamond pyramid head (Micromet 5104, Buehler, Lake Blutt, Illinois, USA), to produce an indent on the surface of the specimen. The subsequent indentation pattern creates diagonal lines which are then measured using a micrometer screw gauge contained within the microscope attachment of the machine to determine the average diagonal distance. The Vickers hardness was obtained by calculating the surface area of the indent in accordance with Equation 3.3 where the harder the material the shallower the indentation and therefore an increased Vickers hardness value.

$$VH = \frac{2P}{D^2}(\sin 68^\circ) \qquad \text{Equation (3.3)}$$

where P was the predetermined load applied (g), D was the diagonal distance (μm) and 68° was the angle of the diamond pyramid head tip of the indenter.

Three specimens for each group irradiated with the QTH (Table 3.2) and LED (Table 3.3) LCUs were prepared in accordance with the specimen preparation procedures outlined in Section 3.2.1.1 and 3.2.1.2, respectively. The 13mm tip diameter (which required three overlapping irradiations on the top surface) formed three non-overlapped and two overlapped regions for the top and bottom surfaces of each RBC specimen. The 11mm tip diameter resulted in four non-overlapped and three overlapped regions while five

overlapping irradiations were required with the 8mm tip diameter thereby creating five non-overlapped and four overlapped regions on the top and bottom surfaces of each specimen of Z100™, Filtek™ Z250, Filtek™ P60 and Filtek™ Supreme XT. Employing the QTH with the 25mm 'one-hit' tip diameter resulted in only one non-overlapped and no overlapped regions on the top and bottom surfaces of each RBC specimen.

Two Vickers indentations were applied, with a load of 300g for 15s at room temperature, to each of the non-overlapped and overlapped regions of the rectangular bar-shaped specimens. This resulted in a total of six non-overlapped and four overlapped Vickers indentations on the top and bottom surface of each of the three specimens irradiated with a 13mm tip diameter. With the 11mm tip diameter, eight non-overlapped and six overlapped Vickers indentations were produced on the top and bottom surface of each of the three specimens. For the 8mm tip diameter, ten non-overlapped and eight overlapped Vickers indentations were made on the top and bottom surface of each of the three specimens. On each of the three 'one-hit' specimens a total of fifteen non-overlapped Vickers indentations were made on the top and bottom surfaces.

3.4.2 QTH handheld LCU

3.4.2.1 Standard mode ($_S$)

The Vickers hardness data for the non-overlapped ($_{NO}$) and overlapped ($_O$) regions was grouped for the top surface ($_T$) of each RBC material irradiated in standard mode ($_S$). The

13mm tip diameter resulted in grouped data for Z100™ (Group $A_{s(NO)T}$ and Group $A_{s(O)T}$), Filtek™ Z250 (Group $B_{s(NO)T}$ and Group $B_{s(O)T}$), Filtek™ P60 (Group $C_{s(NO)T}$ and Group $C_{s(O)T}$) and Filtek™ Supreme XT (Group $D_{s(NO)T}$ and Group $D_{s(O)T}$). The grouped data for the 11mm tip diameter were Z100™ (Group $E_{s(NO)T}$ and Group $E_{s(O)T}$), Filtek™ Z250 (Group $F_{s(NO)T}$ and Group $F_{s(O)T}$), Filtek™ P60 (Group $G_{s(NO)T}$ and Group $G_{s(O)T}$) and Filtek™ Supreme XT (Group $H_{s(NO)T}$ and Group $H_{s(O)T}$). For the 8mm tip diameter the data was grouped as Z100™ (Group $I_{s(NO)T}$ and Group $I_{s(O)T}$), Filtek™ Z250 (Group $J_{s(NO)T}$ and Group $J_{s(O)T}$), Filtek™ P60 (Group $K_{s(NO)T}$ and Group $K_{s(O)T}$) and Filtek™ Supreme XT (Group $L_{s(NO)T}$ and Group $L_{s(O)T}$). In addition, a total of fifteen Vickers indentations were recorded on the top surface ($_T$) for each of the three 'one-hit' specimens of each RBC material, namely Z100™ (Group $M_{s(NO)T}$), Filtek™ Z250 (Group $N_{s(NO)T}$), Filtek™ P60 (Group $O_{s(NO)T}$) and Filtek™ Supreme XT (Group $P_{s(NO)T}$) (Table 3.4).

For the bottom surfaces ($_B$) the Vickers hardness data for the non-overlapped ($_{NO}$) and two overlapped ($_O$) regions was also grouped when irradiated in standard mode ($_s$) with the 13mm tip diameter (Z100™ (Group $A_{s(NO)B}$ and Group $A_{s(O)B}$), Filtek™ Z250 (Group $B_{s(NO)B}$ and Group $B_{s(O)B}$), Filtek™ P60 (Group $C_{s(NO)B}$ and Group $C_{s(O)B}$) and Filtek™ Supreme XT (Group $D_{s(NO)B}$ and Group $D_{s(O)B}$)). The Vickers hardness data for the bottom surface of the specimens irradiated with the 11mm tip diameter were grouped as Z100™ (Group $E_{s(NO)B}$ and Group $E_{s(O)B}$), Filtek™ Z250 (Group $F_{s(NO)B}$ and Group $F_{s(O)B}$), Filtek™ P60 (Group $G_{s(NO)B}$ and Group $G_{s(O)B}$) and Filtek™ Supreme XT (Group $H_{s(NO)B}$ and Group $H_{s(O)B}$). Similarly, the Vickers indentations on the bottom surface of the three specimens irradiated with an 8mm tip diameter were grouped as Z100™ (Group $I_{s(NO)B}$

Table 3.4: The non-overlapped and overlapped groups on the top and bottom surfaces for each RBC material when irradiated with the 13, 11, 8, 25 and 8mm 'Turbo' tip diameters using the QTH LCU in standard mode.

RBCl	Surface	Region	Tip diameter				
			13mm	11mm	8mm	25mm	8mm 'Turbo'
Z100™	Top	Non-overlapped	Group $A_{s(NO)T}$	Group $E_{s(NO)T}$	Group $I_{s(NO)T}$	Group $M_{s(NO)T}$	Group $I_{st(NO)T}$
		Overlapped	Group $A_{s(O)T}$	Group $E_{s(O)T}$	Group $I_{s(O)T}$		Group $I_{st(O)T}$
	Bottom	Non-overlapped	Group $A_{s(NO)B}$	Group $E_{s(NO)B}$	Group $I_{s(NO)B}$	Group $M_{s(NO)B}$	Group $I_{st(NO)B}$
		Overlapped	Group $A_{s(O)B}$	Group $E_{s(O)B}$	Group $I_{s(O)B}$		Group $I_{st(O)B}$
Filtek™ Z250	Top	Non-overlapped	Group $B_{s(NO)T}$	Group $F_{s(NO)T}$	Group $J_{s(NO)T}$	Group $N_{s(NO)T}$	Group $J_{st(NO)T}$
		Overlapped	Group $B_{s(O)T}$	Group $F_{s(O)T}$	Group $J_{s(O)T}$		Group $J_{st(O)T}$
	Bottom	Non-overlapped	Group $B_{s(NO)B}$	Group $F_{s(NO)B}$	Group $J_{s(NO)B}$	Group $N_{s(NO)B}$	Group $J_{st(NO)B}$
		Overlapped	Group $B_{s(O)B}$	Group $F_{s(O)B}$	Group $J_{s(O)B}$		Group $J_{st(O)B}$
Filtek™ P60	Top	Non-overlapped	Group $C_{s(NO)T}$	Group $G_{s(NO)T}$	Group $K_{s(NO)T}$	Group $O_{s(NO)T}$	Group $K_{st(NO)T}$
		Overlapped	Group $C_{s(O)T}$	Group $G_{s(O)T}$	Group $K_{s(O)T}$		Group $K_{st(O)T}$
	Bottom	Non-overlapped	Group $C_{s(NO)B}$	Group $G_{s(NO)B}$	Group $K_{s(NO)B}$	Group $O_{s(NO)B}$	Group $K_{st(NO)B}$
		Overlapped	Group $C_{s(O)B}$	Group $G_{s(O)B}$	Group $K_{s(O)B}$		Group $K_{st(O)B}$
Filtek™ Supreme XT	Top	Non-overlapped	Group $D_{s(NO)T}$	Group $H_{s(NO)T}$	Group $L_{s(NO)T}$	Group $P_{s(NO)T}$	Group $L_{st(NO)T}$
		Overlapped	Group $D_{s(O)T}$	Group $H_{s(O)T}$	Group $L_{s(O)T}$		Group $L_{st(O)T}$
	Bottom	Non-overlapped	Group $D_{s(NO)B}$	Group $H_{s(NO)B}$	Group $L_{s(NO)B}$	Group $P_{s(NO)B}$	Group $L_{st(NO)B}$
		Overlapped	Group $D_{s(O)B}$	Group $H_{s(O)B}$	Group $L_{s(O)B}$		Group $L_{st(O)B}$

and Group $I_{s(O)B}$), Filtek™ Z250 (Group $J_{s(NO)B}$ and Group $J_{s(O)B}$), Filtek™ P60 (Group $K_{s(NO)B}$ and Group $K_{s(O)B}$) and Filtek™ Supreme XT (Group $L_{s(NO)B}$ and Group $L_{s(O)B}$). Fifteen indentations were produced on the bottom surface ($_B$) of the three 'one-hit' specimens of each RBC material examined were grouped as Z100™ (Group $M_{s(NO)B}$), Filtek™ Z250 (Group $N_{s(NO)B}$), Filtek™ P60 (Group $O_{s(NO)B}$) and Filtek™ Supreme XT (Group $P_{s(NO)B}$) (Table 3.4).

3.4.2.2 Boosted mode ($_b$)

The Vickers hardness data for the top surface irradiated in boosted mode ($_b$) was grouped for each RBC irradiated with the 13mm tip diameter (Z100™ (Group $A_{b(NO)T}$ and Group $A_{b(O)T}$), Filtek™ Z250 (Group $B_{b(NO)T}$ and Group $B_{b(O)T}$), Filtek™ P60 (Group $C_{b(NO)T}$ and Group $C_{b(O)T}$) and Filtek™ Supreme XT (Group $D_{b(NO)T}$ and Group $D_{b(O)T}$)), 11mm tip diameter (Z100™ (Group $E_{b(NO)T}$ and Group $E_{b(O)T}$), Filtek™ Z250 (Group $F_{b(NO)T}$ and Group $F_{b(O)T}$), Filtek™ P60 (Group $G_{b(NO)T}$ and Group $G_{b(O)T}$) and Filtek™ Supreme XT (Group $H_{b(NO)T}$ and Group $H_{b(O)T}$)) and 8mm tip diameters (Z100™ (Group $I_{b(NO)T}$ and Group $I_{b(O)T}$), Filtek™ Z250 (Group $J_{b(NO)T}$ and Group $J_{b(O)T}$), Filtek™ P60 (Group $K_{b(NO)T}$ and Group $K_{b(O)T}$) and Filtek™ Supreme XT (Group $L_{b(NO)T}$ and Group $L_{b(O)T}$)). A further fifteen Vickers indentations were made on the top surface ($_T$) for each of the three 'one-hit' specimens of each RBC material, namely Z100™ (Group $M_{b(NO)T}$), Filtek™ Z250 (Group $N_{b(NO)T}$), Filtek™ P60 (Group $O_{b(NO)T}$) and Filtek™ Supreme XT (Group $P_{b(NO)T}$) (Table 3.5).

Similarly, the Vickers hardness data for the bottom surface irradiated in boosted mode ($_{b}$) was grouped for each RBC irradiated with the 13mm tip diameter, (Z100™ (Group $A_{b(NO)B}$ and Group $A_{b(O)B}$), Filtek™ Z250 (Group $B_{b(NO)B}$ and Group $B_{b(O)B}$), Filtek™ P60 (Group $C_{b(NO)B}$ and Group $C_{b(O)B}$) and Filtek™ Supreme XT (Group $D_{b(NO)B}$ and Group $D_{b(O)B}$)), 11mm tip diameter (Z100™ (Group $E_{b(NO)B}$ and Group $E_{b(O)B}$), Filtek™ Z250 (Group $F_{b(NO)B}$ and Group $F_{b(O)B}$), Filtek™ P60 (Group $G_{b(NO)B}$ and Group $G_{b(O)B}$) and Filtek™ Supreme XT (Group $H_{b(NO)B}$ and Group $H_{b(O)B}$)) and 8mm tip diameters (Z100™ (Group $I_{b(NO)B}$ and Group $I_{b(O)B}$), Filtek™ Z250 (Group $J_{b(NO)B}$ and Group $J_{b(O)B}$), Filtek™ P60 (Group $K_{b(NO)B}$ and Group $K_{b(O)B}$) and Filtek™ Supreme XT (Group $L_{b(NO)B}$ and Group $L_{b(O)B}$)). The bottom surface ($_{B}$) was also subjected to fifteen indentations of the three 'one-hit' specimens of each RBC material examined and grouped as Z100™ (Group $M_{b(NO)B}$), Filtek™ Z250 (Group $N_{b(NO)B}$), Filtek™ P60 (Group $O_{b(NO)B}$) and Filtek™ Supreme XT (Group $P_{b(NO)B}$) (Table 3.5).

3.4.2.3 Turbo tip standard ($_{st}$) and boosted mode ($_{bt}$)

The 8mm 'Turbo' tip diameter in standard mode ($_{st}$) resulted in a total of ten non-overlapped ($_{NO}$) and eight overlapped ($_{O}$) indentations on the top surface ($_{T}$) of each group of three rectangular bar-shaped specimens of Z100™ (Group $I_{st(NO)T}$ and Group $I_{st(O)T}$), Filtek™ Z250 (Group $J_{st(NO)T}$ and Group $J_{st(O)T}$), Filtek™ P60 (Group $K_{st(NO)T}$ and Group $K_{st(O)T}$) and Filtek™ Supreme XT (Group $L_{st(NO)T}$ and Group $L_{st(O)T}$) (Table 3.4). The Vickers hardness was also grouped for the bottom surface ($_{B}$) of each of the three rectangular bar-shaped specimens (Z100™ (Group $I_{st(NO)B}$ and Group $I_{st(O)B}$), Filtek™

Table 3.5: The non-overlapped and overlapped groups on the top and bottom surfaces for each RBC material when irradiated with the 13, 11, 8, 25 and 8mm 'Turbo' tip diameters using the QTH LCU in boosted mode.

RBC	Surface	Region	Tip diameter				
			13mm	11mm	8mm	25mm	8mm 'Turbo'
Z100™	Top	Non-overlapped	Group $A_{b(NO)T}$	Group $E_{b(NO)T}$	Group $I_{b(NO)T}$	Group $M_{b(NO)T}$	Group $I_{bt(NO)T}$
		Overlapped	Group $A_{b(O)T}$	Group $E_{b(O)T}$	Group $I_{b(O)T}$		Group $I_{bt(O)T}$
	Bottom	Non-overlapped	Group $A_{b(NO)B}$	Group $E_{b(NO)B}$	Group $I_{b(NO)B}$	Group $M_{b(NO)B}$	Group $I_{bt(NO)B}$
		Overlapped	Group $A_{b(O)B}$	Group $E_{b(O)B}$	Group $I_{b(O)B}$		Group $I_{bt(O)B}$
Filtek™ Z250	Top	Non-overlapped	Group $B_{b(NO)T}$	Group $F_{b(NO)T}$	Group $J_{b(NO)T}$	Group $N_{b(NO)T}$	Group $J_{bt(NO)T}$
		Overlapped	Group $B_{b(O)T}$	Group $F_{b(O)T}$	Group $J_{b(O)T}$		Group $J_{bt(O)T}$
	Bottom	Non-overlapped	Group $B_{b(NO)B}$	Group $F_{b(NO)B}$	Group $J_{b(NO)B}$	Group $N_{b(NO)B}$	Group $J_{bt(NO)B}$
		Overlapped	Group $B_{b(O)B}$	Group $F_{b(O)B}$	Group $J_{b(O)B}$		Group $J_{bt(O)B}$
Filtek™ P60	Top	Non-overlapped	Group $C_{b(NO)T}$	Group $G_{b(NO)T}$	Group $K_{b(NO)T}$	Group $O_{b(NO)T}$	Group $K_{bt(NO)T}$
		Overlapped	Group $C_{b(O)T}$	Group $G_{b(O)T}$	Group $K_{b(O)T}$		Group $K_{bt(O)T}$
	Bottom	Non-overlapped	Group $C_{b(NO)B}$	Group $G_{b(NO)B}$	Group $K_{b(NO)B}$	Group $O_{b(NO)B}$	Group $K_{bt(NO)B}$
		Overlapped	Group $C_{b(O)B}$	Group $G_{b(O)B}$	Group $K_{b(O)B}$		Group $K_{bt(O)B}$
Filtek™ Supreme XT	Top	Non-overlapped	Group $D_{b(NO)T}$	Group $H_{b(NO)T}$	Group $L_{b(NO)T}$	Group $P_{b(NO)T}$	Group $L_{bt(NO)T}$
		Overlapped	Group $D_{b(O)T}$	Group $H_{b(O)T}$	Group $L_{b(O)T}$		Group $L_{bt(O)T}$
	Bottom	Non-overlapped	Group $D_{b(NO)B}$	Group $H_{b(NO)B}$	Group $L_{b(NO)B}$	Group $P_{b(NO)B}$	Group $L_{bt(NO)B}$
		Overlapped	Group $D_{b(O)B}$	Group $H_{b(O)B}$	Group $L_{b(O)B}$		Group $L_{bt(O)B}$

Z250 (Group $J_{st(NO)B}$ and Group $J_{st(O)B}$), Filtek™ P60 (Group $K_{st(NO)B}$ and Group $K_{st(O)B}$) and Filtek™ Supreme XT (Group $L_{st(NO)B}$ and Group $L_{st(O)B}$)) (Table 3.4).

In boosted mode ($_{bt}$), the Vickers hardness data was grouped for the top surface, namely Z100™ (Group $I_{bt(NO)T}$ and Group $I_{bt(O)T}$), Filtek™ Z250 (Group $J_{bt(NO)T}$ and Group $J_{bt(O)T}$), Filtek™ P60 (Group $K_{bt(NO)T}$ and Group $K_{bt(O)T}$) and Filtek™ Supreme XT (Group $L_{bt(NO)T}$ and Group $L_{bt(O)T}$) (Table 3.4) and bottom surface, namely Z100™ (Group $I_{bt(NO)B}$ and Group $I_{bt(O)B}$), Filtek™ Z250 (Group $J_{bt(NO)B}$ and Group $J_{bt(O)B}$), Filtek™ P60 (Group $K_{bt(NO)B}$ and Group $K_{bt(O)B}$) and Filtek™ Supreme XT (Group $L_{bt(NO)B}$ and Group $L_{bt(O)B}$) of the RBCs (Table 3.5).

3.4.3 LED handheld LCU

3.4.3.1 Elipar™ Freelight ($_{l}$)

The Elipar™ Freelight LED LCU ($_{l}$) irradiated with a 13mm tip diameter required a total of six and four non-overlapped and overlapped Vickers indentations, respectively on the top surface. The data was grouped for each of the RBC materials investigated, namely Z100™ (Group $Q_{l(NO)T}$ and Group $Q_{l(O)T}$), Filtek™ Z250 (Group $R_{l(NO)T}$ and Group $R_{l(O)T}$), Filtek™ P60 (Group $S_{l(NO)T}$ and Group $S_{l(O)T}$) and Filtek™ Supreme XT (Group $T_{l(NO)T}$ and Group $T_{l(O)T}$) for the 13mm tip diameter. For the top surface irradiated with the 8mm tip diameter the data was grouped for each of the RBC materials, namely Z100™ (Group $U_{l(NO)T}$ and Group $U_{l(O)T}$), Filtek™ Z250 (Group $V_{l(NO)T}$ and Group

$V_{l(O)T}$), Filtek™ P60 (Group $W_{l(NO)T}$ and Group $W_{l(O)T}$) and Filtek™ Supreme XT (Group $X_{l(NO)T}$ and Group $X_{l(O)T}$) (Table 3.6).

The Vickers indentation procedure outlined above was repeated on the bottom surface ($_B$) with the 13mm tip diameter (Z100™ (Group $Q_{l(NO)B}$ and Group $Q_{l(O)B}$), Filtek™ Z250 (Group $R_{l(NO)B}$ and Group $R_{l(O)B}$), Filtek™ P60 (Group $S_{l(NO)B}$ and Group $S_{l(O)B}$) and Filtek™ Supreme XT (Group $T_{l(NO)B}$ and Group $T_{l(O)B}$)). Similarly, the 8mm tip diameter data was grouped for each of the RBC materials investigated, namely (Group $U_{l(NO)B}$ and Group $U_{l(O)B}$), Filtek™ Z250 (Group $V_{l(NO)B}$ and Group $V_{l(O)B}$), Filtek™ P60 (Group $W_{l(NO)B}$ and Group $W_{l(O)B}$) and Filtek™ Supreme XT (Group $X_{l(NO)B}$ and Group $X_{l(O)B}$) (Table 3.7).

3.4.3.2 Elipar™ Freelight 2 ($_h$)

The Elipar™ Freelight 2 LED LCU ($_h$) was also used to irradiate the top surface of the rectangular bar-shaped specimens with a 13mm tip diameter. The data was grouped for each of the RBC materials investigated, namely Z100™ (Group $Q_{h(NO)T}$ and Group $Q_{h(O)T}$), Filtek™ Z250 (Group $R_{h(NO)T}$ and Group $R_{h(O)T}$), Filtek™ P60 (Group $S_{h(NO)T}$ and Group $S_{h(O)T}$) and Filtek™ Supreme XT (Group $T_{h(NO)T}$ and Group $T_{h(O)T}$). With the 8mm tip diameter the data was grouped as Z100™ (Group $U_{H(NO)T}$ and Group $U_{H(O)T}$), Filtek™ Z250 (Group $V_{h(NO)T}$ and Group $V_{h(O)T}$), Filtek™ P60 (Group $W_{h(NO)T}$ and Group $W_{h(O)T}$) and Filtek™ Supreme XT (Group $X_{h(NO)T}$ and Group $X_{h(O)T}$) (Table 3.6).

Table 3.6: The non-overlapped and overlapped specimen groups on the top surface when irradiated with the 13 and 8mm tip diameters using the Elipar™ Freelight and Elipar™ Freelight 2 LED LCUs.

RBC	LED LCU	Elipar™ Freelight		Elipar™ Freelight 2	
		13mm	8mm	13mm	8mm
Z100™	Non-overlapped	Group $Q_{l(NO)T}$	Group $U_{l(NO)T}$	Group $Q_{h(NO)T}$	Group $U_{h(NO)T}$
	Overlapped	Group $Q_{l(O)T}$	Group $U_{l(O)T}$	Group $Q_{h(O)T}$	Group $U_{h(O)T}$
Filtek™ Z250	Non-overlapped	Group $R_{l(NO)T}$	Group $V_{l(NO)T}$	Group $R_{h(NO)T}$	Group $V_{h(NO)T}$
	Overlapped	Group $R_{l(O)T}$	Group $V_{l(O)T}$	Group $R_{h(O)T}$	Group $V_{h(O)T}$
Filtek™ P60	Non-overlapped	Group $S_{l(NO)T}$	Group $W_{l(NO)T}$	Group $S_{h(NO)T}$	Group $W_{h(NO)T}$
	Overlapped	Group $S_{l(O)T}$	Group $W_{l(O)T}$	Group $S_{h(O)T}$	Group $W_{h(O)T}$
Filtek™ Supreme XT	Non-overlapped	Group $T_{l(NO)T}$	Group $X_{l(NO)T}$	Group $T_{h(NO)T}$	Group $X_{h(NO)T}$
	Overlapped	Group $T_{l(O)T}$	Group $X_{l(O)T}$	Group $T_{h(O)T}$	Group $X_{h(O)T}$

Table 3.7: The non-overlapped and overlapped specimen groups on the bottom surface when irradiated with the 13 and 8mm tip diameters using the Elipar™ Freelight and Elipar™ Freelight 2 LED LCUs.

RBC	LED LCU	Elipar™ Freelight		Elipar™ Freelight 2	
		13mm	8mm	13mm	8mm
Z100™	Non-overlapped	Group $Q_{l(NO)B}$	Group $U_{l(NO)B}$	Group $Q_{h(NO)B}$	Group $U_{h(NO)B}$
	Overlapped	Group $Q_{l(O)B}$	Group $U_{l(O)B}$	Group $Q_{h(O)B}$	Group $U_{h(O)B}$
Filtek™ Z250	Non-overlapped	Group $R_{l(NO)B}$	Group $V_{l(NO)B}$	Group $R_{h(NO)B}$	Group $V_{h(NO)B}$
	Overlapped	Group $R_{l(O)B}$	Group $V_{l(O)B}$	Group $R_{h(O)B}$	Group $V_{h(O)B}$
Filtek™ P60	Non-overlapped	Group $S_{l(NO)B}$	Group $W_{l(NO)B}$	Group $S_{h(NO)B}$	Group $W_{h(NO)B}$
	Overlapped	Group $S_{l(O)B}$	Group $W_{l(O)B}$	Group $S_{h(O)B}$	Group $W_{h(O)B}$
Filtek™ Supreme XT	Non-overlapped	Group $T_{l(NO)B}$	Group $X_{l(NO)B}$	Group $T_{h(NO)B}$	Group $X_{h(NO)B}$
	Overlapped	Group $T_{l(O)B}$	Group $X_{l(O)B}$	Group $T_{h(O)B}$	Group $X_{h(O)B}$

The Vickers indentation procedure outlined above was repeated on the bottom surface with the 13mm tip diameter and grouped, namely Z100™ (Group $Q_{h(NO)B}$ and Group $Q_{h(O)B}$), Filtek™ Z250 (Group $R_{h(NO)B}$ and Group $R_{H(O)B}$), Filtek™ P60 (Group $S_{H(NO)B}$ and Group $S_{h(O)B}$) and Filtek™ Supreme XT (Group $T_{h(NO)B}$ and Group $T_{h(O)B}$). With an 8mm tip diameter the data was also grouped for each of the RBC materials, namely Z100™ (Group $U_{h(NO)B}$ and Group $U_{h(O)B}$), Filtek™ Z250 (Group $V_{h(NO)B}$ and Group $V_{h(O)B}$), Filtek™ P60 (Group $W_{h(NO)B}$ and Group $W_{h(O)B}$) and Filtek™ Supreme XT (Group $X_{h(NO)B}$ and Group $X_{h(O)B}$) (Table 3.7).

3.5 Statistical analysis

3.5.1 Three-point flexure strength data

Multiple comparisons of the group means for the three-point flexure strength data for each RBC (Z100™, Filtek™ Z250, Filtek™ P60 and Filtek™ Supreme XT), irradiated with varying tip diameters (13, 11, 8 and 25mm for the QTH and 13 and 8mm for the LED) and LCU irradiances in standard and boosted modes were made utilising a one-way ANOVA and Tukey's multiple range tests at a significance level of $P<0.05$. In addition, multiple comparisons of the means for the grouped three-point flexure strength data for the 8mm 'Turbo' and 8mm conventional tip diameters irradiated in standard and boosted mode, for each of the RBCs, were made using a one-way ANOVA and Tukey's multiple range test at a significance level of $P<0.05$.

3.5.2 Reliability of the flexure strength data

Weibull analyses were employed to assess the reliability of the three-point flexure strength data by evaluating the strength distribution in mathematical terms. Weibull (1951) derived an equation which described a distribution of strength data in order to assess the probability with which failure occurs within a material at a given level of applied load. The Weibull equation assumes that the most critical flaw in a specimen is responsible for failure and therefore the Weibull distribution is based on the concept of the failure of the weakest link (Weibull, 1951). The basic form of the Weibull distribution is

$$P_f = 1 - \exp\left[-V\left(\frac{\sigma - \sigma_u}{\sigma_0}\right)^m\right] \qquad \text{Equation 3.4}$$

where σ is the applied stress at failure (MPa), σ_u, σ_o and m are all constants. The threshold stress (σ_u) in MPa is the stress at which the failure probability approaches zero and Davis (1973) and Stanley et al. (1973) demonstrated that for brittle materials σ_u can be assumed to be zero since there is always a finite probability that a critical flaw may be present in the material under investigation before it is stressed. σ_o is normally referred to as the normalising or scaling constant and V is the specimen volume. As the sample size and specimen volume of each RBC material tested in the current investigation remained constant throughout the flexure strength testing, the volume term, V can be ignored. Trustrum and Jayatilaka (1979) gave physical meaning to the Weibull modulus (m) as characterising the 'brittleness' of a material since m describes the flaw size distribution and therefore the resultant scatter and associated reliability of the flexure strength data

(Zeng et al., 1996). A closer grouping of the flexure strength data is manifested as a higher value of m. P_f is the probability of failure, which varies from zero to one

$$P_f = \left(\frac{n}{N^* + 1} \right) \qquad \text{Equation 3.5}$$

where N^* was the total number of specimens and n was the ranking number of the specimen when the flexure strength of the specimen were ranked in ascending order. Consequently, Equation 3.4 can be reduced to the form

$$P_s = 1 - P_f = 1 - \left(1 - \exp\left[- \left(\frac{\sigma}{\sigma_0} \right)^m \right] \right) \qquad \text{Equation 3.6}$$

The flexure strength data was graphically displayed on a Weibull plot by further simplifying Equation 3.6 using natural logarithms to the form y=mx+c (Equation 3.7)

$$\ln \ln \left(\frac{1}{P_s} \right) = m \ln(\sigma) - m \ln(\sigma_0) \qquad \text{Equation 3.7}$$

P_s was the probability of survival (since P_s = 1-P_f), m was the gradient of the graph calculated by superimposing a regression line along the specimen data points and the y-axis intercepted the x-axis at -$m$ln(σ_o) and Ritter et al. (1981) identified that the number of nominally identical specimens used in the calculation of the m for brittle materials determines the accuracy of the Weibull analysis. The standard deviation of the Weibull modulus was calculated and derived from statistical theory (Trustrum and Jayatilaka, 1979) to be a function of the sample size (N)

$$\text{Standard deviation } (m) = \frac{m}{\sqrt{N}} \qquad \text{Equation 3.8.}$$

Statistically significant differences in the Weibull modulus between groups were considered to be significant when the 95% confidence intervals did not overlap (Fleming, 1998).

3.5.3 Three-point flexure modulus data

Multiple comparisons of the group means for the three-point flexure modulus data for each RBC (Z100™, Filtek™ Z250, Filtek™ P60 and Filtek™ Supreme XT), irradiated with varying tip diameters (13, 11, 8 and 25mm for the QTH and 13 and 8mm for the LED) and LCU irradiances in standard and boosted modes were made utilising a one-way ANOVA and Tukey's multiple range tests at a significance level of $P<0.05$. In addition, multiple comparisons of the means for the grouped three-point flexure modulus data for the 8mm 'Turbo' and 8mm conventional tip diameters irradiated in standard and boosted mode, for each of the RBCs, were made using a one-way ANOVA and Tukey's multiple range test at a significance level of $P<0.05$.

3.5.4 Vickers hardness data

The analysis of the Vickers hardness data was dependent on the fact that the design was intrinsically unbalanced in respect of site (actual location of the measurement) and region (non-overlapped and overlapped), the numbers of these categories being determined by the tip diameter size. Therefore for the QTH LCU, with the 8 mm tip diameter there were five non-overlapped and four overlapped regions, the 11mm tip diameter there were four

non-overlapped and three overlapped regions, the 13mm tip diameter there were three non-overlapped and two overlapped regions and the 25mm tip there were no overlapped regions. For the LED LCUs, with the 8mm tip diameter there were five non-overlapped and four overlapped regions and the 13mm tip diameter there were three non-overlapped and two overlapped regions. A progressive pooling of the design was therefore used to reduce the dimensionality of the problem by eliminating non-significant classificatory variables.

A two-way ANOVA design using site × region as the independent variables were checked to ensure that no site effect emerged within each RBC for both top and bottom surfaces. A three-way ANOVA were performed on each RBC using tip diameter (13, 11, 8 and 25mm), surface (top and bottom) and region (non-overlapped and overlapped) as the independent variables.

CHAPTER 4 Results

4.1 ISO4049: The influence of LCU tip diameter

The efficacy of the overlapping irradiation regime was investigated by modifying the specimen manufacture protocol in ISO 4049: 2000 to exacerbate the potential for uncontrolled initiation on polymerisation and decrease the homogeneity of polymerisation along the length of the specimen.

QTH Irradiance

When an assessment of the irradiance of the QTH LCU was measured seven consecutive times with tip diameters of 13, 11, 8 and 25mm using the radiometer, irradiances of 640 ± 18mW/cm^2 in standard mode and 790 ± 18mW/cm^2 in boosted mode were recorded. In addition, when an 8mm 'Turbo' tip diameter was used in standard and boosted modes the irradiances were 880 ± 18 and 1040 ± 28mW/cm^2, respectively.

4.1.1 Three-point flexure strength

4.1.1.1 Standard mode

When the 13mm LCU tip diameter was employed the mean three-point flexure strength and associated standard deviation for Z100™ (Group A_s) were 93 ± 14MPa with a range of three-point flexure strengths varying from 74 to 121MPa. When Filtek™ Z250,

Filtek™ P60 and Filtek™ Supreme XT were tested following irradiation with the 13mm tip diameter, the mean three-point flexure strengths and associated standard deviations were 156 ± 15MPa (Group B_s), 162 ± 16MPa (Group C_s), 140 ± 10MPa (Group D_s), respectively. The range of the three-point flexure strengths for Filtek™ Z250, Filtek™ P60 and Filtek™ Supreme XT varied from a low of 128MPa to a high of 180MPa for Group B_s specimens, from 126 to 184MPa for Group C_s specimens and from a minimum of 108MPa to a maximum of 157MPa for Group D_s specimens (Table 4.1).

Employing the overlapping irradiation regime with an 11mm tip diameter resulted in a range of the three-point flexure strengths for Z100™ (Group E_s) from 79 to 122MPa, Filtek™ Z250 (Group F_s) from a minimum of 133MPa to a maximum of 180MPa, Filtek™ P60 (Group G_s) from 125 to 185MPa and Filtek™ Supreme XT (Group H_s) from a low of 125MPa to a high of 185MPa. The mean three-point flexure strengths and associated standard deviations for the four RBC materials investigated, namely Z100™, Filtek™ Z250, Filtek™ P60 and Filtek™ Supreme XT were 99 ± 14MPa, 151 ± 14MPa, 154 ± 16MPa and 141 ± 10MPa, respectively (Table 4.1).

With an 8mm tip diameter the range of the three-point flexure strengths varied for Z100™ from a minimum of 78MPa to a maximum of 131MPa (Group I_s), Filtek™ Z250 from 141 to 189MPa (Group J_s), Filtek™ P60 from a minimum of 127MPa to a maximum of 186MPa (Group K_s) and Filtek™ Supreme XT from a lowest recorded strength of 120MPa to a highest recorded strength of 158MPa (Group L_s), respectively. The mean three-point flexure strengths and associated standard deviations were 103 ±

Table 4.1: The range and mean three-point flexure strengths (associated standard deviations) for the RBC specimens irradiated using a QTH LCU with 8, 11, 13 and 25 mm tip diameters using the QTH LCU in standard and boosted modes.

RBC	Property	Mode	Tip Diameter			
			8mm	11mm	13mm	25mm
Z100™	Three-point flexure strength (MPa)	Standard	101 (16)	99 (14)	93 (14)	104 (15)
	Range of strengths (MPa)		78-131	79-122	74-121	76-135
	Three-point flexure strength (MPa)	Boosted	101 (16)	93 (15)	95 (14)	105 (16)
	Range of strengths (MPa)		76-130	75-122	75-119	79-141
Filtek™ Z250	Three-point flexure strength (MPa)	Standard	164 (16)	152 (14)	156 (15)	157 (15)
	Range of strengths (MPa)		141-189	133-180	128-180	122-179
	Three-point flexure strength (MPa)	Boosted	154 (15)	153 (14)	156 (15)	156 (15)
	Range of strengths (MPa)		137-190	124-184	126-182	123-176
Filtek™ P60	Three-point flexure strength (MPa)	Standard	165 (16)	154 (16)	162 (16)	165 (17)
	Range of strengths (MPa)		127-186	125-185	126-184	128-184
	Three-point flexure strength (MPa)	Boosted	164 (16)	161 (16)	164 (15)	154 (13)
	Range of strengths (MPa)		136-189	128-184	124-186	129-172
Filtek™ Supreme XT	Three-point flexure strength (MPa)	Standard	140 (10)	141 (10)	140 (10)	133 (12)
	Range of strengths (MPa)		120-158	124-158	108-157	115-154
	Three-point flexure strength (MPa)	Boosted	142 (9)	141 (12)	140 (12)	133 (9)
	Range of strengths (MPa)		129-158	120-155	123-157	105-145

15MPa (Group I_s), 164 ± 16MPa (Group J_s), 165 ± 16MPa (Group K_s) and 140 ± 10MPa (Group L_s) (Table 4.1). The mean three-point flexure strengths and associated standard deviations for a 'one-hit' irradiation for Z100™, Filtek™ Z250, Filtek™ P60 and Filtek™ Supreme XT were 104 ± 15MPa (Group M_s), 157 ± 15MPa (Group N_s), 165 ± 17MPa (Group O_s) and 133 ± 12Pa (Group P_s), respectively. The range of three-point flexure strengths varied for Z100™ from a minimum of 76MPa to a maximum of 135MPa, Filtek™ Z250 from 128 to 180MPa, Filtek™ P60 from a low of 128MPa to a high of 184MPa and Filtek™ Supreme XT from a minimum recorded value of 115MPa to a maximum recorded value of 155MPa (Table 4.1).

4.1.1.1.1 Statistical analysis: Standard mode: tip diameter

Multiple comparisons of the group means for the three-point flexure strength data for each RBC (Z100™, Filtek™ Z250, Filtek™ P60 and Filtek™ Supreme XT), irradiated with varying tip diameters (13, 11, 8 and 25mm, respectively) at 640 ± 18mW/cm^2, were made utilising a one-way ANOVA and Tukey's multiple range tests at a significance level of $P<0.05$. No significant differences in the group means of the three-point flexure strengths were identified for Z100™ when irradiated with the varying tip diameters (13, 11, 8 and 25mm) utilising the one-way ANOVA (F value=1.944; P=0.130). When the group means of the three-point flexure strengths for Filtek™ Z250 were analysed no significant differences in the one-way ANOVA (F value=2.302; P=0.840) were evident with varying tip diameters. The group means of the three-point flexure strengths with varying tip diameters highlighted no significant differences for Filtek™ P60 and Filtek™

Supreme XT utilising the one-way ANOVA (F value=1.924; P=0.133 and F value=2.582; P=0.600, respectively).

4.1.1.2 Boosted mode

With a 13mm tip diameter the mean three-point flexure strengths and associated standard deviations for Z100™ (Group A_b) were 95 ± 14MPa, Filtek™ Z250 (Group B_b) were 156 ± 15MPa, Filtek™ P60 (Group C_b) were 164 ± 15MPa and Filtek™ Supreme XT (Group D_b) were 140 ± 12MPa. The range of three-point flexure strengths varied from a low of 78MPa to a high of 131MPa for Group A_b specimens, from a minimum of 141MPa to a maximum of 189MPa for Group B_b specimens, from 127 to 186MPa for Group C_b specimens and from a low of 120MPa to a high of 158MPa for Group D_b specimens, respectively.

For the 11mm tip diameter required four overlapping irradiations on the top surface. The mean three-point flexure strength and associated standard deviations for Z100™ (Group E_b) were 93 ± 15MPa, Filtek™ Z250 (Group F_b) were 153 ± 14MPa, Filtek™ P60 (Group G_b) were 161 ± 16MPa and Filtek™ Supreme XT (Group H_b) were 141 ± 12MPa. The range of three-point flexure strengths varied from a low of 75MPa to a high of 119MPa for Group E_b specimens, from 126 to 182MPa for Group F_b specimens, from a minimum of 124MPa to a maximum of 186MPa for Group G_b specimens and from 123 to 157MPa for Group H_b specimens.

When the 8mm tip diameter was used the mean three-point flexure strengths and associated standard deviations for Z100™ (Group I_b) were 101 ± 16MPa, for Filtek™ Z250 (Group J_b) were 154 ± 15MPa, for Filtek™ P60 (Group K_b) were 164 ± 16MPa and for Filtek™ Supreme XT (Group L_b) were 142 ± 9MPa. The range of three-point flexure strengths varied from a maximum of 76MPa to a minimum of 130MPa for Group I_b specimens, from 137MPa to 190MPa for Group J_b specimens, a low of 136MPa to a high of 189MPa for Group K_b specimens and from 129 to 158MPa for Group L_b specimens, respectively.

The 'one-hit' irradiation resulted in three-point flexure strengths from a low of 79MPa to a high of 141MPa for Z100™ (Group M_b), from 123 to 176MPa for Filtek™ Z250 (Group N_b), from a minimum of 129MPa to a maximum of 172MPa for Filtek™ P60 (Group O_b) and from 105 to 145MPa for Filtek™ Supreme XT (Group P_b). The mean three-point flexure strength and associated standard deviation were 105 ± 16MPa for Group M_b specimens, 156 ± 15MPa for Group N_b specimens, 154 ± 13MPa for Group O_b specimens and 133 ± 9MPa for Group P_b specimens, respectively.

4.1.1.2.1 Statistical analysis: Boosted mode: tip diameter

A one-way ANOVA and Tukey's multiple range test at a significance level of $P<0.05$ were used to make multiple comparisons of the group means for the three-point flexure strength data for each of the RBC materials investigated (Z100™, Filtek™ Z250, Filtek™ P60 and Filtek™ Supreme XT) with tip diameters of 13, 11, 8 and 25mm using the

Optilux 501 LCU operating at an irradiance of 790 ± 18mW/cm^2. For Z100™, no significant differences in the group means of the three-point flexure strengths were identified when irradiated with tip diameters of 13mm (Group A_b), 11mm (Group E_b), 8mm (Group I_b) and 25mm (Group M_b) utilising the one-way ANOVA (F value=2.422; P=0.720). Analysis of the group means of the three-point flexure strengths for Filtek™ Z250 following irradiation with tip diameters of 13mm (Group B_b), 11mm (Group F_b), 8mm (Group J_b) and 25mm (Group N_b) resulted in no significant differences in the one-way ANOVA (F value=0.217; P=0.884). Filtek™ P60 rectangular bar-shaped specimens irradiated with a tip diameters of 13mm (Group C_b), 11mm (Group G_b), 8mm (Group K_b) and 25mm (Group O_b) identified no significant differences in the group means of the three-point flexure strengths when utilising the one-way ANOVA (F value=1.884; P=0.139). Analysis following irradiation of the Filtek™ Supreme XT specimens with tip diameters of 13mm (Group D_b), 11mm (Group H_b), 8mm (Group L_b) and 25mm (Group P_b) revealed no significant differences in the group means of the three-point flexure strengths with the one-way ANOVA (F value=2.976; P=0.370).

4.1.1.3 Grouped data (standard and boosted mode)

Multiple comparisons of the group means for the three-point flexure strength data for the tip diameters, irradiated in standard and boosted modes, for each of the RBCs investigated, were made using a one-way ANOVA and Tukey's multiple range test at a significance level of $P<0.05$. Analysis of the grouped means of the three-point flexure strength data for Z100™ revealed no significant differences with the one-way ANOVA

(F value=2.503; P=0.066). Analysis of the group means of the three-point flexure strength data for Filtek™ Z250 resulted in no significant differences in the one-way ANOVA (F value=1.426; P=0.242). For Filtek™ P60, no significant differences in the group means of the three-point flexure strength data were identified utilising the one-way ANOVA (F value=2.546; P=0.062). Filtek™ Supreme XT also showed that analysis of the group means of the three-point flexure strength data identified no significant differences when utilising the one-way ANOVA (F value=0.745; P=0.529).

4.1.2 Reliability of fracture strength data

4.1.2.1 Standard mode

Weibull analyses of the three-point flexure strength data were performed on the groups of 20 rectangular bar-shaped specimens for each of the RBC materials investigated. The Weibull moduli and associated standard deviations for Z100™ specimens irradiated with tip diameters of 13mm (Group A_s), 11mm (Group E_s), 8mm (Group I_s) or 25mm (Group M_s) were 7.2 ± 1.6, 7.6 ± 1.7, 7.1 ± 1.6 and 7.5 ± 1.7, respectively. The 95% confidence intervals of the Weibull moduli varied from a minimum of 6.2 to a maximum of 8.2 for Group A_s specimens, from 6.5 to 8.6 for Group E_s specimens, from a minimum of 6.1 to a maximum of 8.0 for Group I_s specimens and from a lowest value of 6.9 to a highest of 8.1 for Group M_s specimens. There was no significant difference in the Weibull moduli of the three-point flexure strength data for Z100™ as the 95% confidence intervals overlapped (Table 4.2). The Weibull analysis for Filtek™ Z250 specimens produced

Weibull moduli and associated standard deviations with tip diameters of 13mm (Group B_s) of 10.9 ± 2.4, 11mm (Group F_s) of 10.9 ± 2.4, 8mm (Group J_s) of 10.4 ± 2.3 and 25mm (Group N_s) of 10.9 ± 2.4. The associated 95% confidence intervals ranged from a minimum of 10.0 to a maximum of 11.8 for Group B_s specimens, from 8.6 to 13.2 for Group F_s specimens, from a low of 8.7 to a high of 12.0 for Group J_s specimens and from a minimum of 10.4 to a maximum of 11.4 for Group N_s specimens. The Weibull moduli of Filtek™ Z250 (Group B_s, Group F_s, Group J_s, Group N_s) were considered to be non-significant since the 95% confidence intervals overlapped (Table 4.2). The Weibull moduli and associated standard deviations for the series of Filtek™ P60 specimens irradiated using tip diameters of 13, 11, 8 and 25mm were 10.7 ± 2.4 for Group C_s specimens, 10.6 ± 2.4 for Group G_s specimens, 10.7 ± 2.4 for Group K_s specimens and 9.6 ± 2.1 for Group O_s specimens, respectively. The regression analysis of the three-point flexure strength data resulted in 95% confidence intervals which ranged from a low of 9.6 to a high of 11.9 (Group C_s), from 9.5 to 11.6 (Group G_s), from a minimum of 9.9 to a maximum of 11.4 (Group K_s) and from a minimum of 8.5 to a maximum of 10.7 (Group O_s). The 95% confidence intervals of Filtek™ P60 specimens overlapped and therefore the Weibull moduli were considered to be non-significant (Table 4.2). The Weibull analysis of the three-point flexure strength data of Filtek™ Supreme XT produced Weibull moduli and associated standard deviations for the groups irradiated with tip diameters of 13mm (Group D_s) of 13.0 ± 2.9, 11mm (Group H_s) of 14.1 ± 3.2, 8mm (Group L_s) of 14.2 ± 3.2 and 25mm (Group P_s) of 11.9 ± 2.7. The 95% confidence intervals varied from a low of 10.3 to a high of 15.7 for Group D_s specimens, from a minimum of 12.2 to a maximum of 16.0 for Group H_s specimens, from 12.9 to 15.6 for

Table 4.2: The Weibull moduli and 95% confidence intervals for the RBC specimens irradiated using a QTH LCU with 8, 11, 13 and 25 mm tip diameters using the QTH LCU in standard and boosted modes.

RBC	Property	Mode	Tip Diameter			
			8mm	11mm	13mm	25mm
Z100™	Weibull modulus	Standard	7.1 (1.6)	7.6 (1.7)	7.2 (1.6)	7.5 (1.7)
	95% Confidence Intervals		6.1-8.0	6.5-8.6	6.2-8.2	6.9-8.1
	Weibull modulus	Boosted	6.5 (1.5)	6.3 (1.4)	6.7 (1.5)	7.1 (1.6)
	95% Confidence Intervals		5.8-7.2	5.0-7.6	5.7-7.8	6.3-7.8
Filtek™ Z250	Weibull modulus	Standard	10.4 (2.3)	10.9 (2.4)	10.9 (2.4)	10.9 (2.4)
	95% Confidence Intervals		8.7-12.0	8.6-13.2	10.0-11.8	10.4-11.4
	Weibull modulus	Boosted	10.5 (2.4)	11.2 (2.7)	10.6 (2.4)	10.9 (2.4)
	95% Confidence Intervals		8.0-13.0	10.0-12.5	9.8-11.3	10.2-11.5
Filtek™ P60	Weibull modulus	Standard	10.7 (2.4)	10.6 (2.4)	10.7 (2.4)	9.6 (2.1)
	95% Confidence Intervals		9.9-11.4	9.5-11.6	9.6-11.9	8.5-10.7
	Weibull modulus	Boosted	10.8 (2.4)	10.3 (2.3)	10.7 (2.4)	11.9 (2.7)
	95% Confidence Intervals		9.3-12.3	9.3-11.2	9.6-11.9	10.8-13.1
Filtek™ Supreme XT	Weibull modulus	Standard	14.2 (3.2)	14.1 (3.2)	13.0 (2.9)	11.9 (2.7)
	95% Confidence Intervals		12.9-15.6	12.2-16.0	10.3-15.7	10.5-13.3
	Weibull modulus	Boosted	15.8 (3.5)	12 (2.7)	11.6 (2.6)	13.6 (3.0)
	95% Confidence Intervals		13.2-18.3	10.4-13.6	9.6-13.6	10.1-17.2

Group L_s specimens and from a low of 10.5 to a high of 13.3 for Group P_s specimens. Since the confidence intervals of Filtek™ Supreme XT specimen groups, (Group D_s, Group H_s, Group L_s, Group P_s) overlapped the Weibull moduli were considered to be not significant (Table 4.2).

4.1.2.2 Boosted mode

The three-point flexure strength data for each of the RBC materials investigated were also subjected to Weibull analyses. The irradiation of Z100™ specimens using tip diameters 13, 11, 8 and 25mm resulted in Weibull moduli and associated standard deviations of 6.7 ± 1.5 for Group A_b specimens, 6.3 ± 1.4 for Group E_b specimens, 6.5 ± 1.5 for Group I_b specimens and 7.1 ± 1.6 Group M_b specimens, respectively (Table 4.2). The 95% confidence intervals calculated from regression analysis of the three-point flexure strength data ranged for Group A_b specimens from a minimum of 5.7 to a maximum of 7.8, for Group E_b specimens from 5.0 to 7.6, for Group I_b specimens from a low of 5.8 to a high of 7.2 and for Group M_b specimens from a minimum recorded value of 6.3 to a maximum recorded value of 7.8. As the 95% confidence intervals of the three-point flexure strength data of the Z100™ specimens overlapped, each associated Weibull moduli were therefore not significantly different. Filtek™ Z250 specimens resulted in Weibull moduli and associated standard deviations of 10.6 ± 2.4, 11.2 ± 2.7, 10.5 ± 2.4 and 10.9 ± 2.4 for Group B_b, Group F_b, Group J_b and Group N_b specimens, respectively (Table 4.2). The 95% confidence intervals ranged from a low of 9.8 to a high of 11.3 for Group B_b specimens, from 10.0 to 12.5 for Group J_b specimens, from a minimum of 8.0

to a maximum of 13.0 for Group J_b specimens and from 10.2 to 11.5 for Group N_b specimens. The associated Weibull moduli of Filtek™ Z250 specimens were considered to be non-significant since the 95% confidence intervals overlapped for the groups investigated, namely Group B_b, Group F_b, Group J_b and Group N_b. The Weibull analysis of Filtek™ P60 specimens resulted in Weibull moduli and associated standard deviations for Group C_b, Group G_b, Group K_b and Group O_b specimens of 10.7 ± 2.4, 10.3 ± 2.3, 10.8 ± 2.4 and 11.9 ± 2.7, respectively (Table 4.2). The lower and upper 95% confidence intervals ranged for Group C_b specimens from 9.6 to 11.9, for Group G_b specimens from a minimum of 9.3 to a maximum of 11.2, for Group K_b specimens from 9.3 to 12.3 and for Group O_b specimens from a low of 10.8 to a high of 13.1. The associated Weibull moduli of the three-point flexure strength data for Filtek™ P60 specimens were considered to be non-significant since the 95% confidence intervals overlapped. The irradiation of Filtek™ Supreme XT specimens produced Weibull moduli and associated standard deviations for Group D_b of 11.6 ± 2.6, Group H_b of 12.0 ± 2.7, Group L_b of 15.8 ± 3.5 and Group P_b of 13.6 ± 3.0 (Table 4.2). The associated 95% confidence intervals were reported to ranged from a minimum of 9.6 to a maximum of 13.6 for Group D_b specimens, from 10.4 to 13.6 for Group H_b specimens, from a low of 13.2 to a high of 18.3 for Group L_b specimens and from a minimum recorded value of 10.1 to a maximum recorded value of 17.2 for Group P_b specimens. The 95% confidence intervals of the Weibull moduli for Filtek™ Supreme XT specimens groups, namely Group D_b, Group H_b, Group L_b, Group P_b overlapped indicating no significant differences.

4.1.3 Three-point flexure modulus testing

4.1.3.1 Standard mode

When employing the 13mm tip diameter the mean three-point flexure moduli and associated standard deviations for Z100™, Filtek™ Z250, Filtek™ P60 and Filtek™ Supreme XT were 14.4 ± 1.6GPa for Group A_s specimens, 10.8 ± 0.8GPa for Group B_s specimens, 12.4 ± 1.5GPa for Group C_s specimens and 9.6 ± 0.8GPa for Group D_s specimens, respectively. The range of the three-point flexure moduli varied for Z100™ from a minimum of 12GPa to a maximum of 18GPa (Group I_s), for Filtek™ Z250 from 10 to 12GPa (Group J_s), for Filtek™ P60 from a minimum of 8GPa to a maximum of 14GPa (Group K_s) and for Filtek™ Supreme XT from a lowest recorded flexure modulus of 9GPa to a highest flexure modulus of 11GPa (Group L_s), respectively (Table 4.3).

When Z100™ (Group E_s), Filtek™ Z250 (Group F_s), Filtek™ P60 (Group G_s) and Filtek™ Supreme XT (Group H_s) were irradiated with an 11mm tip diameter the mean three-point flexure moduli and associated standard deviations were 14.8 ± 1.6GPa, 11.0 ± 1.0GPa, 11.2 ± 0.9GPa, 10.2 ± 0.9GPa, respectively. The range of the three-point flexure moduli varied from a low of 11GPa to a high of 18GPa for group E_s specimens, from a minimum of 9GPa to a maximum of 13GPa for Group F_s specimens, from 9 to 13GPa for group G_s specimens and from a minimum of 9GPa to a maximum of 12GPa for group H_s specimens, respectively (Table 4.3).

Table 4.3: The range and mean three-point flexure moduli (associated standard deviations) for the RBC specimens irradiated using a QTH LCU with 8, 11, 13 and 25 mm tip diameters using the QTH LCU in standard and boosted modes.

RBC	Property	Mode	Tip Diameter			
			8mm	11mm	13mm	25mm
Z100™	Three-point flexure modulus (GPa)	Standard	13.6 (1.7)	14.8 (1.6)	14.4 (1.6)	14.9 (1.5)
	Range of moduli (GPa)		9-16	11-18	12-18	13-20
	Three-point flexure modulus (GPa)	Boosted	14.3 (1.5)	14.7 (1.5)	14.2 (1.0)	13.6 (1.3)
	Range of moduli (GPa)		12-19	12-18	13-16	10-17
Filtek™ Z250	Three-point flexure modulus (GPa)	Standard	11.4 (1.3)	11.0 (1.0)	10.8 (0.8)	10.8 (1.4)
	Range of moduli (GPa)		9-13	9-13	10-12	7-13
	Three-point flexure modulus (GPa)	Boosted	11.9 (0.8)	11.4 (0.6)	11.4 (1.1)	10.9 (1.7)
	Range of moduli (GPa)		10-13	10-13	10-14	7-13
Filtek™ P60	Three-point flexure modulus (GPa)	Standard	12.2 (1.0)	11.2 (0.9)	12.4 (1.5)	12.2 (0.9)
	Range of moduli (GPa)		11-15	9-13	8-14	11-15
	Three-point flexure modulus (GPa)	Boosted	12.0 (0.9)	11.6 (1.0)	11.5 (1.2)	11.5 (1.3)
	Range of moduli (GPa)		10-13	10-14	10-14	9-13
Filtek™ Supreme XT	Three-point flexure modulus (GPa)	Standard	10.0 (0.8)	10.2 (0.9)	9.6 (0.8)	9.5 (1.1)
	Range of moduli (GPa)		8-11	9-12	9-11	7-11
	Three-point flexure modulus (GPa)	Boosted	10.3 (0.7)	9.7 (0.6)	9.5 (1.0)	9.6 (0.9)
	Range of moduli (GPa)		8-11	8-11	8-11	8-11

The 8mm tip diameter resulted in three-point flexure moduli for Z100™ (Group A_s) varying from 9 to 16GPa, Filtek™ Z250 (Group B_s) from a minimum of 9GPa to a maximum of 13GPa, Filtek™ P60 (Group C_s) from 11 to 15GPa and Filtek™ Supreme XT (Group D_s) from a low of 8GPa to a high of 11GPa. The mean three-point flexure moduli and associated standard deviations for Z100™ (Group I_s) were 13.6 ± 1.7GPa, for Filtek™ Z250 (Group J_s) were 11.4 ± 1.3GPa, for Filtek™ P60 (Group K_s) were 12.2 ± 1.0GPa and for Filtek™ Supreme XT (Group L_s) were 10.0 ± 0.8GPa, respectively (Table 4.3).

With the custom made fibre optic light guide the range of three-point flexure moduli varied for Z100™ (Group M_s) from a minimum of 13GPa to a maximum of 20GPa, Filtek™ Z250 (Group N_s) from 7 to 13GPa, Filtek™ P60 (Group O_s) from a low of 11GPa to a high of 15GPa and Filtek™ Supreme XT (G roup P_s) from a minimum recorded value of 7GPa to a maximum recorded value of 11GPa. The mean three-point flexure moduli and associated standard deviations for the RBC materials Z100™ (Group M_s) were 14.9 ± 1.5GPa, for Filtek™ Z250 (Group N_s) were 10.8 ± 1.4GPa, for Filtek™ P60 (Group O_s) were 12.2 ± 0.9GPa and for Filtek™ Supreme XT (Group P_s) were 9.5 ± 1.1GPa, respectively (Table 4.3).

4.1.3.1.1 Statistical analysis: Standard mode: tip diameter

For each of the RBC materials multiple comparisons of the group means for the three-point flexure modulus data were made utilising a one-way ANOVA and Tukey's multiple

range tests at a significance level of $P<0.05$ irradiated at 640 ± 18mW/cm^2 (standard mode) with varying tip diameters of 13, 11, 8 and 25mm. When the group means of the three-point flexure modulus data for Z100™ were analysed no significant differences in the one-way ANOVA (F value=2.885; P=0.041) were evident. On irradiation of Filtek™ Z250 with varying tip diameters (13, 11, 8 and 25) the group means of the three-point flexure modulus data identified no significant differences utilising the one-way ANOVA (F value=1.098; P=0.355). In addition, no significant differences in the group means of the three-point flexure modulus data were identified for Filtek™ P60 when utilising the one-way ANOVA (F value=5.427; P=0.200). Similarly, when the group means of the three-point flexure modulus data for Filtek™ Supreme XT were analysed no significant differences in t he one-way ANOVA (F value=2.486; P=0.067) regardless of the tip diameter (13, 11, 8 and 25mm).

4.1.3.2 Boosted mode

The mean three-point flexure moduli and associated standard deviations for the RBC materials investigated with the 13mm tip diameter were 14.2 ± 1.0GPa for Group A_b specimens, 11.4 ± 1.1GPa for Group B_b specimens, 11.5 ± 1.2GPa for Group C_b specimens and 9.5 ± 1.0GPa for Group D_b specimens, respectively. The range of three-point flexure modulus data varied from a minimum of 13GPa to a maximum of 16GPa for Group A_b specimens, from 10 to 14GPa for Group B_b specimens, from a low of 10GPa to a high of 14GPa for Group C_b specimens and from 8 to 11GPa for Group D_b specimens, respectively (Table 4.3).

When the 11mm tip diameter was employed the range of three-point flexure moduli for the four RBC materials varied from a low of 12GPa to a high of 18GPa for Group E_b specimens, from a minimum of 10GPa to a maximum of 13GPa for Group F_b specimens, from 10 to 14GPa for Group G_b specimens and from a low of 8GPa to a high of 11GPa for Group H_b specimens, respectively. The mean three-point flexure moduli and associated standard deviation for Z100™ (Group E_b) were 14.7 ± 1.5GPa, Filtek™ Z250 (Group F_b) were 11.4 ± 0.6GPa, Filtek™ P60 (Group G_b) were 11.6 ± 1.0GPa and Filtek™ Supreme XT (Group H_b) were 9.7 ± 0.6GPa, respectively (Table 4.3).

With the 8mm tip diameter the mean three-point flexure moduli and associated standard deviation for Z100™ (Group I_b) were 14.3 ± 1.5GPa, Filtek™ Z250 (Group J_b) were 11.9 ± 0.8GPa, Filtek™ P60 (Group K_b) were 12.0 ± 0.9GPa and Filtek™ Supreme XT (Group L_b) were 10.3 ± 0.7GPa. The range of three-point flexure moduli varied from a low of 12GPa to a high of 19GPa for Group I_b specimens, from 10 to 13GPa for Group J_b specimens, from a minimum of 10GPa to a maximum of 13GPa for Group J_b specimens and from 8 to 11GPa for Group L_b specimens, respectively (Table 4.3).

The'one-hit' irradiation of the entire specimen resulted in a range of three-point flexure modulus data varying from a low of 10GPa to a high of 17GPa for Z100™ (Group M_b), from 7 to 13GPa for Filtek™ Z250 (Group N_b), from a minimum of 9GPa to a maximum of 13GPa for Filtek™ P60 (Group O_b) and from 8 to 11GPa for Filtek™ Supreme XT (Group P_b) (Table 4.3). The mean three-point flexure moduli and associated standard deviations were 13.6 ± 1.3GPa for Group M_b specimens, 10.9 ± 1.7GPa for Group N_b

specimens, 11.5 ± 1.3GPa for Group O_b specimens, and 9.6 ± 0.9GPa for Group P_b specimens, respectively.

4.1.3.2.1 Statistical analysis: Boosted mode: tip diameter

A one-way ANOVA and Tukey's multiple range tests at a significance level of $P<0.05$ was used to make multiple comparisons of the group means for the three-point flexure modulus data for each of the RBC materials irradiated in boosted mode at an irradiance of 790 ± 18mW/cm^2 with varying tip diameters of 13, 11, 8 and 25mm. Analysis of the group means of the three-point flexure modulus data for Z100™ following irradiation with varying tip diameters (13, 11, 8 and 25mm showed no significant differences in the one-way ANOVA (F value=2.148; P=0.101). The group means of the three-point flexure modulus data for Filtek™ Z250 indicated no significant differences when irradiated with tip diameters of 13, 11, 8 and 25mm by employing the one-way ANOVA (F value=2.919; P=0.085). Irradiation of Filtek™ P60 with varying tip diameters (13, 11, 8 and 25mm) identified no significant differences in the group means of the three-point flexure modulus data when using the one-way ANOVA (F value=0.909; P=0.441). No significant differences of the group means of the three-point flexure modulus d ata for Filtek™ Supreme XT were evident when irradiated with the tip diameters of 13, 11, 8 and 25mm when using the one-way ANOVA (F value=2.668; P=0.054).

4.1.3.3 Grouped data (standard and boosted mode)

Multiple comparisons of the grouped means for the three-point flexure modulus data for the tip diameters investigated, irradiated in standard and boosted mode, for each of the RBC materials, were made using a one-way ANOVA and Tukey's multiple range test at a significance level of $P<0.05$. Analysis of the grouped means of the three-point flexure modulus data for Z100™ revealed no significant differences with the one-way ANOVA (F value=2.355; P=0.260). Analysis of the group means of the three-point flexure modulus data for Filtek™ Z250 resulted in no significant differences in the one-way ANOVA (F value=2.120; P=0.450). For Filtek™ P60, no significant differences in the group means of the three-point flexure modulus data were identified utilising the one-way ANOVA (F value=2.283; P=0.310). Filtek™ Supreme XT showed that analysis of the group means of the three-point flexure modulus data identified no significant differences when utilising the one-way ANOVA (F value=2.212; P=0.360).

4.1.4 Vickers hardness testing

Vickers hardness measurements were made to investigate the influence of the overlapping irradiation regime on rectangular bar-shaped specimens with uncontrolled initiation on polymerisation (Mehl et al., 1997; Manhart et al., 2000), non-homogeneously cured specimens (Ferracane et al., 2003) and inconsistent polymerisation along the length of the bar-shaped specimen (Palin et al., 2003, 2005) since certain areas would receive twice the irradiance (overlapped) than the adjacent region (non-overlapped).

4.1.4.1 Standard mode

4.1.4.1.1 Top

When the top surface was irradiated with a 13mm tip diameter the mean Vickers hardness and associated standard deviations of the non-overlapped region of Z100™, Filtek™ Z250, Filtek™ P60 and Filtek™ Supreme XT were 101.6 ± 1.9, 80.7 ± 0.8, 85.2 ± 1.4 and 72.1 ± 1.6, respectively. For the overlapped region, the mean Vickers hardness and associated standard deviations for Z100™ were 102.0 ± 1.2, Filtek™ Z250 were 80.7 ± 0.9, Filtek™ P60 were 84.5 ± 1.0 and Filtek™ Supreme XT were 70.9 ± 1.8. (Table 4.4)

Following irradiation with an 11mm tip diameter the mean Vickers hardness and associated standard deviations of the non-overlapped region for Z100™, Filtek™ Z250, Filtek™ P60 and Filtek™ Supreme XT were 101.3 ± 4.1, 80.8 ± 1.0, 85.8 ± 1.9 and 71.1 ± 1.2, respectively. For the overlapped region the mean Vickers hardness and associated standard deviations were 101.4 ± 3.2 (Z100™), 80.6 ± 0.8 (Filtek™ Z250), 85.9 ± 1.8 (Filtek™ P60) and 71.1 ± 1.6 (Filtek™ Supreme XT), respectively (Table 4.4).

Irradiation with the 8mm tip diameter resulted in the mean Vickers hardness and associated standard deviations of the non-overlapped region of 100.1 ± 2.3 for Z100™, 79.8 ± 1.1 for Filtek™ Z250, 84.7 ± 0.8 for Filtek™ P60 specimens and 71.1 ± 2.5 for Filtek™ Supreme XT. For the overlapped region on the top surface the mean Vickers hardness and associated standard deviations for Z100™ were 100.1 ± 1.4, Filtek™ Z250

were 79.8 ± 1.1, Filtek™ P60 were 84.8 ± 0.9 and Filtek™ Supreme XT were 71.1 ± 2.4 (Table 4.4).

When the custom made fibre optic light guide was employed to irradiate the RBCs, the mean Vickers hardness and associated standard deviations of the non-overlapped region for the RBC materials Z100™, Filtek™ Z250, Filtek™ P60 and Filtek™ Supreme XT were 99.2 ± 5, 79.5 ± 4.2, 85.3 ± 2.8 and 70.5 ± 2.5, respectively (Table 4.4).

4.1.4.1.2 Bottom

For the non-overlapped region on the bottom surface the mean Vickers hardness and associated standard deviations following irradiation with a 13mm tip diameter were 97.9 ± 2.1 for Z100™, 79.8 ± 1.9 for Filtek™ Z250, 80.1 ± 1.3 for Filtek™ P60 and 68.8 ± 1.5 for Filtek™ Supreme XT. The mean Vickers hardness and associated standard deviations of the overlapped region were 97.5 ± 3.7 (Z100™), 79.1 ± 2.1 (Filtek™ Z250), 79.7 ± 3.7 (Filtek™ P60) and 69.0 ± 3.6 (Filtek™ Supreme XT), respectively (Table 4.4).

The mean Vickers hardness and associated standard deviations of the non-overlapped region when irradiated with the 11mm tip diameter for Z100™, Filtek™ Z250, Filtek™ P60 and Filtek™ Supreme XT were 98.4 ± 3.0, 79.1 ± 1.9, 84.7 ± 1.8 and 68.0 ± 6.2, respectively. For the overlapped region the mean Vickers hardness and associated standard deviations for Z100™ were 97.6 ± 1.8, Filtek™ Z250 were 79.4 ± 1.7, Filtek™ P60 were 83.7 ± 1.9 and Filtek™ Supreme XT were 67.0 ± 3.5 (Table 4.4).

Table 4.4: The non-overlapped and overlapped Vickers hardness data for the top and bottom surfaces for each RBC material when irradiated with the 13, 11, 8 and 25mm tip diameters using the QTH LCU in standard mode.

RBC	Surface	Region	Tip diameter			
			13mm	11mm	8mm	25mm
Z100™	Top	Non-overlapped	101.6 ± 1.9	101.3 ± 4.1	100.1 ± 2.3	99.2 ± 5
		Overlapped	102.0 ± 1.2	101.4 ± 3.2	100.1 ± 1.4	
	Bottom	Non-overlapped	97.9 ± 2.1	98.4 ± 3.0	98.6 ± 2.1	95.1 ± 1.8
		Overlapped	97.5 ± 3.7	97.6 ± 1.8	99.0 ± 2.1	
Filtek™ Z250	Top	Non-overlapped	80.7 ± 0.8	80.8 ± 1.0	79.8 ± 1.1	79.5 ± 4.2
		Overlapped	80.7 ± 0.9	80.6 ± 0.8	79.8 ± 1.1	
	Bottom	Non-overlapped	79.8 ± 1.9	79.1 ± 1.9	78.8 ± 1.6	78.4 ± 1.4
		Overlapped	79.1 ± 2.1	79.4 ± 1.7	78.3 ± 1.4	
Filtek™ P60	Top	Non-overlapped	85.2 ± 1.4	85.8 ± 1.9	84.7 ± 0.8	85.3 ± 2.8
		Overlapped	84.5 ± 1.0	85.9 ± 1.8	84.8 ± 0.9	
	Bottom	Non-overlapped	80.1 ± 1.3	84.7 ± 1.8	82.6 ± 1.8	82.5 ± 3.8
		Overlapped	79.7 ± 3.7	83.7 ± 1.9	82.4 ± 2.0	
Filtek™ Supreme XT	Top	Non-overlapped	72.1 ± 1.6	71.1 ± 1.2	71.1 ± 2.5	70.5 ± 2.5
		Overlapped	70.9 ± 1.8	71.1 ± 1.6	71.1 ± 2.4	
	Bottom	Non-overlapped	68.8 ± 1.5	68.0 ± 6.2	69.6 ± 2.6	66.7 ± 3.0
		Overlapped	69.0 ± 3.6	67.0 ± 3.5	69.6 ± 2.2	

The mean Vickers hardness and associated standard deviations of the non-overlapped region following irradiation with the 8mm tip diameter were 98.6 ± 2.1 for Z100™, 78.8 ± 1.6 for Filtek™ Z250, 82.6 ± 1.8 for Filtek™ P60 and 69.6 ± 2.6 for Filtek™ Supreme XT, respectively. For the overlapped region the mean Vickers hardness and associated standard deviations for Z100™ were 99.0 ± 2.1, Filtek™ Z250 were 78.3 ± 1.4, Filtek™ P60 were 82.4 ± 2.0 and Filtek™ Supreme XT were 69.6 ± 2.2 (Table 4.4).

When the 'one-hit' irradiation was employed the non-overlapped region resulted in the mean Vickers hardness and associated standard deviation for Z100™ were 95.1 ± 1.8, Filtek™ Z250 were 78.4 ± 1.4, Filtek™ P60 were 82.5 ± 3.8 and Filtek™ Supreme XT were 66.7 ± 3.0 (Table 4.4).

4.1.4.1.3 Statistical analysis: Standard mode: tip diameter

A two-way ANOVA design using site × region as the independent variables were then checked to ensure that no site effect emerged within each RBC and for both top and bottom surfaces. No significant differences in the Vickers hardness data were observed. Following the progressive pooling of the Vickers hardness data site variations were eliminated from the analysis. A three-way ANOVA were performed on each RBC using tip diameter (13, 11, 8 and 25mm), surface (top and bottom) and region (non-overlapped and overlapped) as the independent variables. For Z100™ the three-way ANOVA highlighted no significant differences with the effect of region ($P=0.837$), however, the effect of tip diameter ($P<0.0001$) and surface ($P<0.0001$) highlighted significant

differences. In addition, no significant differences were highlighted for the effect of region for Filtek™ Z250 (P=0.386), Filtek™ P60 (P=0.154) and Filtek™ Supreme XT (P=0.388). However, the effect of tip diameter for Filtek™ Z250, Filtek™ P6 0 and Filtek™ Supreme XT indicated significant differences (P<0.0001). Significant differences were also evident with the effect of surface for Filtek™ Z250 (P<0.0001), Filtek™ P60 (P<0.0001) and Filtek™ Supreme XT (P<0.005).

4.1.4.2 Boosted mode

4.1.4.2.1 Top

The mean Vickers hardness and associated standard deviations of the non-overlapped region on the top surface with a 13mm tip diameter for the four RBC materials investigated, namely Z100™, Filtek™ Z250, Filtek™ P60 and Filtek™ Supreme XT were 103.1 ± 2.0, 80.1 ± 2.9, 80.0 ± 1.1 and 98.4 ± 1.8, respectively. For the overlapped region on the top surface the mean Vickers hardness and associated standard deviations for Z100™ were 103.0 ± 1.6, Filtek™ Z250 were 81.4 ± 2.1, Filtek™ P60 were 80.2 ± 0.9 and Filtek™ Supreme XT were 68.7 ± 1.4 (Table 4.5).

For the four RBC materials, namely Z100™, Filtek™ Z250, Filtek™ P60 and Filtek™ Supreme XT following irradiation with the 11mm tip diameter, the mean Vickers hardness and associated standard deviations of the non-overlapped region on the top surface were 103.7 ± 3.0, 80.3 ± 0.9, 79.9 ± 2.2 and 69.1 ± 1.3, respectively. For the

overlapped region on the top surface the mean Vickers hardness and associated standard deviations for Z100™ were 103.6 ± 3.2, Filtek™ Z250 were 80.2 ± 0.1, Filtek™ P60 were 81.5 ± 2.6 and Filtek™ Supreme XT were 68.7 ± 1.2 (Table 4.5).

The mean Vickers hardness and associated standard deviations when irradiated with an 8mm tip diameter was employed of the non-overlapped region on the top surface for the RBC materials investigated, namely Z100™, Filtek™ Z250, Filtek™ P60 and Filtek™ Supreme XT were 103.6 ± 2.6, 80.0 ± 3.1, 80.2 ± 1.7 and 69.5 ± 1.3, respectively. For the overlapped region on the top surface the mean Vickers hardness and associated standard deviations for the RBC materials Z100™ were 103.4 ± 2.8, Filtek™ Z250 were 80.7 ± 2.0, Filtek™ P60 were 80.4 ± 1.2 and Filtek™ Supreme XT were 69.3 ± 1.4 (Table 4.5).

For the non-overlapped region on the top surface when employing the 'one hit' irradiation the mean Vickers hardness and associated standard deviation for the RBC materials investigated, namely Z100™ were 103.0 ± 3.7, Filtek™ Z250 were 81.3 ± 2.9, Filtek™ P60 were 81.4 ± 2.6 and Filtek™ Supreme XT were 69.3 ± 1.1.

4.1.4.2.2 Bottom

The mean Vickers hardness and associated standard deviations of the non-overlapped region on the bottom surface for the four RBC materials investigated, namely Z100™, Filtek™ Z250, Filtek™ P60 and Filtek™ Supreme XT following irradiation with a 13mm tip diameter were 96.4 ± 1.5, 73.5 ± 1.7, 73.9 ± 0.8 and 59.3 ± 3.2, respectively. On the

bottom surface for the overlapped region, the mean Vickers hardness and associated standard deviations were 96.5 ± 1.7, 73.3 ± 1.7, 73.1 ± 1.1 and 58.5 ± 2.9, respectively (Table 4.5).

Following irradiation with an 11mm tip diameter the mean Vickers hardness and associated standard deviations of the non-overlapped region on the bottom surface for Z100™, Filtek™ Z250, Filtek™ P60 and for Filtek™ Supreme XT were 96.8 ± 2.6, 74.7 ± 1.3, 73.8 ± 2.1 and 62.1 ± 1.9, respectively when irradiated with an 8mm tip diameter. On the bottom surface for the overlapped region the mean Vickers hardness and associated standard deviations were 96.2 ± 2.5 (Z100™), 74.7 ± 1.2 (Filtek™ Z250), 74.0 ± 2.1 (Filtek™ P60) and 62.5 ± 1.5 (Filtek™ Supreme XT), respectively (Table 4.5).

For the non-overlapped region on the bottom surface the mean Vickers hardness and associated standard deviations were 96.7 ± 2.9 for Z100™, 74.9 ± 2.1 for Filtek™ Z250, 74.0 ± 0.7 for Filtek™ P60 and 63.7 ± 1.5 for Filtek™ Supreme XT, respectively. The mean Vickers hardness and associated standard deviations of the overlapped region on the bottom surface for the RBC materials investigated, namely Z100™ were 96.0 ± 1.4, Filtek™ Z250 were 74.9 ± 1.4, Filtek™ P60 were 74.0 ± 0.5 and Filtek™ Supreme XT were 63.5 ± 1.2 (Table 4.5).

The mean Vickers hardness and associated standard deviations of the non-overlapped region on the bottom surface for the RBC materials investigated, namely Z100™, Filtek™ Z250, Filtek™ P60 and Filtek™ Supreme XT were 96.2 ± 2.3, 72.2 ± 3.0, 75.5 ±

Table 4.5: The non-overlapped and overlapped Vickers hardness data for the top and bottom surfaces for each RBC material when irradiated with the 13, 11, 8 and 25mm 'Turbo' tip diameters using the QTH LCU in boosted mode.

RBC	Surface	Region	Tip diameter			
			13mm	11mm	8mm	25mm
Z100™	Top	Non-overlapped	103.1 ± 2.0	103.7 ± 3.0	103.6 ± 2.6	103.0 ± 3.7
		Overlapped	103.0 ± 1.6	103.6 ± 3.2	103.4 ± 2.8	
	Bottom	Non-overlapped	96.4 ± 1.5	96.8 ± 2.6	96.7 ± 2.9	96.2 ± 2.3
		Overlapped	96.5 ± 1.7	96.2 ± 2.5	96.0 ± 1.4	
Filtek™ Z250	Top	Non-overlapped	80.1 ± 2.9	80.3 ± 0.9	80.0 ± 3.1	81.3 ± 2.9
		Overlapped	81.4 ± 2.1	80.2 ± 0.1	80.7 ± 2.0	
	Bottom	Non-overlapped	73.5 ± 1.7	74.7 ± 1.3	74.9 ± 2.1	72.2 ± 3.0
		Overlapped	73.3 ± 1.7	74.7 ± 1.2	74.9 ± 1.4	
Filtek™ P60	Top	Non-overlapped	80.0 ± 1.1	79.9 ± 2.2	80.2 ± 1.7	81.4 ± 2.6
		Overlapped	80.2 ± 0.9	81.5 ± 2.6	80.4 ± 1.2	
	Bottom	Non-overlapped	73.9 ± 0.8	73.8 ± 2.1	74.0 ± 0.7	75.5 ± 2.2
		Overlapped	73.1 ± 1.1	74.0 ± 2.1	74.0 ± 0.5	
Filtek™ Supreme XT	Top	Non-overlapped	68.4 ± 1.8	69.1 ± 1.3	69.5 ± 1.3	69.3 ± 1.1
		Overlapped	68.7 ± 1.4	68.7 ± 1.2	69.3 ± 1.4	
	Bottom	Non-overlapped	59.3 ± 3.2	62.1 ± 1.9	63.7 ± 1.5	63.2 ± 3.2
		Overlapped	58.5 ± 2.9	62.5 ± 1.5	63.5 ± 1.2	

2.2 and 63.2 ± 3.2, respectively following irradiation with a custom made fibre optic light guide (Table 4.5).

4.1.4.2.3 Statistical analysis: Boosted: tip diameter

A two-way ANOVA (site × region) within each RBC and for both top and bottom surfaces was undertaken. No significant differences in the Vickers hardness data were evident for site therefore the Vickers hardness data was pooled and site eliminated from the analysis. A three-way ANOVA (tip diameter × surface × region) was performed on each RBC. For Z100™ the three-way ANOVA highlighted no significant differences with the effect of region ($P=0.478$) and tip diameter ($P=0.733$), however, the effect of surface highlighted a significant difference ($P<0.0001$). Additionally, no significant differences were highlighted for the effect of region for Filtek™ Z250 ($P=0.478$), Filtek™ P60 ($P=0.286$) and Filtek™ Supreme XT ($P=0.560$). However, the effect of tip diameter and surface for Filtek™ Z250, Filtek™ P60 and Filtek™ Supreme XT indicated significant differences ($P<0.0001$).

4.2 ISO4049: The influence of LED LCU tip diameter

When evaluating RBC materials using ISO 4049 (ISO 4049: 2000) it is essential that there is standardisation and reproducibility of the testing methodologies between test centres since the type of LCU is not stated.

LED irradiance

When the irradiance of the Elipar™ Freelight LED LCU was measured seven consecutive times using the radiometer with tip diameters of 13 and 8mm, irradiances of 151 ± 18 and 246 ± 15mW/cm^2, respectively were identified. When assessing the irradiance of the Elipar™ Freelight 2 LED LCU seven consecutive times using the radiometer with tip diameters of 13 and 8mm identified irradiances of 769 ± 65mW/cm^2 and 1160 ± 60mW/cm^2.

4.2.1 Three-point flexure strength

4.2.1.1 Elipar™ Freelight

With a 13mm tip diameter the range of the three-point flexure strengths varied for Z100™ from a minimum of 77MPa to a maximum of 138MPa (Group Q_l), for Filtek™ Z250 from 129 to 177MPa (Group R_l), for Filtek™ P60 from a minimum of 117MPa to a maximum of 173MPa (Group S_l) and for Filtek™ Supreme XT from a strength of 119MPa to a strength of 159MPa (Group T_l). The mean three-point flexure strengths and associated standard deviations were 101 ± 15MPa (Group Q_l), 147 ± 15MPa (Group R_l), 146 ± 16MPa (Group S_l) and 132 ± 10MPa (Group T_l), respectively (Table 4.6).

Table 4.6: The range and mean three-point flexure strengths (associated standard deviations) for the RBC specimens irradiated with the Elipar™ Freelight and Elipar™ Freelight 2 LED LCUs using tip diameters of 8 and 13mm.

RBC	Property	Elipar™ Freelight		Elipar™ Freelight 2	
		8mm	13mm	8mm	13mm
Z100™	Three-point flexure strength (MPa)	100 (15)	104 (18)	101 (15)	104 (15)
	Range of strengths (MPa)	77-129	77-138	74-136	77-125
Filtek™ Z250	Three-point flexure strength (MPa)	146 (15)	158 (15)	147 (15)	160 (15)
	Range of strengths (MPa)	112-173	129-177	118-177	138-183
Filtek™ P60	Three-point flexure strength (MPa)	157 (16)	149 (15)	146 (16)	151 (15)
	Range of strengths (MPa)	125-190	117-173	124-179	124-179
Filtek™ Supreme XT	Three-point flexure strength (MPa)	135 (9)	133 (9)	133 (10)	141 (10)
	Range of strengths (MPa)	123-153	119-159	113-141	118-154

The mean three-point flexure strength and associated standard deviations when irradiated with an 8mm tip diameter for Z100™ (Group U_I) was 100 ± 15MPa, Filtek™ Z250 (Group V_I) was 146 ± 15MPa, Filtek™ P60 (Group W_I) was 157 ± 16MPa and Filtek™ Supreme XT (Group X_I) was 135 ± 9MPa. The range of three-point flexure strengths for the four RBC materials investigated varied from a low of 77MPa to a high of 129MPa for Group U_I specimens, from a minimum of 112MPa to a maximum of 173MPa for Group V_I specimens, from 125 to 190MPa for Group W_I specimens and from a low of 123MPa to a high of 153MPa for Group X_I specimens, respectively (Table 4.6).

4.2.1.1.1 Statistical analysis

No significant differences in the group means of the three-point flexure strength data were identified for Z100™ when irradiated with tip diameters of 13 and 8mm with the Elipar™ Freelight LED LCU utilising the one-way ANOVA (F value=0.368; P=0.776). When the group means of the three-point flexure strength data for Filtek™ Z250 were analysed following irradiation no significant differences in the one-way ANOVA (F value=5.063; P=0.053) were evident. For the groups of 20 rectangular bar-shaped specimens of Filtek™ P60 the group means of the three-point flexure strength data highlighted no significant differences when utilising the one-way ANOVA (F value=2.067; P=0.112). Similarly when the group means of the three-point flexure strength data for Filtek™ Supreme XT were analysed no significant differences in the one-way ANOVA (F value=2.871; P=0.062) were identified in the current study.

4.2.1.2 Elipar™ Freelight 2

The mean three-point flexure strengths and associated standard deviations following irradiation with 13mm tip diameter for the RBCs, namely Z100™, Filtek™ Z250, Filtek™ P60 and Filtek™ Supreme XT were 104 ± 14MPa (Group Q_h), 160 ± 15MPa (Group R_h), 151 ± 15MPa (Group S_h) and 141 ± 10MPa (Group T_h), respectively. The range of three-point flexure strengths varied for Z100™ from a minimum of 77MPa to a maximum of 125MPa, for Filtek™ Z250 from 138 to 183MPa, for Filtek™ P60 from a

low of 124MPa to a high of 179MPa and for Filtek™ Supreme XT from a minimum recorded value of 118MPa to a maximum recorded value of 154MPa (Table 4.6).

Irradiation with an 8mm tip diameter resulted in a range of three-point flexure strengths varying from a low of 74MPa to a high of 136MPa for Z100™ (Group U_h), from 118 to 177MPa for Filtek™ Z250 (Group V_h), from a minimum of 124MPa to a maximum of 179MPa for Filtek™ P60 (Group W_h) and from 113MPa to 141MPa for Filtek™ Supreme XT (Group X_h). The mean three-point flexure strength and associated standard deviation were 101 ± 15MPa for Group U_h specimens, 147 ± 15MPa for Group V_h specimens, 146 ± 16MPa for Group W_h specimens and 133 ± 10MPa for Group X_h specimens (Table 4.6).

4.2.1.2.1 Statistical analysis

For Z100™ no significant differences in the group means of the three-point flexure strength data were identified when irradiated with the Elipar™ Freelight 2 LED LCU with tip diameters of 13 and 8mm utilising the one-way ANOVA (F value=0.368; P=0.776). Analysis of the group means of the three-point flexure strength data for Filtek™ Z250 resulted in no significant differences in the one-way ANOVA (F value=5.063; P=0.053). The manufacture of Filtek™ P60 rectangular bar-shaped specimens showed that analysis of the group means of the three-point flexure strength data identified no significant differences when utilising the one-way ANOVA (F value=2.067; P=0.112). Analysis following irradiation of Filtek™ Supreme XT also

revealed no significant differences in the group means of the three-point flexure strength data with the one-way ANOVA (F value=2.871; P=0.062).

4.2.2 Reliability of fracture strength data

4.2.2.1 Elipar™ Freelight

The Weibull moduli and associated standard deviations for the series of Z100™ specimens when irradiated using tip diameters of 13 and 8mm were 6.9 ± 2.2 for Group Q_I specimens and 7.2 ± 2.1 for Group U_I specimens, respectively (Table 4.7). The regression analysis of the three-point flexure strength data resulted in 95% confidence intervals ranging from a low of 6.0 to a high of 7.8 (Group Q_I) and from a minimum of 6.1 to a maximum of 8.2 (Group U_I), respectively. The 95% confidence intervals of the Z100™ specimens irradiated with tip diameters of 13 and 8mm overlapped and the Weibull moduli were therefore considered to be non-significant. Tip diameters of 13 and 8mm used to irradiate Filtek™ Z250 specimens resulted in Weibull moduli and associated standard deviations of 10.1 ± 2.1 for Group Q_I specimens and 9.7 ± 1.2 for Group U_I specimens, respectively with the lower and upper 95% confidence intervals varying for Group Q_I and for Group U_I specimens from a minimum of 9.2 to a maximum of 11.0 and from a low of 7.1 to a high of 12.2, respectively (Table 4.7). The 95% confidence intervals of the Weibull moduli for Filtek™ Z250 specimens irradiated using 13 and 8mm tip diameters overlapped indicating no significant differences. The Weibull analysis for the series of Filtek™ P60 specimens produced Weibull moduli and associated

standard deviations using tip diameters of 13mm (Group Q_l) of 10.5 ± 1.7 and 8mm (Group U_l) of 9.9 ± 1.4, respectively (Table 4.7). The 95% confidence intervals varied from a low of 9.4 to a high of 11.7 for Group Q_l specimens and from 8.9 to 10.9 for Group U_l specimens, respectively. Since the 95% confidence intervals of Filtek™ P60 specimen groups investigated, namely Group Q_l and Group U_l overlapped, the Weibull moduli were considered to be non significant. The irradiation of Filtek™ Supreme XT specimens produced Weibull moduli and associated standard deviations using tip diameters of 13mm (Group Q_l) of 14.7 ± 2.1 and 8mm (Group U_l) of 13.0 ± 1.3, respectively (Table 4.7). The 95% confidence intervals calculated from regression analysis of the three-point flexure strength data ranged for Group Q_l specimens from 11.7 to 17.6 and for Group U_l specimens from a minimum value of 10.2 to a maximum value of 15.9, respectively. As the 95% confidence intervals of the three-point flexure strength data of the Filtek™ Supreme XT specimen irradiated using 13 and 8mm tip diameter overlapped, each associated Weibull moduli were not considered to be significantly different.

4.2.2.2 Elipar™ Freelight 2

Z100™ resulted in Weibull moduli and associated standard deviations with tip diameters of 13mm (Group Q_h) of 7.5 ± 1.1 and 8mm (Group U_h) of 5.4 ± 2.1, respectively (Table 4.7). The 95% confidence intervals varied from a minimum of 6.9 to a maximum of 8.2 for Group Q_h specimens and from of 4.7 to of 6.0 for Group U_h specimens. The associated Weibull moduli of Z100™ specimen groups, namely Group Q_h and Group U_h

were considered to be non-significant since the 95% confidence intervals overlapped. The irradiation of Filtek™ Z250 specimens with tip diameters 13 and 8mm resulted in Weibull moduli and associated standard deviations of 11.3 ± 1.0 for Group Q_h specimens and 10.3 ± 2.0 for Group U_h specimens, respectively (Table 4.7). The 95% confidence intervals ranged from a low of 9.3 to a high of 13.2 (Group Q_h) and from 9.0 to 11.6 (Group U_h), respectively. The associated Weibull moduli of the three-point flexure strength data for Filtek™ Z250 specimens irradiated with tip diameters 13 and 8mm were considered to be non-significant as the 95% confidence intervals overlapped. The resultant Weibull moduli and associated standard deviations for the specimens fabricated from Filtek™ P60 when irradiated using tip diameters of 13mm (Group Q_h), and 8mm (Group U_h) were 10.9 ± 1.9 and 10.2 ± 1.1, respectively (Table 4.7). Filtek™ P60 was reported with the associated 95% confidence intervals ranging from 9.9 to 11.8 for Group Q_h specimens and from a minimum recorded value of 9.3 to a maximum recorded value of 11.1 for Group U_h specimens. The Weibull moduli of the three-point flexure strength data of the specimens fabricated from the RBC material Filtek™ P60 and irradiated using tip diameters of 13 and 8mm were considered to be non-significant since the 95% confidence intervals overlapped. Tip diameters of 13 and 8mm used to irradiate Filtek™ Supreme XT specimens resulted in Weibull moduli and associated standard deviations of 14.6 ± 2.3 for Group Q_h specimens and 15.1 ± 1.6 for Group U_h specimens, respectively with the associated 95% confidence intervals ranging from a minimum of 13.0 to a maximum of 16.1 for Group Q_h specimens and from 12.8 to 17.5 for Group U_h specimens (Table 4.7). The Weibull moduli of Filtek™ Supreme XT specimen groups, namely

Group Q_h and Group U_h, were considered to be non-significant as the 95% confidence intervals overlapped.

Table 4.7: The Weibull moduli and 95% confidence intervals for the RBC specimens irradiated with the Elipar™ Freelight and Elipar™ Freelight 2 LED LCUs using tip diameters of 8 and 13mm.

RBC	Property	Elipar™ Freelight		Elipar™ Freelight 2	
		8mm	13mm	8mm	13mm
Z100™	Weibull modulus	7.2 (2.1)	6.9 (2.2)	5.4 (2.1)	7.5 (1.1)
	95% Confidence Intervals	6.1-8.2	6.0-7.8	4.7-6.0	6.9-8.2
Filtek™ Z250	Weibull modulus	9.7-1.2	10.1 (2.1)	10.3 (2.0)	11.3 (1.0)
	95% Confidence Intervals	7.1-12.2	9.2-11.0	9.0-11.6	9.3-13.2
Filtek™ P60	Weibull modulus	9.9 (1.4)	10.5 (1.7)	10.2 (1.1)	10.9 (1.9)
	95% Confidence Intervals	8.9-10.9	9.4-11.7	9.3-11.1	9.9-11.8
Filtek™ Supreme XT	Weibull modulus	13.0 (1.3)	14.7 (2.1)	15.1 (1.6)	14.6 (2.3)
	95% Confidence Intervals	10.2-15.9	11.7-17.6	12.8-17.5	13.0-16.1

4.2.3 Three-point flexure modulus testing

4.2.3.1 Elipar™ Freelight

The mean three-point flexure moduli and associated standard deviations following irradiation with a 13mm tip diameter for Z100™ (Group Q_l) were 13.8 ± 1.1GPa, for Filtek™ Z250 (Group R_l) were 10.3 ± 1.2GPa, for Filtek™ P60 (Group S_l) were 10.6 ± 0.6GPa and for Filtek™ Supreme XT (Group T_l) were 8.2 ± 1.0GPa. The range of the

three-point flexure moduli varied from a low of 12GPa to a high of 16GPa for Group Q_I specimens, from a minimum of 8GPa to a maximum of 13GPa for Group R_I specimens, from 10 to 12GPa for group S_I specimens and from a minimum of 6GPa to a maximum of 10GPa for group T_I specimens, respectively (Table 4.8).

Table 4.8: The range and mean three-point flexure moduli (associated standard deviations) for the RBC specimens irradiated with the Elipar™ Freelight and Elipar™ Freelight 2 LED LCUs using tip diameters of 8 and 13mm.

RBC	Property	Elipar™ Freelight		Elipar™ Freelight 2	
		8mm	13mm	8mm	13mm
Z100™	Three-point flexure modulus (GPa)	13.2 (1.2)	13.8 (1.1)	13.1 (1.1)	13.8 (1.2)
	Range of moduli (GPa)	11-15	12-16	11-15	12-17
Filtek™ Z250	Three-point flexure modulus (GPa)	10.6 (0.6)	10.3 (1.2)	10.9 (1.4)	10.7 (1.0)
	Range of moduli (GPa)	10-12	8-13	9-15	9-12
Filtek™ P60	Three-point flexure modulus (GPa)	11.0 (1.7)	10.6 (0.6)	11.3 (1.4)	10.9 (0.6)
	Range of moduli (GPa)	9-16	10-12	7-14	10-13
Filtek™ Supreme XT	Three-point flexure modulus (GPa)	8.5 (0.6)	8.2 (1.0)	8.7 (0.7)	8.7 (0.3)
	Range of moduli (GPa)	7-10	6-10	7-10	8-9

The mean three-point flexure moduli and associated standard deviations when irradiated with an 8mm tip diameter for Z100™ (Group U_I) were 13.2 ± 1.2GPa, for Filtek™ Z250 (Group V_I) were 10.6 ± 0.6GPa, for Filtek™ P60 (Group W_I) were 11.0 ± 1.7GPa and for Filtek™ Supreme XT (Group X_I) were 8.5 ± 0.6GPa. For the four RBC materials investigated, the range of the three-point flexure moduli varied from a minimum of 11GPa to a maximum of 15GPa (Group U_I), from 10 to 12GPa (Group V_I), from a

minimum of 9GPa to a maximum of 16GPa (Group W_I) and from 7GPa to 10GPa (Group X_I), respectively (Table 4.8).

4.2.3.1.1 Statistical analysis

For each RBC a one-way ANOVA and Tukey's multiple range tests at a significance level of $P<0.05$ were used to make multiple comparisons of the group means of the three-point flexure modulus data. The Elipar™ Freelight was used with tip diameters of 13 and 8mm. When the group means of the three-point flexure modulus data for Z100™ were analysed with tip diameters of 13mm (Group Q_I), and 8mm (Group U_I) no significant differences in the one-way ANOVA (F value=2.460; P=0.969) were evident. The groups of 20 rectangular bar-shaped specimens of Filtek™ Z250 irradiated with tip diameters of 13mm (Group R_I) and 8mm (Group V_I) resulted in no significant differences in the group means of the three-point flexure modulus data when analysed utilising the one-way ANOVA (F value=0.985; P=0.404). No significant differences in the group means of the three-point flexure modulus data were identified for Filtek™ P60 when irradiated with tip diameters of 13mm (Group S_I) and 8mm (Group W_I) when utilising the one-way ANOVA (F value=1.276; P=0.289). Similarly when the group means of the three-point flexure modulus data for Filtek™ Supreme XT were analysed following irradiation with tip diameters of 13mm (Group T_I) and 8mm (Group X_I) no significant differences in the one-way ANOVA (F value=1.830; P=0.149) were identified.

4.2.3.2 Elipar™ Freelight 2

Following irradiation with a 13mm tip diameter the range of three-point flexure moduli for the four RBC materials varied from a low of 12GPa to a high of 17GPa for Group Q_h specimens, from a minimum of 9GPa to a maximum of 12GPa for Group R_h specimens, from 10 to 13GPa for Group S_h specimens and from a low of 8GPa to a high of 9GPa for Group T_h specimens, respectively. The mean three-point flexure moduli and associated standard deviations for Z100™ (Group Q_h) were 13.8 ± 1.2GPa, Filtek™ Z250 (Group R_h) were 10.7 ± 1.0GPa, Filtek™ P60 (Group S_h) were 10.9 ± 0.6GPa and Filtek™ Supreme XT (Group T_h) were 8.7 ± 0.3GPa.

Employing the overlapping irradiation regime using an 8mm tip diameter, the mean three-point flexure moduli and associated standard deviations for Z100™ (Group U_h) were 13.1 ± 1.1GPa, Filtek™ Z250 (Group V_h) were 10.9 ± 1.4GPa, Filtek™ P60 (Group W_h) were 11.3 ± 1.4GPa and Filtek™ Supreme XT (Group X_h) were 8.7 ± 0.7GPa. The range of three-point flexure moduli varied from a low of 11GPa to a high of 15GPa for Group U_h specimens, from 9 to 15GPa for Group V_h specimens, from a minimum of 7GPa to a maximum of 14GPa for Group W_h specimens and from 7 to 10GPa for Group X_h specimens, respectively.

4.2.3.2.1 Statistical analysis

Statistical analysis following irradiation of the Z100™ specimens with tip diameters of 13mm (Group Q_h) and 8mm (Group U_h) revealed no significant differences in the group means of the three-point flexure modulus data with the one-way ANOVA (F value=2.460; P=0.069). Analysis of the group means of the three-point flexure modulus data for Filtek™ Z250 following irradiation with tip diameters of 13mm (Group R_h) and 8mm (Group V_h) also resulted in no significant differences in the one-way ANOVA (F value=0.985; P=0.404). For Filtek™ P60, no significant differences in the group means of the three-point flexure modulus data were identified following irradiation with tip diameters of 13mm (Group S_h) and 8mm (Group W_h) utilising the one-way ANOVA (F value=1.276; P=0.289). Filtek™ Supreme XT rectangular bar-shaped specimens irradiated with tip diameters of 13mm (Group T_h) and 8mm (Group X_h) highlighted no significant differences in grouped means of the three-point flexure modulus data when utilising the one-way ANOVA (F value=1.830; P=0.149).

4.2.4 Vickers hardness testing

The influence of tip diameter when employing the overlapping regime to irradiate rectangular bar-shaped specimens was investigated using Vickers hardness measurements.

4.2.4.1 Elipar™ Freelight

4.2.4.1.1 Top

Irradiation from the top surface of the specimen using the 13mm tip diameter resulted in the mean Vickers hardness and associated standard deviations for the non-overlapped region of 103.2 ± 1.5 for Z100™, 74.7 ± 2.1 for Filtek™ Z250, 78.3 ± 4.2 for Filtek™ P60 and 67.6 ± 1.8 for Filtek™ Supreme XT. For the overlapped region the mean Vickers hardness and associated standard deviations were 103.7 ± 1.8 (Z100™), 74.9 ± 1.7 (Filtek™ Z250), 78.0 ± 2.2 (Filtek™ P60) and 67.4 ± 1.8 (Filtek™ Supreme XT) (Table 4.9).

The mean Vickers hardness and associated standard deviations for the non-overlapped region on the top surface irradiated with an 8mm tip diameter were 104.0 ± 2.6 for Z100™, 75.1 ± 2.9 for Filtek™ Z250, 78.5 ± 1.9 for Filtek™ P60 and 66.1 ± 1.8 for Filtek™ Supreme XT. The mean Vickers hardness and associated standard deviations for the overlapped region for Z100™ were 103.5 ± 2.4, Filtek™ Z250 were 74.0 ± 2.4, Filtek™ P60 were 79.4 ± 2.8 and Filtek™ Supreme XT were 67.1 ± 1.8 (Table 4.9).

Table 4.9: The non-overlapped and overlapped Vickers hardness data for the top surface for each RBC material when irradiated with the 13 and 8mm tip diameters using the LED LCUs.

RBC	LED LCU	Elipar™ Freelight		Elipar™ Freelight 2	
		13mm	8mm	13mm	8mm
Z100™	Non-overlapped	103.2 ± 1.5	104.0 ± 2.6	103.1 ± 2.1	103.7 ± 2.3
	Overlapped	103.7 ± 1.8	103.5 ± 2.4	103.3 ± 2.3	105.2 ± 2.3
Filtek™ Z250	Non-overlapped	74.7 ± 2.1	75.1 ± 2.9	75.0 ± 1.9	75.5 ± 3.1
	Overlapped	74.9 ± 1.7	74.0 ± 2.4	75.2 ± 2.2	77.2 ± 2.2
Filtek™ P60	Non-overlapped	78.3 ± 4.2	78.5 ± 1.9	77.8 ± 2.6	79.6 ± 2.5
	Overlapped	78.0 ± 2.2	79.4 ± 2.8	78.2 ± 2.1	79.8 ± 2.5
Filtek™ Supreme XT	Non-overlapped	67.6 ± 1.8	66.1 ± 1.8	68.2 ± 2.9	67.8 ± 2.8
	Overlapped	67.4 ± 1.8	67.1 ± 1.8	67.6 ± 1.9	67.8 ± 1.6

4.2.4.1.2 Bottom

Following irradiation with a 13mm tip diameter the mean Vickers hardness and associated standard deviations for the non-overlapped region on the bottom surface were 83.3 ± 2.3 for Z100™, 58.6 ± 2.4 for Filtek™ Z250, 63.1 ± 3.6 for Filtek™ P60 and 45.1 ± 2.7 for Filtek™ Supreme XT. The mean Vickers hardness and associated standard deviation for the overlapped region on the bottom surface were 81.7 ± 2.3 for Z100™,

60.6 ± 1.7 for Filtek™ Z250, 64.1 ± 2.8 for Filtek™ P60 and 46.9 ± 2.5 for Filtek™ Supreme XT (Table 4.10)

Table 4.10: The non-overlapped and overlapped Vickers hardness data for the bottom surfaces for each RBC material when irradiated with the 13 and 8mm tip diameters using the LED LCUs.

RBC	LED LCU	Elipar™ Freelight		Elipar™ Freelight 2	
		13mm	8mm	13mm	8mm
Z100™	Non-overlapped	83.3 ± 2.3	83.2 ± 2.0	99.0 ± 2.9	101.2 ± 2.9
	Overlapped	81.7 ± 2.3	82.6 ± 2.5	99.4 ± 2.4	102.4 ± 2.7
Filtek™ Z250	Non-overlapped	58.6 ± 2.4	61.8 ± 2.4	74.5 ± 2.1	74.5 ± 2.1
	Overlapped	60.6 ± 1.7	63.4 ± 2.0	74.8 ± 2.3	74.3 ± 1.1
Filtek™ P60	Non-overlapped	63.1 ± 3.6	64.5 ± 2.6	74.5 ± 2.2	76.1 ± 2.2
	Overlapped	64.1 ± 2.8	64.5 ± 2.6	73.2 ± 2.6	76.2 ± 2.3
Filtek™ Supreme XT	Non-overlapped	45.1 ± 2.7	46.9 ± 2.7	59.1 ± 3.1	65.7 ± 2.6
	Overlapped	46.9 ± 2.5	44.6 ± 2.5	59.0 ± 2.3	66.0 ± 2.0

The mean Vickers hardness and associated standard deviations for the non-overlapped region on the bottom surface following irradiation with the 8mm light tip diameter were 83.2 ± 2.0 (Z100™), 61.8 ± 2.4 (Filtek™ Z250), 64.5 ± 2.6 (Filtek™ P60) and 46.9 ± 2.7 (Filtek™ Supreme XT). For the overlapped region the mean Vickers hardness and

associated standard deviations were 82.6 ± 2.5 for Z100™, 63.4 ± 2.0 for Filtek™ Z250, 64.5 ± 2.6 for Filtek™ P60 and 44.6 ± 2.5 for Filtek™ Supreme XT (Table 4.10).

4.2.4.1.3 Statistical analysis: Elipar™ Freelight

A two-way ANOVA design using site × region as the independent variables were undertaken to ensure that no site effect emerged within each RBC and for both top and bottom surfaces. No significant differences in the Vickers hardness data were observed. Following the progressive pooling of the Vickers hardness data site variations were eliminated from the analysis. The three-way ANOVA (tip diameter × surface × region) highlighted no significant differences with the effect of region for Z100™ (P=0.141), Filtek™ Z250 (P=0.136), Filtek™ P60 (P=0.402) and Filtek™ Supreme XT (P=0.924) and tip diameter for Z100™ (P=0.364), Filtek™ P60 (P=0.078) and Filtek™ Supreme XT (P=0.118), however, a significant effect was indicated for Filtek™ Z250 (P=0.002). The effect of surface highlighted a significant difference (P<0.0001) for Z100™ (P<0.0001), Filtek™ Z250 (P<0.0001), Filtek™ P60 (P<0.0001) and Filtek™ Supreme XT (P<0.0001).

4.2.4.2 Elipar™ Freelight 2

4.2.4.2.1 Top

When the top surface was irradiated with a 13mm tip diameter the mean Vickers hardness and associated standard deviations for the non-overlapped region were 103.1 ± 2.1 for Z100™, 75.0 ± 1.9 for Filtek™ Z250, 77.8 ± 2.6 for Filtek™ P60 and 68.2 ± 2.9 for Filtek™ Supreme XT. For the overlapped region the mean Vickers hardness and associated standard deviations were 103.3 ± 2.3 (Z100™), 75.2 ± 2.2 (Filtek™ Z250), 78.2 ± 2.1 (Filtek™ P60) and 67.6 ± 1.9 (Filtek™ Supreme XT), respectively (Table 4.9).

Following irradiation with an 8mm tip diameter resulted in mean Vickers hardness and associated standard deviations for the non-overlapped region of 103.7 ± 2.3 for Z100™, 75.5 ± 3.1 for Filtek™ Z250, 79.6 ± 2.5 for Filtek™ P60 and 67.8 ± 2.8 for Filtek™ Supreme XT. For the overlapped region the mean Vickers hardness and associated standard deviations were 105.2 ± 2.3 (Z100™), 77.2 ± 2.2 (Filtek™ Z250), 79.8 ± 2.5 (Filtek™ P60) and 67.8 ± 1.6 (Filtek™ Supreme XT) (Table 4.9).

4.2.4.2.2 Bottom

The mean Vickers hardness and associated standard deviations following irradiation with the 13mm tip diameter for the non-overlapped region on the bottom surface were 99.0 ± 2.9 for Z100™, 74.5 ± 2.1 for Filtek™ Z250, 74.5 ± 2.2 for Filtek™ P60 and 59.1 ± 3.1

for Filtek™ Supreme XT. The mean Vickers hardness and associated standard deviation for the overlapped region for Z100™ were 99.4 ± 2.4, Filtek™ Z250 were 74.8 ± 2.3, Filtek™ P60 were 73.2 ± 2.6 and Filtek™ Supreme XT were 59.0 ± 2.3 (Table 4.10).

The mean Vickers hardness and associated standard deviations for the non-overlapped region on the bottom surface following irradiation with the 8mm tip diameter were 101.2 ± 2.9 (Z100™), 74.5 ± 2.1 (Filtek™ Z250), 76.1 ± 2.2 (Filtek™ P60), and 65.7 ± 2.6 (Filtek™ Supreme XT). The mean Vickers hardness and associated standard deviations for the overlapped region for Z100™, Filtek™ Z250, Filtek™ P60 and Filtek™ Supreme XT were 102.4 ± 2.7, 74.3 ± 1.1, 76.2 ± 2.3 and 66.0 ± 2.0, respectively (Table 4.10).

4.2.4.2.3 Statistical analysis: Elipar™ Freelight 2

A two-way ANOVA (site × region) were undertaken to ensure that no site effect emerged within each RBC for both the top and bottom surfaces. No significant differences in the Vickers hardness data were evident for site therefore the Vickers hardness data was pooled and site eliminated from the analysis. A three-way ANOVA (tip diameter × surface × region) was performed on each RBC. The three-way ANOVAs highlighted no significant differences with the effect of region for Z100™ ($P=0.095$), Filtek™ Z250 ($P=0.978$), Filtek™ P60 ($P=0.690$) and Filtek™ Supreme XT ($P=0.685$). However, a significant difference was identified for the effect of tip diameter ($P<0.0001$) and surface ($P<0.0001$) for all RBC materials.

4.3 ISO4049: The influence of QTH LCU irradiance

The three-point flexural properties have been reported to be influenced by the operating irradiance and the overlapping irradiation protocol during specimen manufacture in accordance with ISO 4049.

4.3.1 Three-point flexure strength

4.3.1.1 QTH

4.3.1.1.1 Standard mode

When the 8mm 'Turbo' tip diameter was used to irradiate the RBCs, the range of three-point flexure strengths varied for Z100™ from a low of 69MPa to a high of 130MPa (Group I_{st}), Filtek™ Z250 from 124 to 183MPa (Group J_{st}), Filtek™ P60 from a minimum of 128MPa to a maximum of 187MPa (Group K_{st}) and Filtek™ Supreme XT from a lowest value of 130MPa to a highest value of 167MPa (Group L_{st}), respectively. The mean three-point flexure strengths and associated standard deviations for Z100™, Filtek™ Z250, Filtek™ P60, Filtek™ Supreme XT were 104 ± 14MPa, 157 ± 16MPa, 164 ± 16MPa and 140 ± 10MPa, respectively (Table 4.11).

Table 4.11: The range and mean three-point flexure strength (associated standard deviations) for the RBC specimens irradiated using a QTH LCU in standard and boosted modes with the 8mm 'Turbo' tip diameter.

RBC	Property	8mm 'Turbo'	
		Standard	Boosted
Z100™	Three-point flexure strength (MPa)	104 (14)	107 (15)
	Range of strengths (MPa)	69-130	87-134
Filtek™ Z250	Three-point flexure strength (MPa)	157 (16)	156 (16)
	Range of strengths (MPa)	124-183	131-182
Filtek™ P60	Three-point flexure strength (MPa)	164 (16)	153 (14)
	Range of strengths (MPa)	128-187	128-178
Filtek™ Supreme XT	Three-point flexure strength (MPa)	140 (10)	137 (11)
	Range of strengths (MPa)	130-167	112-159

4.3.1.1.1.1 Statistical analysis

A one-way ANOVA and Tukey's multiple range tests at a significance level of $P<0.05$ was used to make multiple comparisons of the group means for the three-point flexure strength data for the RBC materials irradiated at irradiances of 640 ± 18 and 880 ± 18mW/cm^2 with the 8mm and 8mm 'Turbo' LCU tip diameters, respectively. No significant differences in the group means of the three-point flexure strength data were identified for Z100™ utilising the one-way ANOVA (F value=0.721; P=0.543). The group means of the three-point flexure strength data for Filtek™ Z250 also showed no significant differences in the one-way ANOVA (F value=1.529; P=0.214). When Filtek™ P60 was irradiated with tip diameters of 8mm (Group K_s) or 8mm 'Turbo' (Group K_{st}) the group means of the three-point flexure strength data highlighted no significant

differences utilising the one-way ANOVA (F value=3.713; P=0.150). Similarly, analysis of the group means of the three-point flexure strength data for Filtek™ Supreme XT indicated no significant differences in the one-way ANOVA (F value=0.699; P=0.555).

4.3.1.1.2 Boosted mode

The mean three-point flexure strengths and associated standard deviations following irradiation with the 8mm 'Turbo' tip diameter for Z100™ (Group I_{bt}) were 107 ± 15MPa, Filtek™ Z250 (Group J_{bt}) were 156 ± 16MPa, Filtek™ P60 (Group K_{bt}) were 153 ± 14MPa and Filtek™ Supreme XT (Group L_{bt}) were 137 ± 11MPa. The range of three-point flexure strengths varied from a low of 87MPa to a high of 134MPa (Group I_{bt}), from 131 to 182MPa (Group J_{bt}), from a minimum of 128MPa to a maximum of 178MPa (Group K_{bt}) and from a low of 112MPa to a high of 159MPa (Group L_{bt}), respectively (Table 4.11).

4.3.1.1.2.1 Statistical analysis

For each of the four RBC materials investigated (Z100™, Filtek™ Z250, Filtek™ P60 and Filtek™ Supreme XT) multiple comparisons of the group means for the three-point flexure strength data were made with a one-way ANOVA and Tukey's multiple range tests at a significance level of $P<0.05$ at irradiances of 790 ± 18mW/cm^2 and 1040 ± 28mW/cm^2 using tip diameters of 8mm and 8mm 'Turbo', respectively. No significant differences in the group means of the three-point flexure strengths were identified when

employing the one-way ANOVA for Z100™ (F value=0.721; P=0.543), Filtek™ Z250 (F value=1.529; P=0.214), Filtek™ P60 (F value=3.713; P=0.150) and Filtek™ Supreme XT (F value=0.699; P=0.555).

4.3.2 Reliability of the fracture strength data

4.3.2.1 Standard mode

The three-point flexure strength data was subjected to Weibull analyses for each of the groups of 20 rectangular bar-shaped specimens fabricated from the RBC materials Z100™, Filtek™ Z250, Filtek™ P60 and Filtek™ Supreme XT with the 8mm 'Turbo' tip diameter. The irradiation of the specimen groups, namely Group I_{st}, Group J_{st}, Group K_{st} and Group L_{st} resulted in Weibull moduli and associated standard deviations of 6.5 ± 1.5, 10.7 ± 2.4, 10.4 ± 2.3 and 16.4 ± 3.6, respectively (Table 4.12). The 95% confidence intervals varied from a low of 5.8 to a high of 7.2 (Group I_{st}), from a minimum of 10.0 to a maximum of 11.3 (Group J_{st}), from 9.7 to 11.1 (Group K_{st}) and from a low of 14.2 to a high of 17.9 (Group L_{st}). Since the 95% confidence intervals for Group I_s and Group I_{st}, Group J_s and Group J_{st}, Group K_s and Group K_{st} and Group L_s and Group L_{st} overlapped, each associated Weibull moduli were considered not to be significantly different.

Table 4.12: The Weibull moduli and 95% confidence intervals for the RBC specimens irradiated using a QTH LCU in standard and boosted modes with the 8mm 'Turbo' tip diameter.

RBC	Property	8mm 'Turbo'	
		Standard	Boosted
Z100™	Weibull modulus	13.2 (1.2)	14.1 (1.1)
	95% Confidence Intervals	11-16	12-17
Filtek™ Z250	Weibull modulus	11.3 (0.9)	11.6 (0.7)
	95% Confidence Intervals	10.0-12	10-13
Filtek™ P60	Weibull modulus	12.7 (1.3)	12.8 (1.1)
	95% Confidence Intervals	10-16	10-15
Filtek™ Supreme XT	Weibull modulus	10.3 (0.7)	9.9 (1.0)
	95% Confidence Intervals	5-12	9-12

4.3.2.2 Boosted mode

Irradiation with an 8mm 'Turbo' tip diameter produced Weibull moduli and associated standard deviations for Z100™ of 7.5 ± 1.7 for Group I_{bt} specimens, for Filtek™ Z250 of 10.6 ± 2.4 for Group J_{bt} specimens, for Filtek™ P60 of 11.8 ± 2.6 for Group K_{bt} specimens and for Filtek™ Supreme XT of 15.0 ± 3.4 for Group L_{bt} specimens, respectively (Table 4.12). The investigated RBC materials at the 95% confidence intervals calculated from regression analysis varied from a low of 6.2 to a high of 8.8 (Group I_{bt}), from 9.4 to 11.8 (Group J_{bt}), from a minimum of 10.6 to a maximum of 13.0 (Group K_{bt}) and from 12.5 to 17.5 (Group L_{bt}). When the Weibull moduli of the three-point flexure strength data for Group I_b and Group I_{bt}, Group J_b and Group J_{bt}, Group K_b

and Group K_{bt} and Group L_b and Group L_{bt} specimens were examined, no significant differences were indicated as the 95% confidence intervals overlapped.

4.3.3 Three-point flexure modulus

4.3.3.1 Standard mode

When using the 8mm 'Turbo' tip diameter the mean three-point flexure moduli and associated standard deviations for Z100™ (Group I_{st}) were 13.2 ± 1.2GPa, Filtek™ Z250 (Group J_{st}) were 11.3 ± 0.9GPa, Filtek™ P60 (Group K_{st}) were 12.7 ± 1.3GPa and Filtek™ Supreme XT (Group L_{st}) were 10.3 ± 0.7GPa. The range of three-point flexure moduli varied from a low of 11GPa to a high of 16GPa (Group I_{st}), from 10 to 12GPa (Group J_{st}), from a minimum of 10GPa to a maximum of 16GPa (Group K_{st}) and from a low of 5GPa to a high of 12GPa (Group L_{st}), respectively (Table 4.13).

4.3.3.1.1 Statistical analysis

Multiple comparisons of the group means for the three-point flexure modulus data were made utilising a one-way ANOVA and Tukey's multiple range tests at a significance level of $P<0.05$ for the RBCs investigated (Z100™, Filtek™ Z250, Filtek™ P60 and Filtek™ Supreme XT) with tip diameters of 8mm and 8mm 'Turbo' at irradiances of 640 ± 18mW/cm^2 and 880 ± 18mW/cm^2 in standard mode, respectively. No significant differences in the group means of the three-point flexure strengths were identified when

employing the one-way ANOVA for Z100™ (F value=2.503; P=0.066), Filtek™ Z250 (F value=1.426; P=0.242), Filtek™ P60 (F value=2.546; P=0.062) and Filtek™ Supreme XT (F value=0.745; P=0.529)

Table 4.13: The range and mean three-point flexure moduli (associated standard deviations) for the RBC specimens irradiated using a QTH LCU in standard and boosted modes with the 8mm 'Turbo' tip diameter.

RBC	Property	8mm 'Turbo'	
		Standard	Boosted
Z100™	Three-point flexure modulus (GPa)	6.5 (1.5)	7.5 (1.7)
	Range of moduli (GPa)	5.8-7.2	6.2-8.8
Filtek™ Z250	Three-point flexure modulus (GPa)	10.7 (2.4)	10.6 (2.4)
	Range of moduli (GPa)	10.0-11.3	9.4-11.8
Filtek™ P60	Three-point flexure modulus (GPa)	10.4 (2.3)	11.8 (2.6)
	Range of moduli (GPa)	9.7-11.1	10.6-13.0
Filtek™ Supreme XT	Three-point flexure modulus (GPa)	16.1 (3.6)	15.0 (3.4)
	Range of moduli (GPa)	14.2-17.9	12.5-17.5

4.3.3.2 Boosted mode

The range of three-point flexure moduli with the 8mm 'Turbo' tip diameter varied for Z100™ from a low of 12GPa to a high of 17GPa (Group I_{bt}), Filtek™ Z250 from 10 to 13GPa (Group J_{bt}), Filtek™ P60 from a minimum of 10GPa to a maximum of 15GPa (Group K_{bt}) and Filtek™ Supreme XT from a lowest value of 9GPa to a highest value of 12GPa (Group L_{bt}). The mean three-point flexure moduli and associated standard deviations for the RBC materials investigated were 14.1 ± 1.1GPa for Group I_{bt}

specimens, 11.6 ± 0.7GPa for Group J_{bt} specimens, 12.8 ± 1.1GPa for Group K_{bt} specimens and 9.9 ± 1.0GPa for Group L_{bt} specimens, respectively (Table 4.13).

4.3.3.2.1 Statistical analysis

For each of the RBCs investigated (Z100™, Filtek™ Z250, Filtek™ P60 and Filtek™ Supreme XT), a one-way ANOVA and Tukey's multiple range tests at a significance level of $P<0.05$ was used to make multiple comparisons of the group means for the three-point flexure modulus data at irradiances of 790 ± 18mW/cm^2 and 1040 ± 28mW/cm^2 with an 8mm and 8mm 'Turbo' tip diameters, respectively. When Z100™ was irradiated the group means of the three-point flexure modulus data identified no significant differences when utilising the one-way ANOVA (F value=2.503; P=0.066). Similarly analysis of the group means of the three-point flexure modulus data for Filtek™ Z250 indicated no significant differences in the one-way ANOVA (F value=1.426; P=0.242). No significant differences in the group means of the three-point flexure modulus data were identified for Filtek™ P60, when utilising the one-way ANOVA (F value=0.2.546; P=0.062). The group means of the three-point flexure modulus data for Filtek™ Supreme XT when analysed also highlighted no significant differences in the one-way ANOVA (F value=0.745; P=0.529).

4.3.4 Vickers hardness testing

Vickers hardness measurements were made to investigate the influence of the operating output intensity during specimen manufacture when using the modified ISO 4049 overlapping irradiation regime.

4.3.4.1 Standard mode

4.3.4.1.1 Top

When using the 8mm 'Turbo' tip diameter to irradiate the RBCs, the mean Vickers hardness and associated standard deviations of the non-overlapped region on the top surface of Z100™, Filtek™ Z250, Filtek™ P60 and Filtek™ Supreme XT were 99.7 ± 2.6, 80.9 ± 1.7, 84.1 ± 1.3 and 71.5 ± 1.0, respectively. For the overlapped region the mean Vickers hardness and associated standard deviation for Z100™ was 100.8 ± 2.2, Filtek™ Z250 was 79.9 ± 2.4, Filtek™ P60 was 84.8 ± 1.5 and Filtek™ Supreme XT was 71.2 ± 1.4 (Table 4.14).

4.3.4.1.2 Bottom

For the RBC materials investigated the mean Vickers hardness and associated standard deviations of the non-overlapped region on the bottom surface when irradiated with the 8mm 'Turbo' tip diameter were 97.9 ± 2.8, 77.9 ± 2.8, 82.3 ± 2.4 and 70.8 ± 2.2 for

Z100™, Filtek™ Z250, Filtek™ P60 and Filtek™ Supreme XT, respectively. The mean Vickers hardness and associated standard deviations for the RBC materials investigated, namely Z100™ was 98.3 ± 2.8, Filtek™ Z250 was 78.7 ± 2.8, Filtek™ P60 was 81.8 ± 3.5 and Filtek™ Supreme XT was 70.6 ± 2.7 (Table 4.14).

Table 4.14: The non-overlapped and overlapped Vickers hardness data for the top and bottom surfaces for each RBC material when irradiated with the 8mm 'Turbo' tip diameter using the QTH LCU in standard and boosted modes.

RBC	Surface	Region	8mm 'Turbo'	
			Standard	Boosted
Z100™	Top	Non-overlapped	99.7 ± 2.6	102.6 ± 2.9
		Overlapped	100.8 ± 2.2	103.6 ± 1.3
	Bottom	Non-overlapped	97.9 ± 2.8	96.8 ± 2.7
		Overlapped	98.3 ± 2.8	97.8 ± 1.6
Filtek™ Z250	Top	Non-overlapped	80.9 ± 1.7	79.8 ± 4.4
		Overlapped	79.9 ± 2.4	79.8 ± 4.6
	Bottom	Non-overlapped	77.9 ± 2.8	73.8 ± 1.4
		Overlapped	78.7 ± 2.8	73.4 ± 1.4
Filtek™ P60	Top	Non-overlapped	84.1 ± 1.3	80.0 ± 4.3
		Overlapped	84.8 ± 1.5	80.3 ± 4.1
	Bottom	Non-overlapped	82.3 ± 2.4	73.8 ± 1.5
		Overlapped	81.8 ± 3.5	74.0 ± 1.7
Filtek™ Supreme XT	Top	Non-overlapped	71.5 ± 1.0	69.3 ± 1.3
		Overlapped	71.2 ± 1.4	69.0 ± 1.6
	Bottom	Non-overlapped	70.8 ± 2.2	62.8 ± 1.3
		Overlapped	70.6 ± 2.7	62.6 ± 0.9

4.3.4.1.3 Statistical analysis: standard mode: irradiance

Analysis of site × region was carried out using a two-way ANOVA within each RBC for both the top and bottom surfaces. No significant differences in the Vickers hardness data were evident for site therefore the Vickers hardness data was pooled and site eliminated from the analysis. The three-way ANOVA (irradiance × surface × region) highlighted no significant differences with the effect of region for Z100™ ($P=0.161$), Filtek™ Z250 ($P=0.444$), Filtek™ P60 ($P=0.975$) and Filtek™ Supreme XT ($P=0.714$) and irradiance for Z100™ ($P=0.347$), Filtek™ Z250 ($P=0.522$), Filtek™ P60 ($P=0.147$) and Filtek™ Supreme XT ($P=0.300$). However, the effect of surface highlighted a significant difference for all RBCs investigated ($P<0.0001$).

4.3.4.2 Boosted mode

4.3.4.2.1 Top

For the RBC materials, Z100™, Filtek™ Z250, Filtek™ P60 and Filtek™ Supreme XT, the mean Vickers hardness and associated standard deviations of the non-overlapped region on the top surface when irradiated with the 8mm 'Turbo' tip diameter were 102.6 ± 2.9, 79.8 ± 4.4, 80.0 ± 4.3 and 69.3 ± 1.3, respectively. The mean Vickers hardness and associated standard deviations for the overlapped region of Z100™ were 103.6 ± 1.3, Filtek™ Z250 were 79.8 ± 4.6, Filtek™ P60 were 80.3 ± 4.1 and Filtek™ Supreme XT were 69.0 ± 1.6 (Table 4.14).

4.3.4.2.2 Bottom

The mean Vickers hardness and associated standard deviations of the non-overlapped region on the bottom surface irradiated with the 8mm 'Turbo' tip diameter were 96.8 ± 2.7, 73.8 ± 1.4, 73.8 ± 1.5 and 62.8 ± 1.3, respectively. For the overlapped region the mean Vickers hardness and associated standard deviation for Z100™ were 97.8 ± 1.6, Filtek™ Z250 were 73.4 ± 1.4, Filtek™ P60 were 74.0 ± 1.7 and Filtek™ Supreme XT were 62.6 ± 0.9 (Table 4.14).

4.3.4.2.3 Statistical analysis: boosted mode: irradiance

For each RBC material and both top and bottom surfaces a two-way ANOVA (site × region) was conducted. Since no effect of site was evident the Vickers hardness data was pooled and site eliminated from the analysis. A three-way ANOVA (irradiance × surface × region) undertaken highlighted no significant differences with the effect of region for Z100™ (P=0.405), Filtek™ Z250 (P=0.776), Filtek™ P60 (P=0.573) and Filtek™ Supreme XT (P=0.266) and irradiance for Z100™ (P=0.426) and Filtek™ P60 (P=0.608). However, a significant effect for irradiance was indicated for Filtek™ Z250 (P=0.016) and Filtek™ Supreme XT (P=0.001). In addition, the effect of surface for Filtek™ Z250 (P<0.0001), Filtek™ P60 (P<0.0001) and Filtek™ Supreme XT (P<0.0001) indicated significant differences.

4.4 ISO4049: The influence of LED LCU irradiance

4.4.1 Three-point flexure strength

4.4.1.1 Statistical analysis Elipar™ Freelight

No significant differences in the group means of the three-point flexure strength data was identified when irradiated at 151 ± 18 and 246 ± 15mW/cm^2 (tip diameters of 13 and 8mm, respectively) with the Elipar™ Freelight LED LCU utilising the one-way ANOVA for Z100™ (F value=0.368; P=0.776), Filtek™ Z250 (F value=5.063; P=0.053), Filtek™ P60 (F value=2.067; P=0.112) and Filtek™ Supreme XT (F value=2.871; P=0.062).

4.4.1.2 Statistical analysis: Elipar™ Freelight 2

When the RBCs examined were irradiated at irradiances of 769 ± 65 and 1160 ± 60mW/cm^2 (tip diameters of 13 and 8mm, respectively) with the Elipar™ Freelight 2 LED LCU, no significant differences in the group means of the three-point flexure strength data was identified utilising the one-way ANOVA for Z100™ (F value=0.368; P=0.776), Filtek™ Z250 (F value=5.063; P=0.053), Filtek™ P60 (F value=2.067; P=0.112) and Filtek™ Supreme XT (F value=2.871; P=0.062).

4.4.2 Three-point flexure modulus

4.4.2.1 Statistical analysis: Elipar™ Freelight

No significant differences in the group means of the three-point flexure moduli were identified when irradiated at 151 ± 18 and 246 ± 15mW/cm^2 (tip diameters of 13 and 8mm, respectively) with the Elipar™ Freelight LED LCU utilising the one-way ANOVA for Z100™ (Group Q_I and Group U_I) (F value=2.460; P=0.069), Filtek™ Z250 (Group R_I and Group V_I) (F value=0.985; P=0.404), Filtek™ P60 (Group S_I and Group W_I) (F value=1.276; P=0.289) and Filtek™ Supreme XT (Group T_I and Group X_I) (F value=1.830; P=0.149).

4.4.2.2 Statistical analysis: Elipar™ Freelight 2

When the RBCs materials investigated were irradiated at 769 ± 65 and 1160 ± 60mW/cm^2 (with tip diameters of 13 and 8mm, respectively) with the Elipar™ Freelight 2 LED LCU, no significant differences in the group means of the three-point flexure moduli were identified utilising the one-way ANOVA for Z100™ (F value=2.460; P=0.069), Filtek™ Z250 (F value=0.985; P=0.404), Filtek™ P60 (F value=1.276; P=0.289) and Filtek™ Supreme XT (F value=1.830; P=0.149).

4.4.3 Vickers hardness

4.4.3.1 Statistical analysis: Elipar™ Freelight

For each RBC material and both top and bottom surfaces a two-way ANOVA (site × region) was conducted. No significant differences in the Vickers hardness data were evident for site therefore the Vickers hardness data was pooled and site eliminated from the analysis. The three-way ANOVA (irradiance × surface × region) highlighted no significant differences with the effect of region for Z100™ (P=0.268), Filtek™ Z250 (P=0.939), Filtek™ P60 (P=0.368) and Filtek™ Supreme XT (P=0.346) and irradiance for Z100™ (P=0.347), Filtek™ Z250 (P=0.522), Filtek™ P60 (P=0.147) and Filtek™ Supreme XT (P=0.300). However, the effect of surface highlighted a significant difference (P<0.0001).

4.4.3.2 Statistical analysis: Elipar™ Freelight 2: irradiance

Analysis of site × region was carried out using a two-way ANOVA within each RBC and for both top and bottom surfaces. Since no effect of site was evident the Vickers hardness data was pooled and site eliminated from the analysis. A three-way ANOVA (irradiance × surface × region) undertaken highlighted no significant differences with the effect of region for Z100™ (P=0.749), Filtek™ Z250 (P=0.179), Filtek™ P60 (P=0.908) and Filtek™ Supreme XT (P=0.274). In addition, significant effects of irradiance were indicated for Z100™, Filtek™ Z250, Filtek™ P60 and Filtek™ Supreme XT (P<0.0001)

and the effect of surface for Z100™, Filtek™ Z250, Filtek™ P60 and Filtek™ Supreme XT also indicated significant differences ($P<0.0001$).

CHAPTER 5 Discussion

5.1 QTH

5.1.1 Irradiance

When an 8mm 'Turbo' tip diameter was used in standard and boosted modes the irradiances were increased compared with when a conventional 8mm tip diameter was employed. The light guides themselves consist of fused hexagonal fibres which run from the adit (the LCU side) to the exit (the LCU tip). The adit diameter of the 8mm 'Turbo' tip diameter was 12.1mm compared with an adit diameter of 7.4mm for the conventional 8mm tip diameter. The adit diameter of the latter being modified with a metal sleeve to limit the irradiance going into the hexagonal fibres of the LCU light guides. The similar diameters of the 8mm 'Turbo' and 8mm conventional exit windows, means in short, that the broader adit diameter of the 8mm 'Turbo' tip will capture and therefore emit more irradiance at the proximal portion of the light cone generated. This results in the associated increase in irradiance with the 8mm 'Turbo' tip diameter compared with the conventional 8mm tip diameter identified in the current study. The increase in irradiance in boosted compared with standard mode is a result of the manufactures increasing the current available to the LCU power source with the associated increase in irradiance reported in Section 4.1.

5.1.2 Tip diameter

The assessment of the irradiance of the QTH LCU with tip diameters of 13, 11, 8 and 25mm identified consistent results in standard and boosted modes. Examination of the 13, 11 and 8mm light tip guides with an optical microscope (Measuring microscope MM-40, Nikon, Japan) revealed a 14mm adit diameter. The hexagonal fibres run from the adit to the exit window, however, to control the level of irradiance captured and therefore emitted at the proximal portion of the light cone generated, the effective adit diameter was modified with a metal sleeve together with a modification of the dimensions of the hexagonal fibres of the LCU light guides.

In reality the 13, 11 and 8mm adit diameters were 12.1. 10.3 and 7.4mm. In addition, the variation in the fibre spacing and fibre diameter at the adit of the 13mm tip diameter were 26.8 and 184μm, respectively compared with 36.9 and 278μm and 14.3 and 119μm, respectively for 11 and 8mm tip diameters, respectively. Additionally, the fibre spacing and fibre diameter at the exit of the 13mm tip diameter were 26.7 and 191μm, respectively compared with 34.5 and 280μm for the 11mm tip diameter, respectively and 15.0 and 115μm for the 8mm tip diameter, respectively. Larger tip diameters would be expected to result in a reduction in the irradiance compared with the smaller tip diameters (Leonard et al., 1999, Liberman et al., 1990). However, the similar irradiances demonstrated with the 13, 11, and 8mm tip diameters were achieved by the manufacturer by controlling the amount of light entering the adit side of the LCU tips together with modifying the number and dimensions of the hexagonal fibres in the LCU tips. Therefore,

all the tip diameters used with the QTH LCU were just as effective in the irradiances they generated.

5.2 LED

5.2.1 Irradiance

When the irradiance of the two LED LCUs investigated were measured with the same tip diameter different irradiances were identified. The idea that LED LCUs would replace QTH LCUs and become commonplace in dental surgeries worldwide within 10 years was boldly proposed in a letter to the British Dental Journal in 1995 by Mills (1995) depite the fact that the technology was not yet available. The transformation of the idea to reality did not come about by accident with many technological challenges having to be overcome. The low powered blue LEDs available in 1995 were based on silicon carbide technology with an output of 7μW per LED available (Mills et al., 1999). The problem was overcome in part with the development of an LED based on gallium-nitride technology with over 400 times more output power (3mW per LED) (Nakamura et al., 1995) such that by 2002 prototype LED LCUs with irradiances similar to QTH LCUs (in excess of 500mW/cm^2) were developed. The performance of these prototype LED LCUs is well reported in the dental literature and polymerised RBCs with reported inferior depth of cure (penetrometer assembly) (Harrington and Wilson, 1993; Uhl et al., 2003), similar depth of cure (Barol hardness) (Mills et al., 2002), similar compressive fracture strengths (Mills et al., 2002) and Knoop hardness values (Uhl et al., 2003). The variously

reported data was a combination of the rapid development from 27 blue LEDs to in excess of 63 LEDs per LCU resulting in an associated increase in irradiance with the further development of LED LCUs, the irradiation conditions namely, the exposure time and distance (Bennett and Watts, 2004), and the tip diameter of the light guide (Nitta, 2005). The technological advancements that occurred from the time the Elipar™ Freelight (a first generation) LED LCU was marketed consisting of 19 separate LEDs grouped in the head of the LCU, to the launch of the Elipar™ Freelight 2 consisting of a single more powerful LED resulted in the increase irradiance for the Elipar™ Freelight 2 employing a 13mm tip diameter (151 ± 18 to 769 ± 65mW/cm^2, respectively) or an 8mm tip diameter (246 ± 15 to 1160 ± 60mW/cm^2, respectively).

5.2.2 Tip diameter

The manufacturer's claimed irradiance for the Elipar™ Freelight (240mW/cm^2) and the Elipar™ Freelight 2 (1040mW/cm^2) LED LCUs appears to refer to the irradiance whilst employing the 8mm LCU tip diameter. The light guides themselves consist of fused hexagonal fibres which run from the adit (the LCU side) to the exit (the LCU tip) with tapers that are negative for the 8mm and positive for the 13mm tip diameters. The ratio between the outputs of the tip diameters are 1.63 for the Elipar™ Freelight and 1.51 for the Elipar™ Freelight 2. These values can be compared with the ratios of the LCU tip exit diameters (1.63) and the LCU tip exit areas (2.64). The fibre spacing and fibre diameter are 9.7 and 210μm, respectively are similar for the 8 and 13mm tip diameters at the adit end. However variations in fibre spacing and fibre diameter were evident when the exit

ends were compared for the 8mm negative taper (13.5 and 167μm, respectively) and the 13mm positive taper (17.0 and 276μm, respectively) tip diameters. This suggests that the complexities of the attenuation arising from negative fibre taper (roughly, as the square of the diameter ratio) (Duke, 2001) are such as to preclude simple predictions of irradiance. Even so, variations in irradiance across the LED tip exit window, with a central peak value, have been reported (Nitta, 2005), and the pattern also depends on the distance from the end of the fibres (Corcionali et al., 2008) as the optical behaviour is complicated. In short, narrower tip diameters at the exit window are prone to emit more irradiance (Corcionali et al., 2008) and illuminance (Nitta, 2005) at a distance of 5mm from the exit window to the RBC material resulting in the associated increase in irradiance with the 8mm tip diameter compared with the 13mm tip diameter.

5.3 Characterisation techniques: Mechanical properties

5.3.1 ISO 4049: 2000

For the range of testing methodologies employed to assess RBC performance and stated in ISO 4049 (The International Standard for Dentistry - polymer-based filling, restorative and luting materials (ISO 4049, 2000)) it is imperative that there is standardisation and reproducibility of the testing methodologies between test centres when evaluating RBCs using the ISO 4049 (ISO 4049, 2000) so that any material tested under ISO 4049 conditions should produce consistent test results.

The three-point flexure properties of RBC materials determined using the protocol set out in ISO 4049 (ISO 4049, 2000) involves the fabrication of rectangular bar-shaped specimens with length, width and height dimensions of 25 x 2 x 2mm, respectively. As the length of the rectangular-bar exceeds the LCU tip diameter, an overlapping light irradiation procedure is required. The efficiency of the overlapping irradiation regime has been questioned by a number of authors in the dental literature recently in terms of uncontrolled initiation on polymerisation (Mehl et al., 1997; Manhart et al., 2000), non-homogeneously cured specimens (Ferracane et al., 2003) and inconsistent polymerisation along the length of the bar-shaped specimen (Palin et al., 2003, 2005). Alternative irradiation methodologies including oven-LCUs (Peutzfeldt and Asmussen, 2000; Ferracane et al., 2003; Palin et al., 2005), the use of a scanning motion with a handheld-LCU along the length of the bar-shaped specimen (Mehl et al., 1997; Manhart et al., 2000) or employing a custom made fibre optic light guide enabling a 'one-hit' irradiation of the entire specimen (Musanje et al., 2001) have been advocated to control initiation on polymerisation and produce homogeneous specimens and consistent polymerisation along the length of the specimen.

5.3.2 LCU tip diameter

Mehl et al. (1997) and Manhart et al. (2000) advocated employing three LCUs placed along-side one another with no gaps between the LCU tip diameters to irradiate the three-point rectangular bar-shaped specimens in an effort to prevent uncontrolled initiation on polymerisation by avoiding the effect of light scattering. However, Mehl et al. (1997) and

Manhart et al. (2000) did not investigate the overlapping irradiation regime against their technique of employing three LCUs placed along-side one another and therefore it was not possible to assess whether their technique was beneficial in preventing uncontrolled initiation on polymerisation by avoiding the effects of light scattering. Ferrancane et al. (2003) also expressed concern that the overlapping irradiation regime would influence the homogeneity of the irradiated specimen. Ferracane et al. (2003) compared nine RBC materials irradiated using a Triad II (Caulk/Densply, Milford, DE, USA) oven-LCU with a QTH LCU and 'overall' the authors identified 'practically equivalent' three-point flexure properties when either the oven- or QTH LCUs were employed. Ferrancane et al. (2003) suggested the two irradiation methods were 'interchangeable' for most RBCs and advocated using the oven-LCU due to the time saving during specimen manufacture allowing for the simultaneous polymerisation of multiple specimens. Palin et al. (2003) suggested that the overlapping irradiation regime stipulated in ISO 4049 may result in inconsistent polymerisation along the length of the three-point flexure rectangular bar-shaped specimen thereby producing a different defect population to that expected for a 'one-hit' irradiation. These suggestions were further emphasised by Palin et al. (2005) when the three-point flexure strength data from an overlapping irradiation regime with a handheld QTH LCU was compared with a single exposure Visio-Beta (3M ESPE, Seefeld, Germany) oven-LCU. Although equivalent three-point flexure strengths were achieved, the authors highlighted a significant reduction in the reliability of the three-point flexure strength data when an overlapping irradiation regime was employed.

Palin et al. (2005) proposed that residual tensile stresses were created by the overlapping irradiation regime and therefore a non-homogenous polymerisation stress distribution existed along the length of the bar-shaped specimens which was manifested as a reduction in the reliability of the flexure strength data, namely the Weibull modulus. A range of light tip diameters are currently available to dental practitioners ranging from 8 to 13mm. Consequently, the 8, 11 and 13mm tip diameters would require nine, seven and five overlapping irradiations on each side of the specimen to adequately polymerise the 25mm length of the ISO bar-shaped specimens according to the standard protocol. In the current study, to exacerbate the potential for uncontrolled initiation on polymerisation and decrease the homogeneity of polymerisation along the length of the specimen, the exit window was moved by three-quarters (not half) the diameter along the specimen so that some areas received twice the irradiation of adjacent areas. Additionally, to further exacerbate the potential for a non-homogenous polymerisation stress distribution along the length of the specimens, irradiation was from the top surface only resulting in five, four and three overlapping irradiations with the 8, 11 and 13mm tip diameters, respectively. Accordingly, decreasing the LCU tip diameter (from 13 to 11 and 8mm) would be expected to progressively decrease the efficiency of the polymerisation process along the length of the RBC specimens compared with a 'one-hit' irradiation (25mm tip diameter). This would be expected to be manifested as a reduction in the reliability of the three-point flexure strength data if the theory proposed by Palin et al. (2005) regarding residual tensile stress generation were to hold true.

However, when the reliability of the three-point flexure strength data was analysed for the four RBCs tested, no change in the reliability of the three-point flexure strength data was evident when irradiated using tip diameters of 13, 11, 8 and 25mm with the QTH LCU at the two irradiances investigated (Table 4.2). In addition, similar Weibull moduli and associated 95% confidence intervals were achieved following irradiation with the LED LCUs regardless of the tip diameter (8 or 13mm) employed (Table 4.7). It is therefore evident that the previously theory proposed by Palin et al. (2003, 2005) was not entirely correct. If the central region of the bar-shaped specimen is irradiated and the gel-point reached, the setting stresses are accommodated by the adjacent resin-ends which are only partially-irradiated by light scattering (Mehl et al., 1997; Manhart et al., 2000). Palin et al. (2005) postulated that when the partially irradiated end regions are irradiated that the associated post-gel shrinkage stresses place the central region under tensile stress. If the proposed theory was correct then increasing the number of overlapping irradiations (decreasing the light tip diameter) would be expected to progressively decrease the homogeneity of the irradiated bar-shaped specimens resulting in an increased irradiation variability. The irradiation variability would be expected to result in a reduction in the reliability of the three-point flexure strength data, manifested as non-overlapping associated 95% confidence intervals, which did not occur in the current study for the QTH (Table 4.2) or LED (Table 4.7) LCUs.

In addition, Palin et al. (2003) suggested the strength data generated using the overlapping regime was partially dependent on the relative shrinkage constraints. In the study by Palin et al. (2003) only one material was used (Filtek™ Z250), however, in the

current study four methacrylate RBCs with markedly varying shrinkage characteristics were employed and no shrinkage constraint effect was observed.

Additionally, no effect due to overlapping, which corresponds to a doubling of the irradiation time at such sites, on Vickers hardness was detected. It can be concluded that the recommended irradiation times, per spot, effectively put the material on the 'plateau' of the response surface, and it is expected then not to show any further change on prolonged irradiation (Musanje and Darvell, 2003). Even so, it should be noted that there is unavoidably much scatter occurring within the material such as, firstly, to make the distinction between regions unsharp and, secondly, make any such effect (if one did exist) at the lower surface even less obvious: the effectively irradiated area must be larger than the tip diameter. While this does not provide such a strong test of doubled exposure time as might be desired, it provides strong confirmation that there is no detriment to the specimens from overlapping irradiation sites, on the assumption that 'full' irradiation is desired, and confidence both that the modified ISO 4049 irradiation methodology is sound thereby implying the ISO 4049 irradiation methodology is also sound. As a result from a clinical point of view, extra irradiation is sensible should doubt about the adequacy of the exposure arise for any reason. Incidentally, variation in irradiance across the exit window can be expected to be of relatively little significance, given the scatter that occurs. An overall value is therefore probably adequate for characterisation, greater detail being pointless.

There was, however, a highly-significant difference between the top and bottom surfaces indicating that attenuation over the depth of the specimen was enough to lead to 'incomplete' polymerisation on the bottom, taking note of the failure to detect a difference between non-overlapped and overlapped regions on the top surface, where it would be most expected to show. The constant, presumably 'saturated' result for the top surface contrasts markedly with the bottom surface, noting that saturation was not attained even at the highest irradiance for that thickness (2mm), *i.e.* at the bottom of the recommended maximum increment. It is apparent that the plateau value cannot be expected at the bottom of such an increment, even allowing for the multiple exposures that occurred from scatter unless the top surface irradiance is appreciably increased. Whether longer exposure will compensate, as might be expected, but this does indicate that the ISO protocol, with bottom surface irradiation, could achieve greater uniformity. In any case, the recommended maximum increment thickness, for the recommended exposure, is excessive, and more realistic values, as discussed elsewhere (Musanje and Darvell, 2006) are necessary, noting that inadequate depth of full cure compromises the restoration but that this is not detectable clinically.

5.3.2.1 Summary: tip diameter

The efficiency of the overlapping irradiation regime in ISO 4049 has been questioned by a number of authors in the dental literature recently (Mehl et al., 1997; Ferrancane et al., 2003; Palin et al., 2003, 2005). The authors postulated that alternative irradiation methodologies including oven-LCUs (Peutzfeldt and Asmussen, 2000; Ferracane et al.,

2003, 2005), the use of a scanning motion with a handheld-LCU along the length of the bar-shaped specimen (Mehl et al., 1997; Manhart et al., 2000) or employing a custom made fibre optic light guide enabling a 'one-hit' irradiation of the entire specimen (Musanje et al., 2001) would control initiation on polymerisation and produce homogeneous specimens and consistent polymerisation along the length of the specimen. The objective of the current study was to investigate light irradiation variables (tip diameter, irradiance, irradiation protocol and LCU) on the flexural strength, flexural modulus and Vickers hardness of four RBCs. The hypothesis tested was that the flexural strength, flexural modulus and the Vickers hardness for the RBCs would be similar regardless of the irradiation variables and the internal control for the investigations was the 25mm custom made fibre optic light guide.

In the current study the irradiation protocol in ISO 4049 was modified to exacerbate the potential for uncontrolled initiation on polymerisation and decrease the homogeneity of polymerisation along the length of the specimen postulated previously. The efficacy of the modified overlapping irradiation regime was upheld for the conditions tested (tip diameter, irradiance, irradiation protocol, LCU). No manifestations of uncontrolled initiation on polymerisation, decreased homogeneity and consistency of polymerisation along the length of the specimen for four methacrylate RBCs were evident. It is suggested that while novel irradiation techniques such as oven-LCUs (Peutzfeldt and Asmussen, 2000; Ferracane et al., 2003; Palin et al., 2005), the use of a scanning motion with a handheld-LCU along the length of the bar-shaped specimen (Mehl et al., 1997; Manhart et al., 2000) or employing a custom made fibre optic light guide enabling a 'one-hit'

irradiation of the entire specimen (Musanje et al., 2001) do not provide for controlled initiation on polymerisation or produce more homogeneous specimens with consistent polymerisation along the length of the specimen.

5.3.3 Light energy density

In general, when assessing the flexure properties of RBCs, researchers routinely quote flexure strength, flexure modulus and Vickers hardness values determined following the delivery of a specific irradiance for a predetermined time period (Mehl et al., 1997; Unterbrink and Muessner, 1995; Miyazaki et al., 1996; Asmussen and, Peutzfeldt, 2004) while few authors quote the energy density delivered at the specific irradiance (Ferracane et al., 2003; Palin et al., 2005; Calherios et al., 2006). The conventional wisdom regarding the total energy delivered, namely the energy density (J/cm^2), is calculated from the irradiation time (t) with a LCU of a specific irradiance (I). However, the irradiation of a photo-sensitised RBC results primarily (and inefficiently) in the formation of an excited state photo-sensitiser molecule which after several (inefficient) steps, including diffusion to react with the amine initiator, may result in the formation of a free radical which can initiate a polymerisation chain reaction. Both the photo-sensitiser and the amine must be present at low concentrations for reasons of colour, strength and stiffness, but this makes the rate of free radical production low, and thus the rate of initiation (Yoshida and Greener, 1994; Venhoven et al., 1996). However, the mobility of the amine free radical species means that mutual annihilation can dominate chain initiation if the concentration rises too high, and likewise the termination of live chains.

Mutual reaction of live chains is of low probability because of their relatively low diffusibility, with polymerisation relying on the higher mobility of monomer to permit the reaction to proceed, remembering that continuation of the polymerisation occurs long after irradiation has ceased for this very reason: light only initiates the first stage of the process (Musanje and Darvell, 2006). Hence, too great a rate of amine radical production is counterproductive, leading to loss of polymerisation initiating radicals and the termination of existing chains (Venhoven et al., 1996) which is expected to adversely influence strength, stiffness and hardness (Ferracane and Greener, 1986).

There is a second factor. The CQ (or other photo-sensitiser) must first be excited from the ground state, CQ^0, to the so-called excited singlet state, CQ* (by the absorption of one quantum of light) before it can be converted to the active form, the triplet state, CQ^T. This is essentially a random and low probability event, but the rate of which is proportional to the concentration of CQ*. The rate of formation of radicals is proportional to both the concentration of CQ^T and the amine. The rate of formation of CQ* depends on the concentration of CQ^0 and the irradiance, but total CQ = CQ^0 + CQ* + CQ^T (ignoring for the moment the consumption of the CQ by the process of radical production). Thus, since the rate of formation of CQ* is proportional to CQ^0 at a given irradiance, this becomes less efficient as the irradiance is raised. Indeed, it leads to an exponentially asymptotic approach to saturation (in the absence of any consumption) such that it is only at (relatively) low irradiances that an approach to a simple proportionality between the concentration of CQ* (and thus the rate of production of CQ^T) can be made. Thus,

fundamentally, no such system can show proportionality in any respect to irradiance, although it does, in the limit, approximate this at low irradiance.

It must be noted, however, that the CQ supply is limited, and this is indeed consumed by the process of radical production. That is, for a constant irradiation, the rate of production of radicals must fall, and eventually cease, whereupon further irradiation can have no further effect (Tirtha et al., 1982). It follows then that adding in the effect of the mutual annihilation of radicals, when deterioration in mechanical properties must ensue, leads to the conclusion that reciprocity is an impossibility except as the limiting behaviour at low irradiance and low CQ and amine concentrations, that is, doubling irradiance is not equivalent to doubling exposure time. The question of importance, nevertheless, is at what magnitude of irradiance does this reciprocity failure become of practical importance. Effectively, as this is a trade-off between the rates of polymerisation reaction initiation and annihilation of radicals, the expectation is of a peak in the value of the mechanical property of interest as a function of irradiance. This is not the case but an approach to the plateau value with respect to time is evident, as shown in the results of Musanje and Darvell (2003).

There is, in any case, a maximum value for the strength, stiffness and hardness that may be attained for any material, nominally corresponding to complete conversion of all monomer double bonds to network-contributory single bonds. In practice, this is not attainable as vitrification effectively brings reactions to a halt through inhibition of diffusion. The maximum conversion of double bonds is typically between about 40 and

70% in hand. Thus there is an asymptotic approach to the maximum attainable values of such mechanical properties (at a given temperature). Further irradiation, whether by increasing irradiance or exposure time, cannot change this. This point is demonstrated clearly in the study by Peutzfeldt and Asmussen (2000) where the authors investigated the effects of post-irradiation methods on the mechanical properties including three-point flexure strength for two RBC materials one of which was Z100™ which was used in the current study. Following initial irradiation with an 8mm tip diameter at an irradiance of 480mW/cm^2 the authors employed post-irradiation techniques ranging from 10 minutes in a Triad II (Caulk/Densply, Milford, DE, USA) oven-LCU to a conventional heat oven (Heraeus, Hanau, Germany). While the degree of conversion for Z100™ was increased with post-irradiation, this was not reflected in the three-point flexure strengths achieved which would appear to preclude post-irradiation as an effective means of improving the mechanical properties of Z100™.

In line with the conventional wisdom regarding energy densities, energy densities ranging from 12.8 to 41.6J/cm^2 were employed in the current study with the results indicating no significant differences between the three-point flexure strengths of the four RBCs investigated. The differences in the three-point flexure strength data reported in the dental literature for the RBCs investigated in the current study varied from 79-184MPa for Z100™ MP Restorative (Peutzfeld and Asmussen, 2000; Cesar et al., 2001; Yap et al., 2002; Adabo et al., 2003; Palin et al., 2003; Beun et al., 2007), 92-245MPa for Filtek™ Z250 (Ferracane et al., 2003; Mitra et al., 2003; Palin et al., 2003; Yap et al., 2003; Palin et al., 2005; Calherios et al., 2006), 138-170MPa for Filtek™ P60 (Adabo et al., 2003;

Ferracane et al., 2003) and 113-153MPa for Filtek™ Supreme XT (Mitra et al., 2003; Beun et al., 2007). The three-point flexure modulus data reported in the dental literature varied from 5.8-17GPa for Z100™ MP Restorative (Unterbrink and Muessner, 1995; Miyazaki et al., 1996; Choi et al., 2000; Peutzefeldt and Asmussen, 2000; Stahl et al., 2000; Asmussen and Peutzefeldt, 2004; Beun et al., 2007), 8.4-14GPa for Filtek™ Z250 (Musanje et al., 2004; Walker et al., 2005; Calheiros et al., 2006), 10-18GPa for Filtek™ P60 (Papadogiannis et al., 2008) with little published data available for Filtek™ Supreme XT (Beun et al., 2007; Papadogiannis et al., 2008).

The variously reported three-point flexure properties were reported to be indicative of the degree of conversion (Ferracane et al., 2003; Calherios et al., 2006), irradiance (Miyazaki et al., 1996; Calherios et al., 2006), type of mould (Peutzfeld and Asmussen, 2000; Palin et al., 2003; Beun et al., 2007) and light source (Ferracane et al., 2003; Palin et al., 2003; Palin et al., 2005) employed although different operators would be expected to manipulate the materials differently as well. Examination of the three-point flexure strength and three-point flexure modulus data in the dental literature following evaluation of the total energy density delivered for these studies suggests no significant differences for Z100™ at energy densities of 12J/cm^2 delivered for 30s at 400mW/cm^2, 60s at 200mW/cm^2 or 120s at 100mW/cm^2 (Miyazaki et al., 1996). In addition, Asmussen and Peutzfeldt (2004) identified no significant differences in the three-point flexure strength and three-point flexure modulus data when Z100™ was irradiated at energy densities of 15.5-23 J/cm^2, using either a single or two-step light irradiation regime. Palin et al. (2005) identified no significant differences in the three-point flexure strength data for

Filtek™ Z250 for an equivalent energy density of 14J/cm^2 from a handheld- and oven-LCUs. Ferracane et al. (2003) identified 'practically equivalent' three-point flexure strength and three-point flexure modulus data using a handheld- and oven-LCU for approximate energy densities of 24 and 8.8J/cm^2, respectively for a range of RBCs. Interestingly, Utterbrink and Muessner (1995) identified a significant reduction in the three-point flexure strength and three-point flexure modulus data for Z100™ irradiated for energy densities of 18 and 10J/cm^2, respectively. Calheiros et al. (2006) investigated the three-point flexure strength and three-point flexure modulus of Filtek™ Z250 irradiated for energy densities of 6, 12, 24 and 36J/cm^2. The authors identified no significant differences in the three-point flexure modulus data for Filtek™ Z250 but a significant reduction in the flexure strength when irradiated at energy densities of 6 and 12J/cm^2 compared with 24 and 36J/cm^2.

In line with the discussion of the flexure properties, that reciprocity between irradiance and time does not hold, the Vickers hardness results can be explained. The non-significant differences in the non-overlapped and overlapped regions on the top and bottom surfaces are self-explanatory based on the irradiance exceeding the influence of shade, monomeric reactivity, refractive index mismatch, light scattering and absorption (Shortall et al., 2008). However, the current study employed specimens of a 2mm depth and higher irradiance has been shown to result in an increased Vickers hardness on the bottom surface resulting in the significant Vickers hardness differences encountered in the current study between the top and bottom surfaces.

Inadequate polymerisation of RBC materials can result in reduced three-point flexural properties but in the current study reducing the irradiance from 1040 to 240mW/cm^2 had no significant impact on the flexure properties. However, variations were evident when the Vickers hardness data following irradiation using the QTH LCU in standard or boosted mode were examined as a result of the increased irradiance. Additionally, variations were evident when the LED Vickers hardness data following irradiation with 8 and 13mm LCU tip diameters were examined as a result of the increased irradiance due to the negative and positive taper of the light guides, respectively. A bottom to top hardness value of 80–90% has previously been suggested as an indicator for the minimum depth of cure to be acceptable (Skeeters et al., 1983; Johnston et al., 1985; Yearn, 1985). However, this value has been the subject of considerable controversy amongst dental material scientists and clinicians alike in terms of the clinical significance of a bottom to top hardness value of 80–90%. Previous studies have reported that reducing the depth of cure of RBC materials is manifested as a decrease in the surface hardness (Cook, 1980; Baharav et al., 1988; Rueggeberg et al., 1994; Price et al., 2002). For reduced exposure periods the concentration of unexcited CQ molecules decreases with distance from the irradiation source within the RBC specimens following the cessation of light irradiation. With increasing specimen thickness, fewer photons are able to reach the CQ molecules within the resin and as a result fewer molecules are activated and raised to the 'triple' (excited) state. Therefore at reduced light exposure periods, the quantity of CQ molecules at the lower surface of the specimen in the triplet state that are able to collide with an amine will be reduced and as a result are incapable of producing free radicals to initiate polymerisation. Thus, an increase in irradiance for a constant

irradiation time would be expected to result in an increase in the Vickers hardness of the bottom and top surfaces (Pilo and Cardash, 1992). These studies further emphasise that there is an asymptotic approach to the maximum attainable values of three-point flexure strength and three-point flexure modulus data (at a given temperature) and further emphasise that the relationship between the development of mechanical properties with energy density, namely irradiance and time is not linear (Musanje and Darvell, 2003; Asmussen and Peutzfeld, 2005).

5.3.3.1 Summary: irradiance

The Vickers hardness data indicated that for each LCU and tip diameter utilised there was no significant difference between the non-overlapped and overlapped regions on the top surface. However, there were significant differences highlighted between the non-overlapped and overlapped regions on the bottom surface (compared with the corresponding region on the top surface) at the range of intensities investigate with the LCU tip diameters employed. However, the differences in Vickers hardness data with varying irradiances did not influence the flexural properties of each of the RBC materials investigated. These results from the current investigation further emphasise that the relationship between the development of three-point flexure properties and Vickers hardness with energy density, namely irradiance and time is not linear (Musanje and Darvell, 2003; Asmussen and Peutzfeld, 2005). In addition, the current study provides confidence both that the ISO method is sound and that, clinically, extra irradiation is sensible should doubt about the adequacy of the exposure arise for any reason.

5.3.4 RBC material

The polymerisation process for light activated RBCs involves a complex series of interactions which can be influenced by the resin photo-activation system (Cook, 1982), the LCU spectral distribution (Pradhan et al., 2002; Obici et al., 2005) and the energy density (J/cm^2) (Peutzfeld and Asmussen, 2005). In the current study, RBCs from the same manufacturer were chosen to ensure the same photo-activation system was employed, namely CQ and the LCUs used produced specific irradiances (I) for specific irradiation times (t) to provide discrete energy densities. Differences between materials require no elaboration as the effects of formulation have been discussed at length elsewhere in the literature. The RBCs (Filtek™ Z250, Filtek™ P60 and Filtek™ Supreme XT) were chosen as the same monomeric constituents were present with similar filler loadings (although different packing fraction designs) was to insure that the effects being measured were mostly related to the variables of light curing (tip diameter, irradiance, irradiation protocol, LCU) and not to the compositions of the RBCs. As expected increasing filler content resulted in improved three-point flexure strength and flexure modulus data for Filtek™ Z250, Filtek™ P60 and Filtek™ Supreme XT given the monomeric constituents. Z100™ despite the higher filler volume (66%), the increased TEGDMA concentration in the monomeric constituents resulted in decreased flexural strength and increased brittleness (elastic modulus) compared with Filtek™ Z250, Filtek™ P60 and Filtek™ Supreme XT. Similarly, as the indentation hardness is dependent upon the monomeric constituents involved in polymerisation, filler particle size, shape and volume, type and density of cross linking and degree of conversion

(Musanje and Darvell, 2006) the Vickers hardness results reported are therefore material specific.

5.3.5 Implications for further research

Within the limitations of the experiment (specimen thickness, RBC shade, photo-activation system, irradiances chosen, LCU) tip diameter, irradiance and irradiation protocol had no influence on three-point flexural strength and modulus data although there are some clinical implications which are further addressed in Part II of the current study.

PART II

THE INFLUENCE OF IRRADIATION DISTANCE ON RESIN-BASED COMPOSITE PERFORMANCE

CHAPTER 6 Introduction

In Part I of the current study the RBCs were irradiated directly from the top surface to a maximum depth of 2mm. Clinically, the influence of shade, monomeric reactivity, refractive index mismatch, light scattering and absorption all have an impact on the irradiance available to the RBC (Shortall et al., 2008). The clinical recommendation most commonly quoted involves holding the LCU tip 1mm from the top surface of the RBC (Swartz et al., 1983; Pires et al., 1993; Kanca, 1995) as irradiance decreases with distance. However, close proximity is not always possible, particularly in the case of class II restorations where interproximal boxes exceed 7mm in depth, since the placement of the gingival increment has a negative correlation between irradiance delivered and the depth of the cavity, (Sakaguchi and Berge, 1998). Although clear matrix bands and wedges have been developed to enable irradiance to access previously inaccessible areas, other factors such as reflectance of the dentine and enamel are more difficult to assess. The range of RBC placement variables highlighted leads to a significant reduction in irradiance delivered to the RBC which may have implications for strength and modulus development when irradiated with the LCUs employed in the current study. In addition, the problem is further compounded for QTH LCUs where clinical studies (Barghi et al., 1994; Martin et al., 1998; Pilo et al., 1999; El-Mowafy et al., 2005) have shown that dental practitioners do not maintain their LCUs to produce the optimum irradiance with 33% of QTH LCUs found to be operating at an irradiance of less than 200mW/cm^2. Therefore the implications of RBC placement variables (particularly in the case of the

placement of the gingival increment in class II restorations) and irradiance degradation of QTH LCUs was further investigated.

Dental RBCs have disadvantages namely, marginal leakage due to polymerisation shrinkage (Eick and Welch, 1986; Walls et al., 1988; Davidson and Feilzer, 1997; Chen et al., 2001; Ferracane, 2008) and inadequate wear resistance under high masticatory loading in large restorations (Lutz et al., 1984; Mair et al., 1990; Suzuki and Leinfelder, 1993; Hu et al., 1999) which limit their application for clinical use. Polymerisation shrinkage is complex in terms of how the contraction stresses are measured (Bowen, 1967; Feilzer et al., 1987; Bouschlicher et al., 1997; Condon and Ferracane, 1998, Watts et al., 2003; Sakaguchi et al., 2004; Lee et al., 2007; Ferracane, 2008) and are outside the scope of the current study. However, the clinical performance of the RBC materials investigated has been extended for the implications of RBC placement variables and irradiance degradation of QTH LCUs to include *in-vitro* wear simulation. The testing methodology rapidly allows RBC assessment prior to the placement in the mouth and a variety of machines including the Materials Testing and Simulation (MTS) artificial oral environment (DeLong and Douglas, 1983), the Academisch Centrum for Tandheelkunde Amsterdam (ACTA) wear machine (De Gee et al., 1986), the University of Alabama wear machine (Leinfelder et al., 1989) and the Oregon Health Science University (OHSU) oral wear simulator (Condon and Ferracane, 1996) have been used previously. In the current study the *in-vitro* wear resistance was investigated using the OHSU oral wear simulator. Unfortunately, the three-point flexure specimens were not compatible with the wear chambers of the oral wear simulator and disc-shaped specimens (12mm

diameter) were required. Therefore the *in-vitro* wear simulation data was compared with bi-axial flexure strength results to provide further information on the irradiance effects on mechanical property development.

6.1 Aims and Objectives

The objective of Part II of the current study was to investigate the RBC placement variables (principally irradiation distance) which may have implications for strength and modulus development when irradiated with the LCUs employed in the current study. In addition, the influence of QTH LCU irradiation distance on bi-axial flexure strength and short- and long-term *in-vitro* wear resistance of the four RBCs were also assessed. The hypothesis tested was that the flexural strength and short- and long-term *in-vitro* wear resistance would be dependent on the irradiation distance and therefore the irradiance delivered.

CHAPTER 7 Materials and Methods

The RBC materials tested in the Part II of the current study were Z100™, Filtek™ Z250, Filtek™ P60 and Filtek™ Supreme XT and were manufactured by 3M ESPE Dental Products Division, St. Paul, MN, USA. Details of the formulation of the RBCs are provided in Table 3.1. The QTH LCU used to irradiate the RBCs was an Optilux 501 used in conjunction with an 8mm tip diameter in standard mode. The LED LCUs employed were the Elipar™ Freelight and the Elipar™ Freelight 2 which were irradiated with an 8mm tip diameter for testing the flexure properties and with a 13mm tip diameter for bi-axial strength and *in-vitro* wear resistance. Details of the LCUs are provided in Section 3.1.2.

7.1 Three-point flexure properties

During the placement of the gingival increment in class II restorations, the LCU tip is often positioned at varying distances from the RBC resulting in irradiance variation during clinical placement. To investigate irradiance variation on the flexure properties of RBCs, the modified ISO 4049 specimen manufacture protocol (outlined in Section 3.2) was employed by placing the tip diameter at varying distances (0, 7 and 15mm) from the top surface of the RBCs examined prior to irradiation.

7.1.1 QTH irradiance variation

The irradiance of the QTH LCU was measured seven consecutive times using a radiometer incorporated within the Optilux 501 QTH LCU with an 8mm tip diameter when placed in contact with the radiometer (at a distance of 0mm) and at distances of 7, and 15mm from the radiometer. In addition, the irradiance was measured seven consecutive times at distances of 0, 3, 5, 7, 9, 11, 13 and 15mm for bi-axial flexure and in-vitro wear determination using a 13mm tip diameter.

7.1.2 LED irradiance variation

The irradiance of the Elipar™ Freelight and the Elipar™ Freelight 2 LED LCUs were also measured consecutively seven times using the radiometer incorporated within the QTH LCU when employed with tip diameters of 8mm at distances of 0, 7 and 15mm.

7.1.3 Specimen preparation

Prior to the irradiation protocol being implemented, acrylic spacers had to be prepared to the required distances from which the three-point flexure specimens were to be irradiated, namely 7 and 15mm. A two part cold-setting acrylic resin (Varidur, Beuhler, Lake Bluff, IL, USA) was mixed according to the manufacturers instructions and poured into a stainless steel mould (30.0 ± 0.1mm height and 20.0 ± 0.1mm diameter) which had an 8.0 ± 0.1mm stainless steel plunger placed centrally. The acrylic resin was allowed to set for 30mins after which time the stainless steel plunger was removed. A diamond saw

(Beulher, Lake Bluff, IL, USA) with water as a lubricant was used to cut the acrylic spacers to the approximate lengths required. The acrylic spacers were then ground with P1200 Silicaon Carbide (SiC) abrasive paper on a Beta grinder-polisher machine (Beulher, Lake Bluff, IL, USA) at a force of 20N with water as a lubricant to the exact thicknesses required.

Twenty rectangular bar-shaped specimens (25.0 ± 0.1mm length, 2.0 ± 0.1mm width and 2.0 ± 0.1mm thickness) of each RBC material were fabricated using the knife-edged split aluminium mould in accordance with the modified ISO overlapping irradiation protocol as outlined in Section 3.2. The exit window was moved by three-quarters (not half) the diameter along the specimen so that certain areas received twice the irradiation of adjacent areas. Each specimen was irradiated by placing the LCU tip diameter in contact with the acetate strip until the entire length of the specimen was irradiated (at a distance of 0mm). The procedure was then repeated with the aid of the acrylic spacer which enabled alignment of the LCU at distances of 7 and 15mm.

7.1.3.1 QTH LCU

When the QTH LCU was employed with the 8mm tip diameter five overlapping irradiations were required. Irradiation when in contact with the acetate strip on the top surface of the RBC (at a distance of 0mm) resulted in groups of 20 specimens for Z100™ (Group A_Q), Filtek™ Z250 (Group B_Q), Filtek™ P60 (Group C_Q) and Filtek™ Supreme XT (Group D_Q). Additionally specimens were irradiated at a distance of 7mm from the

top surface of each specimen resulted in groups for Z100™ (Group E_Q), Filtek™ Z250 (Group F_Q), Filtek™ P60 (Group G_Q) and Filtek™ Supreme XT (Group H_Q). A distance of 15mm from the top surface of each RBC specimen resulted in groups of 20 specimens for Z100™ (Group I_Q), Filtek™ Z250 (Group J_Q), Filtek™ P60 (Group K_Q) and Filtek™ Supreme XT (Group L_Q) (Table 7.1).

Table 7.1: The specimen groups for each RBC material irradiated in contact with the top surface (at a distance of 0mm) and at distances of 7 and 15mm from the top surface when employing the 8mm tip diameter with the QTH LCU.

RBC	Irradiation Distance		
	0mm	**7mm**	**15mm**
Z100™	Group A_Q	Group E_Q	Group I_Q
Filtek™ Z250	Group B_Q	Group F_Q	Group J_Q
Filtek™ P60	Group C_Q	Group G_Q	Group K_Q
Filtek™ Supreme XT	Group D_Q	Group H_Q	Group L_Q

7.1.3.2 LED LCU

7.1.3.2.1 Elipar™ Freelight ($_I$)

Five overlapping irradiations with the 8mm tip diameter were required to irradiate the RBC materials at distances of 0, 7 and 15mm from the top surface resulting in specimen groups for Z100™ (Group A_I, Group E_I and Group I_I, respectively), Filtek™ Z250 (Group

B_l, Group F_l and Group J_l, respectively), Filtek™ P60 (Group C_l , Group G_l and Group K_l, respectively) and Filtek™ Supreme XT (Group D_l , Group H_l and Group L_l, respectively) (Table 7.2).

Table 7.2: The specimen groups for each RBC material irradiated in contact with the top surface (at a distance of 0mm) and at distances of 7 and 15mm from the top surface when employing the 8mm tip diameter with the Elipar™ Freelight LCU.

RBC	Irradiation Distance		
	0mm	**7mm**	**15mm**
Z100™	Group A_l	Group E_l	Group I_l
Filtek™ Z250	Group B_l	Group F_l	Group J_l
Filtek™ P60	Group C_l	Group G_l	Group K_l
Filtek™ Supreme XT	Group D_l	Group H_l	Group L_l

7.1.3.2.2 Elipar™ Freelight 2 ($_h$)

Similarly when employing the 8mm LCU tip diameter with the Elipar™ Freelight 2 to irradiate the RBC materials investigated from the top surface at distances of 0, 7 and 15mm, specimen groups for Z100™ (Group A_h, Group E_h and Group I_h, respectively), Filtek™ Z250 (Group B_h, Group F_h and Group J_h, respectively), Filtek™ P60 (Group C_h , Group G_h and Group K_h, respectively) and Filtek™ Supreme XT (Group D_h , Group H_h and Group L_h, respectively) were prepared (Table 7.3).

Table 7.3: The specimen groups for each RBC material irradiated in contact with the top surface (at a distance of 0mm) and at distances of 7 and 15mm from the top surface when employing the 8mm tip diameter with the Elipar™ Freelight 2 LCU.

RBC	Irradiation Distance		
	0mm	**7mm**	**15mm**
Z100™	Group A_h	Group E_h	Group I_h
Filtek™ Z250	Group B_h	Group F_h	Group J_h
Filtek™ P60	Group C_h	Group G_h	Group K_h
Filtek™ Supreme XT	Group D_h	Group H_h	Group L_h

Following irradiation the cellulose acetate strip was discarded, the mould dismantled, the specimen removed and checked for surface imperfections. Specimens with defects were eliminated and the remaining specimens stored in a light-proof container containing 50ml of deionised water and placed in a climate controlled chamber maintained at 37 ± 1°C at 55% relative humidity for 24h prior to testing and analysis.

7.1.4 Three-point flexure testing

The rectangular bar-shaped specimens with the irradiated side uppermost were centrally loaded with a 0.3mm width knife-edge indenter across a support span of 20mm at a crosshead speed of 1mm/min and the maximum load to fracture was recorded (Section 3.3). The three-point flexure strength was calculated using Equation 3.1 (ISO 4049, 2000)

and the three-point flexure modulus was determined using Equation 3.2 (ISO 4049: 2000).

7.1.4.1 Statistical analysis

Analysis of the group means for the three-point flexure strength and flexure modulus data for each RBC (Z100™, Filtek™ Z250, Filtek™ P60 and Filtek™ Supreme XT) irradiated at distances of 0, 7 and 15mm from the top surface of the specimen using the QTH or LED LCUs were made utilising a one-way ANOVA and Tukey's multiple range tests at a significance level of $P<0.05$. The initial analysis carried out involved three one-way ANOVAs. The first one-way ANOVA was in terms of RBC material, for each LCU at each irradiated distance. The second one-way ANOVA was in terms of LCU employed, for each RBC material and irradiated distance. The final one-way ANOVA was in terms of the irradiation distance for each RBC material and LCU employed.

7.2 Bi-axial flexure properties

Dental RBCs have disadvantages namely, marginal leakage due to polymerisation shrinkage (Eick and Welch, 1986; Walls et al., 1988; Davidson and Feilzer, 1997; Chen et al., 2001; Ferracane, 2008) and inadequate wear resistance under high masticatory loading in large restorations (Lutz et al., 1984; Mair et al., 1990; Suzuki and Leinfelder, 1993; Hu et al., 1999). Clinical studies have shown that 27% of 214 QTH LCUs surveyed in Australia (Martin et al., 1998), 33% of 130 QTH LCUs in Israel (Pilo et al., 1999),

30% of 209 QTH LCUs in Texas (Barghi et al., 1994) and 4.2% of 214 QTH LCUs in Toronto had an irradiance of less than 200mW/cm^2 (El-Mowafy et al., 2005) highlighting that many dental practitioners do not maintain their LCUs to produce the optimum irradiance. The influence of QTH LCU irradiation distance on bi-axial flexure strength and short- and long-term *in-vitro* wear resistance of the four RBCs were assessed.

7.2.1 Specimen preparation

Prior to preparation and irradiation of the disc-shaped RBC specimens for bi-axial flexure strength testing and short- and long-term *in-vitro* wear resistance determination, acrylic spacers (similar to those prepared for the three-point flexure specimens (Section 7.1.3)) were made. The two part cold-setting acrylic resin was poured into a stainless steel mould (30.0 ± 0.1mm height and 20.0 ± 0.1mm diameter), with a 13.0 ± 0.1mm stainless steel plunger placed centrally. The acrylic resin was allowed to set, the stainless steel plunger was removed and a diamond saw (with water as a lubricant) was used to cut the acrylic spacers to the approximate lengths required. The acrylic spacers were ground at a force of 20N with water as a lubricant with P1200 SiC abrasive paper to the exact thicknesses (3, 5, 7, 9, 11, 13 and 15mm) required.

Disc-shaped specimens were prepared by using the acrylic spacers placed at distances of 0, 3, 5, 7, 9, 11, 13 and 15mm from the top surface of the four RBCs investigated. The uncured RBC paste was packed into an acrylic mould (12.0 ± 0.1mm diameter and 2.0 ± 0.1mm thickness). The mould was placed on an aluminium base plate and the uncured

resin was placed into the mould with the top surface covered with a cellulose acetate strip. A glass microscope slide and a load of 1kg was applied for 20s to ensure consistent and reproducible packing of the disc-shaped specimens. The load and microscope slide were removed and the specimen irradiated at ambient room temperature (23 ± 1°C) for the manufacturers recommended exposure times (40s for of Z100™ and 20s for Filtek™ Z250, Filtek™ P60 and Filtek™ Supreme XT).

Irradiation of the RBC specimens with the 13mm tip diameter placed in contact with the top surface (at a distance of 0mm) required one irradiation to ensure the entire area of each specimen of Z100™ (Group A_0), Filtek™ Z250 (Group B_0), Filtek™ P60 (Group C_0) and Filtek™ Supreme XT (Group D_0) was irradiated. In addition further specimen groups were prepared and irradiated from varying distances from the top surface of the RBCs at 3, 5, 7, 9, 11, 13 and 15mm resulting in specimen groups for Z100™ (Group A_3, Group A_5, Group A_7, Group A_9, Group A_{11}, Group A_{13} and Group A_{15}, respectively), Filtek™ Z250 (Group B_3, Group B_5, Group B_7, Group B_9, Group B_{11}, Group B_{13} and Group B_{15}, respectively), Filtek™ P60 (Group C_3, Group C_5, Group C_7, Group C_9, Group C_{11}, Group C_{13} and Group C_{15}, respectively) and Filtek™ Supreme XT (Group D_3, Group D_5, Group D_7, Group D_9, Group D_{11}, Group D_{13} and Group D_{15}, respectively) (Table 7.4).

7.2.2 Bi-axial flexural strength

The bi-axial flexure strength was determined by imposing a central load using a 3mm ball indenter on a 10mm diameter ring support at a crosshead speed of 1mm/min with the

irradiated side uppermost on the groups of 20 disc-shaped specimens. To assist in uniform loading of the ball indenter on the specimen surface, a thin sheet of rubber was placed between the sample and the ring support. The samples were loaded using a universal testing machine (Model 5565, Instron Ltd., High Wycombe, UK) and flexure strengths were calculated from Equation 7.1 (Timoshenko and Woinowsky-Krieger, 1959)

$$\sigma_{max} = \frac{P}{h^2}\left\{(1+v)\left[0.485 \times \ln\left(\frac{a}{h}\right) + 0.52\right] + 0.48\right\} \qquad \text{Equation 7.1}$$

where σ_{max} is the maximum flexure stress, P the measured load at fracture, h the specimen thickness, v the Poisson's ratio for the material (0.225) (Ban and Anusavice, 1990) and a the radius of the ring support (5mm).

7.2.2.1 Statistical analysis

A one-way (irradiated distance) ANOVA and Tukey's multiple range tests at a significance level of $P<0.05$ was initially performed. A two-way (irradiated distance × RBC material) ANOVA and Tukey's multiple range test at a significance level of $P<0.05$ were then undertaken on the group means of the bi-axial flexure strength data when irradiated at distances of 0, 3, 5, 7, 9, 11, 13 and 15mm from the top surface of the RBC specimens.

Table 7.4: The specimen groups for each RBC material irradiated in contact with the top surface (at a distance of 0mm) and at distances of 3, 5, 7, 9, 11, 13 and 15mm from the top surface when employing the 13mm tip diameter with the QTH LCU.

RBC	Irradiation Distance							
	0mm	**3mm**	**5mm**	**7mm**	**9mm**	**11mm**	**13mm**	**15mm**
Z100™	Group A_0	Group A_3	Group A_5	Group A_7	Group A_9	Group A_{11}	Group A_{13}	Group A_{15}
Filtek™ Z250	Group B_0	Group B_3	Group B_5	Group B_7	Group B_9	Group B_{11}	Group B_{13}	Group B_{15}
Filtek™ P60	Group C_0	Group C_3	Group C_5	Group C_7	Group C_7	Group C_{11}	Group C_{13}	Group C_{15}
Filtek™ Supreme XT	Group D_0	Group D_3	Group D_5	Group D_7	Group D_9	Group D_{11}	Group D_{13}	Group D_{15}

7.3 *In-vitro* wear testing

For *in-vitro* wear testing determination four specimens for each RBC were irradiated at a distance of 0mm (Z100™ (Group Aw_0), Filtek™ Z250 (Group Bw_0), Filtek™ P60 (Group Cw_0) and Filtek™ Supreme XT (Group Dw_0)) or at distances of 3, 5, 7, 9, 11, 13 and 15mm from the top surface of the RBCs. Following irradiation of the resultant groups (Z100™: Group Aw_3, Group Aw_5, Group Aw_7, Group Aw_9, Group Aw_{11}, Group Aw_{13} and Group Aw_{15}, respectively, Filtek™ Z250: Group Bw_3, Group Bw_5, Group Bw_7, Group Bw_9, Group Bw_{11}, Group Bw_{13} and Group Bw_{15}, respectively, Filtek™ P60: Group Cw_3, Group Cw_5, Group Cw_7, Group Cw_9, Group Cw_{11}, Group Cw_{13} and Group Cw_{15}, respectively and Filtek™ Supreme XT: Group Dw_3, Group Dw_5, Group Dw_7, Group Dw_9, Group Dw_{11}, Group Dw_{13} and Group Dw_{15}, respectively) the cellulose acetate strips were discarded, the specimens removed from the mould, checked for surface imperfections and stored in a light-proof container (containing 50ml of deionised water) in a climate controlled chamber at 37 ± 1°C at 55% relative humidity for 23h prior to testing and analysis (Table 7.5).

Twenty-three hours after wet storage the disc-shaped RBC specimens were mounted in a two part cold-setting acrylic resin to produce cylinders (25.0 ± 0.1mm diameter and 10.0 ± 0.1mm height) compatible with the chambers of the wear testing apparatus. Prior to mixing the acrylic resin the specimens were centrally located at the centre of individual cylindrical mounting cups (Metset Cups, Beuhler, Lake Bluff, IL, USA). The acrylic resin was mixed, using a mixing ratio of 2g of powder to 1ml of liquid in accordance with

the manufacturers instructions for 30s, and the plastic mass poured into the cylindrical mounting cups containing the specimens. The mounted specimens were removed from the cylindrical mounting cups 45mins after the commencement of mixing. The mounted specimens were wet ground using water as the lubricant on a Beta grinder-polisher with P600 SiC abrasive paper at a force of 10N per specimen for 30s and at a force of 10N per specimen for 30s on P1200 SiC abrasive paper to provide a reproducible surface roughness conductive to wear testing (Condon and Ferracane, 1996).

The 24h *in-vitro* wear was assessed for each RBC group investigated using the OHSU four chamber oral wear simulator (Condon and Ferracane, 1996). The wear regime utilises steatite antagonists to simultaneously produce abrasion and attrition wear in the form of a tear drop wear facet in the presence of a food-like slurry. Abrasion wear is caused by the sliding action of one surface over another and attrition wear is caused by direct static forces acting between opposing surfaces (Mair et al., 1996; Mortensen, 2007). The wear regime imposed by the OHSU oral wear simulator brings the steatite antagonist into direct contact with the specimen to impart a 20N sliding abrasion force along a 7mm linear path (Condon and Ferracane, 1996, 1997a,b). A direct static 90N force was applied at the end of the 7mm path for each specimen to simulate attrition wear (Condon and Ferracane, 1996, 1997a,b). At the end of each wear cycle the steatite antagonist is raised and returns to the start of the 7mm path and the wear regime repeats at a frequency of 1Hz.

Table 7.5: The specimen groups for each RBC material irradiated in contact with the top surface (at a distance of 0mm) and at distances of 3, 5, 7, 9, 11, 13 and 15mm from the top surface when employing the 13mm tip diameter with the QTH LCU.

RBC	Irradiation Distance							
	0mm	**3mm**	**5mm**	**7mm**	**9mm**	**11mm**	**13mm**	**15mm**
Z100™	Group Aw_0	Group Aw_3	Group Aw_5	Group Aw_7	Group Aw_9	Group Aw_{11}	Group Aw_{13}	Group Aw_{15}
Filtek™ Z250	Group Bw_0	Group Bw_3	Group Bw_5	Group Bw_7	Group Bw_9	Group Bw_{11}	Group Bw_{13}	Group Bw_{15}
Filtek™ P60	Group Cw_0	Group Cw_3	Group Cw_5	Group Cw_7	Group Cw_7	Group Cw_{11}	Group Cw_{13}	Group Cw_{15}
Filtek™ Supreme XT	Group Dw_0	Group Dw_3	Group Dw_5	Group Dw_7	Group Dw_9	Group Dw_{11}	Group Dw_{13}	Group Dw_{15}

Steatite spheres of 10.0 ± 0.1mm diameter have wear characteristics similar to enamel when opposing dental restorative materials (Wassell et al., 1994; Condon and Ferracane, 1997a, 2003). Prior to the commencement of wear testing the steatite antagonists (placed atop of nylon screws) were positioned into the OHSU oral wear simulator and the height adjusted using a custom made jig to ensure the antagonist was 1mm above the disc shaped RBC specimen to be tested. Each of the four specimens to be tested were secured into individual wear chambers of the wear simulator and a food-like slurry, (1.0g of ground poppy seeds (Holland & Barrett, Burton-upon-Trent, UK), 0.5g of PMMA beads (Special Tray, Dentsply DeTrey, Kanstanz, Germany) and 5ml of distilled water), was added to each chamber prior to testing. The wear rates produced with the slurry mixture for various dental restorative materials were identified to be comparable with clinical studies (Lutz et al., 1984; De Gee, 1986). Fragmentation of the poppy seeds was achieved by grinding in a ceramic pestle and mortar for 100 strokes.

7.3.1 Short-term *in-vitro* wear resistance

Four specimens of each RBC material investigated and irradiated at distances of 0, 3, 5, 7, 9, 11, 13 and 15mm from the LCU tip diameter were subjected to 50,000 wear cycles at a frequency of 1Hz which was equivalent to 6 months wear in the oral environment (Condon and Ferracane, 1996). The tear drop wear facet produced (Figure 7.1) on the surface of each specimen was analysed using a non-contact optical profilometer (Talysurf CLI 2000, Taylor-Hobson Precision, Leicester, UK) with a 3mm range chromatic length aberration gauge with a resolution of 0.1µm (z-direction) scanning at 2mm/s.

Longitudinal traces were taken at 4μm intervals (x-direction) across the wear facet with a measurement recorded at 40μm intervals (y-direction) generating a three dimensional (3D) profile using the TalyMap analysis software package (Talysurf CLI 2000, Taylor-Hobson Precision, Leicester, UK). The mean total volumetric wear and mean maximum wear depth measurements were determined using the non-worn areas around the wear facet as a reference (Dowling and Fleming, 2007).

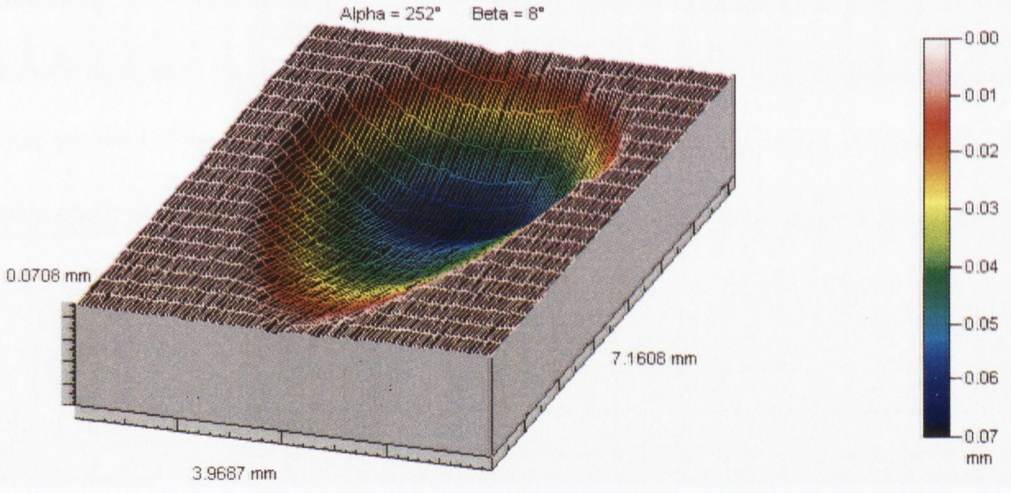

Figure 7.1: A three-dimensional representation of the total wear facet for the 7mm sliding path produced from the wear regime employed using the OHSU oral wear simulator.

7.3.1.1 Statistical analysis

The raw data for the short-term *in-vitro* wear resistance were analysed using one- (irradiated distance) and two-way (irradiated distance × RBC material) ANOVAs and Tukey's multiple range tests at a significance level of $P<0.05$ of the mean total

volumetric wear data and mean maximum wear depth when irradiated at distances of 0, 3, 5, 7, 9, 11, 13 and 15mm from the top surface of the RBC specimens.

7.3.2 Long-term *in-vitro* wear resistance

Four specimens of each RBC material investigated and irradiated at distances of 0, 7 and 15mm from the LCU tip diameter were subjected to extended wear regimes. Following analysis of the wear facets after 50,000 wear cycles at 1Hz using the non-contact optical profilometer, the samples were aligned into the individual wear chambers and a fresh food-like slurry was added. A further 100,000 wear cycles at 1Hz were performed and analysis of the wear facets (after 150,000 wear cycles) was performed using the non-contact optical profilometer prior to realignment of the samples into the individual wear chambers. A fresh food-like slurry was added. An additional 150,000 wear cycles at 1Hz were performed and analysis of the wear facets (after 300,000 wear cycles) with the profilometer was undertaken prior to realignment of the samples into the individual wear chambers with a fresh food-like slurry. A final 200,000 wear cycles at 1Hz were performed and the final analysis of the wear facets (after 500,000 wear cycles) with the profilometer was undertaken.

7.3.2.1 Statistical analysis

The long-term *in-vitro* wear resistance data was analysed using one- (irradiated distance) and two-way (irradiated distance × RBC material) ANOVAs and Tukey's multiple range

tests ($P<0.05$) of the mean total volumetric wear data and mean maximum wear depth when irradiated at distances of 0, 7 and 15mm from the top surface of the RBC specimens.

CHATER 8 Results

8.1 The influence of irradiation distance

The influence of irradiation distance was investigated by modifying the specimen manufacture protocol in ISO 4049 by placing the LCU tip diameter at varying distances from the RBC top surfaces to reflect the output intensities routinely encountered clinically when placing the gingival increment of a large mesio-occlusal-distal (MOD) restoration.

8.1.1 QTH LCU irradiance variation

The irradiance of the Optilux 501 QTH LCU was 650 ± 14mW/cm^2 when in contact with the radiometer (at a distance of 0mm), 350 ± 8mW/cm^2 at a distance of 7mm from the radiometer and 150 ± 8mW/cm^2 when positioned 15mm from the radiometer when employing an 8mm tip diameter.

8.1.2 LED LCU irradiance variation

When employing an 8mm tip diameter, the irradiance of the Elipar™ Freelight LED LCU was 246 ± 8mW/cm^2 in contact with the radiometer, 186 ± 14mW/cm^2 at 7mm from the radiometer and less than 100mW/cm^2 when 15mm from the radiometer. The irradiance of the Elipar™ Freelight 2 LED LCU was 1160 ± 8mW/cm^2 at a distance of 0mm, 469 ±

8mW/cm^2 when placed 7mm and 129 ± 14mW/cm^2 when positioned 15mm from the radiometer.

8.2 Three-point flexure strength

8.2.1 Optilux 501 QTH LCU

When the 8mm LCU tip diameter was employed to irradiate the RBCs, in contact with the top surface (at a distance of 0mm), the range of the three-point flexure strengths varied for Z100™ from a minimum of 67MPa to a maximum of 137MPa (Group A_Q), Filtek™ Z250 from 132 to 196MPa (Group B_Q), Filtek™ P60 from a minimum of 118MPa to a maximum of 209MPa (Group C_Q) and Filtek™ Supreme XT from a lowest recorded strength of 105MPa to a highest recorded strength of 169MPa (Group D_Q), respectively. The mean three-point flexure strengths and associated standard deviations were 111 ± 18MPa (Group A_Q), 151 ± 17MPa (Group B_Q), 155 ± 22MPa (Group C_Q) and 139 ± 15MPa (Group D_Q) (Table 8.1).

The mean three-point flexure strengths and associated standard deviations when irradiated at a distance of 7mm from the top surface of Z100™, Filtek™ Z250, Filtek™ P60 and Filtek™ Supreme XT were 96 ± 17MPa (Group E_Q), 132 ± 14MPa (Group F_Q), 138 ± 20MPa (Group G_Q) and 129 ± 10Pa (Group H_Q), respectively. The range of three-point flexure strengths varied for Z100™ from a minimum of 69MPa to a maximum of 124MPa, Filtek™ Z250 from 111 to 152MPa, Filtek™ P60 from a low of 112MPa to a

high of 165MPa and Filtek™ Supreme XT from a minimum recorded value of 105MPa to a maximum value of 143MPa (Table 8.1).

Table 8.1: The range and mean three-point flexure strengths (associated standard deviations) for the RBC specimens irradiated in contact with the top surface (at a distance of 0mm) and at distances of 7 and 15mm using the QTH LCU.

RBC	Property	Irradiation Distance		
		0mm	7mm	15mm
Z100™	Three-point flexure strength (MPa)	111 (18)	96 (17)	83 (19)
	Range of strengths (MPa)	67-137	69-124	47-125
Filtek™ Z250	Three-point flexure strength (MPa)	151 (17)	132 (14)	124 (25)
	Range of strengths (MPa)	132-196	111-152	74-159
Filtek™ P60	Three-point flexure strength (MPa)	155 (22)	138 (20)	127 (11)
	Range of strengths (MPa)	118-209	112-165	109-146
Filtek™ Supreme XT	Three-point flexure strength (MPa)	139 (15)	129 (10)	111 (8)
	Range of strengths (MPa)	105-169	105-143	98-123

When irradiated at 15mm from the top surface of the RBCs, the three-point flexure strengths varied from a low of 47MPa to a high of 125MPa for Z100™ (Group I_Q), from 74 to 159MPa for Filtek™ Z250 (Group J_Q), from a minimum of 109MPa to a maximum of 146MPa for Filtek™ P60 (Group K_Q) and from 98 to 123MPa for Filtek™ Supreme XT (Group L_Q). The mean three-point flexure strengths and associated standard deviations were 83 ± 19MPa for Group I_Q specimens, 124 ± 25MPa for Group J_Q specimens, 127 ± 11MPa for Group K_Q specimens and 111 ± 8MPa for Group L_Q specimens, respectively (Table 8.1).

8.2.2 Elipar™ Freelight LED LCU

When the RBC materials were irradiated with the 8mm tip diameter in contact with the top surface the range of the three-point flexure strengths varied for Z100™ from a minimum of 88MPa to a maximum of 156MPa (Group A_1), Filtek™ Z250 from 130 to 178MPa (Group B_1), Filtek™ P60 from a minimum of 119MPa to a maximum of 181MPa (Group C_1) and Filtek™ Supreme XT from a lowest recorded strength of 100MPa to a highest recorded strength of 156MPa (Group D_1), respectively. The mean three-point flexure strengths and associated standard deviations were 125 ± 20MPa (Group A_1), 154 ± 13MPa (Group B_1), 147 ± 15MPa (Group C_1) and 128 ± 18MPa (Group D_1) (Table 8.2).

Table 8.2: The range and mean three-point flexure strengths (associated standard deviations) for the RBC specimens irradiated in contact and at distances of 7 and 15mm from the top surface of the specimens using the Elipar™ Freelight LCU.

RBC	Property	Irradiation Distance		
		0mm	7mm	15mm
Z100™	Three-point flexure strength (MPa)	125 (20)	97 (23)	91 (13)
	Range of strengths (MPa)	88-156	58-138	63-115
Filtek™ Z250	Three-point flexure strength (MPa)	154 (13)	140 (16)	109 (11)
	Range of strengths (MPa)	130-178	109-163	92-129
Filtek™ P60	Three-point flexure strength (MPa)	147 (15)	129 (10)	111 (10)
	Range of strengths (MPa)	119-181	110-153	87-127
Filtek™ Supreme XT	Three-point flexure strength (MPa)	128 (18)	83 (10)	53 (11)
	Range of strengths (MPa)	100-156	63-101	41-78

Employing the modified ISO 4049 overlapping irradiation regime at 7mm from the top surface resulted in a range of the three-point flexure strengths for Z100™ (Group E_l) of 58 to 138MPa, Filtek™ Z250 (Group F_l) from a minimum of 109MPa to a maximum of 163MPa, Filtek™ P60 (Group G_l) from 110 to 153MPa and Filtek™ Supreme XT (Group H_l) from a low of 63MPa to a high of 101MPa. The mean three-point flexure strengths and associated standard deviations for Z100™, Filtek™ Z250, Filtek™ P60 and Filtek™ Supreme XT were 97 ± 23MPa, 140 ± 16MPa, 129 ± 10MPa and 83 ± 10MPa, respectively (Table 8.2).

Irradiation at a distance of 15mm from the top surface of the RBC specimens resulted in three-point flexure strengths that varied from a low of 63MPa to a high of 115MPa for Z100™ (Group I_l), from 92 to 129MPa for Filtek™ Z250 (Group J_l), from a minimum of 87MPa to a maximum of 127MPa for Filtek™ P60 (Group K_l) and from 41 to 78MPa for Filtek™ Supreme XT (Group L_l). The mean three-point flexure strengths and associated standard deviations were 91 ± 13MPa for Group I_l specimens, 109 ± 11MPa for Group J_l specimens, 111 ± 10MPa for Group K_l specimens and 53 ± 11MPa for Group L_l specimens, respectively (Table 8.2).

8.2.3 Elipar™ Freelight 2 LED LCU

The mean three-point flexure strength and associated standard deviations for Z100™ (Group A_h) were 121 ± 26MPa, for Filtek™ Z250 (Group B_h) were 146 ± 14MPa, for Filtek™ P60 (Group C_h) were 159 ± 14MPa and for Filtek™ Supreme XT (Group D_h)

were 137 ± 14MPa when irradiated at a distance of 0mm. The range of three-point flexure strengths varied from a low of 80MPa to a high of 166MPa for Group A_h specimens, from 116 to 172MPa for Group B_h specimens, from a minimum of 113MPa to a maximum of 179MPa for Group C_h specimens and from 103 to 153MPa for Group D_h specimens (Table 8.3).

Table 8.3: The range and mean three-point flexure strengths (associated standard deviations) for the RBC specimens irradiated in contact and at distances of 7 and 15mm from the top surface using the Elipar™ Freelight 2 LCU.

RBC	Property	Irradiation Distance		
		0mm	7mm	15mm
Z100™	Three-point flexure strength (MPa)	121 (26)	103 (27)	95 (24)
	Range of strengths (MPa)	80-166	62-143	53-143
Filtek™ Z250	Three-point flexure strength (MPa)	146 (14)	136 (15)	128 (10)
	Range of strengths (MPa)	116-172	102-171	106-145
Filtek™ P60	Three-point flexure strength (MPa)	159 (14)	149 (18)	137 (17)
	Range of strengths (MPa)	113-179	116-181	107-179
Filtek™ Supreme XT	Three-point flexure strength (MPa)	137 (14)	126 (10)	117 (11)
	Range of strengths (MPa)	103-153	107-147	99-137

At a distance of 7mm the mean three-point flexure strengths and associated standard deviations for Z100™ (Group E_h) were 103 ± 27MPa, Filtek™ Z250 (Group F_h) were 136 ± 15MPa, Filtek™ P60 (Group G_h) were 149 ± 18MPa and Filtek™ Supreme XT (Group H_h) were 126 ± 10MPa. The range of three-point flexure strengths varied from a minimum of 62MPa to a maximum of 143MPa for Group E_h specimens, 102MPa to

171MPa for Group F_h specimens, a low of 116MPa to a high of 181MPa for Group G_h specimens and 107 to 147MPa for Group H_h specimens, respectively (Table 8.3).

Irradiating the RBC specimens at a distance of 15mm resulted in three-point flexure strengths varying from a low of 53MPa to a high of 143MPa for Z100™ (Group I_h), 106 to 145MPa for Filtek™ Z250 (Group J_h), a minimum of 107MPa to a maximum of 179MPa for Filtek™ P60 (Group K_h) and 99 to 137MPa for Filtek™ Supreme XT (Group L_h). The mean three-point flexure strengths and associated standard deviations were 95 ± 24MPa for Group I_h specimens, 128 ± 10MPa for Group J_h specimens, 137 ± 17MPa for Group K_h specimens and 117 ± 11MPa for Group L_h specimens, respectively (Table 8.3).

8.2.4 Statistical analysis

The data was checked for a normal distribution and an analysis of the group means for the three-point flexure strength data for each RBC (Z100™, Filtek™ Z250, Filtek™ P60 and Filtek™ Supreme XT) irradiated at distances of 0, 7 and 15mm from the top surface of the specimen (with an 8mm tip diameter) were made utilising a one-way ANOVAs and Tukey's multiple range test at a significance level of $P<0.05$. The initial analysis carried out involved three one-way ANOVAs.

In terms of RBC material, the one-way ANOVA for each LCU (QTH or LED) at the irradiated distances (0, 7 and 15mm) highlighted no significant differences in the group means of the three-point flexure strengths between Filtek™ Z250 and Filtek™ P60 (all P

values were greater than 0.10) regardless of the LCU employed at the irradiation distances investigated.

In terms of LCU (QTH and LED), for each RBC material, at the irradiated distances (0, 7 and 15mm), the one-way ANOVA highlighted no significant differences in the group means of the three-point flexure strengths when irradiated at a distance of 0mm from the top surface of Z100™ (F=2.377; P=0.102), Filtek™ Z250 (F=1.510; P=0.230), Filtek™ P60 (F=2.736; P=0.073) and Filtek™ Supreme XT (F=2.826; P=0.068). In addition, no significant differences in the group means of the three-point flexure strengths were evident when irradiated at a distance of 7mm from the top surface of Z100™ (F=0.586; P=0.560) and Filtek™ Z250 (F=1.252; P=0.294) and when irradiated at a distance of 15mm from the top surface of Z100™ (F=1.927; P=0.155).

In terms of irradiation distances (0, 7 and 15mm), for each RBC material and LCU (QTH or LED), the one-way ANOVA highlighted no significant differences in the group means of the three-point flexure strengths with the QTH LCU employed at 7 and 15mm from the top surface of Z100™ (P=0.086), Filtek™ Z250 (P=0.410) and Filtek™ P60 (P=0.143). Similarly, no significant differences in the group means of the three-point flexure strengths were highlighted when the Elipar™ Freelight LCU was employed at 7 and 15mm from the top surface of Z100™ (P=0.517) and the Elipar™ Freelight 2 LCU was employed at 7 and 15mm from the top surface of Z100™ (P=0.596), Filtek™ Z250 (P=0.145) and Filtek™ P60 (P=0.071). Interestingly, significant differences were highlighted for Filtek™ Supreme XT at the irradiated distances investigated (0, 7 and

15mm) when employing an 8mm tip diameter in conjunction with the Optilux 501 QTH ($F=29.501$; $P<0.0001$), Elipar™ Freelight ($F=161.505$; $P<0.0001$) and Elipar™ Freelight 2 ($F=14.988$; $P<0.0001$) LCUs.

8.3 Three-point flexure modulus

8.3.1 Optilux 501 QTH LCU

Irradiating the RBC specimens in contact with the top surface resulted in three-point flexure moduli for Z100™ (Group A_Q) varying from 9 to 16GPa, Filtek™ Z250 (Group B_Q) from a minimum of 9GPa to a maximum of 14GPa, Filtek™ P60 (Group C_Q) from 10 to 16GPa and Filtek™ Supreme XT (Group D_Q) from a low of 9GPa to a high of 13GPa. The mean three-point flexure moduli and associated standard deviations for Z100™ (Group A_Q) were 13.5 ± 1.5GPa, Filtek™ Z250 (Group B_Q) were 11.3 ± 1.2GPa, Filtek™ P60 (Group C_Q) were 12.4 ± 1.2GPa and Filtek™ Supreme XT (Group D_Q) were 11.1 ± 1.1GPa, respectively (Table 8.4).

When Z100™ (Group E_Q), Filtek™ Z250 (Group F_Q), Filtek™ P60 (Group G_Q) and Filtek™ Supreme XT (Group H_Q) were irradiated 7mm from the top surface of the RBCs the mean three-point flexure moduli and associated standard deviations were 12.4 ± 1.4GPa, 9.9 ± 1.6GPa, 10.6 ± 1.0GPa, 9.1 ± 0.8GPa, respectively. The range of the three-point flexure moduli varied from a low of 11GPa to a high of 15GPa for Group E_Q specimens, from a minimum of 6GPa to a maximum of 13GPa for Group F_Q specimens,

from 9 to 13GPa for Group G_Q specimens and from a minimum of 7GPa to a maximum of 11GPa for Group H_Q specimens, respectively (Table 8.4).

When irradiated at 15mm the range of three-point flexure moduli varied from a low of 6GPa to a high of 14GPa for Group I_Q specimens, from a minimum of 6GPa to a maximum of 12GPa for Group J_Q specimens, from 9 to 16GPa for Group K_Q specimens and from a low of 7GPa to a high of 10GPa for Group L_Q specimens, respectively. The mean three-point flexure moduli and associated standard deviations for Z100™ (Group I_Q) were 10.9 ± 2.7GPa, Filtek™ Z250 (Group J_Q) were 9.6 ± 1.9GPa, Filtek™ P60 (Group K_Q) were 10.7 ± 2.1GPa and Filtek™ Supreme XT (Group L_Q) were 8.9 ± 1.1GPa, respectively (Table 8.4).

Table 8.4: The range and mean three-point flexure moduli (associated standard deviations) for the RBC specimens irradiated at a distance of 0, 7 and 15mm from the top surface of the specimens using the QTH LCU.

RBC	Property	Irradiation Distance		
		0mm	7mm	15mm
Z100™	Three-point flexure modulus (GPa)	13.5 (1.5)	12.4 (1.4)	10.9 (2.7)
	Range of moduli (GPa)	9-16	11-15	6-14
Filtek™ Z250	Three-point flexure modulus (GPa)	11.3 (1.2)	9.9 (1.6)	9.6 (1.9)
	Range of moduli (GPa)	9-14	6-13	6-12
Filtek™ P60	Three-point flexure modulus (GPa)	12.4 (1.2)	10.6 (1.0)	10.7 (2.1)
	Range of moduli (GPa)	10-16	9-13	9-16
Filtek™ Supreme XT	Three-point flexure modulus (GPa)	11.1 (1.1)	9.1 (0.8)	8.9 (1.1)
	Range of moduli (GPa)	9-13	7-11	7-10

8.3.2 Elipar Freelight LED LCU

When using the 8mm tip diameter to irradiate the RBC specimens in contact with the top surface, the mean three-point flexure moduli and associated standard deviations for Z100™ (Group A_l) were 14.2 ± 1.4GPa, Filtek™ Z250 (Group B_l) were 12.5 ± 1.2GPa, Filtek™ P60 (Group C_l) were 13.3 ± 1.4GPa and Filtek™ Supreme XT (Group D_l) were 11.7 ± 1.1GPa. The range of three-point flexure moduli varied from a low of 12GPa to a high of 16GPa for Group A_l specimens, from 10 to 15GPa for Group B_l specimens, from a minimum of 11GPa to a maximum of 16GPa for Group C_l specimens and from 10 to 13GPa for Group D_l specimens, respectively (Table 8.5).

Irradiating the RBCs at a distance of 7mm resulted in a range of three-point flexure moduli data varying from a low of 10GPa to a high of 14GPa for Z100™ (Group E_l), from 7 to 13GPa for Filtek™ Z250 (Group F_l), from a minimum of 9GPa to a maximum of 13GPa for Filtek™ P60 (Group G_l) and from 7 to 11GPa for Filtek™ Supreme XT (Group H_l). The mean three-point flexure moduli and associated standard deviations were 12.2 ± 1.0GPa for Group E_l specimens, 10.5 ± 1.2GPa for Group F_l specimens, 10.5 ± 1.1GPa for Group G_l specimens, and 8.6 ± 1.3GPa for Group H_l specimens, respectively (Table 8.5).

Table 8.5: The range and mean three-point flexure moduli (associated standard deviations) for the RBC specimens irradiated in contact and at distances of 7 and 15mm from the top surface of the specimens using the Elipar™ Freelight LCU.

RBC	Property	Irradiation Distance		
		0mm	7mm	15mm
Z100™	Three-point flexure modulus (GPa)	14.2 (1.4)	12.2 (1.0)	11.9 (1.3)
	Range of moduli (GPa)	12-16	10-14	10-14
Filtek™ Z250	Three-point flexure modulus (GPa)	12.5 (1.2)	10.5 (1.2)	10.7 (0.8)
	Range of moduli (GPa)	10-15	7-13	9-12
Filtek™ P60	Three-point flexure modulus (GPa)	13.3 (1.4)	10.5 (1.1)	10.7 (1.4)
	Range of moduli (GPa)	11-16	9-13	9-13
Filtek™ Supreme XT	Three-point flexure modulus (GPa)	11.7 (1.1)	8.6 (1.3)	8.1 (0.6)
	Range of moduli (GPa)	10-13	7-11	8-9

When Z100™ (Group I_l), Filtek™ Z250 (Group J_l), Filtek™ P60 (Group K_l) and Filtek™ Supreme XT (Group L_l) were irradiated from a distance of 15mm from the top surface of the RBC specimens the mean three-point flexure moduli and associated standard deviations were 11.9 ± 1.3GPa, 10.7 ± 0.8GPa, 10.7 ± 1.4GPa, 8.1 ± 0.6GPa, respectively. The range of the three-point flexure moduli varied from a low of 10GPa to a high of 14GPa for Group I_l specimens, from a minimum of 9GPa to a maximum of 12GPa for Group J_l specimens, from 9 to 13GPa for Group K_l specimens and from a minimum of 8GPa to a maximum of 9GPa for Group L_l specimens, respectively (Table 8.5).

8.3.3 Elipar Freelight 2 LED LCU

The mean three-point flexure moduli and associated standard deviations for the RBC specimens irradiated in contact were 14.6 ± 1.5GPa for Group A_h specimens, 12.4 ± 1.6GPa for Group B_h specimens, 12.1 ± 1.9GPa for Group C_h specimens and 11.3 ± 1.0GPa for Group D_h specimens, respectively. The range of three-point flexure moduli varied from a minimum of 12GPa to a maximum of 18GPa for Group A_h specimens, from 10 to 16GPa for Group B_h specimens, from a low of 10GPa to a high of 15GPa for Group C_h specimens and from 8 to 13GPa for Group D_h specimens, respectively (Table 8.6).

RBCs specimens irradiated 7mm from the top surface resulted in a range of three-point flexure moduli for Z100™ (Group E_h) varying from a minimum of 12GPa to a maximum of 15GPa, Filtek™ Z250 (Group F_h) from 8 to 13GPa, Filtek™ P60 (Group G_h) from a low of 7GPa to a high of 11GPa and Filtek™ Supreme XT (Group H_h) from a minimum recorded value of 7GPa to a maximum recorded value of 10GPa. The mean three-point flexure moduli and associated standard deviations for Z100™ (Group E_h) were 13.0 ± 0.8GPa, Filtek™ Z250 (Group F_h) were 10.1 ± 1.5GPa, Filtek™ P60 (Group G_h) were 10.5 ± 1.0GPa and Filtek™ Supreme XT (Group H_h) were 8.5 ± 0.7GPa, respectively (Table 8.6).

Table 8.6: The range and mean three-point flexure moduli (associated standard deviations) for the RBC specimens irradiated at distances of 0, 7 and 15mm from the top surface using the Elipar™ Freelight 2 LCU.

RBC	Property	Irradiation Distance		
		0mm	7mm	15mm
Z100™	Three-point flexure modulus (GPa)	15 (2)	13 (1)	11 (1)
	Range of moduli (GPa)	12-18	12-15	9-12
Filtek™ Z250	Three-point flexure modulus (GPa)	12 (2)	10 (2)	10 (1)
	Range of moduli (GPa)	10-16	8-13	8-12
Filtek™ P60	Three-point flexure modulus (GPa)	12 (2)	11 (1)	10 (1)
	Range of moduli (GPa)	10-15	7-11	8-12
Filtek™ Supreme XT	Three-point flexure modulus (GPa)	11 (1)	9 (1)	9 (1)
	Range of moduli (GPa)	8-13	7-10	8-9

Employing the 8mm tip diameter 15mm from the top surface of the RBC specimens resulted in the mean three-point flexure moduli and associated standard deviations for Z100™, Filtek™ Z250, Filtek™ P60 and Filtek™ Supreme XT of 10.5 ± 0.7GPa for Group I_h specimens, 10.1 ± 1.3GPa for Group J_h specimens, 9.7 ± 1.1GPa for Group K_h specimens and 8.5 ± 0.5GPa for Group L_h specimens, respectively. The range of the three-point flexure moduli varied for Z100™ from a minimum of 9GPa to a maximum of 12GPa (Group I_h), Filtek™ Z250 from 8 to 12GPa (Group J_h), Filtek™ P60 from a minimum of 8GPa to a maximum of 12GPa (Group K_h) and Filtek™ Supreme XT from a lowest recorded flexure modulus of 8GPa to a highest flexure modulus of 9GPa (Group L_h), respectively (Table 8.6).

8.3.4 Statistical analysis

Three one-way ANOVAs and Tukey's multiple range tests at a significance level of $P<0.05$ were used to make multiple comparisons of the group means for the three-point flexure modulus data in terms of the RBC material, LCU employed (QTH and LED) and irradiated distance (0, 7 and 15mm) when an 8mm LCU tip diameter was employed.

In terms of RBC material, the one-way ANOVA of the group means of the three-point flexure moduli identified no significant differences between Filtek™ Z250 and Filtek™ P60 when irradiated using the QTH LCU at distances of 7 or 15mm and the Elipar Freelight or Elipar Freelight 2 LCUs at distances of 0, 7 or 15mm (all P values were greater than 0.24). No significant differences in the group means of the three-point flexure moduli were highlighted for Z100™ when compared with Filtek™ Z250 ($P=0.192$) and Filtek™ P60 ($P=0.992$) when irradiated using the QTH LCU at a 15mm. Similarly, no significant difference in the group means of the three-point flexure moduli were evident for Z100™ when compared with Filtek™ P60 ($P=0.104$) irradiated at a distance of 0mm with the Elipar Freelight LCU and at 15mm with the Elipar Freelight 2 LCU ($P=0.659$). In addition, no significant differences in the group means of the three-point flexure moduli were identified for Filtek™ Supreme XT when compared with Filtek™ Z250 irradiated with the QTH LCU at distances of 0mm ($P=0.969$), 7mm ($P=0.157$) and 15mm ($P=0.694$) and the Elipar Freelight 2 LCU at 0mm ($P=0.117$).

The one-way ANOVA for the LCU employed highlighted significant differences in the mean three-point flexure moduli for Filtek™ Z250 when irradiated at a distance of 0mm using the QTH compared with the Elipar Freelight (P=0.021) and the Elipar Freelight 2 (P=0.048) LCUs and at 15mm using the QTH compared with the Elipar Freelight LCU (P=0.037). No significant differences were highlighted in the mean three-point flexure moduli following irradiation with the QTH, Elipar Freelight or Elipar Freelight 2 LCUs at distances of 0mm for Z100™ (P=0.102), Filtek™ P60 (P=0.073) and Filtek™ Supreme XT (P=0.073), 7mm for Z100™ (P=0.102), Filtek™ Z250 (P=0.230), Filtek™ P60 (P=0.073) and Filtek™ Supreme XT (P=0.073) or at 15mm for Z100™ (P=0.230), Filtek™ P60 (P=0.073) and Filtek™ Supreme XT (P=0.073).

The one-way ANOVA for the irradiated distance revealed no significant differences in the mean three-point flexure moduli for irradiated distance of 7 and 15mm for each RBC material and each LCU employed (all P values were greater than 0.60) with the exception of Z100™ when irradiated at 7 and 15mm with the Elipar Freelight 2 LCU (P<0.0001). Significant differences in the grouped means of the three-point flexure moduli were also highlighted at distances of 0 and 7mm and 0 and 15mm for all the RBC materials investigated with each LCU employed (P<0.0001) with the exception of Z100™ irradiated at distances of 0 and 7mm using the QTH LCU (P=0.149).

8.4 Bi-axial flexure strength

8.4.1 QTH LCU irradiance variation

The irradiance of the Optilux 501 QTH LCU was 650 ± 14mW/cm^2 when in contact with the radiometer (at a distance of 0mm) employing a 13mm tip diameter. Increasing the irradiation distance to 3, 5, 7, 9, 11, 13 and 15 mm resulted in irradiances of 530 ± 8, 420 ± 14, 350 ± 8, 270 ± 8, 230 ± 14, 190 ± 8 and 150 ± 8mW/cm^2 when employing a 13mm tip diameter.

8.4.2 Bi-axial flexure strength

The mean bi-axial flexure strengths and associated standard deviations of the RBC specimens irradiated with a 13mm tip diameter in contact with the top surface and at irradiation distances of 3, 5, 7, 9, 11, 13 and 15 mm are highlighted in Table 8.7.

8.4.3 Statistical analysis

Analysis of the group means of the bi-axial flexure strength data was conducted using one- (irradiated distance) and two-way (irradiated distance × RBC material) ANOVAs and Tukey's multiple range tests at a significance level of $P<0.05$ when irradiated at distances of 0, 3, 5, 7, 9, 11, 13 and 15mm from the top surface of the RBC specimens. When the one-way ANOVAs for each RBC material were investigated, no significant

Table 8.7: The range and mean bi-axial flexure strengths (associated standard deviations) for the RBC specimens irradiated in contact with the top surface (at a distance of 0mm) and at distances of 3, 5, 7, 9, 11, 13 and 15mm from the top surface of the specimens using the QTH LCU.

RBC	Property	Irradiation Distance							
		0mm	3mm	5mm	7mm	9mm	11mm	13mm	15mm
Z100™	Bi-axial flexure strength (MPa)	161 (27)	163 (27)	158 (16)	154 (16)	156 (19)	146 (23)	145 (20)	145 (29)
	Range of strengths (MPa)	109-161	107-201	120-188	124-203	111-209	117-190	115-210	91-229
Filtek™ Z250	Bi-axial flexure strength (MPa)	165 (30)	164 (14)	153 (16)	154 (16)	162 (25)	154 (21)	154 (18)	153 (16)
	Range of strengths (MPa)	60-205	125-204	120-206	109-195	83-195	90-201	114-203	122-190
Filtek™ P60	Bi-axial flexure strength (MPa)	164 (14)	157 (15)	153 (18)	153 (15)	156 (18)	151 (16)	150 (20)	149 (20)
	Range of strengths (MPa)	127-183	117-179	123-183	121-185	123-181	119-187	125-181	104-181
Filtek™ Supreme XT	Bi-axial flexure strength (MPa)	143 (24)	143 (17)	142 (17)	137 (17)	141 (21)	131 (19)	130 (23)	130 (14)
	Range of strengths (MPa)	96-185	112-166	93-176	91-172	100-178	97-185	99-169	102-149

differences in the group means of the bi-axial flexure strengths were identified with irradiated distance for Z100™ (P=0.145), Filtek™ Z250 (P=0.194), Filtek™ P60 (P=0.087) and Filtek™ Supreme XT (P=0.162). The two-way ANOVA identified a significant difference in the group means of the bi-axial flexure strengths for irradiated distance (P<0.0001) with the Tukey's multiple range test revealing significant differences in the group means of the bi-axial flexure strengths identified for irradiated distances of 11, 13 and 15mm compared with 0mm (all P values were less than 0.0001) and 3mm (all P values were less than 0.0001). A significant difference in the group means of the bi-axial flexure strengths were also highlighted for Filtek™ Supreme XT (P<0.0001) when the Tukey's multiple range test were analysed and compared with Z100™ (P<0.0001), Filtek™ Z250 (P<0.0001) and Filtek™ P60 (P<0.0001).

8.5 *In-vitro* wear testing

The 24h *in-vitro* wear was assessed for each RBC group investigated using the OHSU four chamber oral wear simulator (Condon and Ferracane, 1996).

8.5.1 Short-term *in-vitro* wear resistance

In 1996 the developers of the OHSU oral wear simulator reported that both abrasion and attrition wear produced by the action of an enamel antagonist could be quantified (Condon and Ferracane, 1996). However the reproducibility of average wear depth results between different test centers was limited and a comparison of the mean wear depth

measurements for abrasive wear (20N) and attrition wear (70-90N) identified differences of 33-56% and 31-78%, respectively for three RBC materials (Heintze, 2006). As a result mean total volumetric wear and mean maximum wear depth of the tear drop wear facet and not the individual regions (abrasion and attrition) were used for data reporting.

8.5.1.1 Mean total volumetric wear

Irradiation of the RBC specimens in direct contact resulted in mean total volumetric wear and associated standard deviations of 0.03 ± 0.01mm^3 for Z100™ (Group Aw_0), 0.05 ± 0.01mm^3 for Filtek™ Z250 (Group Bw_0), 0.08 ± 0.01mm^3 for Filtek™ P60 (Group Cw_0) and 0.06 ± 0.02mm^3 for Filtek™ Supreme XT (Group Dw_0), respectively. The range of the mean total volumetric wear for Filtek™ Z100, Filtek™ Z250, Filtek™ P60 and Filtek™ Supreme XT varied from a low of 0.02mm^3 to a high of 0.04mm^3 for Group Aw_0 specimens, from 0.04 to 0.07mm^3 for Group Bw_0 specimens from a minimum of 0.09mm^3 to a maximum of 0.13mm^3 for Group Cw_0 specimens and from a low of 0.04mm^3 to a high of 0.06mm^3 for Group Dw_0

When the RBC materials were irradiated from a distance of 3mm the mean total volumetric wear and associated standard deviations for Z100™ (Group Aw_3), Filtek™ Z250 (Group Bw_3), Filtek™ P60 (Group Bw_3) and Filtek™ Supreme XT (Group Bw_3) were 0.02 ± 0.01mm^3, 0.07 ± 0.01mm^3, 0.09 ± 0.04mm^3 and 0.05 ± 0.03mm^3, respectively. The range of mean total volumetric wear for Z100™ (Group Aw_3) varied from a minimum of 0.02mm^3 to a maximum of 0.03mm^3, for Filtek™ Z250 (Group Bw_3)

from 0.06 to 0.07mm^3, for Filtek™ P60 (Group Cw_3) from a low of 0.09mm^3 to a high of 0.11mm^3 and for Filtek™ Supreme XT (Group Dw_3) from a minimum recorded value of 0.02mm^3 to a maximum value of 0.08mm^3.

The mean total volumetric wear and associated standard deviations irradiated from a distance of 5mm were 0.05 ± 0.02mm^3 for Z100™ (Group Aw_5), 0.05 ± 0.02mm^3 for Filtek™ Z250 (Group Bw_5), 0.06 ± 0.04mm^3 for Filtek™ P60 (Group Cw_5) and 0.06 ± 0.03mm^3 for Filtek™ Supreme XT (Group Dw_5). The range of the mean total volumetric wear varied for Group Aw_5 from 0.03 to 0.08mm, for Group Bw_5 from a minimum of 0.03mm to a maximum of 0.08mm, for Group Cw_5 from 0.02 to 0.11mm and for Group Dw_5 from a low of 0.03mm to a high of 0.09mm.

Specimens irradiated at a distance of 7mm from the top surface resulted in the mean total volumetric wear and associated standard deviations for Z100™ (Group Aw_7), Filtek™ Z250 (Group Bw_7), Filtek™ P60 (Group Cw_7) and Filtek™ Supreme XT (Group Dw_7) of 0.03 ± 0.01mm^3, 0.05 ± 0.01mm^3, 0.05 ± 0.00mm^3 and 0.04 ± 0.02mm^3, respectively. The range of the mean total volumetric wear varied from a maximum of 0.02mm^3 to a minimum of 0.04mm^3 for Group Aw_7 specimens, from 0.04mm^3 to 0.07mm^3 for Group Bw_7 specimens, a low of 0.05mm^3 to a high of 0.06mm^3 for Group Cw_7 specimens and from 0.03 to 0.06mm^3 for Group Dw_7 specimens, respectively.

The RBC specimens irradiated from a distance of 9mm resulted in mean total volumetric wear for Z100™ (Group Aw_9) varying from 0.03 to 0.06mm^3, for Filtek™ Z250 (Group

Bw_9) from a minimum of 0.02mm^3 to a maximum of 0.06mm^3, for Filtek™ P60 (Group Cw_9) from 0.04 to 0.10mm^3 and for Filtek™ Supreme XT (Group Dw_9) from a low of 0.01mm^3 to a high of 0.04mm^3. The mean total volumetric wear and associated standard deviations were 0.04 ± 0.01mm^3 for Group Aw_9, 0.04 ± 0.02mm^3 for Group Bw_9, 0.07 ± 0.03mm^3 for Group Dw_9 and 0.03 ± 0.02mm^3 for Group Dw_9.

The mean total volumetric wear and associated standard deviations of the RBCs irradiated 11mm from the top surface were 0.04 ± 0.02mm^3 for Z100™ (Group Aw_{11}), 0.04 ± 0.01mm^3 for Filtek™ Z250 (Group Bw_{11}), 0.06 ± 0.03mm^3 for Filtek™ P60 (Group Cw_{11}) and 0.05 ± 0.02mm^3 for Filtek™ Supreme XT (Group Dw_{11}). The range of the mean total volumetric wear varied from a low of 0.02mm^3 to a high of 0.06mm^3 for Group Aw_{11} specimens, from 0.03 to 0.06mm^3 for Group Bw_{11} specimens from a minimum of 0.03mm^3 to a maximum of 0.10mm^3 for Group Cw_{11} specimens and from a low of 0.04mm^3 to a high of 0.04mm^3 for Group Dw_{11}.

When the RBC materials were irradiated from a distance of 13mm from the top surface the mean total volumetric wear and associated standard deviations were 0.04 ± 0.02mm^3 for Z100™ (Group Aw_{13}), 0.06 ± 0.01mm^3 for Filtek™ Z250 (Group Bw_{13}), 0.05 ± 0.02mm^3 for Filtek™ P60 (Group Cw_{13}) and 0.02 ± 0.00mm^3 for Filtek™ Supreme XT (Group Dw_{13}). The range of mean total volumetric wear for Group Aw_{13} varied from a minimum of 0.02mm^3 to a maximum of 0.10mm^3, for Group Bw_{13} from 0.05 to 0.07mm^3, for Group Cw_{13} from a low of 0.03mm^3 to a high of 0.08mm^3 and for Group Dw_{13} from a minimum recorded value of 0.02mm^3 to a maximum value of 0.06mm^3.

Table 8.8: The mean total volumetric wear and mean maximum wear depth (associated standard deviations) at 50,000 wear cycles for the RBC specimens irradiated in contact with the top surface (at a distance of 0mm) and at distances of 3, 5, 7, 9, 11, 13 and 15mm from the top surface of the specimens using the QTH LCU.

RBC	Property	Irradiation Distance							
		0mm	3mm	5mm	7mm	9mm	11mm	13mm	15mm
Z100™	Mean total volumetric wear (mm^3)	0.03 (0.01)	0.02 (0.01)	0.05 (0.02)	0.03 (0.01)	0.04 (0.01)	0.04 (0.02)	0.04 (0.02)	0.03 (0.01)
	Mean maximum wear depth (mm)	0.05 (0.01)	0.04 (0.01)	0.06 (0.02)	0.05 (0.00)	0.05 (0.02)	0.05 (0.01)	0.05 (0.01)	0.06 (0.02)
Filtek™ Z250	Mean total volumetric wear (mm^3)	0.05 (0.01)	0.07 (0.01)	0.05 (0.02)	0.05 (0.01)	0.04 (0.02)	0.04 (0.01)	0.06 (0.01)	0.07 (0.01)
	Mean maximum wear depth (mm)	0.06 (0.01)	0.06 (0.01)	0.06 (0.02)	0.07 (0.01)	0.07 (0.02)	0.07 (0.00)	0.06 (0.01)	0.07 (0.02)
Filtek™ P60	Mean total volumetric wear (mm^3)	0.08 (0.01)	0.09 (0.04)	0.06 (0.04)	0.05 (0.00)	0.07 (0.03)	0.06 (0.03)	0.05 (0.02)	0.09 (0.03)
	Mean maximum wear depth (mm)	0.08 (0.01)	0.09 (0.00)	0.06 (0.02)	0.07 (0.01)	0.07 (0.03)	0.06 (0.02)	0.06 (0.02)	0.04 (0.01)
Filtek™ Supreme XT	Mean total volumetric wear (mm^3)	0.06 (0.02)	0.05 (0.03)	0.06 (0.03)	0.04 (0.02)	0.03 (0.02)	0.05 (0.02)	0.02 (0.00)	0.04 (0.02)
	Mean maximum wear depth (mm)	0.07 (0.04)	0.06 (0.01)	0.07 (0.02)	0.06 (0.01)	0.07 (0.02)	0.05 (0.01)	0.05 (0.01)	0.05 (0.01)

The mean total volumetric wear and associated standard deviations of the RBCs irradiated 15mm from the top surface for Z100™ (Group Aw_{15}), Filtek™ Z250 (Group Bw_{15}), Filtek™ P60 (Group Cw_{15}) and Filtek™ Supreme XT (Group Dw_{15}) were 0.03 ± 0.01mm^3, 0.07.1 ± 0.01mm^3, 0.09 ± 0.03mm^3 and 0.04 ± 0.02mm^3, respectively. The the mean total volumetric wear for Group Aw_{15} ranged from 0.01 to 0.04mm^3, for Group Bw_{15} from a minimum of 0.06mm^3 to a maximum of 0.08mm^3, for Group Cw_{15} from 0.06 to 0.18mm^3 and for Group Dw_{15} from a low of 0.02mm^3 to a high of 0.07mm^3.

8.5.1.2 Mean maximum wear depth

The mean maximum wear depth and associated standard deviations of the RBC specimens irradiated at distances of 0, 3, 5, 7, 9, 11, 13 and 15mm are also recorded in Table 8.8

8.5.1.3 Statistical analysis

The mean total volumetric wear data was analysed using one- (irradiated distance) and two-way (irradiated distance × RBC material) ANOVAs and Tukey's multiple range tests at a significance level of $P<0.05$ when irradiated at distances of 0, 3, 5, 7, 9, 11, 13 and 15mm from the top surface of the RBC specimens.

The one-way ANOVA of the group means of the total volumetric wear for Z100™ ($P=0.394$), Filtek™ Z250 ($P=0.076$), Filtek™ P60 ($P=0.279$) and Filtek™ Supreme XT

(P=0.504) identified no significant differences in mean total volumetric wear for each RBC material at the irradiated distances investigated. The two-way ANOVA identified no significant effect for irradiated distance (P=0.317), however, a significant effect was highlighted for RBC material (P<0.0001). The Tukey's multiple range tests revealed significant differences for the group means of the total volumetric wear of Z100™ compared with Filtek™ Z250 (P=0.003) and Filtek™ P60 (P<0.0001). In addition, the Tukey's multiple range tests revealed significant differences for the group means of the total volumetric wear of Filtek™ P60 compared with Z100™ (P<0.0001), Filtek™ Z250 (P=0.033) and Filtek™ Supreme XT (P<0.0001).

One- and two-way ANOVAs, at a significance level of P<0.05, were used to analyse the group means of the maximum wear depth data in terms of irradiated distance and irradiated distance × RBC material, respectively (P>0.05). When the one-way ANOVA was performed no significant differences in group means of the maximum wear depth data were identified with irradiated distance for Z100™ (P=0.079), Filtek™ Z250 (P=0.816), Filtek™ P60 (P=0.059) and Filtek™ Supreme XT (P=0.462). The two-way ANOVA of the group means of the maximum wear depth data with irradiated distance × material identified no significant effect for irradiated distance (P=0.207), however, a significant effect was evident for RBC material (P<0.0001). The Tukey's multiple range tests revealed a significant differences for the group means of the maximum wear depth data of Z100™ compared with Filtek™ Z250 (P=0.007) and Filtek™ P60 (P<0.0001) and also for Filtek™ P60 compared with Filtek™ Supreme XT (P=0.007).

8.5.2 Long-term *in-vitro* wear resistance

8.5.2.1 *In-vitro* wear resistance at 150,000 cycles

The RBC materials irradiated at a distance of 0mm resulted in mean total volumetric wear and associated standard deviations of 0.05 ± 0.02mm^3 for Z100™ (Group Aw_0), 0.09 ± 0.03mm^3 for Filtek™ Z250 (Group Bw_0), 0.10 ± 0.01mm^3 for Filtek™ P60 (Group Cw_0) and 0.07 ± 0.02mm^3 for Filtek™ Supreme XT (Group Dw_0), respectively following 150,000 wear cycles (Figure 8.1). Mean maximum wear depth and associated standard deviations of 0.09 ± 10.03mm for Z100™, 0.09 ± 0.01mm for Filtek™ Z250, 0.10 ± 0.01mm for Filtek™ P60 and 0.08 ± 0.01mm for Filtek™ Supreme XT (Group Dw_0), respectively were also recorded (Figure 8.2). The range of the mean total volumetric wear and the mean maximum wear depths are reported in Table 8.9.

When irradiated at a distance of 7mm the mean total volumetric wear and associated standard deviations following 150,000 wear cycles for Z100™ (Group Aw_7) were 0.09 ± 0.02mm^3, Filtek™ Z250 (Group Bw_7) were 0.11 ± 0.04mm^3, Filtek™ P60 (Group Cw_7) were 0.13 ± 0.02mm^3 and Filtek™ Supreme XT (Group Dw_7) were 0.11 ± 0.04mm^3. The mean maximum wear depth and associated standard deviations were 0.12 ± 0.03mm for Group Aw_7, 0.08 ± 0.02mm Group Bw_7, 0.11 ± 0.03mm for Group Cw_7 and 0.08 ± 0.02mm for Group Dw_7, respectively. The range of the mean total volumetric wear and mean maximum wear depths are reported in Table 8.9.

Table 8.9: The mean total volumetric wear and mean maximum wear depths (associated standard deviations) following 150,000 wear cycles for the RBC specimens irradiated at a distance of 0, 7 and 15mm.

RBC	Property	Irradiation Distance		
		0mm	7mm	15mm
Z100™	Mean total volumetric wear (mm^3)	0.05 (0.02)	0.09(0.02)	0.12 (0.03)
	Mean maximum wear depth (mm)	0.09 (0.03)	0.12 (0.03)	0.12 (0.02)
Filtek™ Z250	Mean total volumetric wear (mm^3)	0.09 (0.03)	0.11 (0.04)	0.20 (0.06)
	Mean maximum wear depth (mm)	0.09 (0.01)	0.08 (0.02)	0.09 (0.03)
Filtek™ P60	Mean total volumetric wear (mm^3)	0.10 (0.01)	0.13 (0.02)	0.17 (0.02)
	Mean maximum wear depth (mm)	0.10 (0.01)	0.11 (0.03)	0.12 (0.04)
Filtek™ Supreme XT	Mean total volumetric wear (mm^3)	0.07 (0.02)	0.11 (0.04)	0.13 (0.04)
	Mean maximum wear depth (mm)	0.08 (0.01)	0.08 (0.02)	0.10 (0.02)

Following 150,000 wear cycles the RBCs irradiated from a distance of 15mm resulted in mean total volumetric wear and associated standard deviations of $0.12 \pm 0.03mm^3$ for Z100™ (Group Aw_{15}), $0.20 \pm 0.06mm^3$ for Filtek™ Z250 (Group Bw_{15}), $0.17 \pm 0.02mm^3$ for Filtek™ P60 (Group Cw_{15}) and $0.13 \pm 0.04mm^3$ for Filtek™ Supreme XT (Group Dw_{15}) (Figure 8.1). The mean maximum wear depth and associated standard deviations for Group Aw_{15} were 0.12 ± 0.02mm, Group Bw_{15} were 0.09 ± 0.03mm, Group Cw_{15} were 0.12 ± 0.04mm and Group Dw_{15} were 0.10 ± 0.02mm (Figure 8.2). The range of the mean total volumetric wear and mean maximum wear depths are reported in Table 8.9.

8.5.2.2 *In-vitro* wear resistance at 300,000 cycles

When RBC specimens were irradiated in contact with the top surface the mean total volumetric wear and associated standard deviations for Z100™ (Group Aw_0), Filtek™ Z250 (Group Bw_0), Filtek™ P60 (Group Cw_0) and Filtek™ Supreme XT (Group Dw_0) were 0.09 ± 0.03mm^3, 0.14 ± 0.02mm^3, 0.14 ± 0.02mm^3 and 0.12 ± 0.03mm^3, respectively following 300,000 wear cycles (Figure 8.1). The mean maximum wear depth and associated standard deviations for Z100™ (Group Aw_0), Filtek™ Z250 (Group Bw_0), Filtek™ P60 (Group Cw_0) and Filtek™ Supreme XT (Group Dw_0) were 0.11 ± 0.04mm, 0.12 ± 0.00mm, 0.15 ± 0.03mm and 0.11 ± 0.01mm, respectively (Figure 8.2). The range of the mean total volumetric wear and mean maximum wear depths are reported in Table 8.10.

Following 300,000 wear cycles the mean total volumetric wear and associated standard deviations when irradiated at a distance of 7mm were 0.12 ± 0.02mm^3 for Z100™ (Group Aw_7), 0.16 ± 0.04mm^3 for Filtek™ Z250 (Group Bw_7), 0.15 ± 0.02mm^3 for Filtek™ P60 (Group Cw_7) and 0.19 ± 0.06mm^3 for Filtek™ Supreme XT (Group Dw_7). The mean maximum wear depth and associated standard deviations of 0.13 ± 0.03mm for Group Aw_7, 0.11 ± 0.04mm for Group Bw_7, 0.16 ± 0.01mm for Group Cw_7 and 0.12 ± 0.02mm for Group Dw_7.The range of the mean total volumetric wear and mean maximum wear depths are reported in Table 8.10.

Table 8.10: The mean total volumetric wear and mean maximum wear depth (associated standard deviations) following 300,000 wear cycles wear cycles for the RBC specimens irradiated at a distance of 0, 7 and 15mm.

RBC	Property	Irradiation Distance		
		0mm	7mm	15mm
Z100™	Mean total volumetric wear (mm^3)	0.09 (0.03)	0.12 (0.02)	0.22 (0.05)
	Mean maximum wear depth (mm)	0.11 (0.04)	0.13 (0.03)	0.16 (0.04)
Filtek™ Z250	Mean total volumetric wear (mm^3)	0.14 (0.02)	0.16 (0.04)	0.28 (0.06)
	Mean maximum wear depth (mm)	012 (0.00)	0.11 (0.04)	0.13 (0.04)
Filtek™ P60	Mean total volumetric wear (mm^3)	0.14 (0.02)	0.15 (0.02)	0.18 (0.02)
	Mean maximum wear depth (mm)	015 (0.03)	016 (0.01)	0.22 (0.07)
Filtek™ Supreme XT	Mean total volumetric wear (mm^3)	0.12 (0.03)	0.19 (0.06)	0.21 (0.03)
	Mean maximum wear depth (mm)	0.11 (0.01)	0.12 (0.02)	0.12 (0.03)

Irradiation at a distance of 15mm from RBC specimen resulted in the mean total volumetric wear and associated standard deviations for Z100™, Filtek™ Z250, Filtek™ P60 and Filtek™ Supreme XT of 0.22 ± 0.05mm^3, 0.28 ± 0.10mm^3, 0.18 ± 0.02mm^3 and 0.21 ± 0.03mm^3, respectively following 3000,000 wear cycles (Figure 8.1). The mean maximum wear depth and associated standard deviations were 0.16 ± 0.04mm for Z100™ (Group Aw_{15}), 0.13 ± 0.04mm for Filtek™ Z250 (Group Bw_{15}), 0.22 ± 0.07mm for Filtek™ P60 (Group Cw_{15}) specimens and 0.12 ± 0.03mm for Filtek™ Supreme XT (Group Dw_{15}) (Figure 8.2). The range of the mean total volumetric wear and mean maximum wear depths are reported in Table 8.10.

Figure 8.1: The mean total volumetric wear at 50,000, 150,000, 300,000 and 500,000 wear cycles for Z100™, Filtek™ Z250, Filtek™ P60 and Filtek™ Supreme XT irradiated at distances of 0, 7 and 15mm using a QTH handheld LCU at irradiances of 650 ± 14, 350 ± 8, and 150 ± 8mW/cm^2, respectively.

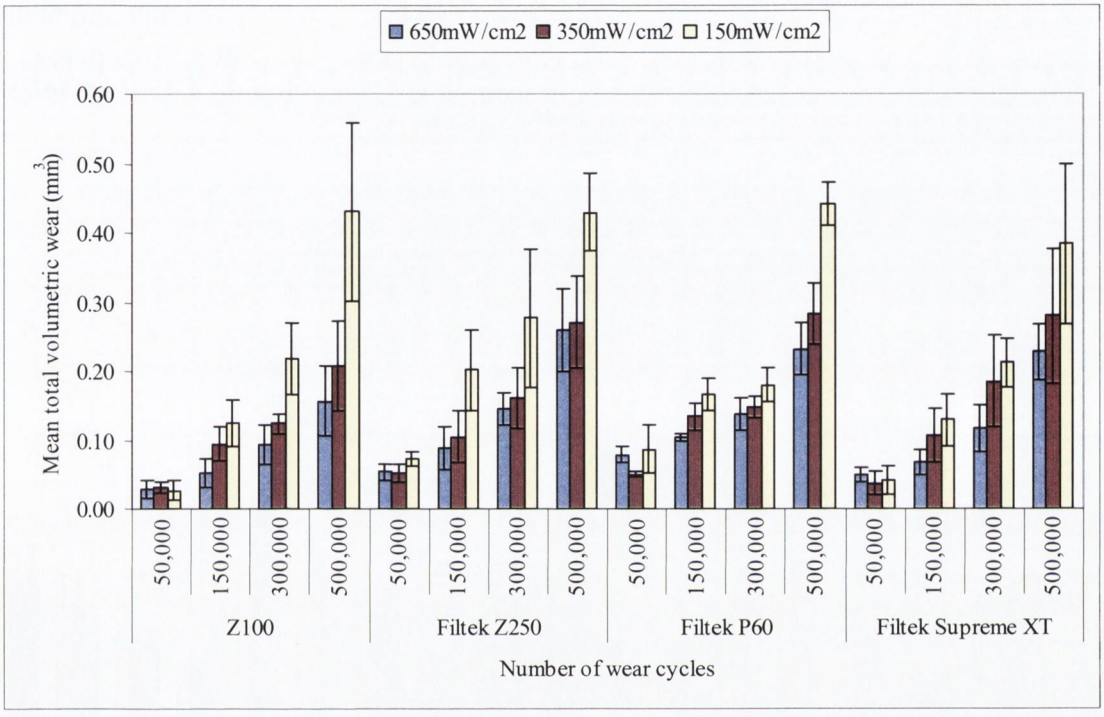

8.5.2.3 *In-vitro* wear resistance at 500,000 cycles

Following 500,000 wear cycles the mean total volumetric wear and associated standard deviations when irradiated at a distance of 0mm for Z100™ (Group Aw_0) were 0.16 ± 0.05mm^3, Filtek™ Z250 (Group Bw_0) were 0.26 ± 0.06mm^3, Filtek™ P60 (Group Cw_0) were 0.23 ± 0.04mm^3 and Filtek™ Supreme XT (Group Dw_0) were 0.23 ± 0.04mm^3. The mean maximum wear depth and associated standard deviations for Z100™, Filtek™ Z250, Filtek™ P60 and Filtek™ Supreme XT were 0.16 ± 0.03mm, 0.14 ± 0.01mm, 0.19

± 0.04mm and 0.14 ± 0.03mm, respectively (Figure 8.2). The range of the mean total volumetric wear and mean maximum wear depths are reported in Table 8.11.

Figure 8.2: The mean maximum wear depth at 50,000, 150,000, 300,000 and 500,000 wear cycles for Z100™, Filtek™ Z250, Filtek™ P60 and Filtek™ Supreme XT irradiated at distances of 0, 7 and 15mm using a QTH handheld LCU at irradiances of 650 ± 14, 350 ± 8, and 150 ± 8mW/cm^2, respectively

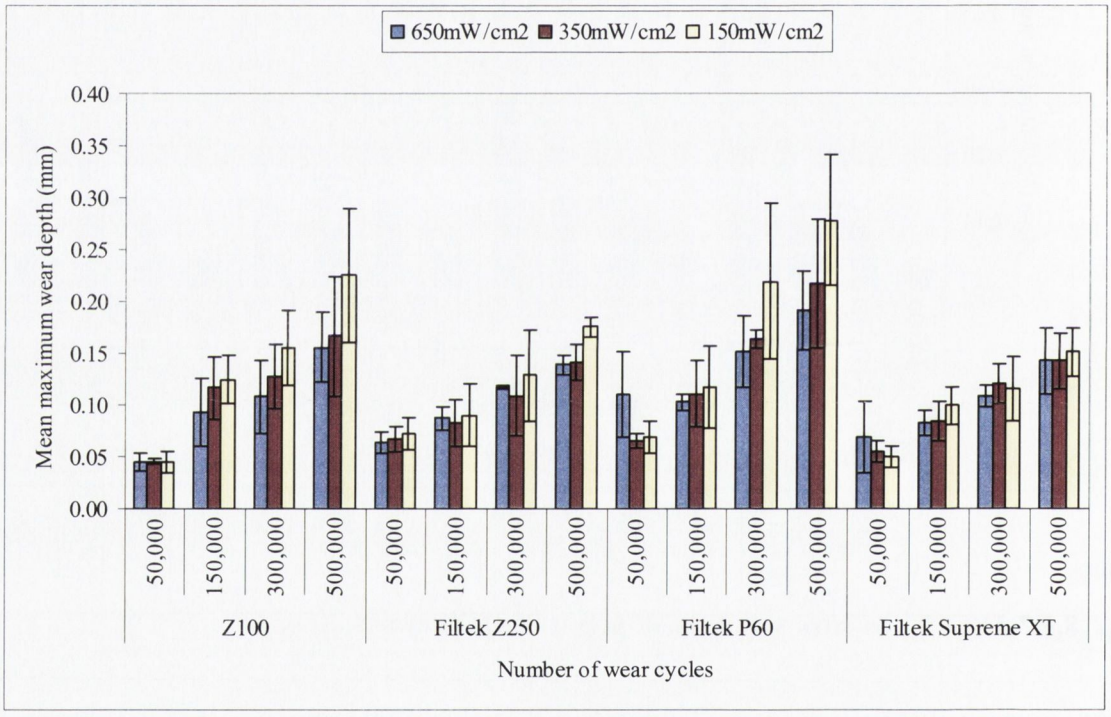

The mean total volumetric wear and associated standard deviations following 500,000 wear cycles and irradiaion at a distance of 7mm were 0.21 ± 0.07mm^3 for Group Aw_7, 0.27 ± 0.07mm^3 for Group Bw_7, 0.28 ± 0.04mm^3 for Group Cw_7 specimens and 0.28 ± 0.10mm^3 for Group Dw_7 (Figure 8.1). The mean maximum wear depth and associated standard deviations were 0.17 ± 0.06mm for Z100™ (Group Aw_7), 0.14 ± 0.02mm for Filtek™ Z250 (Group Bw_7), 0.22 ± 0.06mm for Filtek™ P60 (Group Cw_7) and 0.14 ±

0.03mm for Filtek™ Supreme XT (Group Dw_7), respectively. The range of the mean total volumetric wear and mean maximum wear depths are reported in Table 8.11.

Irradiating the RBC materials at a distance of 15mm before *in-vitro* wear testing for 500,000 wear cycles resulted in mean total volumetric wear and associated standard deviations for Z100™ (Group Aw_{15}) of 0.43 ± 0.13mm^3, for Filtek™ Z250 (Group Bw_{15}) of 0.43 ± 0.06mm^3, for Filtek™ P60 (Group Cw_{15}) of 0.44 ± 0.03mm^3 and for Filtek™ Supreme XT (Group Dw_{15}) of 0.38 ± 0.11mm^3 (Figure 8.1). The mean maximum wear depth and associated standard deviations were 0.23 ± 0.06mm, 0.18 ± 0.01mm, 0.28 ± 0.06mm and 0.15 ± 0.02mm for Z100™, Filtek™ Z250, Filtek™ P60 and Filtek™ Supreme XT, respectively (Figure 8.2). The range of the mean total volumetric wear and mean maximum wear depths are reported in Table 8.11.

Table 8.11: The mean total volumetric wear and mean maximum wear depth (associated standard deviations) at 500,000 wear cycles wear cycles for the RBC specimens irradiated at a distance of 0, 7 and 15mm

RBC	Property	Irradiation Distance		
		0mm	7mm	15mm
Z100™	Mean total volumetric wear (mm^3)	0.16 (0.05)	0.21 (0.07)	0.43 (0.13)
	Mean maximum wear depth (mm)	0.16 (0.03)	0.17 (0.06)	0.23 (0.06)
Filtek™ Z250	Mean total volumetric wear (mm^3)	0.26 (0.06)	0.27 (0.07)	0.43 (0.43)
	Mean maximum wear depth (mm)	0.14 (0.01)	0.14 (0.02)	0.18 (0.01)
Filtek™ P60	Mean total volumetric wear (mm^3)	0.23 (0.04)	0.28 (0.04)	0.44 (0.03)
	Mean maximum wear depth (mm)	0.19 (0.04)	0.22 (0.06)	0.28 (0.06)
Filtek™ Supreme XT	Mean total volumetric wear (mm^3)	0.23 (0.04)	0.28 (0.10)	0.38 (0.11)
	Mean maximum wear depth (mm)	0.14 (0.03)	0.14 (0.03)	0.15 (0.02)

8.5.2.4 Statistical analysis

For the long-term wear resistance two- (irradiated distance × number of wear cycles) and three-way (irradiated distance × RBC material × number of wear cycles) ANOVAs and Tukey's multiple range tests were undertaken at a significance level of $P<0.05$ for analysis of the mean total volumetric wear following 150,000, 300,000 and 500,000 wear cycles when irradiated at distances of 0, 7 and 15mm from the top surface of the RBC specimens.

The two-way ANOVA of the group means of the total volumetric wear identified a significant effect of irradiated distance ($P<0.001$) and number of wear cycles ($P<0.001$) for Z100™, Filtek™ Z250, Filtek™ P60, and Filtek™ Supreme XT. The Tukey's multiple range tests analysis revealed no significant differences for the group means of the total volumetric wear when compared with irradiated distances of 7 and 15mm for each investigated RBC material (all P values were greater than 0.1). The three-way ANOVA (irradiated distance × RBC material × number of wear cycles) identified a significant interactions for the group means of the total volumetric wear with irradiated distance ($P<0.0001$), RBC material ($P<0.0001$) and number of wear cycles ($P<0.0001$).

Two- (irradiated distance × number of wear cycles) and three-way (irradiated distance × RBC material × number of wear cycles) ANOVAs and Tukey's multiple range tests at a significance level of $P<0.05$ were considered for the RBC materials for analysis of the mean maximum wear depth at 150,000, 300,000 and 500,000 wear cycles when irradiated at distances of 0, 7 and 15mm.

The two-way ANOVA of the group means of the maximum wear depth highlighted a significant effect of number of wear cycles ($P<0.0001$), however, no significant effect of irradiated distance for Filtek™ Z250 ($P=0.083$), Filtek™ P60 ($P=0.055$) and Filtek™ Supreme XT ($P=0.996$) was indicated for the group means of the maximum wear depths. The three-way ANOVA (irradiated distance × RBC material × number of wear cycles) undertaken identified a significant effect for irradiated distance ($P<0.0001$), RBC

material ($P<0.0001$) and number of wear cycles ($P<0.0001$) in the group means of the maximum wear depths reported in the current study.

CHAPTER 9 Discussion

9.1 LCU irradiance degradation

Increasing the LCU exit window distance from the RBC top surface results in a reduction in the irradiance (Corcionali et al., 2008) at the proximal portion of the light cone generated from the exit window to the RBC material. Darvell (2002) highlighted that as a result of beam spreading, the irradiance reaching the RBC material top surface falls rapidly as the exit window is moved away from the RBC. This phenomenon of irradiance degradation with distance from the LCU has also previously been reported in the dental literature (Pires et al 1993; Sakaguchi and Berge, 1998) which corresponds well with the irradiance degradation with irradiation distance for the LCUs identified in the current study. While the irradiance reaching the top surface of the RBC is decreased the phenomenon is further exacerbated when, light transmission characteristics of the RBC depending upon the influence of shade, monomeric reactivity, refractive index mismatch, light scattering and absorption (Sakaguchi and Berge, 1998; Shortall et al., 2008) are taken into consideration.

9.2 Three-point flexure properties

In the three-point flexure testing methodology rectangular bar-shaped specimens of brittle materials are subjected to three-point flexure loading, where a pure state of tension (Berenbaum and Brodie, 1959) is placed on one side of the specimen (not the irradiated

side). A major disadvantage of the three-point flexure testing methodology is that the stress in the loaded section is not uniform (Williams and Smith, 1971) varying from zero at the neutral plane to a maximum compressive stress at the irradiated surface (for specimens tested in the current study) to a maximum tensile stress on the non-irradiated surface. This non-uniform stress distribution accentuates the influence of surface flaws on the measured strength (Ruidnick et al., 1963) such that the test results are in excess of the true tensile strength of the material in question (Wright, 1955; Ruidnick et al., 1963; Earnshaw and Smith, 1966).

Strength is not an intrinsic material property (Darvell, 1990; Kelly, 1995) as the dimensions of the rectangular bar-shaped specimens influences the load to failure and therefore the mean three-point flexure strength (Darvell, 1990; Ashby and Jones, 1998). In theory, the larger the specimen volume the greater the likelihood of introducing crack initiating defects and therefore one would expect a lower mean compressive fracture strength (Ashby and Jones, 1998). However, it is clear from the information available in the dental literature that differences in the three-point flexure strengths are routinely achieved for RBC specimens with similar dimensions. For the RBCs investigated the three-point flexure strengths varied from 79-184MPa for Z100™ MP Restorative (Peutzfeld and Asmussen, 2000; Cesar et al., 2001; Yap et al., 2002; Adabo et al., 2003; Palin et al., 2003; Beun et al., 2007), 92-245MPa for Filtek™ Z250 (Ferracane et al., 2003; Mitra et al., 2003; Palin et al., 2003; Yap et al., 2003; Palin et al., 2005; Calherios et al., 2006), 138-170MPa for Filtek™ P60 (Adabo et al., 2003; Ferracane et al., 2003) and 113-153MPa for Filtek™ Supreme XT (Mitra et al., 2003; Beun et al., 2007). The

variously reported three-point flexure properties were reported to be indicative of the degree of conversion (Ferracane et al., 2003; Calherios et al., 2006), irradiance (Miyazaki et al., 1996; Calherios et al., 2006), type of mould (Peutzfeld and Asmussen, 2000; Palin et al., 2003; Beun et al., 2007) and light source (Ferracane et al., 2003; Palin et al., 2003, 2005) employed, although different operators would be expected to manipulate the materials differently as well.

It is known that the elastic modulus which is calculated from the ratio of stress to strain in the elastic range of the RBC offers a further insight into material performance, as the elastic modulus is an intrinsic material property independent of specimen dimensions. Additionally, the elastic modulus can be linked directly to the bonding between atoms (Askeland and Phulé, 2005) and therefore is not sensitive to microstructure or crack initiating defects in the same way as three-point flexure strength (Kelly, 1995). Whilst one might expect consistency in the three-point flexure modulus data reported in the dental literature for RBC specimens of similar dimensions, this was unfortunately not the case. For the RBCs investigated the three-point flexure modulus data varied from 5.8-17GPa for Z100™ MP Restorative (Unterbrink and Muessner, 1995; Miyazaki et al., 1996; Choi et al., 2000; Peutzefeldt and Asmussen, 2000; Stahl et al., 2000; Asmussen and Peutzefeldt, 2004; Beun et al., 2007), 8.4-14GPa for Filtek™ Z250 (Musanje et al., 2004; Walker et al., 2006; Calheiros et al., 2006), 10-18GPa for Filtek™ P60 (Papadogiannis et al., 2008) with little published data available for Filtek™ Supreme XT (Beun et al., 2007; Papadogiannis et al., 2008). The degree of conversion (Ferracane et al., 2003; Calherios et al., 2006), irradiance (Miyazaki et al., 1996; Calherios et al., 2006)

and type of mould (Peutzfeld and Asmussen, 2000; Beun et al., 2007) and light source (Ferracane et al., 2003) employed, during specimen manufacture all contribute to the variations in the three-point flexure moduli reported.

9.2.1 Irradiation distance

In the current study the type of mould was consistent as was the irradiation time (as specified for each RBC material) such that the only variable was the irradiance for each LCU assessed. For the four dimethacrylate RBC materials increasing the irradiation distance from 0 to 15mm resulted in significant differences in the group means of the three-point flexure strengths and the three-point flexure moduli when irradiated with each LCU. Additionally, increasing the irradiation distance from 0 to 7mm also resulted in significant differences in the group means of the three-point flexure strengths and the three-point flexure moduli when irradiated with all LCUs investigated with the exception of the three-point flexure modulus for Z100™ when irradiated at distances of 0 to 7mm with the Optilux 501 QTH LCU.

In the current study, the measured irradiance decreased with irradiation distance (0, 7 and 15mm) from 650 ± 14mW/cm^2 to 350 ± 8mW/cm^2 and 150 ± 8mW/cm^2 for the QTH LCU, from 246 ± 8mW/cm^2 to 186 ± 14mW/cm^2 and less than 100mW/cm^2 for the Elipar™ Freelight LED LCU and 1160 ± 8mW/cm^2 to 469 ± 8mW/cm^2 and 129 ± 14mW/cm^2 for the Elipar™ Freelight 2 LED LCU. This phenomenon of irradiance decreasing with distance from the LCU was previously reported in the dental literature

(Pires et al 1993; Sakaguchi and Berge, 1998). In RBC materials, irradiation forms an excited state photo-sensitiser which has to react with the amine initiator and may then result in a free radical being formed (inefficiently) since the photo-sensitiser and the amine are present at low concentrations. This makes the rate of free radical production and therefore the rate of initiation for the process low. In current study, the process is compounded further by the magnitude of the irradiance where reciprocity failure became of practical importance for the three-point flexure properties. Therefore the deviation from the predicted approach to the plateau value (for a constant irradiation time) as described by Musanje and Darvell (2003) occurred at irradiation distances between 0 and 7mm for the RBCs investigated although the irradiation distance may have been considerably lower than the 7mm since the depth of cure is reduced with increasing distance.

The maximum three-point flexure properties (strength and modulus) that may be attained for the RBCs investigated would be expected to correspond to between 40 and 70% conversion of double bonds (at a given temperature). In view of the absorption by the photo-sensitiser (the irradiance is reduced as it travels through the 2mm bar-shaped specimens) according to Beer-Lamberts law, in combination with light scattering by the high volume of filler particles the resultant attainment of the three-point flexure properties is compromised. This was the case in the current study at irradiation distances between 0 and 7mm manifested as a reduction in the three-point flexure properties which was further compounded on comparing the flexure properties when irradiated at a distance of 15mm. It is suggested that the non-significant difference in three-point flexure

moduli for Z100™ when irradiated at distances of 0 to 7mm with the Optilux 501 QTH LCU may have been a result of the different monomeric formulation compared with the other RBCs investigated for the absorption spectrum generated by the Optilux 501 QTH LCU.

Since the deviation from the maximum three-point flexure properties (strength and modulus) from the predicted approach to the plateau value (for a constant irradiation time) as described by Musanje and Darvell (2003) occurred at irradiation distances between 0 and 7mm it is not surprising that increasing the irradiation distance to 15mm would further compound the deviation from the maximum three-point flexure properties although variations from 7 to 15mm were in general non-significant.

9.2.2 RBC material

Generally, in terms of RBC material, the one-way ANOVA for each LCU at 0, 7 and 15mm irradiated distances no significant differences in the group means of the three-point flexure properties were highlighted between Filtek™ Z250 and Filtek™ P60. The methacrylate RBCs (Filtek™ Z250 and Filtek™ P60) contain exactly the same monomeric resin constituents and filler loadings (60 and 61vol.%, respectively (Table 3.1)) such that it would be expected that both materials would perform in a similar manner when tested in three-point flexure. Whilst one may expect Filtek™ Supreme XT, which contains exactly the same monomeric resin constituents and a similar filler loading (59.5vol%), to behave in the same manner to Filtek™ Z250 and Filtek™ P60, the nano-

filler technology in the Filtek™ Supreme XT must play a role in disrupting the light attenuation trough the material. This is further emphasised in the three-point flexure strength data for Filtek™ Supreme XT where significant differences between group means were identified for all LCUs irradiated for all distances. Comparison of the three-point flexure strength data with then recommendations in ISO 4049 are interesting. The standard suggests that if three of five three-point flexure specimens fail to reach the 80MPa specified limit the RBC is deemed to 'have failed absolutely'. In the current study Filtek™ Supreme XT would have failed to meet the ISO criteria if irradiated with the Elipar™ Freelight LED LCU at irradiation distances of 7 and 15mm which may have clinical implications with respect to the flexure strength, modulus, marginal integrity and wear resistance when using Filtek™ Supreme XT.

9.3 Reliability of the flexure strength data

The distribution of flexure strengths of quasi-brittle RBC materials can be more properly described by Weibull statistics rather than mean fracture strengths determined from a Gaussian strength distribution. In the three-point flexure strength data for irradiation distances in excess of 0mm (namely 7 and 15mm) the data are normally distributed and is perfectly well described using mean and standard deviation. The graphical display of the quality of the fit to a Weibull distribution was not at all convincing. In the USA the use of the Weibull Modulus to predict brittleness would be considered contentious since it is really a combination of the characteristic value and the Weibull modulus which will indicate the chances of finding a specimen which fractures at low strength. Therefore

given the reduced depth of cure at the bottom surfaces of the RBC specimens irradiated at distances of 7 and 15mm the most appropriate statistical method was identified to be adequately described using mean and standard deviation.

9.4 Bi-axial flexure strength

An alternative testing methodology to the three-point flexure test is the bi-axial flexure strength test (Giovan & Sines, 1979; Ban & Anusavice, 1990; Ban et al., 1992) where a disc-shaped specimen is centrally loaded so that the maximum tensile stresses occurs at the centre of the specimen and decreases rapidly with increased radial distance from the centre of the disc (Ban et al., 1992). This technique eliminates spurious edge failures, offers controllable specimen geometry, sample preparation is simple and the disc-shaped specimens have a surface to volume ratio more closely related to that of actual restorations than conventional three-point flexure specimens (Piddock et al., 1987). Ritter et al. (1980) and Shetty et al. (1980) showed in their literature reviews of bi-axial flexure strength testing that several variations of test method exist including the ring-on-ring, piston-on-three-ball and ball-on-ring tests. In the ring-on-ring test a plate shaped specimen is supported by a ring and loaded with a smaller coaxial ring. However, Ritter et al. (1980) identified a stress concentration under the loading ring using finite element analysis modeling techniques so that if fracture initiates in this region then the fracture stress as well as the area and volume subjected to the maximum stress are significantly less than that assumed by theoretical considerations. In the piston-on-three-ball flexure test, developed by Kirstein & Woolley (1967), a plate shaped specimen is peripherally

supported by three equi-spaced balls and centrally loaded with a flat piston. While the piston-on-three-ball test allows for the fracture of slightly warped specimens the stress under the flat piston is non-uniform and difficult to model so that the calculation of the flexure stress is uncertain (De With & Wagemans, 1989). In the ball-on-ring bi-axial flexure strength test (Shetty et al., 1980) a plate shaped specimen is supported on a ring and loaded centrally with a ball. Because minimal friction exists between the test specimen and jig during loading the ball-on-ring or shell test was advocated by De With & Wagemans (1989) as being the most reliable bi-axial flexure strength test method. This suggests that because of the elimination of friction clinically relevant strengths are obtained with greater clinical significance of the results.

Further advantages of the disc-shaped specimens are that they can be irradiated in a 'one-hit' irradiation and as a result specimen manufacture time is markedly reduced as is the volume of RBC materials required for sample preparation. The deviation of the maximum bi-axial flexure strengths occurred at irradiation distances from 11mm compared with the 7mm identified for the three-point flexure properties. The variation in distance from 7 to 11mm is indicative of the testing methodology as different stress distributions are placed on the three-point and bi-axial flexure test specimens. It is suggested that the less irradiated bottom surface, from which the crack initiates, does not provide a sensitive enough fracture mechanism to enable an accurate representation of the true tensile strength of the RBC materials tested. This is reinforced by the results of the one-way ANOVA indicating no significant differences in the bi-axial flexure strengths between the irradiation distances investigated. However, significant differences in the group

means of the bi-axial flexure strengths were highlighted by the two-way ANOVA for Filtek™ Supreme XT ($P<0.0001$) when the Tukey's multiple range test were analysed and compared with Z100™ ($P<0.0001$), Filtek™ Z250 ($P<0.0001$) and Filtek™ P60 ($P<0.0001$). It is again suggested that the nano-filler technology in the Filtek™ Supreme XT must play a role in disrupting the light attenuation through the material manifested as a significant difference in the group means of the bi-axial flexure strengths.

9.5 *In-vivo* wear resistance

Mair et al. (1996) described wear is a tribological process that due to the interaction of opposing surfaces results in the loss of material from the softer of the two mating surfaces. Mair et al. (1996) further suggested that in the oral environment the wear of dental restoratives can result from a variety of mechanical interactions including abrasion, attrition, adhesion, fatigue and erosion or indeed a combination of two or more of these interactions. The assessment of the wear of restorations *in-vivo* was initially conducted through either direct observation of the restoration at regular patient visits (Cvar and Ryge, 1971) or by the indirect analysis of tooth replicas of the restorations, proposed by Leinfelder et al. in 1986. The Cvar and Ryge technique was adopted as the United States Public Health Service (USPHS) technique in 1980 (Ryge, 1980). Two or more independent clinical observers directly evaluated the wear of restorations after regular time intervals and rated them as either clinically ideal (Alpha), clinically acceptable (Bravo) or clinically unacceptable (Charlie) as defined by specific criteria (Ryge, 1980). One of the major drawbacks of the USPHS technique was that clinical

observers were subjective in their assessment and often disagreed over ratings such that restorations were rated as Bravo at one visit and Alpha at a later revisit (Taylor et al., 1989) when wear would be expected to increase with time. In addition, further problems included the difficulty in achieving continuity of clinical observers for subsequent patient visits, notwithstanding patient attendance, expense and compliance issues. The quantitative indirect assessment of dental restorative wear, namely the technique reported by Leinfelder et al. (1986), compared stone cast replicas of teeth containing restorations to six standard casts which corresponded to specific wear depths. The requirement of the Leinfelder technique was for both positive and negative impressions of the restored teeth to be taken. However, a major shortcoming was that both dental impression materials and dental stone materials were susceptible to varying dimensional instability on setting, thereby impeding the dimensional precision of the replicas and as a result, clinical confidence in the wear data. The imprecision of both the direct (USPHS) and indirect (Leinfelder technique) *in-vivo* method ologies, routinely employed to assess the wear resistance of restorative materials, meant the dental profession had to pursue alternative technologies to assess the *in-vivo* wear of dental structures. The potential of computerised three-dimensional (3D) mapping techniques such as the Michigan computer graphic technique (McDowell et al., 1988) and 3D profilometry techniques (Conry et al., 1992) were championed as revolutionary methodologies which could produce consistent *in-vivo* wear measurements for dental restoratives when placed in the oral environment.

Over the last 30 years there were numerous attempts to develop *in-vitro* wear simulators, namely devices that would mimic the masticatory processes that occur in the oral

environment, which could provide an initial screening for the use of potential restorative materials (Forss et al., 1991). The advantage of such an *in-vitro* wear simulator would be realised most effectively in the assessment of the wear resistance, of potential dental materials designed for use in occlusal restorations, prior to placement in the mouth which would avert the need for expensive and time consuming clinical trials on substandard materials. A variety of *in-vitro* wear simulators were developed including the Materials Testing and Simulation (MTS) artificial oral environment (DeLong and Douglas, 1983), the Academisch Centrum for Tandheelkunde Amsterdam (ACTA) wear machine (De Gee et al., 1986), the University of Alabama wear machine (Leinfelder et al., 1989) and the Oregon Health Science University (OHSU) oral wear simulator (Condon and Ferracane, 1996). Internationally there is no recognised standard for the *in-vitro* wear assessment of dental restoratives which is more than likely a result of the difficulties involved in simulating the complex wear behaviour routinely encountered in the oral environment. As a result, currently there is no single *in-vitro* wear simulator that can simulate clinical wear in the oral environment as the *in-vitro* wear machines (MTS, ACTA, University of Alabama and OHSU) simulate one or two of the individual wear mechanisms outlined by Mair et al. (1996). Therefore there is considerable difficulty in correlating *in-vitro* and *in-vivo* wear study measurements in the dental literature.

The OHSU four chamber oral wear simulator (Condon and Ferracane, 1996) used in the current study utilises steatite antagonists (10.0 ± 0.1mm diameter), which have wear characteristics similar to enamel when opposing dental restorative materials (Wassell et al., 1994; Condon and Ferracane, 2002), to simultaneously produce abrasion and attrition

wear in the form of a tear drop wear facet (Figure 7.1) in the presence of a food-like slurry. Abrasion wear was described by Mair et al. (1996) as being caused by the sliding action of one surface over another and attrition wear by direct static forces acting between opposing surfaces (Mortensen, 2007). The wear regime imposed by the OHSU oral wear simulator brings the steatite antagonist into direct contact with the specimen in the presence of a food-like slurry to impart a 20N sliding abrasion force along a 7mm linear path (Condon and Ferracane, 1996, 1997a,b). A direct static 90N force is also applied at the end of the 7mm path for each specimen to simulate attrition wear (Condon and Ferracane, 1996, 1997a, and 1997b). At the end of each wear cycle the steatite antagonist is raised and returns to the start of the 7mm path and the wear regime is repeated at a frequency of 1Hz. The food-like slurry mixture consisting of 1.0g of poppy seeds ground for 100 strokes in a ceramic pestle and mortar, 0.5g of PMMA beads (50-100μm diameter) and 5ml of distilled water has been reported (Lutz et al., 1984; De Gee, 1986) to produce wear rates for a range of dental restorative materials that are comparable with clinical studies.

Traditionally, the *in-vitro* wear resistance of dental restoratives, namely dental amalgam (Condon and Ferracane, 1996) and RBCs (Condon and Ferracane, 1996, 1997a,b), tested in the OHSU were quantified in terms of the mean wear depths due to abrasion and attrition. The tear drop wear facets were analysed using a diamond-tipped profilometer by making ten equally spaced traces perpendicular to the wear facet length. According to the authors, following "profilometric and visual examination" of the wear traces, the abrasion region was determined to be 40-60% of the wear facet trace and the attrition region was

80-90% of the wear facet trace based on the average wear depth measurements (Condon and Ferracane, 1996). However, examination of the dental literature on the OHSU (Heintze, 2006) highlighted that mean wear depths measured in the abrasion and attrition regions differed by 33-56% and 31-78%, respectively when RBCs (Heliomolar, Herculite and Z100™) were tested using the same protocol (20 N abrasion force and 70-90 N attrition force in the presence of a food-like slurry) (Condon and Ferracane, 2002; Sorensen and Pham, 2002; Seghi et al., 2002). A recent study (Dowling and Fleming, 2007) employed the OHSU, using the same protocol (20 N abrasion force and 90 N attrition force in the presence of the food-like slurry) to assess glass-ionomer restoratives and suggested further difficulties with using mean wear depths due to abrasion and attrition to report the *in-vitro* wear resistance. The authors used a non-contact optical profilometer (Talysurf CLI 2000, Taylor-Hobson Precision, Leicester, UK) with a 3mm range chromatic length aberration gauge with a resolution of 0.1μm (z-direction) scanning at 2mm/s such that longitudinal traces were taken at 4μm intervals (x-direction) across the wear facet with a measurement recorded at 40μm intervals (y-direction) compared with the 0.7mm intervals (y-direction) used by Condon and Ferracane (1996). Dowling and Fleming (2007) identified variations of 0.22 and 0.19mm in the wear depth measured over the abrasion and attrition regions of the wear facet, respectively emphasising that the abrasion and attrition regions were not uniform which coincides with the previously reported differences of 33-56% and 31-78%, respectively for RBCs using the same protocol. Unfortunately, no detail of the resolution of the profilometer in the y-direction was not reported in the previous studies (Condon and Ferracane, 2002; Sorensen and Pham, 2002; Seghi et al., 2002). More recently, studies employing the

OHSU (Turssi et al., 2006, Correr et al., 2006) have performed up to 125 perpendicular traces across the wear facet (using a resolution in the x- and y-direction of 50 and 80μm, respectively) to determine the wear depth measurements over the abrasion and attrition regions of the wear facet. Given the improvements in the scanning resolution, accuracy, precision and speed of profilometric scanning devices, since the OHSU was first employed, it is understandable that the number of traces utilised to analyse the wear depths measured over the abrasion and attrition regions of the wear facets has increased. However, the study by Dowling and Fleming (2007) has highlighted that a minimum of 100 traces (y-axis spacing of 40μm) for maximum wear depths measured are required to provide an accurate and precise representation of *in-vitro* wear resistance.

Interestingly, more recently when questioning the "need for *in-vitro* wear simulating devices" Ferracane concluded wear testing data reporting (depth, area or volume) needed to be standardised (Ferracane, 2006). The calculation of material removed due to the interaction of contacting surfaces was suggested by Archard in 1953 to be more accurately described in terms of volume loss (Archard, 1953). Archard's wear equation calculated wear as the volume V (mm^3) per unit sliding distance L (mm) which was dependant upon the dimensionless wear coefficient k, the applied load P (N) and the radii of the contacting asperities a (mm) as shown in Equation 9.1

$$Wear = \frac{V}{L} = \frac{kP}{3a} \qquad \text{Equation 9.1.}$$

DeLong et al. (1985) evaluated the *in-vitro* wear of dental amalgam in the MTS by measuring the volume of material removed and suggested wear volume as being an "indirect measure of wear" and a measure of the work done to remove material, implying

that the wear volume was a material property independent of occlusal factors (DeLong, 2006). This was demonstrated by the variation in tooth wear *in-situ* in young adults over a 2-year period (Pintado et al., 1997). As a result, DeLong (2006) suggested that the determination of the mean total volumetric wear of the facet was a more accurate parameter for evaluating material loss due to wear. Therefore, the authors of the current study whilst reporting mean wear depth measurements have also focused on the maximum wear volume as an appropriate wear quantity. A recent review (DeLong, 2006) also appeared to be more concerned with the confidence in the accuracy and precision of results presented, therefore, the results presented are in terms of the resolution in the x-, y- and z-directions for the *in-vitro* wear simulation. In addition, the technique of data reporting employed to quantify the wear facets in the current study quantify both the mean maximum wear depth measurements and total wear volumes of the tear drop wear facets rather than the individual abrasion and attrition regions in accordance with the views of Ferracane (2006).

9.5.1 Short-term *in-vitro* wear resistance

In the current study, the wear data analysed for the four RBCs tested at 50,000 cycles (at scanning resolutions in the x-, y- and z-directions of 4, 40 and 0.1μm, respectively) demonstrated that reducing QTH LCU irradiance resulted in no significant difference in the mean total volumetric wear and mean maximum wear depth. The constant mean total volumetric wear and mean maximum wear depths (Table 8.8) showed clearly that the top surface of the RBCs was adequately cured within the range of intensities employed,

presumably due to the maximum conversion of C=C double bonds to C-C single bonds for the top surface. In the dental literature, Halverson et al. (2002) showed that even with low irradiances (200mW/cm^2) and short exposure times (10s), nearly maximum conversion could be achieved at the irradiated top surface to achieve 90% of the maximum conversion. Therefore, it is not surprising that no significant differences were evident in mean total volumetric wear and mean maximum wear depth following irradiation at distances of 0 to 15mm from the top surface of the RBCs (irradiances of 650 ± 14 to 150 ± 8mW/cm^2). The question of importance, nevertheless, is at what magnitude of irradiance does this reciprocity failure become of practical importance again here for the short-term *in-vitro* wear resistance. The expectation may be for a peak in the value for the short-term *in-vitro* wear resistance as a function of irradiance, but an approach to the plateau value was identified, as shown in the mechanical property results of Musanje and Darvell (2003).

9.5.2 Long-term *in-vitro* wear resistance

The two-way ANOVA of the long-term *in-vitro* wear resistance (irradiation distance × number of wear cycles) highlighted significant interactions for the mean total volumetric wear for each RBC material (all P values were less than 0.026) but not the mean maximum wear depth for Z100™ (P=0.400), Filtek™ Z250 (P=0.746) and Filtek™ Supreme XT (P=0.737). The increased number of ploughing actions of the antagonist on the RBC results in increased friction which would be expected to play a major role in the wear process (Palin et al., 2005). Increasing the number of wear cycles results in a

significant increase in the mean total volumetric wear observed over time which is exacerbated with increasing QTH LCU irradiance distances. Interestingly the mean maximum wear depth observed with increasing number of wear cycles was manifested as a non-significant increase in the mean maximum wear depth observed for all materials with the exception of Filtek™ P60 over time with varying QTH LCU irradiance distances. It is suggested that in line with the findings of Archard (1953) and DeLong et al. (1985) that the determination of the mean total volumetric wear was a more accurate parameter for evaluating material loss due to wear since difficulties with the mean maximum wear depth measurements for data reporting are routinely encountered in the dental literature (Heintze, 2006; DeLong, 2006). The differences identified between RBC materials require little elaboration as the effects of monomeric resin formulation have been discussed extensively in the dental literature.

A further disadvantage to using the wear depth measurement would be when trying to correlate *in-vivo* and *in-vitro* studies. In the oral environment the opposing teeth do not wear linearly with time. As teeth wear against each other, dynamic changes occur in the occlusal parameters, namely the centric contacts move, the orientation of the teeth in relation to each other changes and the areas of contact increase. Therefore it is possible that wear may cease in one location and move to another location leading to the problem of trying to quantify the *in-vivo* wear. Volumes are additive, however, for depth or area measurements the problem may be complicated by overlapping wear regions (DeLong, 2006). It is suggested that this result further emphasises the arguments for the employment of volume (DeLong, 2006) and for standardised data reporting (Ferracane,

2006), for evaluating material loss due to wear following *in-vitro* wear simulation of RBCs.

Previously in the dental literature when long-term wear studies with increasing number of cycles were considered the slurry was often not changed for the duration of the experiment (Hu et al., 2002; Barkmeier et al., 2008) so that the abrasiveness of the slurry increased with removal of RBC filler particles which exacerbated the wear phenomenon. In the current study, the wear media was changed to prevent this phenomenon occurring to more accurately reflect the clinical situation. In addition, the degree of conversion within an RBC material is reduced depending upon the influence of shade, monomeric reactivity, refractive index mismatch, light scattering and absorption (Shortall et al., 2008). Reducing the LCU output intensity has the effect of further reducing the degree of conversion at varying depths from the LCU such that it becomes easier to remove material following an increased number of cycles. As a result, the proposed hypothesis that exacerbated wear rates would be evident following long-term wear with RBCs irradiated under non-optimised conditions was accepted.

9.5.3 RBC material

In general no significant differences occurred between the methacrylate RBCs (Filtek™ Z250, Filtek™ P60 and Filtek™ Supreme XT) which contained similar monomeric resin constituents and filler loadings and Z100™ despite the higher filler volume and elastic modulus of the more brittle Z100™ RBC (Musanje and Darvell, 2006). This is in

agreement with the volume loss data from Palin et al. (2005) who determined similar frictional coefficients, wear coefficients and volume loss for the monomeric resin constituents investigated resulting in similar fraction of friction results. Therefore it would appear that improved wear performance suggested for nano-filled RBCs (Filtek™ Supreme XT) which were proposed to be less prone to filler plucking due to their irregular shape compared with the hybrid RBCs (Z100™, Filtek™ Z250 and Filtek™ P60) may not be entirely correct (Mitra et al., 2003).

CHAPTER 10 Conclusions

When an 8mm 'Turbo' tip diameter was used in standard and boosted modes the irradiances were increased compared with when a conventional 8mm tip diameter was employed. The broader adit diameter of the 8mm 'Turbo' tip will capture and therefore emit more irradiance at the proximal portion of the light cone generated when compared with the narrower adit diameter of the conventional 8mm tip diameter. The increase in irradiance in boosted compared with standard mode is a result of the manufacturers increasing the current available to the LCU power source with the associated increase in irradiance reported in Section 4.1. Similarly, the 13, 11 and 8mm light guides consist of a 14mm adit diameter which is attached to the LCU. To control the level of irradiance captured and therefore emitted at the proximal portion of the light cone generated, the effective adit diameter was modified with a metal sleeve together with a modification of the dimensions of the hexagonal fibres of the LCU light guides such that in reality the 13, 11 and 8mm adit diameters were 12.1. 10.3 and 7.4mm. In addition, the variation in the fibre spacing and fibre diameter at the adit and exit of the tip diameters were different. It is suggested that the similar irradiances demonstrated with the 13, 11, and 8mm tip diameters were achieved by the manufacturers through controlling the amount of light entering the adit side of the LCU tips together with modifying the number and dimensions of the hexagonal fibres in the LCU tips. Therefore, all the tip diameters used with the QTH LCU were just as effective in the irradiances they generated.

The technological advancements that occurred from the time the Elipar™ Freelight LED LCU was marketed, to the launch of the Elipar™ Freelight 2 resulted in the increase irradiance for the Elipar™ Freelight 2 employing either an 8 or 13mm tip diameter. The manufacturer's claimed irradiance for the Elipar™ Freelight (240mW/cm^2) and the Elipar™ Freelight 2 (1040mW/cm^2) LED LCUs appears to refer to the irradiance whilst employing the 8mm LCU tip diameter. The light guides themselves consist of fused hexagonal fibres which run from the adit (the LCU side) to the exit (the LCU tip) with tapers that are negative for the 8mm and positive for the 13mm tip diameters. Although the fibre spacing and fibre diameter were similar for the 8 and 13mm tip diameters at the adit end, variations in fibre spacing and fibre diameter were evident when the exit ends were compared for the 8mm negative taper and the 13mm positive taper tip diameters. In short, narrower tip diameters at the exit window are prone to emit more irradiance and illuminance at the proximal portion of the light cone.

The efficiency of the overlapping irradiation regime has been questioned by a number of authors in the dental literature recently in terms of uncontrolled initiation on polymerisation, non-homogeneously cured specimens and inconsistent polymerisation along the length of the bar-shaped specimen. Accordingly, decreasing the LCU tip diameter (from 13 to 11 and 8mm) would be expected to progressively decrease the efficiency of the polymerisation process along the length of the RBC specimens compared with a 'one-hit' irradiation (25mm tip diameter). This would be expected to be manifested as a reduction in the reliability of the three-point flexure strength data if the theory proposed by Palin et al. (2005) regarding residual tensile stress generation were to

hold true. However, when the reliability of the three-point flexure strength data was analysed for the four RBCs tested, no change in the reliability of the three-point flexure strength data was evident when irradiated using tip diameters of 13, 11, 8 and 25mm with the QTH LCU at the two irradiances investigated (Table 4.2). In addition, similar Weibull moduli and associated 95% confidence intervals were achieved following irradiation with the LED LCUs regardless of the tip diameter (8 or 13mm) employed (Table 4.7). It is therefore evident that the previously theory proposed by Palin et al. (2003, 2005) was not entirely correct.

Additionally, no effect due to overlapping, which corresponds to a doubling of the irradiation time at such sites, on Vickers hardness was detected. It can be concluded that the recommended irradiation times, per spot, effectively put the material on the 'plateau' of the response surface, and it is expected then not to show any further change on prolonged irradiation (Musanje and Darvell, 2003). Even so, it should be noted that there is unavoidably much scatter occurring within the material such as, firstly, to make the distinction between regions unsharp and, secondly, make any such effect (if one did exist) at the lower surface even less obvious: the effectively irradiated area must be larger than the tip diameter. While this does not provide such a strong test of doubled exposure time as might be desired, it provides strong confirmation that there is no detriment to the specimens from overlapping irradiation sites, on the assumption that 'full' irradiation is desired, and confidence both that the modified ISO 4049 irradiation methodology is sound thereby implying the ISO 4049 irradiation methodology is also sound. The Vickers hardness data indicated that for each LCU and tip diameter utilised there was no

significant difference between the non-overlapped and overlapped regions on the top surface. However, there were significant differences highlighted between the non-overlapped and overlapped regions on the bottom surface (compared with the corresponding region on the top surface) at the range of intensities investigate with the LCU tip diameters employed. However, the differences in Vickers hardness data with varying irradiances did not influence the flexural properties of each of the RBC materials investigated. These results from the current investigation further emphasise that the relationship between the development of three-point flexure properties and Vickers hardness with energy density, namely irradiance and time is not linear. In addition, the current study provides confidence both that the ISO method is sound and that, clinically, extra irradiation is sensible should doubt about the adequacy of the exposure arise for any reason.

Increasing the LCU exit window distance from the RBC top surface results in a reduction in the irradiance at the proximal portion of the light cone generated from the exit window to the RBC material. While the irradiance reaching the top surface of the RBC is decreased the phenomenon is further exacerbated when, light transmission characteristics of the RBC depending upon the influence of shade, monomeric reactivity, refractive index mismatch, light scattering and absorption are taken into consideration. The maximum flexure properties (strength and modulus) that may be attained for the RBCs investigated would be expected to correspond to between 40 and 70% conversion of double bonds (at a given temperature). In view of the absorption by the photo-sensitiser (the irradiance is reduced as it travels trough the 2mm bar-shaped specimens) according

to Beer-Lamberts law, in combination with light scattering by the high volume of filler particles the resultant attainment of the flexure properties was compromised with irradiation distance.

For the short-term *in-vitro* wear resistance, the constant mean total volumetric wear and mean maximum wear depths (Table 8.8) showed clearly that the top surface of the RBCs was adequately cured within the range of intensities employed, presumably due to the maximum conversion of C=C double bonds to C-C single bonds for the top surface. Therefore, it is not surprising that no significant differences were evident in mean total volumetric wear and mean maximum wear depth following irradiation at distances of 0 to 15mm from the top surface of the RBCs (irradiances of 650 ± 14 to 150 ± 8mW/cm^2). For the long-term *in-vitro* wear, the increased number of ploughing actions of the antagonist on the RBC results in increased friction which would be expected to play a major role in the wear process. Increasing the number of wear cycles results in a significant increase in the mean total volumetric wear observed over time which is exacerbated with increasing QTH LCU irradiance distances. Interestingly the mean maximum wear depth observed with increasing number of wear cycles was manifested as a non-significant increase in the mean maximum wear depth observed for all materials (with the exception of Filtek™ P60) over time with varying QTH LCU irradiance distances. It is suggested that the determination of the mean total volumetric wear was a more accurate parameter for evaluating material loss due to wear since difficulties with the mean maximum wear depth measurements for data reporting are routinely encountered in the dental literature.

CHAPTER 11 Recommendations for further work

Existing data

The objective in the current study was to investigate the efficiency of the overlapping irradiation regime by modifying the specimen manufacture protocol in ISO 4049 using QTH and LED LCUs. The exit window of the LCU was moved by three-quarters (not half) the diameter along the specimen so that some areas received twice the irradiation of adjacent areas, thereby exacerbating the potential for uncontrolled initiation on polymerisation and potentially decreasing the homogeneity of polymerisation along the length of the specimen. In addition, specimens were irradiated from the top surface only to further exacerbate the phenomena investigated. Analysis of the existing data was undertaken for the QTH and LED LCUs however, no comparisons were carried out between the two LCU irradiation technologies. It is suggested that further multiple comparisons of the two irradiation technologies could be undertaken which would provide additional information on the differences in the reliability of the fracture strength associated with the fabrication of three-point flexure bar-shaped specimens.

The ISO 4049 for dental polymer-based restorative materials stipulate that RBCs used in occlusal surfaces should have a three-point flexure strength value in excess of 80 MPa. The standard suggests that if three of five three-point flexure specimens fail to reach the 80MPa specified limit the RBC is deemed to 'have failed absolutely'. In the current study Filtek™ Supreme XT failed to meet the three-point flexure strength ISO criteria. Examination of the existing data in terms of the order they were manufactured and tested

could highlight the failure of the RBC to meet the ISO three-point flexure strength criteria. However, Filtek™ Supreme XT has been used clinically in dental practice for in excess of 5 years with few complications reported suggesting that the ISO 4049 strength criteria test is flawed in terms of the number of specimens required for the test and the reliance on a mean value of 80 MPa.

An indication of the influence of increasing the number of wear cycles for each RBC investigated may be highlighted by exploration of the correlation between the number of wear cycles and the mean total volumetric wear and mean maximum wear depths. The plots would highlight if a linear relationship was followed and if there was a common trend between RBC materials with the different resin constituents and filler volumes.

Further work on existing data

The influence of irradiance on the four RBC materials investigated was assessed in the current study in terms of the mean total volumetric wear and the mean maximum wear depth. The data from the profilometric traces could be further examined by evaluating the influence of irradiance on the RBC surface with increasing depth by investigating the surface roughness when employing the steatite antagonist. Such data could provide further information on the influence that irradiance has in terms of the resin chemistry and filler technology with increasing depth.

The *in-vitro* wear resistance of RBCs tested in the OHSU were quantified in terms of the mean wear depths due to abrasion and attrition (Condon and Ferracane, 1996, 1997a,b).

The tear drop wear facets were analysed using a diamond-tipped profilometer by making ten equally spaced traces perpendicular to the wear facet length. The current study identified variations in the wear depth measured over the abrasion and attrition regions of the wear facet, respectively emphasising that the abrasion and attrition regions were not uniform when using a non-contact optical profilometer making approximately 200 traces. It was therefore proposed that further investigations of the profilometric data would provide additional information of the wear data measured over the abrasion and attrition regions of the wear facets thus enabling a comparison between 10 and 200 traces of the existing data using the Talysurf analysis software.

Future work

Each of the four RBC specimens were tested in the OHSU wear simulator with a food-like slurry added to each chamber consisting of 1.0g of ground poppy seeds, 0.5g of PMMA beads and 5ml of distilled water. Further studies could include an evaluation of the wear volumes and wear depths of the investigated RBCs by using various ethanol/water mixtures added to the poppy seeds and PMMA beads. Investigations with different solvent concentrations would provide a more detailed insight into the wear behaviour at various irradiances under harsher oral environments which could preclude the use of extended wear testing regimes.

Whilst the current study advocates wear volume, which was reported as being an "indirect measure of wear" and a measure of the work done to remove material, when employed to quantify *in-vitro* wear then the picture is clouded by the wear regime chosen.

In line with the developers of the OHSU the current study employed the same testing protocol (20 N abrasion force and 90 N attrition force in the presence of a food-like slurry). It is suggested that improvements in the knowledge of the wear process for both abrasion and attrition would best be achieved by examining the wear mechanisms in isolation rather than together. Therefore it is proposed that applying variable attrition or abrasion loads would be more helpful to understanding the fundamental wear processes that occur in the oral environment.

REFERENCES

Abbas, G., Fleming, G.J.P., Harrington, E., Shortall, A.C.C. and Burke, F.J.T. Cuspal Movement and Microleakage in Premolar Teeth Restored with a Packable Composite Cured in Bulk or in Increments. Journal of Dentistry, 2003; 31: 437-444.

Adabo, G.L., Cruz, C.A.S., Fonseca, R.G. and Vaz, L.G. The Volumetric Fraction of Inorganic Particles and the Flexural Strength of Composites for Posterior Teeth. Journal of Dentistry, 2003; 31: 353-359.

Anusavice, K.J. Restorative Resins. In: Anusavice, K.J. Phillip's Science of Dental Materials (10th Edition). W.B. Saunders Company, 1996a; Philadelphia: Chapter 12, 273-299.

Anusavice, K.J. Restorative Resins. In: Anusavice, K.J. Phillip's Science of Dental Materials (10th Edition). W.B. Saunders Company, 1996b; Philadelphia: Chapter 24, 525-554.

Aravamydhan, K., Floyd, C.J., Rakowski, D., Flaim, G., Dickens, S.H., Eichmiller, F.C. and Fan, P.L. Light-Emitting Diode Curing Light Irradiance and Polymerization of Resin-Based Composite. Journal of the American Dental Association, 2006; 137: 213-223.

Archard, J.F. Contact and Rubbing of Flat Surfaces. Journal of Applied Physics, 1953; 24: 981–988.

Ashby, M.F. and Jones, D.R.H. The Mechanical Properties of Ceramics. In: Ashby, M.F. and Jones, D.R.H., editors. Engineering Materials 2: An Introduction To Microstructures, Processing and Design. 2nd Edition. Oxford: Butterworth-Heinemann Ltd; 1998: 177-84.

Askeland, D.R. and Phulé, P.P. Atomic Structures. In: Askeland, D.R. and Phulé, P.P., editors. The Science and Engineering of Materials. 5th Edition. London: Brooks Cole; 2005: 23-47.

Asmussen, E. and Peutzfeldt, A. Flexural Strength and Modulus of a Step-Cured Resin Composite. Acta Odontologica Scandinavica, 2004; 62: 87-90.

Asmussen, E. and Peutzfeldt, A. Polymerisation Contraction of Resin Composite vs. Energy and Power Density of Light-Cure. European Journal of Oral Science, 2005; 113: 417-421.

Baharav, H., Abraham, D., Cardash, H.S. and Helft, M. Effect of Exposure Time on the Depth of Polymerisation of a Visible Light-Cured Composite Resin. Journal of Oral Rehabilitation, 1988; 15: 167-172.

Ban, S. and Anusavice, K.J. Influence of Test Method on Failure Stress of Brittle Materials. Journal of Dental Research, 1990; 69: 1791-1799.

Ban, S., Hasegawa, J. and Anusavice, K.J. Effect of Loading Conditions on Bi-axial Flexure Strength of Dental Cements. Dental Materials, 1992; 8: 100-104.

Barghi, N., Berry, T. and Hatton, C. Evaluating Intensity Output of Curing Lights in Private Dental Offices. Journal of the American Dental Association, 1994; 25: 992-996.

Barker, G.R. and Setchell, M.R. A Guide to the Use of Composite Resin Materials. Dental Practice, 1972; 22: 174-178.

Barkmeier, W.W., Latta, M.A., Erikson, R.L. and Wilwerding, T.M. Wear Simulation of Resin Composites and the Relationship to Clinical Wear. Operative Dentistry, 2008; 33: 177-182.

Barnes, I.E. and Kidd, E.A.M. Composite Resin Restorative Materials - A Review Part I. Dental Update, 1980; 6: 221-235.

Bennett, A.W. and Watts, D.C. Performance of Two Blue Light Emitting-Diode Dental Light Curing Units with Distance and Irradiation-Time. Dental Materials, 2004; 20: 72-79.

Berenbaum, R. and Brodie, I. Measurements of Tensile Strength of Brittle Materials. British Journal of Applied Physics, 1959; 10: 281-287

Beun, S., Glorieux, T., Devaux, J., Vreven, J. and Leloup, G. Characterization of Nanofilled Compared to Universal and Microfilled Composites. Dental Materials, 2007; 23: 51-59.

Bouschlicher, M.R., Vargas, M.A. and Boyer, DB. Effect of Composite Type, Light Intensity, Configuration Factor and Laser Polymerization on Polymerization Contraction Forces. American Journal of Dentistry, 1997; 10: 88-96.

Bowen, R.L. Adhesive Bonding of Various Materials to Hard Tissues. VI. Forces Developing in Direct-Filling Materials During Hardening. Journal of the American Dental Association, 1967; 74: 439-445.

Bowen, R.L. Dental Filling Materials Comprising of Vinyl-Silane Treated Fused Silica and Binder Consisting of the Reaction Product of Bisphenol and Glycidyl Methacrylate. 1962, US Patent 3,066,112.

Bowen, R.L. Properties of a Silica-Reinforced Polymer for Dental Restorations. Journal of the American Dental Association, 1963; 66: 57-64.

Bowen, R.L. Synthesis of a Silica-Resin Direct Filling Material: Progress Report. Journal of Dental Research, 1958; 37: 90-91.

Brackett, W.W., Haisch, L.D. and Covey, D.A. Effect of Plasma Arc Curing on the Microleakage of Class V Resin-Based Composite Restorations. American Journal of Dentistry, 2000; 13: 121-122.

Braden, M. Selection and Properties of Some New Dental Materials. Dental Update, 1974; 1: 489-501.

Calheiros, F.C., Kawano, Y., Stansbury, J.W. and Braga, R.R. Influence of Radiant Exposure on Contraction Stress, Degree of Conversion and Mechanical Properties of Resin Composites. Dental Materials, 2006; 22: 799-803.

Cesar, P.F., Miranda, W.G. and Braga, R.R. Influence of Shade and Storage Time on the Flexural Strength, Flexural Modulus, and Hardness of Composites Used for Indirect Restorations. Journal of Prosthetic Dentistry, 2001; 86: 289-296.

Chen, H.Y., Manhart, J., Hickel, R. and Kunzelmann, K-H. Polymerisation Contraction Stress in Light-Cured Packable Composite Resins. Dental Materials, 2001; 17: 253-259.

Choi, K.K., Ferracane J.L., Hilton T. and Charlton D. Properties of Packable Dental Composites. Journal of Esthetic Dentistry, 2000; 12: 216-226.

Condon JR, Ferracane JL. Reduction of Composite Contraction Stress Through Non-Bonded Microfiller Particles. Dental Materials, 1998; 14: 256-260.

Condon, J.R. and Ferracane, J.L. Evaluation of Seven Commercial Composites using New *In Vitro* Wear Simulator. Journal of Dental Research, 2002; 81, Special Issue A: A337 Abstract. No. 2683.

Condon, J.R. and Ferracane, J.L. Factors Effecting Dental Composite Wear *In Vitro*. Journal of Biomedical Materials Research, 1997a; 38: 303-313.

Condon, J.R. and Ferracane, J.L. *In Vitro* Wear of Composite with Varied Cure, Filler Level and Filler Treatment. Journal of Dental Research, 1997b; 76: 1405-1411.

Condon, J.R. and Ferracane, J.L.. A New Multi-Mode Oral Wear Simulator. Dental Materials. 1996; 12: 218-226.

Conry, J.P., Beyer, J.P., Pintado, M.R. and Douglas, W.H. Measurement of Preventative Resin Restorations Using Computer Profilometry. Journal of Dentistry for Children, 1992; 59: 177-181.

Cook, W.D. Factors Affecting the Depth of Cure of UV-Polymerised Composites. Journal of Dental Research, 1980; 59: 800-808.

Cook, W.D. Spectral Distributions of Dental Photo-Polymerisation Sources. Journal of Dental Research, 1982; 61: 1436-1438.

Corciolani, G., Vichi, A., Davidson, C.L. and Ferrari, M. The Influence of Tip Geometry and Distance on Light – Curing Efficacy. Operative Dentistry, 2008; 33: 325-331.

Correr, G.M., Alonso, R.C.B., Sobrinho, L.C., Puppin-Rontani, R.M. and Ferracane, J.L. *In Vitro* Wear of Resin-Based Materials – Simultaneous Corrosive and Abrasive Wear. Journal of Biomedical Materials Research B Applied Biomaterials, 2006; 78: 105-114.

Cvar, J.F. and Ryge, G. Criteria for the Clinical Evaluation of Dental Restorative Materials. United States Public Health Service Publication #790-244. San Francisco: US Government Printing Office; 1971.

Dart, E.C., Cantwell, J.R., Traynor, JR., Taworzyn, J.F. and Nemeck, J. Method of Repairing Teeth Using a Composition which is Curable by Irradiation by Visible Light, 1978: US Patent 4,089,763.

Darvell BW. Mechanical Testing. In: Darvell BW, editor. Materials Science for Dentistry. 7th Edition. Hong Kong: University of Hong Kong; 2002; 1-35.

Davidson, C.L. and Feilzer, A.J. Polymerisation Shrinkage and Polymerisation Shrinkage Stress in Polymer-Based Restoratives. Journal of Dentistry, 1997; 25: 435-440.

De Gee, A.J, Pallav, P. and Davidson, C.L. Effect of Abrasion Medium on Wear of Stress-Bearing Composites and Amalgam *in Vitro*. Journal of Dental Research, 1986; 65: 654-658.

De With, G. and Wagemanes, H.H.M. Ball-on-Ring Test Revisited. Journal of the American Ceramic Society, 1989; 72: 1538-1541.

DeLong, R. and Douglas, W.H. Development of an Artificial Oral Environment for the Testing of Dental Restoratives: Bi-axial Force and Movement Control. Journal of Dental Research, 1983; 62: 32-36.

DeLong, R. Intra-Oral Restorative Materials Wear: Rethinking the Current Approaches: How to Measure Wear. Dental Materials, 2006; 22: 702-711

DeLong, R., Sakaguchi, R.L., Douglas, W.H. and Pintado, M.R. The Wear of Dental Amalgam in an Artificial Mouth: A Clinical Correlation. Dental Materials, 1985; 1: 238-242.

Dowling, A.H. and Fleming, G.J.P. The Impact of Montmorillonite Clay Addition on the *In Vitro* Wear Resistance of a Glass-Ionomer Restorative. Journal of Dentistry, 2007; 35: 309-317.

Duke, E.S. Light-Emitting Diodes in Composite Resin Photopolymerization. Compendium, 2001; 22: 722-725.

Earnshaw, R. and Smith, D.C. The Tensile and Compressive Strength of Plaster and Stone. Australian Dental Journal, 1966; 11: 415-422.

Eick, J.D. and Welch, F.H. Polymerisation Shrinkage of Posterior Composite Resins and its Possible Influence on Postoperative Sensitivity. Quintessence International, 1986; 17: 103-111.

Elliott, J.E., Lovell, L.G. and Bowman, C.N. Primary Cyclisation in the Polymerization of Bis-GMA and TEGDMA: A Modelling Approach to Understanding the Cure of Dental Resins. Dental Materials, 2001; 17: 221-229.

El-Mowafy, O., El-Badrawy, W., Lewis, D.W., Shokati, B., Kermallli, J., Sloiman, O., Encioiu, A., Zawi, R. and Rajwani, F. Intensity of Quartz-Tungsten-Halogen-Light-Curing Units used in Private Practices in Toronto. Journal of the American Dental Association, 2005; 136: 766-773.

Farah, J.W. and Dougherty, E.W. Unfilled, Filled and Microfilled Composite Resins. Operative Dentistry, 1981; 6: 95-103.

Feilzer, A.J., De Gee, A.J. and Davidson, C.L. Setting Stress in Composite Resin in Relation to Configuration of the Restoration. Journal of Dental Research, 1987; 66: 1636-1639.

Ferracane, J.L. and Greener, E.H. The Effect of Resin Formulation on the Degree of Conversion and Mechanical Properties of Dental Restorative Resins. Journal of Biomedical Materials Research, 1986; 20: 121-131.

Ferracane, J.L. Current Trends in Dental Composites. Critical Reviews in Oral Biology and Medicine, 1995; 6: 302-318.

Ferracane, J.L. Is the Wear of Dental Composites Still a Clinical Concern?: Is there Still a Need for *In Vitro* Wear Simulating Devices? Dental Materials, 2006; 22: 689-692.

Ferracane, J.L. Placing Dental Composites-A Stressful Experience. Operative Dentistry, 2008; 33: 247-257.

Ferracane, J.L., Berge, H.X. and Condon, J.R. *In Vitro* Aging of Dental Composites in Water - Effect of Degree of Conversion, Filler Volume, and Filler/Matrix Coupling. Journal of Biomedical Materials Research, 1998; 42: 465-472.

Ferracane, J.L., Ferracane, L.L. and Musanje, L. Effect of Light Activation Method on Flexural Properties of Dental Composites. American Journal of Dentistry, 2003; 16: 318–322.

Filtek™ P60 Product Report. 3M ESPE Dental Products, St. Paul, MN, USA, 2001.

Filtek™ Supreme XT Product Report. 3M ESPE Dental Products, St. Paul, MN, USA, 2004.

Filtek™ Z250 Product Report. 3M ESPE Dental Products, St. Paul, MN, USA, 1999.

Fleming, G.J.P., Burke, F.J.T., Watson, D.J. and Owen, F.J. Materials for Restoration of Primary Teeth: 1. Conventional Materials and Early Glass Ionomers. Dental Update, 2001; 28: 486-491.

Forss, H., Seppa, L. and Lappalaimen, R. *In-Vitro* Abrasion Resistance and Hardness of Glass-Ionomer Cements. Dental Materials, 1991; 7: 36-39.

Giovan, M.N. and Sines, G. Biaxial and Uniaxial Data for Statistical Comparison of a Ceramic's Strength. Journal of the American Ceramic Society, 1979; 62: 510-515.

Halvorson, R.H., Erickson, R.L. and Davidson, C.L. Energy Dependent Polymerisation of Resin-Based Composite. Dental Materials, 2002; 18: 463-469

Harrington, E. and Wilson, H.J. Depth of Cure of Radiation-Activated Materials - Effect of Mould Material and Cavity Size. Journal of Dentistry, 1993; 21: 305-331.

Heintze, S.D. How to Qualify and Validate Wear Simulation Devices and Methods. Dental Materials, 2006; 22: 712-734.

Heuer, G.A., Garmara, T.A. and Sherrer, J.D. A Clinical Comparison of a Quartz and Glass-Filled Composite With a Glass-Filled Composite. Journal of the American Dental Association, 1982; 105: 246-254.

Hoffman, N., Hugo, B., Schubert, K. and Klaiber, B. Comparison Between a Plasma Arc Light Source and Conventional Halogen Curing Units Regarding Flexural Strength, Modulus, and Hardness of Photo activated Resin Composites. Clinical Oral Investigations, 2000; 4: 140-147.

Hu, X., Marquis, P.M. and Shortall, A.C. Two-Body *In Vitro* Wear Study of Some Current Dental Composites and Amalgams. Journal of Prosthetic Dentistry, 1999; 82: 214-220.

Hu, X., Shortall, A.C. and Marquis, P.M. Wear of Three Dental Composites Under Different Testing Conditions. Journal of Oral Rehabilitation, 2002; 29: 756-764.

International Standards Organisation. Dentistry - Polymer-Based Filling, Restorative and Luting Materials. ISO 4049, 3rd Edition. 2000: 15-18.

Jandt, K.D., Mills, R.W., Blackwell, G.B. and Ashworth, S.H. Depth of Cure and Compressive Strength of Dental Composites Cured With Blue Light Emitting Diodes (LEDs). Dental Materials, 2000; 16: 41-47.

Johnston, W.M., Leung, R.L. and Fan, P.L. A Mathematical Model for Post-Irradiation Hardening of Photoactivated Composite Resins. Dental Materials, 1985; 1: 191-194.

Jordan, R.E., Boksman, L. and Skinner, D.H. The New Generation of Composite Materials. New York State Dental Journal, 1982; 48: 219-231.

Jorgensen, K.D. and Amussen, E. Occlusal Abrasion of a Composite Restorative Material with an Ultra-Fine Filler - An Initial Study. Quintessence International, 1978; 9: 73-78.

Kanca, J. Maximising the Cure of Posterior Light-Activated Resins. Quintessence International, 1986; 17: 25-27.

Kelly, J.R. Perspectives on Strength. Dental Materials, 1995; 11:103-110.

Kirstein and Woolley. Symmetrical Bending of Thin Circular Plates of Equally Spaced Point Supports. Journal of Research for the National Bureau of Standards, 1967; 71: 1-10.

Kusy, R.P. and Leinfelder, K.F. Pattern of Wear In Posterior Restorations. Journal of Dental Research, 1977; 56: 544-553.

Lee, H.L., Orlowski, J.A. and Rogers, B.J. A Comparison of Ultra-Violet Curing and Self-Curing Polymers in Preventative, Restorative and Orthodontic Dentistry. International Dental Journal, 1976; 26: 134-171.

Lee, S.H., Chang, J., Ferracane, J. and Lee, I.B. Influence of Instrument Compliance and Specimen Thickness on the Polymerization Shrinkage Stress Management of Light-Cured Composites. Dental Materials, 2007; 23: 1093-1100.

Leinfelder, K.F. and Roberson, T.M. Clinical Evaluation of Posterior Composite Resins. Journal of General Dentistry, 1983; 3: 276-281.

Leinfelder, K.F. Posterior Composite Resins: The Materials and Their Clinical Performance. Journal of the American Dental Association, 1995; 126: 663-676.

Leinfelder, K.F. Wear Patterns and Rates of Posterior Composite Resins. International Dental Journal, 1987; 37: 152-157.

Leinfelder, K.F., Sluder T.R. and Sockwell, C.L. Clinical Evaluation of Composite Resins as Anterior and Posterior Restorative Materials. Journal of Prosthetic Dentistry, 1975; 33: 407-416.

Leinfelder, K.F., Taylor, D.F., Barkmeier, W.W. and Goldberg, A.J. Quantitative Wear Measurement of Posterior Composite resins. Dental Materials, 1986; 2: 198-201.

Leonard, D., Charlton, D.G. and Hilton, T.J. Effect of Curing-Tip Diameter on the Accuracy of Dental Radiometers. Operative Dentistry, 1999; 24: 31-37.

Liberman, R., Ben-Amar, A., Gontar, G. and Hirsh, A. The Effect of Posterior Composite Restorations on the Resistance of Cavity Walls to Vertically Applied Occlusal Loads. Journal of Oral Rehabilitation, 1990; 17: 99-105.

Lovell, L.G., Stansbury, J.W., Syrpes, D.C. and Bowman, C.N. The Effects of Composition and Reactivity on the Reaction Kinetics of Dimethacrylate/Dimethacrylate Copolymerisation. Macromolecules, 1999; 32: 3913-3921.

Lutz, F. and Phillips, R.W. A Classification and Evaluation of Composite Resin Systems. Journal of Prosthetic Dentistry, 1983; 50: 480-488.

Lutz, F., Phillips, R.W., Roulet, J.F. and Setcos, J.C. *In Vivo* and *In Vitro* Wear of Potential Posterior Composites. Journal of Dental Research, 1984; 6: 914-920.

Lutz, F., Setcos, J.C., Phillips, R.W. and Roulet, J.F. Dental Restorative Resins - Types and Characteristics. Dental Clinics of North America, 1983; 27: 697-710.

Mair, L.H., Stolarski, T.A., Vowles, R.W. and Lloyd, C.H. Wear: Mechanisms, Manifestations and Measurement. Report of a Workshop. Journal of Dentistry, 1996; 24: 141-148.

Mair, L.H., Voules, RW. and Cunningham, J. The Clinical Wear of Three Posterior Composites. British Dental Journal, 1990; 169: 335-360.

Manhart, J., Kunzelmann, K.H., Chen, H.Y. and Hickel, R. Mechanical Properties of New Composite Restorative Materials. Journal of Biomedical Materials Research, 2000; 53: 353-361.

Martin, F.E. A survey of the Efficiency of Visible Light Curing Units. Journal of Dentistry 1998; 26: 239-243.

McDowell, G.C., Bloem, T.J., Lang, B.R. and Asgar, K. *In-Vivo* Wear. Part 1: The Michigan Computer-Graphic Measuring System. Journal of Prosthetic Dentistry, 1988; 60: 112-120.

Mehl, A., Hickel, R. and Kunzelmann, K.H. Physical Properties and Gap Formation of Light-Cured Composites With and Without Soft-Start Polymerisation. Journal of Dentistry, 1997; 25: 321-330.

Mills RW. Blue Light Emitting Diodes--Another Method of Light Curing? British Dental Journal 1995;178:169.

Mills, R.W., Jandt, K.D. and Ashworth, S.H. Dental Composite Depth of Cure with Halogen and Blue Light Emitting Diode Technology. British Dental Journal, 1999; 186: 388-391.

Mills, R.W., Uhl, A., Blackwell, G.B. and Jandt, K.D. High Power Light Emitting Diode (LED) Arrays Versus Halogen Light Polymerization of Oral Biomaterials: Barcol Hardness, Compressive Strength and Radiometric Properties. Biomaterials, 2002; 23: 2955–2963.

Mitra, S.B., Wu, D. and Holmes, B.N. An Application of Nanotechnology in Advanced Dental Materials. Journal of the American Dental Association, 2003; 134: 1382-1390.

Miyazaki, M., Oshida, Y., Moore, B.K. and Onose, H. Effects of Light Exposures on Fracture Toughness and Flexural Strength of Light-Cured Composites. Dental Materials, 1996; 12: 328-332.

Mortensen A. Biocomposites – Composite Dental Materials Wear. In: Mortensen A, editor. Concise Encyclopaedia of Composite Materials. (2nd Edition) London: Elsevier; 2007. p.174-82.

Munksgaard, E.C., Peutzfeldt, A. and Asmussen, E. Elution of TEGDMA and BisGMA From a Resin and a Resin Composite Cured with Halogen or Plasma Light. European Journal of Oral Science, 2000; 108: 341-345.

Murray, G.A., Yates, J.L. and Newman, S.M. Ultraviolet Light and Ultraviolet-Activated Composite Resins. Journal of Prosthetic Dentistry, 1981; 46: 167-170.

Musanje, L. and Darvell, B.W. Curing-Light Attenuation in Filled-Resin Restorative Materials. Dental Materials, 2006; 22: 804–817.

Musanje, L. and Darvell, B.W. Effects of Strain Rate and Temperature on the Mechanical Properties of Resin Composites. Dental Materials, 2004; 20: 750-765.

Musanje, L. and Darvell, B.W. Polymerisation of Resin Composite Restorative Materials: Exposure Reciprocity. Dental Materials, 2003; 19: 531-541.

Musanje, L., Shu, M. and Darvell, B.W. Water Sorption and Mechanical Behaviour of Cosmetic Direct Restorative Materials in Artificial Saliva. Dental Materials, 2001; 17: 394-401.

Nakamura, S., Senoh, M., Iwasa, N. and Nagahama, S. High-Power InGaN Single-Quantum-Well-Structure Blue and Violet Light-Emitting Diodes. Applied Physics Letters, 1995; 67: 1868-1870.

Nitta, K. Effect of Light Guide Tip Diameter of LED-Light Curing Unit on Polymerization of Light-Cured Composites. Dental Materials, 2005; 21: 217-223.

Nuckles, D.R. and Fingar, W.W. Six-Month and One-Year Clinical Evaluation of a Composite Resin for Class II Restorations. Journal of the American Dental Association, 1975; 91: 1017-1022.

Obici, A.C., Sinhoreti, M.A.C., Frollini, E., Sobrinho, L.C. and Consani, S. Degree of Conversion and Knoop Hardness of Z250 Composite Using Different Photo-Activation Methods. Polymer Testing, 2005; 24: 814-818.

Orefice, R.L., Discacciati, J.A.C., Neves, A.D., Mansur, H.S. and Jansen, W.E. In Situ Evaluation of the Polymerisation Kinetics and Corresponding Evolution of the Mechanical Properties of Dental Composites. Polymer Testing, 2003; 22: 77-81.

Osborne, J.W., Gale, E.N. and Ferguson, G.W. 1 Year and 2 Year Clinical Evaluation of a Composite Resin and an Amalgam. Journal of Prosthetic Dentistry, 1973; 30: 795-800.

Palin, W.M., Fleming, G.J.P. and Marquis, P.M. The Reliability of Standardized Flexure Strength Testing Procedures for a Light-Activated Resin-Based Composite. Dental Materials, 2005; 21: 911-909.

Palin, W.M., Fleming, G.J.P., Burke, F.J.T., Marquis, P.M. and Randall, R.C. The Reliability in Flexural Strength Testing of a Novel Dental Composite. Journal of Dentistry, 2003; 31: 549–557.

Papadogiannis, D.Y., Laes, R.S., Papadogiannis, Y., G Palaghias, G. and Helvatjoglu-Antoniades., M. The Effect of Temperature on the Viscoelastic Properties of Nano-Hybrid Composites. Dental Materials, 2008; 24: 257-266.

Park, Y.P., Chae, K.H. and Rawls, H.R. Development of a New Photoinitiation System for Dental Light-Cure Composite Resins. Dental Materials, 1999; 15: 120-127.

Peutzfeldt, A. and Asmussen, E. Resin Composite Properties and Energy Density of Light Cure. Journal of Dental Research, 2005; 4: 659-662.

Peutzfeldt, A. and Asmussen, E. The Effect of Post-Curing on the Quantity of Remaining Double Bonds, Mechanical Properties, and *In Vitro* Wear of Two Resin Composites. Journal of Dentistry, 2000; 28: 447-452.

Phillips, R.W., Avery, D.R., Mehra, R., Swartz, M.L. and McCune, R.J. Observations on a Composite Resin for Class II Restorations: Three-Year Report. Journal of Prosthetic Dentistry, 1973; 30: 891-897.

Piddock, V., Marquis, P.M. and Wilson, H.J. The Mechanical Strength and Microstructure of All-Ceramic Crowns. Journal of Dentistry, 1987; 15: 153-158.

Pilo, R. and Cardash, H.S. Post-Irradiation Polymerisation of Different Anterior and Posterior Visible Light-Activated Resin Composites. Dental Materials, 1992; 8: 299-304.

Pilo, R., Oelgiesser, D. and Cardash, H.S. A Survey of Output Intensity and Potential for Depth of Cure Among Light-Curing Units in Clinical Use. Journal of Dentistry, 1999; 27: 235-241.

Pintado, M.R., Anderson, G.A., DeLong, R. and Douglas, W.H. Variation in Tooth Wear in Young Adults Over a Two-Year Period. Journal of Prosthetic Dentistry, 1997; 77: 313-320.

Pires, J.A.F., Cvitko, E., Denehy, G.E. and Swift, E.J. Effects of Curig Tip Distance on Light Intensity and Composite Resin Microhardness. Quintessence International, 1993; 24: 517-521

Powers, J.M., Dennison, J.B. and Lepeak, P.J. Parameters That Affect the Colour of Direct Restorative Resins. Journal of Dental Research, 1978; 57: 876-880.

Powers, J.M., Fan, P.L. and Raptis, C.N. Colour Stability on New Composite Restorative Materials Under Accelerated Aging. Journal of Dental Research, 1980; 59: 2071-2074.

Pradhan, R.D., Melikechi, N. and Eichmiller. The Effect of Irradiation Wavelength Bandwidth and Spot Size on the Scraping Depth and Temperature Rise in Composite Exposed to an Argon Laser or a Conventional Quartz-Tungsten-Halogen Source. Dental Materials, 2002; 18: 221-226.

Price, R.B., Derand, T., Loney, R.W. and Andreou, P. Effect of Light Source and Specimen Thickness on the Surface Hardness of Resin Composite. American Journal of Dentistry, 2002; 15: 47-53.

Ritter, J.E., Jakus, K., Batakis, A. and Bandyopadhyay, N. Appraisal of Biaxial Flexure Strength Testing. Journal of Non-Crystalline Solids, 1980; 38 and 39: 419-424.

Rock, W.P. The Use of Ultra-Violet Radiation in Dentistry. British Dental Journal, 1974; 136: 455-458.

Rudnick, A., Hunter, A.R. and Holden, F.C. An Analysis of the Diametral-Compression Test. Materials Research and Standards, 1963; 3: 283-289.

Rueggeberg, F.A., Caughman, W.F. and Comer, R.W. The Effect of Autoclaving on Energy Transmission Through Light-Curing Tips. Journal of the American Dental Association, 1996; 127: 1183-1187.

Rueggeberg, F.A., Caughman, W.F., Curtis, J.W. and Davis, H.C. Effect of Light Intensity and Exposure Duration on Cure of Resin Composite. Operative Dentistry, 1994; 19: 26-32.

Ryge, G. Clinical Criteria. International Dental Journal, 1980; 30: 347-357.

Sahafi, A., Peutzfeldt, A. and Asmussen, E. Soft-Start Polymerisation and Marginal Gap Formation *In Vitro*. American Journal of Dentistry, 2001; 14: 145-147.

Sakaguchi, R.L. and Berge, H.X. Reduced Light Energy Density Decreases Post-Gel Contraction While Maintaining Degree of Conversion in Composites. Journal of Dental Research, 1998; 26: 695-700.

Sakaguchi, R.L., Wiltbank, B.D. and Murchison, C.F. Contraction Force Rate of Polymer Composites is Linearly Correlated with Irradiance. Dental Materials, 2004; 20: 402-407.

Seghi, R., Pollock, M. and Lannutti, J. Wear Resistance of Various Nano-Structured Composites. Journal of Dental Research, 2002; 81, Special Issue A: A414 Abstract. No. 3358.

Shetty, D.K., Wright, I.G., Mincer, P.N. and Clauer, A.H. Indentation Fracture of WC-Co Cerments. Journal of Materials Science, 1985; 20: 1873-1882.

Shortall, A.C., Palin, W.M. and Burtscher, P. Refractive Index Mismatch and Monomer Reactivity Influence Composite Curing Depth. Journal of Dental Research, 2008; 87: 84-88.

Silikas, N., Eliades, G. Watts, D.C. Light Intensity Effects on Resin-Composite Degree of Conversion and Shrinkage Strain. Dental Materials. 2000; 16: 292-296.

Skeeters, T.M., Timmons, J.G. and Mitchell, R.J. Curing Depth of Visible Light Cured Composite Resins. Journal of Dental Research, 1983; 62: 219. Abst. No. 448 (AADR).

Smith, D.C. Posterior Composite Dental Restorative Materials: Materials Development. In: Vanherle, G. and Smith, D.C. International Symposium on Posterior Composite Dental Resin Restorative Materials. P. Szulc Publishing Company: 1985; Netherlands: 47-60.

Sorensen, J.A. and Pham, M. *In Vitro* Wear of Composite Resins Processed with Various Systems. Journal Dental Research, 2002; 81, Special Issue A: A324 Abstract. No. 2578.

Stahl, F., Ashworth, S.H., Jandt, K.D. and Mills, R.W. Light-Emitting Diode (LED) Polymerisation of Dental Composites: Flexural Properties Polymerisation Potential. Biomaterials, 2000; 21: 1379-1385.

Stanford, J.W. The Current Status of Restorative Resins. Dental Clinics of North America, 1971; 15: 57-79.

Suzuki, S. and Leinfelder, K.F. Wear of Enamel Cusps Opposed By Posterior Composite Resin. Quintessence International, 1993; 24: 885-890.

Swartz, M.L., Phillips, R.W. and Rhodes, B. Visible Light-Activated Resins-Depth of Cure. Journal of the American Dental Association, 1983; 106: 634-637.

Taylor, D.F., Bayne, S.C., Sturdevant, J.R. and Wilder, A.D. Comparison of Direct and Indirect Methods for Analysing Wear of Posterior Composite Restorations. Dental Materials, 1989; 5: 157-160.

Timoshenko, S. and Woinowsky-Krieger, S. Symmetrical Bending of Circular Plates. In: Theory of Plates and Shells (2nd Edition). McGraw-Hill, 1959; New York.

Tirtha, R., Fan, P.L., Dennison, J.B. and Powers, J.M. *In Vitro* Depth of Cure of Photo-Activated Composites. Journal of Dental Research, 1982; 61: 1184-1187.

Turssi, C.P., Ferracane, J.L. and Ferracane, L.L. Wear and Fatigue Behaviour of Nano-Structured Dental Resin Composites. Journal of Biomedical Materials Research B Applied Biomaterials, 2006; 78: 196-203.

Uhl, A, Mills, R.W. and Jandt, K.D. Photoinitiator Dependent Composite Depth of Cure and Knoop Hardness with Halogen and LED Light Curing Units. Biomaterials, 2003; 24: 1809-1820.

Uhl, A., Michaelis, C., Mills, R.W. and Jandt, K.D. The Influence of Storage and Indenter Load on the Knoop Hardness of Dental Composites polymerized with LED and Halogen Technologies. Dental Materials, 2004a; 20: 21-28.

Uhl, A., Sigusch, B.W. and Jandt, K.D. Second Generation LEDs for the Polymerization of Oral Biomaterials. Dental Materials, 2004b; 20: 80-87.

Uhl, A., Völpel, A. and Sigusch, B.W. Influence of Heat From Light Curing Units and Dental Composite Polymerization on Cells I*n Vitro*. Journal of Dentistry, 2006; 34: 298-306.

Unterbrink, G.L. and Muessner, R., Influence of Light Intensity on Two Restorative Systems. Journal of Dentistry, 1995; 23: 183-189.

Vanherle, G., Lambrechts, P. and Braem, M. Overview of the Clinical Requirements for Posterior Composites. In: Vanherle, G. and Smith, D.C. International Symposium on Posterior Composite Resin Dental Restorative Materials. P. Szulc Publishing Company, 1985; Netherlands: 21-40.

Venhoven, B.A.M., de Gee, A.J. and Davidson, C.L. Light Initiation of Dental Resins: Dynamics of the Polymerization. Biomaterials, 1996; 17: 2313-2318.

Walker, M.P., Haj-Ali, R., Wang, Y., Hunziker, D. and Williams, KB. Influence of Environmental Conditions on Dental Composite Flexural Properties. Dental Materials, 2006; 22: 1002-1007.

Walls, A.W.G., McCabe, J.F. and Murray, J.J. The Polymerisation Contraction of Visible-Light Activated Composite Resins. Journal of Dentistry, 1988; 16: 177-181.

Wassell, R.W., McCabe, J.F. and Walls, A.W. Wear Characteristics In a Two-Body Wear Test. Dental Materials, 1994; 10: 269-74.

Watts, D.C. and Hindi, A.A. Intrinsic 'Soft-Start' Polymerisation Shrinkage-Kinetics in an Acrylate-Based Resin Composite. Dental Materials, 1999; 15: 39-45.

Watts, D.C., Amer, O.M. and Combe, E.C. Characteristics of Visible Light-Activated Composite Systems. British Dental Journal, 1984; 156: 209-215.

Watts, D.C., Marouf, A.S. and Al-Hindi, A.M. Photo-Polymerization Shrinkage-Stress Kinetics in Resin-Composites: Methods development Dental Materials, 2003; 19: 1-11

Weibull, W. A Statistical Distribution Function of Wide Applicability. Journal of Applied Mechanics 1951; 18: 293-297.

Willems, G., Lambrechts, P., Braem, M. and Vanherle, G. Composite Resins in the 21st Century. Quintessence International, 1993; 24: 641-658.

Williams, P.D. and Smith, D.C. Measurement of Tensile Strength of Dental Resorative Materials by Use of a Diametral Compression Test. Journal of Dental Research, 1971; 50: 436-442.

Wright, P.J.F. Comments on an Indirect Tensile Test on Concrete Cylinders. Magazine of Concrete Research, 1955; 1: 87-96.

Yap, A.U.J. and Teoh, S.H. Comparison of Flexural Properties of Composite Restoratives Using the ISO and Mini-Flexural Tests. Journal of Oral Rehabilitation, 2003; 30: 171-177.

Yap, A.U.J., Chandra, S.P., Chung, S.M. and Lim, C.T. Changes in Flexural Properties of Composite Restoratives After Aging in Water. Operative Dentistry, 2002; 27: 468-474.

Yearn, J.A. Factors Affecting Cure of Visible Light Activated Composites. International Dentistry Journal, 1985; 35: 218-225.

Yoon, T.H., Lee, Y.K., Lim, B.S. and Kim, C.W. Degree of Polymerization of Resin Composites by Different Light Sources. Journal of Oral Rehabilitation, 2002; 29: 1165-1173.

Yoshida, K. and Greener, E.H. Effect of Photoinitiator on Degree of Conversion of Unfilled Light Cured Resin. Journal of Dentistry, 1994; 22: 296-299.

Z100™ Product Report. 3M ESPE Dental Products, St. Paul, MN, USA, 1996.

JOURNAL OF DENTISTRY 36 (2008) 643–650

available at www.sciencedirect.com

ScienceDirect

journal homepage: www.intl.elsevierhealth.com/journals/jden

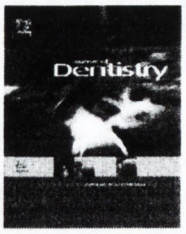

Effects of halogen light irradiation variables (tip diameter, irradiance, irradiation protocol) on flexural strength properties of resin-based composites

Gurcharn S. Bhamra, Garry J.P. Fleming *

Materials Science Unit, Division of Oral Biosciences, Dublin Dental School & Hospital, Trinity College Dublin, Dublin 2, Ireland

ARTICLE INFO

Article history:
Received 15 August 2007
Received in revised form
23 April 2008
Accepted 24 April 2008

Keywords:
Halogen light curing unit tip diameter
Irradiance
Flexure properties
Resin-based composites
Overlapping irradiation protocol

ABSTRACT

Objective: Investigation of halogen light irradiation variables (tip diameter, irradiance, irradiation protocol) on flexural strength and modulus of four methacrylate resin-based composites (RBCs).

Methods: Rectangular bar-shaped specimens (25 mm × 2 mm × 2 mm; $n = 20$ per group) of four RBCs were irradiated at varying irradiances (640 and 790 mW/cm^2; standard and boosted mode) with different tip diameters (8, 11, 13 and 25 mm) and for the 8 mm Turbo light tip diameter at irradiances of 880 and 1040 mW/cm^2 (standard and boosted mode). Following irradiation the specimens were stored in a light-proof container for 24 h at 37 ± 1 °C and tested in three-point flexure. One-way analyses of variance were made at $P = 0.05$, guided as necessary by Tukey's correction in multiple partial analyses, in addition to a Weibull analysis.

Results: The mean three-point flexure strengths, Weibull moduli and flexure moduli of the four RBC materials, irradiated with varying irradiances, tip diameters and irradiation protocols highlighted no significant differences although the values were material specific. Similarly the 8 mm conventional and Turbo tip diameter resulted in no significant differences for varying irradiances and irradiation protocols.

Conclusion: Within the limitations of the experiment halogen tip diameter, irradiance and irradiation protocol have no influence on three-point flexural strength and modulus data. The efficacy of the overlapping irradiation regime was upheld for the conditions tested.

1. Introduction

Dental resin-based composites (RBCs) consist of a high-strength particulate inorganic filler bonded to a lower strength organic polymer resin matrix utilising a silane coupling agent. Most RBCs available to dental practitioners are based on methacrylate chemistry and polymerisation is achieved, using visible light of a specified wavelength (450–470 nm), commonly by activation of the camphoroquinone–amine initiator-activator system.[1] Following irradiation, a proportion of the C=C double bonds of the methacrylate monomer resin are polymerised to C–C single bonds and form polymer chains with an associated closer packing of the molecules.[2] During polymerisation a gelation point is reached where the resin matrix changes from a viscous-plastic to a rigid-elastic phase.[2] The gel-point was defined as the moment at which the viscous flow of the RBC "can no longer keep up with the curing contraction".[2] As a result, bulk contraction or polymerisation shrinkage induces shrinkage stress within RBCs, the magnitude being dependent upon the nature of the polymeric matrix

* *Corresponding author.* Tel.: +353 1 612 7371; fax: +353 1 612 7297.
E-mail address: garry.fleming@dental.tcd.ie (Garry J.P. Fleming).
0300-5712/$ – see front matter
doi:10.1016/j.jdent.2008.04.019

material,[3] the filler load,[4] the viscous-elastic properties of the RBC[5] and the *in-vivo* cavity configuration.[6,7] Clinically, the shrinkage stress on polymerisation may compromise the quality of the bond at the tooth–restoration interface[8] and possibly lead to bacterial micro-leakage[9–11] and ultimately pulpal inflammation or necrosis and secondary caries.[9]

The range of testing methodologies employed to assess RBC performance and stated in ISO 4049 (The International Standard for Dentistry—polymer-based filling, restorative and luting materials[12]) include depth of cure, water sorption and water solubility and three-point flexure strength. It is imperative that there is standardisation and reproducibility of the testing methodologies between test centres when evaluating RBCs using the ISO 4049 standard[12] so that any material tested under ISO 4049 standard conditions should produce consistent test results. However, the differences in the three-point flexure strength data reported in the dental literature for the RBCs investigated in the current study varied from 79 to 184 MPa for Z100™ MP Restorative (3 M ESPE, St Paul, MN, USA),[13–18] 92–245 MPa for Filtek™ Z250 (3 M ESPE, St Paul, MN, USA),[17,19–23] 138–170 MPa for Filtek™ P60 (3 M ESPE, St Paul, MN, USA)[16,19] and 113–153 MPa for Filtek™ Supreme XT (3 M ESPE, St Paul, MN, USA).[18,23] The variously reported three-point flexure strength data was reported to be indicative of the degree of conversion,[19,21] irradiance,[21,24] type of mould[17,18,25] and light source[17,19,20] employed although different operators would be expected to manipulate the materials differently as well. In addition, the polymerisation process for light activated RBCs involves a complex series of interactions which can be influenced by the resin photo-activation system,[26] the light curing unit (LCU) spectral distribution[27,28] and the energy density (J/cm^2).[29] In the current study, RBCs from the same manufacturer were chosen to ensure the same photo-activation system was employed, namely camphorquinone and the QTH LCU used produced two specific irradiances (I) for specific irradiation times (t) to provide two discrete energy densities.

The three-point flexure strength of RBC materials determined using the protocol set out in ISO 4049[12] involves the fabrication of rectangular bar-shaped specimens with length, width and height dimensions of 25 mm × 2 mm × 2 mm, respectively. As the length of the rectangular-bar exceeds the LCU light tip diameter, an overlapping light curing procedure is required. The exit window of the LCU light tip is placed at the centre of the specimen, irradiated for the recommended exposure time which can vary depending upon the composition of the RBC. The exit window is then moved by half the diameter of the exit window along the specimen and the adjacent area irradiated, with the procedure repeated until the entire length of the specimen is irradiated on both the top and bottom surfaces.[12] The efficiency of the overlapping irradiation regime has been questioned by a number of authors in the dental literature recently in terms of uncontrolled initiation on polymerisation,[11] non-homogeneously cured specimens[19] and inconsistent polymerisation along the length of the bar-shaped specimen.[17,20] A range of light tip diameters are currently available to dental practitioners ranging from 8 to 13 mm diameters. Consequently 8, 11 and 13 mm light tip diameters require nine, seven and five overlapping irradiations on each side to adequately polymerise the 25 mm length of the ISO bar-shaped specimens according to the protocol. Alternative irradiation methodologies including oven-LCUs,[13,19,20] the use of a scanning motion with a handheld-LCU along the length of the bar-shaped specimen[11,30] or employing a custom made fibre optic light guide enabling a 'one-hit' irradiation of the entire specimen[31] have been advocated to control initiation on polymerisation and produce homogeneous specimens and consistent polymerisation along the length of the specimen. Mehl et al.[11] and Manhart et al.[30] advocated employing three LCUs placed alongside one another with no gaps between the LCU curing tips to irradiate the three-point rectangular bar-shaped specimens to prevent uncontrolled initiation on polymerisation. However, Mehl et al.[11] and Manhart et al.[30] did not investigate the overlapping irradiation regime against their technique of employing the three LCUs. Ferracane et al.[19] also expressed concern that the overlapping irradiation regime would influence the homogeneity of the irradiated specimen. Ferracane et al.[19] compared a Triad II (Caulk/Densply, Milford, DE, USA) oven-LCU with a QTH LCU and identified 'practically equivalent' three-point flexure strength and flexure modulus data when either LCU was employed. Palin et al.[17] suggested that the overlapping irradiation regime stipulated in ISO 4049 may result in inconsistent polymerisation along the length of the three-point flexure rectangular bar-shaped specimen thereby producing a different defect population to that expected for a 'one-hit' irradiation. These suggestions were further emphasised by Palin et al.[20] when the three-point flexure strength data from an overlapping irradiation regime with a handheld-LCU was compared with a single exposure Visio-Beta (3 M ESPE, Seefeld, Germany) oven-LCU. Although equivalent three-point flexure strength data was achieved, the authors highlighted a significant reduction in the reliability of the three-point flexure strength data when an overlapping irradiation regime was employed. In addition, the survival probability distributions of Palin et al.[20] highlighted a bi-modal defect distribution namely an asymmetry, for the handheld-LCU compared with specimens irradiated using the oven-LCU.

In the current study to exacerbate the potential for uncontrolled initiation on polymerisation and decrease the homogeneity of polymerisation along the length of the specimen, the exit window was moved by three-quarters (not half) the diameter along the specimen so that some areas received twice the irradiation of adjacent areas and irradiation was from the top surface only. The objective was to investigate halogen light irradiation variables (tip diameter, irradiance, irradiation protocol) on flexural strength and modulus of four RBCs. The hypothesis tested was that the flexural strength and flexural moduli for the RBCs would be similar regardless of the halogen light curing variables.

2. Materials and methods

The RBC materials tested in the current study (Table 1) were Z100™ MP Restorative, Filtek™ Z250, Filtek™ P60 and Filtek™ Supreme XT. Twenty rectangular bar-shaped specimens (25 mm length, 2 mm width and 2 mm thickness) were fabricated using a knife-edged split aluminium mould (aluminium alloy 6061) designed to minimise the stresses

Table 1 – The formulation of the resin-based composite materials used in the current study

RBC type	Filler			Resin
	Type	Particle size (μm)	Volume (%)	
Z100™ (shade A3: batch 20050211)	Zirconia and silica	0.01–0.35	66	Bis-GMA and TEGDMA
Filtek™ Z250 (shade A3: batch 20050210)	Zirconia and silica	0.01–0.35	60	Bis-GMA, UDMA, Bis-EMA and TEGDMA
Filtek™ P60 (shade A3: batch 20050329)	Zirconia and silica	0.01–0.35	61	Bis-GMA, UDMA, Bis-EMA and TEGDMA
Filtek™ Supreme XT (shade A3B: batch 20050106)	Zirconia	0.6–1.4	59.5	Bis-GMA, UDMA, Bis-EMA and TEGDMA

Manufacturers details available as of 3 M ESPE Technical Specifications (www.mmm.com/Product/business-units/espe-dental.html) accessed 22 April 2008.

generated on the specimens upon retrieval following irradiation.[30] In addition, the split-mould allowed the flash of excess material to be easily removed and the diverging end walls allowed easy flow of the material and maximised the expulsion of air.[30] A constant excess of uncured resin was placed into the mould, covered with a cellulose acetate strip and a glass microscope slide and a load of 1 kg was applied for 20 s to ensure consistent and reproducible packing of the specimens. The load and microscope slide were removed and the specimen was irradiated using a quartz tungsten halogen (QTH) handheld LCU at ambient room temperature (23 ± 1 °C) in either a standard or boosted mode (Table 2). Prior to the fabrication of each of the 24 specimen groups (4 RBCs × 3 tip diameters × 2 irradiances) of 20 specimens, the output was measured ($n = 7$) at the centre of the exit window using a radiometer incorporated in the LCU for each tip diameter in standard and boosted mode. The entire length of each specimen was irradiated by modifying the ISO 4049 specimen manufacture protocol[12] by moving the exit window by a three-quarters (not half) the diameter along the specimen so that areas received twice the irradiation of adjacent areas using 8, 11 and 13 mm LCU tip diameters, by placing the tip of the light guide in direct contact with the acetate strip. Eight groups were irradiated using the 8 mm Turbo light curing tip diameter with irradiances in standard mode and boosted mode (Table 2). A further eight specimen groups were prepared using a custom made fibre optic light guide, a 10 mm circular collection port with the fibre optics within the bundle randomly arranged to form the exit window,[30] enabling illumination of the entire specimen in 'one-hit' in standard and boosted mode (Table 2). Following polymerisation the cellulose acetate strip was discarded, the mould dismantled and the specimen removed and checked for surface imperfections. The specimens were then stored in a light-proof container and placed in a water-bath maintained at 37 ± 1 °C for 24 h prior to testing.

The rectangular bar-shaped specimens with the cured side uppermost were centrally loaded using a universal testing machine (Model 5565, Instron Ltd., High Wycombe, Berks, England) with a support span of 20 mm at a crosshead speed of 1 mm/min using a 2 kN load cell with a relative uncertainty of measurement of ±0.23%. The maximum load to fracture was recorded and the three-point flexure strength calculated using the following equation[12]:

$$\sigma_{max} = \frac{3PL}{2bd^2} \quad (1)$$

where σ_{max} was the maximum flexure stress, P the measured load at fracture, L the support span distance, b the width and d

Table 2 – Details of the irradiances and energy densities employed for the varying tip diameters when using the QTH handheld LCU (Optilux 501, Kerr Mfg. Co., Orange, CA, USA)

	Tip diameter (mm)									
	8	11	13	25	8T	8	11	13	25	8T
Z100™										
Irradiance (mW/cm²)		640 ± 18			880 ± 18		790 ± 18			1040 ± 28
Energy density (J/cm²)		25.6			35.2		31.6			41.6
Filtek™ Z250										
Irradiance (mW/cm²)		640 ± 18			880 ± 18		790 ± 18			1040 ± 28
Energy density (J/cm²)		12.8			17.6		15.8			20.8
Filtek™ P60										
Irradiance (mW/cm²)		640 ± 18			880 ± 18		790 ± 18			1040 ± 28
Energy density (J/cm²)		12.8			17.6		15.8			20.8
Filtek™ Supreme XT										
Irradiance (mW/cm²)		640 ± 18			880 ± 18		790 ± 18			1040 ± 28
Energy density (J/cm²)		12.8			17.6		15.8			20.8

Table 3 – The mean three-point flexure strengths and associated standard deviations (in parenthesis), the range of three-point flexure strengths, associated Weibull moduli and associated standard deviations (in parenthesis), 95% confidence intervals and mean three-point flexure moduli and associated standard deviations in parenthesis for the RBC specimens irradiated using a QTH LCU with 8, 11, 13 and 25 mm LCU tip diameters at standard (S) and boosted (B) irradiances of 640 and 790 mW/cm², respectively (individual group means connected by the same case letter are not significantly different for Tukey's test comparisons at $P < 0.05$)

	Output intensity (mW/cm²)							
	640				790			
	8 mm	11 mm	13 mm	25 mm	8 mm	11 mm	13 mm	25 mm
Z100™								
Three-point flexure strength (MPa)	103 (15)[a]	99 (14)[a]	93 (14)[a]	104 (15)[a]	101 (16)[a]	93 (15)[a]	95 (14)[a]	105 (16)[a]
Range of three-point flexure strengths (MPa)	78–131	79–122	74–121	76–135	76–130	75–122	75–119	79–141
Weibull modulus	7.1 (1.6)	7.6 (1.7)	7.2 (1.6)	7.5 (1.7)	6.5 (1.5)	6.3 (1.4)	6.7 (1.5)	7.1 (1.6)
95% confidence intervals	6.1–8.0	6.5–8.6	6.2–8.2	6.9–8.1	5.8–7.2	5.0–7.6	5.7–7.8	6.3–7.8
Three-point flexure modulus (GPa)	13.6 (1.7)[b]	14.8 (1.6)[b]	14.4 (1.6)[b]	14.9 (1.5)[b]	14.3 (1.5)[b]	14.7 (1.5)[b]	14.2 (1.0)[b]	13.6 (1.3)[b]
Filtek™ Z250								
Three-point flexure strength (MPa)	164 (16)[c]	151 (14)[c]	156 (15)[c]	157 (15)[c]	154 (15)[c]	153 (14)[c]	156 (15)[c]	156 (15)[c]
Range of three-point flexure strengths (MPa)	141–189	133–180	128–180	122–179	137–190	124–184	126–182	123–176
Weibull modulus	10.4 (2.3)	10.9 (2.4)	10.9 (2.4)	10.9 (2.4)	10.5 (2.4)	11.2 (2.7)	10.6 (2.4)	10.9 (2.4)
95% confidence intervals	8.7–12.0	8.6–13.2	10.0–11.8	10.4–11.4	8.0–13.0	10.0–12.5	9.8–11.3	10.2–11.5
Three-point flexure modulus (GPa)	11.4 (1.3)[d]	11.0 (1.0)[d]	10.8 (0.8)[d]	10.8 (1.4)[d]	11.9 (0.8)[d]	11.4 (0.6)[d]	11.4 (1.1)[d]	10.9 (1.7)[d]
Filtek™ P60								
Three-point flexure strength (MPa)	165 (16)[e]	154 (16)[e]	162 (16)[e]	165 (17)[e]	164 (16)[e]	161 (16)[e]	164 (15)[e]	154 (13)[e]
Range of three-point flexure strengths (MPa)	127–186	125–185	126–184	128–184	136–189	128–184	124–186	129–172
Weibull modulus	10.7 (2.4)	10.6 (2.4)	10.7 (2.4)	9.6 (2.1)	10.8 (2.4)	10.3 (2.3)	10.7 (2.4)	11.9 (2.7)
95% confidence intervals	9.9–11.4	9.5–11.6	9.6–11.9	8.5–10.7	9.3–12.3	9.3–11.2	9.6–11.9	10.8–13.1
Three-point flexure modulus (GPa)	12.2 (1.0)[fg]	11.2 (0.9)[f]	12.4 (1.5)[g]	12.2 (0.9)[fg]	12.0 (0.9)[fg]	11.6 (1.0)[fg]	11.5 (1.2)[fg]	11.5 (1.3)[fg]
Filtek™ Supreme XT								
Three-point flexure strength (MPa)	140 (10)[h]	141 (10)[h]	140 (10)[h]	133 (12)[h]	142 (9)[h]	141 (12)[h]	140 (12)[h]	133 (9)[h]
Range of three-point flexure strengths (MPa)	120–158	124–158	108–157	115–154	129–158	120–155	123–157	105–145
Weibull modulus	14.2 (3.2)	14.1 (3.2)	13.0 (2.9)	11.9 (2.7)	15.8 (3.5)	12 (2.7)	11.6 (2.6)	13.6 (3.0)
95% confidence intervals	12.9–15.6	12.2–16.0	10.3–15.7	10.5–13.3	13.2–18.3	10.4–13.6	9.6–13.6	10.1–17.2
Three-point flexure modulus (GPa)	10.0 (0.8)[i]	10.2 (0.9)[i]	9.6 (0.8)[i]	9.5 (1.1)[i]	10.3 (0.7)[i]	9.7 (0.6)[i]	9.5 (1.0)[i]	9.6 (0.9)[i]

the thickness of the specimens measured using a digital micrometer accurate to 10 μm (Mitutoyo, Kawasaki, Japan).

The three-point flexure modulus was determined using the following equation:

$$E = \left(\frac{\Delta P}{\Delta D}\right)\frac{L^3}{4bd^3} \quad (2)$$

where E was the flexure modulus, L the support span distance, b the width and d the thickness of the specimen and $(\Delta P/\Delta D)$ the gradient of the steepest linear portion of the load–deflection curve.[12]

One-way analyses of variance (ANOVA), were made in software (Sigmaplot 11, Systat Software, Richmond, CA, USA) using a critical significance level of $P = 0.05$, guided as necessary by Tukey's correction in multiple partial analyses. The three-point flexure strength data was ranked in ascending order and Weibull analysis performed. The Weibull distribution can be shown as[32]

$$P_f = 1 - \exp\left[-\left(\frac{\sigma}{\sigma_0}\right)^m\right] \quad (3)$$

where σ was the fracture stress, P_f the probability of failure, m the Weibull modulus and σ_0 the normalising constant—calculated at 63.21% probability of failure. For each specimen group the 95% confidence limits of the Weibull modulus were calculated and considered to be significant when they did not overlap.[32]

3. Result

3.1. *The influence of irradiation tip diameter*

The mean three-point flexure strengths of the rectangular bar-shaped RBC specimens utilised, irradiated with the 8, 11 and 13 mm LCU tip diameters and 'one-hit' irradiation in standard and boosted modes, showed no significant differences between LCU tip diameters at the 95% significance level, although the mean three-point flexure strengths were material specific (Table 3). In addition, the survival probability distributions for the three-point flexure strength data of the four RBC materials investigated possessed a similar symmetry indicative of a single distribution of defects regardless of the irradiation protocol and output intensity employed during fabrication (Fig. 1). The associated Weibull moduli of the three-point flexure strength data in both standard and boosted modes showed no significant differences (as the 95% confidence intervals of the Weibull moduli overlapped) between the RBC specimens irradiated with the different LCU tip diameters and 'one-hit' irradiation although the Weibull modulus again was material specific.

When the mean three-point flexure moduli for the 32 groups of 20 rectangular bar-shaped RBC specimens were analysed at the 95% significance level, no significant differences between LCU tip diameters were identified for 31 of the 32 groups although the mean flexure moduli were material specific (Table 3). The only exception was with Filtek™ P60 when irradiated at 640 mW/cm^2 with the 11 or 13 mm LCU tip diameter ($P = 0.13$).

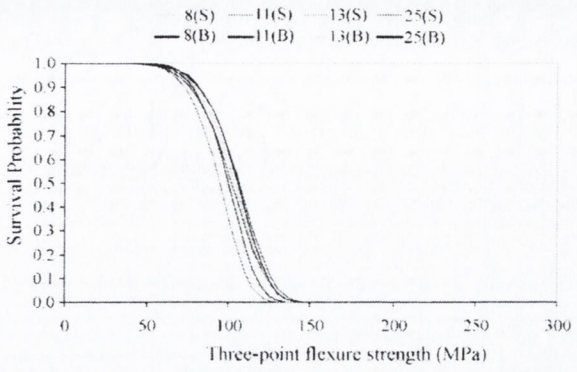

Fig. 1 – The survival probability distributions of three-point flexure strengths for Z100™ specimens irradiated using a QTH LCU with 8, 11, 13 and 25 mm LCU tip diameters at standard (S) and boosted (B) irradiances of 640 and 790 mW/cm^2, respectively highlighting a similar symmetry indicative of a single distribution of defects regardless of the irradiation protocol and irradiance employed during fabrication.

3.2. *The influence of irradiance*

Irradiation of the RBC rectangular bar-shaped specimens with the 8 mm conventional and 8 mm Turbo LCU tip diameters in standard mode or boosted mode resulted in no significant differences in mean three-point flexure strengths (Table 4) for the eight specimen groups of each material at the 95% significance level. The survival probability distributions for the three-point flexure strength data possessed a similar symmetry which was indicative of a single distribution of defects regardless of output intensity employed during fabrication for the four RBC materials investigated (Fig. 2). In addition, the 95% confidence intervals of the Weibull moduli overlapped so that the reliability of the fracture strength data resulted in no significant differences between specimens irradiated with different light intensities for the individual RBC materials investigated.

Analysis of the mean three-point flexure moduli of the RBC rectangular bar-shaped specimens irradiated with the 8 mm conventional and 8 mm Turbo LCU tip diameters in standard mode or boosted mode at the 95% significance level also showed no significant differences between light intensities on the flexure modulus of each individual material (Table 4).

4. Discussion

In the current study differences between materials requires no elaboration as the effects of formulation have been discussed at length elsewhere in the literature. The reason RBCs from the same manufacturer were chosen was to ensure the same photo-activation system was employed. The RBCs (Filtek™ Z250, Filtek™ P60 and Filtek™ Supreme XT) were chosen as the same monomeric constituents were present with similar filler loadings (although different packing fraction designs) was to insure that the effects being measured were mostly

Table 4 – The mean three-point flexure strengths and associated standard deviations in parenthesis, the range of three-point flexure strengths, associated Weibull moduli and associated standard deviations in parenthesis, 95% confidence intervals and mean three-point flexure moduli and associated standard deviations in parenthesis for specimens irradiated at with a conventional 8 mm LCU tip diameter at standard and boosted irradiances of 640 and 790 mW/cm^2, respectively and an 8 mm Turbo LCU tip diameter at standard and boosted irradiances of 880 and 1040mW/cm^2, respectively (individual group means connected by the same case letter are not significantly different for Tukey's test comparisons at $P < 0.05$)

Output intensity (mW/cm^2)	Z100™				Filtek™ Z250			
	640	880	790	1040	640	880	790	1040
Three-point flexure strength (MPa)	101 (16)^j	104 (14)^j	101 (16)^j	107 (15)^j	164 (16)^k	157 (16)^k	154 (15)^k	156 (16)^k
Range of three-point flexure strengths (MPa)	78–131	69–130	76–130	87–134	141–189	124–183	137–190	131–182
Weibull modulus	7.1 (1.6)	6.5 (1.5)	6.7 (1.5)	7.5 (1.7)	10.4 (2.3)	10.7 (2.4)	10.5 (2.4)	10.6 (2.4)
95% confidence intervals	6.1–8.0	5.8–7.2	5.7–7.8	6.2–8.8	8.7–12.0	10.0–11.3	8.0–13.0	9.4–11.8
Three-point flexure modulus (GPa)	13.6 (1.7)^m	13.2 (1.2)^m	14.3 (1.5)^m	14.1 (1.1)^m	11.4 (1.3)^m	11.3 (0.9)^m	11.9 (0.8)^m	11.6 (0.7)^m
Output intensity (mW/cm^2)	Filtek™ P60				Filtek™ Supreme XT			
	640	880	790	1040	640	880	790	1040
Three-point flexure strength (MPa)	165 (16)^n	164 (16)^n	164 (16)^n	151 (14)^n	140 (10)^o	140 (9)^o	142 (9)^o	137 (11)^o
Range of three-point flexure strengths (MPa)	127–186	128–187	136–189	128–178	120–158	124–157	129–158	112–159
Weibull modulus	10.7 (2.4)	10.4 (2.3)	10.8 (2.4)	11.8 (2.6)	14.2 (3.2)	16.1 (3.6)	15.8 (3.5)	15.0 (3.4)
95% confidence intervals	9.9–11.4	9.7–11.1	9.3–12.3	10.6–13.0	12.9–15.6	14.2–17.9	13.2–18.3	12.5–17.5
Three-point flexure modulus (GPa)	12.2 (1.0)^p	12.7 (1.3)^p	12.0 (0.9)^p	12.8 (1.1)^p	10.0 (0.8)^q	10.3 (0.7)^q	10.3 (0.7)^q	9.9 (1.0)^q

related to the variables of halogen light irradiation (tip diameter, irradiance, irradiation protocol) and not to the compositions of the RBCs. As expected increasing filler content resulted in improved three-point flexure strength and modulus data for Filtek™ Z250, Filtek™ P60 and Filtek™ Supreme XT given the monomeric constituents. Z100™ despite the higher filler volume (66%), the increased TEGDMA concentration in the monomeric constituents result in decreased strength and increased brittleness (elastic modulus) compared with Filtek™ Z250, Filtek™ P60 and Filtek™ Supreme XT.[15]

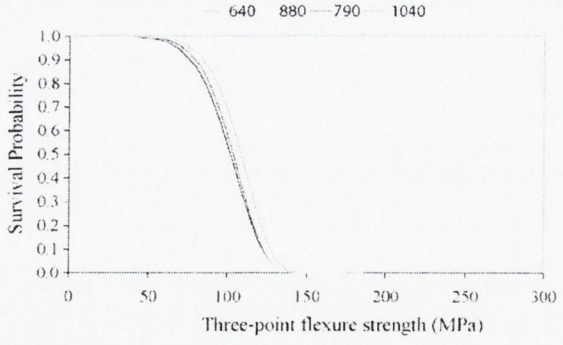

Fig. 2 – The survival probability distributions of three-point flexure strengths for Z100™ specimens irradiated at with a conventional 8 mm LCU tip diameter at standard (S) and boosted (B) output intensities of 640 and 790 mW/cm^2, respectively and an 8 mm Turbo LCU tip diameter at standard (S) and boosted (B) irradiances of 880 and 1040 mW/cm^2, respectively. The survival probability distributions highlighting a similar symmetry indicative of a single distribution of defects regardless of the irradiance employed for an 8 mm LCU tip diameter during fabrication.

4.1. *LCU tip diameter*

The efficacy of the overlapping irradiation regime has been questioned by a number of authors in the dental literature recently.[11,17,19,20,30] Palin et al.[20] proposed that residual tensile stresses were created by the overlapping irradiation regime and therefore a non-homogenous polymerisation stress distribution existed along the length of the bar-shaped specimens manifested as a reduction in the Weibull modulus and the bi-modal defect distribution. Accordingly, decreasing the LCU tip diameter (from 13 to 11 mm and 8 mm) would be expected to progressively decrease the efficiency of the polymerisation process along the length of the RBC specimens compared with a 'one-hit' irradiation, manifested as a reduction in the reliability of the three-point flexure strength. However, when the three-point flexure strength data was analysed for the four RBCs tested at the irradiances investigated, no change in the reliability of the three-point flexure strength data was evident. It is therefore evident that the previously theory proposed by Palin et al.[17,20] was not entirely correct. If the central region of the bar-shaped specimen is

irradiated and the gel-point reached, the setting stresses are accommodated by the adjacent resin-ends which are only partially irradiated by light scattering.[11,30] Palin et al. [20] postulated that when the partially irradiated end regions are irradiated that the associated post-gel shrinkage stresses place the central region under tensile stress. If the proposed theory was correct then increasing the number of overlapping irradiations (decreasing the light tip diameter) would be expected to progressively decrease the homogeneity of the irradiated bar-shaped specimens resulting in an increased curing variability. The irradiation variability would be manifested as a reduction in the reliability of the three-point flexure strength data in addition to an exacerbation of the bimodal defect distribution which did not occur in the survival probability distributions in the current study (Fig. 1). In addition, Palin et al.[17] suggested the strength data generated using the overlapping regime was partially dependent on the relative shrinkage constraints. In the study by Palin et al.[17] only one material was used (Filtek™ Z250), however, in the current study four methacrylate RBCs with markedly varying shrinkage characteristics were employed and no shrinkage constraint effect was observed in the reliability of the three-point flexure strength data.

4.2. *Light energy density*

The conventional wisdom regarding the total energy delivered, namely the energy density (J/cm^2), is calculated from the irradiation time (t) with a LCU of a specific irradiance (I). In general, when assessing the flexure properties of RBCs, researchers routinely quote flexure strength and flexure modulus values determined following the delivery of a specific irradiance for a predetermined time period[11,24,33,34] while few authors quote the energy density delivered at the specific irradiance.[19–21] In line with the conventional wisdom regarding energy densities, energy densities ranging from 12.8 to 41.6 J/cm^2 were employed in the current study with the results indicating no significant differences between the three-point flexure strengths and three-point flexure moduli of the four RBCs investigated. Examination of the three-point flexure strength and three-point flexure modulus data in the dental literature identified no significant differences for a range of RBCs irradiated at energy densities of 19–27 J/cm^2,[11] 12 J/cm^2 (delivered for 30 s at 400 mW/cm^2, 60 s at 200 mW/cm^2 or 120 s at 100 mW/cm^2),[24] 15.5–23 J/cm^2 using either a single or two-step light irradiation regime[34] or 24 and 8.8 J/cm^2 from a handheld- and oven-LCUs, respectively.[19] These results combined with those from the current investigation further emphasise that the relationship between the development of three-point flexure properties with energy density, namely irradiance and time is not linear.[35,36] In the current study, to investigate halogen light irradiation variables (tip diameter, irradiance, irradiation protocol) on flexural strength and modulus, the irradiation protocol (ISO 4049) was modified to exacerbate the potential for uncontrolled initiation on polymerisation and decrease the homogeneity of polymerisation along the length of the specimen. The efficacy of the modified overlapping irradiation regime was upheld for the conditions tested (tip diameter, irradiance, irradiation protocol). No manifestations of uncontrolled initiation on polymerisation, decreased homogeneity and consistency of polymerisation along the length of the specimen for four methacrylate RBCs were evident.

Within the limitations of the experiment (specimen thickness, RBC shade, photo-activation system, irradiances chosen) halogen tip diameter, irradiance and irradiation protocol have no influence on three-point flexural strength and modulus data although there are some clinical implications. The RBCs were irradiated directly from the top surface to a maximum depth of 2 mm in the current study. Clinically, the irradiance available to the RBCs has a negative correlation to the depth of the cavity, particularly in the case of class II restorations where interproximal boxes exceed 7 mm in depth.[37] This combined with the fact that most dentists hold the light curing tip 1 mm or more away from the tooth leads to a significant reduction in irradiance delivered to the RBC which may have implications for strength and modulus development.

5. Conclusion

Within the limitations of the experiment (specimen thickness, RBC shade, photo-activation system, irradiances chosen) halogen tip diameter, irradiance and irradiation protocol have no influence on three-point flexural strength and modulus data. The efficacy of the overlapping irradiation regime was upheld for the conditions tested.

REFERENCES

1. Viljanen EK, Lassila LVJ, Skrifvars M, Vallittu PK. Degree of conversion and flexural properties of a dendrimer/methyl methacrylate copolymer: design of experiments and statistical screening. *Dental Materials* 2005;**21**:172–7.
2. Davidson CL, Feilzer AJ. Polymerization shrinkage and polymerization shrinkage stress in polymer-based restoratives. *Journal of Dentistry* 1997;**25**:435–40.
3. Guggenberger R, Weinmann W. Exploring beyond methacrylates. *American Journal of Dentistry* 2000;**13**:82D–4D.
4. Fleming GJP, Hall D, Shortall ACC, Burke FJT. Cuspal movement and microleakage in premolar teeth restored with posterior filling materials of varying reported volumetric shrinkage values. *Journal of Dentistry* 2005;**33**:139–46.
5. Bragga RR, Ballester RY, Ferracane JL. Factors involved in the development of polymerisation shrinkage stress in resin-composites: a systematic review. *Dental Materials* 2005;**21**:962–70.
6. Feilzer AJ, De Gee AJ, Davidson CL. Setting stress in composite resin in relation to configuration of the restoration. *Journal of Dental Research* 1987;**66**:1636–9.
7. Kleverlaan CJ, Feilzer AJ. Polymerization shrinkage and contraction stress of dental resin composites. *Dental Materials* 2005;**21**:1150–7.
8. Davidson CL, DeGee AJ, Feilzer AJ. The competition between the composite–dentin bond strength and the polymerisation contraction stress. *Journal of Dental Research* 1984;**63**:1396–9.
9. Lutz F, Krejici I, Barbakow F. Quality and durability of marginal adaptation in bonded composite restorations. *Dental Materials* 1991;**7**:107–13.
10. Uno S, Asmussen E. Marginal adaptation of a restorative resin polymerized at reduced rate. *Scandinavian Journal of Dental Research* 1991;**99**:440–4.

11. Mehl A, Hickel R, Kunzelmann K-H. Physical properties and gap formation of light-cured composites with and without 'soft-start polymerization'. *Journal of Dentistry* 1997;**25**: 321–30.
12. International Standards Organisation. *Dentistry—polymer-based filling, restorative and luting materials*. 3rd ed. ISO 4049; 2000. p. 15–8.
13. Peutzfeldt A, Asmussen E. The effect of postcuring on quantity of remaining double bonds, mechanical properties, and in vitro wear of two resin composites. *Journal of Dentistry* 2000;**28**:447–52.
14. Cesar PF, Miranda WG, Braga RR. Influence of shade and storage time on the flexural strength, flexural modulus, and hardness of composites used for indirect restorations. *Journal of Prosthetic Dentistry* 2001;**86**:289–96.
15. Yap AUJ, Chandra SP, Chung SM, Lim CT. Changes in flexural properties of composite restoratives after aging in water. *Operative Dentistry* 2002;**27**:468–74.
16. Adabo GL, Cruz CAS, Fonseca RG, Vaz LG. The volumetric fraction of inorganic particles and the flexural strength of composites for posterior teeth. *Journal of Dentistry* 2003;**31**:353–9.
17. Palin WM, Fleming GJP, Burke FJT, Marquis PM, Randall RC. The reliability in flexural strength testing of a novel dental composite. *Journal of Dentistry* 2003;**31**:549–57.
18. Beun S, Glorieux T, Devaux J, Vreven J, Leloup G. Characterization of nanofilled compared to universal and microfilled composites. *Dental Materials* 2007;**23**:51–59.
19. Ferracane JL, Ferracane LL, Musanje L. Effect of light activation method on flexural properties of dental composites. *American Journal of Dentistry* 2003;**16**:318–22.
20. Palin WM, Fleming GJP, Marquis PM. The reliability of standardized flexure strength testing procedures for a light-activated resin-based composite. *Dental Materials* 2005;**21**:911–9.
21. Calheiros FC, Kawano Y, Stansbury JW, Braga RR. Influence of radiant exposure on contraction stress, degree of conversion and mechanical properties of resin composites. *Dental Materials* 2006;**22**:799–803.
22. Yap AUJ, Teoh SH. Comparison of flexural properties of composite restoratives using the ISO and mini-flexural tests. *Journal of Oral Rehabilitation* 2003;**30**:171–7.
23. Mitra SB, Wu D, Holmes BN. An application of nanotechnology in advanced dental materials. *Journal of American Dental Association* 2003;**134**:1382–90.
24. Miyazaki M, Oshida Y, Moore BK, Onose H. Effects of light exposures on fracture toughness and flexural strength of light-cured composites. *Dental Materials* 1996;**12**:328–32.
25. Peutzfeldt A, Asmussen E. The effect of postcuring on quality of remaing double bonds, mechanical properties, and in vitro wear of two resin composites. *Journal of Dentistry* 2000;**28**:447–52.
26. Cook WD. Spectral distributions of dental photopolymerization sources. *Journal of Dental Research* 1982;**61**:1436–8.
27. Pradhan RD, Melikechi N, Eichmiller. The effect of irradiation wavelength bandwidth and spot size on the scraping depth and temperature rise in composite exposed to an argon laser or a conventional quartz-tungsten-halogen source. *Dental Materials* 2002;**18**:221–6.
28. Obici AC, Sinhoreti MAC, Frollini E, Sobrinho LC, Consani S. Degree of conversion and knoop hardness of Z250 composite using different photo-activation methods. *Polymer Testing* 2005;**24**:814–8.
29. Peutzfeltz A, Asmussen E. Resin composite properties and energy density of light cure. *Journal of Dental Research* 2005;**84**:659–62.
30. Manhart J, Kunzelmann K-H, Chen Y, Hickel R. Mechanical properties and wear behaviour of light-cured packable composite resins. *Dental Materials* 2000;**16**:33–40.
31. Musanje L, Shu M, Darvell BW. Water sorption and mechanical behaviour of cosmetic direct restorative materials in artificial saliva. *Dental Materials* 2001;**17**: 394–401.
32. Weibull W. A statistical distribution function of wide applicability. *Journal of Applied Mechanics* 1951;**18**:293–7.
33. Unterbrink GL, Muessner R. Influence of light intensity on two restorative systems. *Journal of Dentistry* 1995;**23**:183–9.
34. Asmussen E, Peutzfeldt A. Flexural strength and modulus of a step-cured resin composite. *Acta Odontologica Scandinavica* 2004;**62**:87–90.
35. Musanje L, Darvell BW. Polymerisation of resin composite restorative materials: exposure reciprocity. *Dental Materials* 2003;**19**:531–41.
36. Asmussen E, Peutzfeldt A. Polymerisation contraction of resin composite vs. energy and power density of light-cure. *European Journal of Oral Science* 2005;**113**:417–21.
37. Sakaguchi RL, Berge HX. Reduced light energy density decreases post-gel contraction while maintaining degree of conversion in composites. *Journal of Dentistry* 1998;**26**:695–700.

DENTAL MATERIALS XXX (2008) XXX–XXX

available at www.sciencedirect.com

ScienceDirect

journal homepage: www.intl.elsevierhealth.com/journals/dema

Influence of halogen irradiance on short- and long-term wear resistance of resin-based composite materials

*Gurcharn S. Bhamra, Garry J.P. Fleming**

Materials Science Unit, Division of Oral Biosciences, Dublin Dental School & Hospital, Trinity College Dublin, Dublin 2, Ireland

ARTICLE INFO

Article history:
Received 16 April 2008
Received in revised form
19 June 2008
Accepted 20 June 2008

Keywords:
Wear resistance
Resin-based composites
Halogen irradiance
Optical profilometry

ABSTRACT

Objective. The Oregon Health Science University (OHSU) four-chamber oral wear simulator was used to examine the impact of halogen irradiance on the short- and long-term wear behavior of four-methacrylate resin-based composites (RBCs). The hypothesis proposed was that exacerbated wear would occur following the long-term wear of RBCs irradiated under non-optimized irradiance conditions.

Methods. Disc-shaped specimens (12.0 ± 0.1 mm diameter and 2.0 ± 0.1 mm height) of each RBC were prepared at irradiances of 650 ± 14, 530 ± 8, 420 ± 14, 350 ± 8, 270 ± 8, 230 ± 14, 190 ± 8, and 150 ± 8 mW/cm^2, respectively. Short-term three-body wear simulation was carried out for 50,000 cycles and long-term was performed up to 500,000 cycles. The wear facets were analyzed using a non-contact optical profilometer. One-, two-, and three-way analyses of variance (ANOVA) were made at $P = 0.05$, guided as necessary by Tukeys correction in multiple partial analyses of the mean total volumetric wear and mean maximum wear depth.

Results. For the short-term wear resistance, the two-way ANOVA identified no significant difference in the mean total volumetric wear ($P = 0.188$) although the mean total wear depth was identified to be significant ($P = 0.024$). The long-term wear resistance for the mean total volumetric wear identified significant differences for each RBC at varying irradiances with the number of cycles but not for the mean maximum wear depth.

Significance. The increased number of ploughing actions of the antagonist on the RBC (long-term) results in increased friction which would be expected to play a major role in the wear process. The significant increase in the mean total volumetric wear, but not the mean maximum wear depth, observed over time which is exacerbated at reduced halogen irradiances emphasizes the arguments of DeLong for the employment of volume for evaluating material loss due to wear following *in vitro* wear simulation of RBCs.

1. Introduction

Conventional quartz-tungsten halogen (QTH) handheld light curing units (LCUs) are routinely used to irradiate resin-based composites (RBCs) in dental clinics by producing filtered blue light by thermonic emission [1]. Halogen bulbs have a short working life of about 100 h [2], the dielectric pass-band filter, the reflector, and the bulb degrade over time due to the high operating temperatures produced during function [3]. Damage to the fibre optic bundle due to poor handling [4] and repeated

* *Corresponding author.* Tel.: +353 1 612 7371; fax: +353 1 612 7297.
E-mail address: garry.fleming@dental.tcd.ie (G.J.P. Fleming).

0109-5641/$ – see front matter © 2008 Academy of Dental Materials. Published by Elsevier Ltd. All rights reserved.
doi:10.1016/j.dental.2008.06.007

Please cite this article in press as: Bhamra GS, Fleming GJP. Influence of halogen irradiance on short- and long-term wear resistance of resin-based composite materials. Dent Mater (2008), doi:10.1016/j.dental.2008.06.007

sterilization [5] can all lead to a reduction in the irradiance over time. Studies carried out evaluating the irradiance of QTH LCUs used in dental practices revealed that many dental practitioners do not maintain their LCUs. Barghi et al. [6] evaluated 209 LCUs in private dental practices in Texas of which 30% provided an irradiance of less than 200 mW/cm^2. In Australia, 27% of the 214 LCUs investigated by Martin [7] and 33% of 130 LCUs examined by Pilo et al. [8] in Israel, had an irradiance of less than 200 mW/cm^2. Most recently in 2005, El-Mowafy et al. [9] investigated 214 LCUs in dental practices in Toronto and revealed that 16% of the LCUs assessed had an irradiance of less than 200 mW/cm^2. It is evident from these findings that general dental practitioners (GDPs) are unaware of the clinical implications of regular maintenance of their QTH LCUs has on RBC performance. This combined with the fact that most dentists hold the light curing tip 1 mm or more away from the tooth leads to a significant reduction in irradiance delivered to the RBC [10].

The clinical performance of RBC materials in terms of maintaining anatomical contours and contact with food and beverages [11] have been correlated with laboratory *in vitro* wear simulation. The testing methodology rapidly allows RBC assessment prior to the placement in the mouth and a variety of machines including the materials testing and simulation (MTS) artificial oral environment [12], the Academisch Centrum for Tandheelkunde Amsterdam (ACTA) wear machine [13], the University of Alabama wear machine [14] and the Oregon Health Science University (OHSU) oral wear simulator [15] have been used. The resin matrix has been reported to be the most influential factor influencing wear rate along with the filler loading [16–18] although limited information is available regarding the irradiance delivered to the RBC. Analysis of the dental literature available for the OHSU oral wear simulator highlighted there is little standardization of the testing regime (the attrition load (17–20 N), abrasion load (70–90 N), sliding path (5–7 mm) [17], antagonist (enamel or ceramic) [18]) the methods used to quantify the wear facet or the data reporting (wear depth, area or volume) [19,20]. In addition, poor standardization of results between operators in different test centers have resulted from different prototypes of the OHSU oral wear simulator being available over the last 10 years [21,22]. However, long-term wear data from the OHSU oral wear simulator for RBCs is non-existent as the studies to date have been limited to 50,000 and 100,000 wear cycles [15,23,24].

The polymerisation process for light-activated RBCs involves a complex series of interactions which can be influenced by the resin photo-activation system [25], the LCU spectral distribution [26,27] and the energy density (J/cm^2) [28]. In the current study, a recent version of the OHSU four-chamber oral wear simulator was used to examine the impact of QTH LCU irradiance on the short- and long-term wear behavior of four-methacrylate RBCs from the same manufacturer. The RBCs were chosen to ensure the same photo-activation system was employed, namely camphoroquinone and the LCU used produced specific irradiances for specific irradiation times to provide discrete energy densities. The RBCs (Filtek™ Z250, Filtek™ P60, and Filtek™ Supreme XT; 3M ESPE, Seefeld, Germany) contained the same monomeric constituents with similar filler loadings 59.5–61 vol.% (although different packing fraction designs) to insure that the effects being measured were mostly related to the irradiance delivered. Z100™ (3M ESPE, Seefeld, Germany) had a higher filler volume (66%) and an increased diluent concentration in the monomeric constituents.

The hypotheses proposed were that exacerbated wear rates for the RBCs investigated would be evident following: (1) irradiation at increased distances, (2) an increased number of wear cycles, (3) varying the monomeric constituents, and (4) varying the filler packing fraction design.

2. Materials and methods

2.1. *Specimen preparation*

For each of the four-methacrylate RBCs (Table 1) disc-shaped specimens (12.0 ± 0.1 mm diameter and 2.0 ± 0.1 mm depth) were prepared using an acrylic mould placed on an aluminium base plate. The mould was packed with an excess of uncured resin, covered with a cellulose acetate strip and a load of 1 kg was applied for 20 s. Subsequently the load was removed and the four specimens were irradiated in direct contact (0 mm) with the acetate strip using a QTH handheld LCU (Optilux 501, Kerr Mfg. Co., Orange, CA, USA) with an irradiance of 650 ± 14 mW/cm^2 and a 13 mm light tip diameter for the time period specified by the manufacturers. The procedure was repeated and so that further specimen groups of four (for each RBC) were fabricated by irradiating at distances of 3, 5, 7, 9, 11, 13, and 15 mm from the LCU tip resulting in irradiances of 530 ± 8, 420 ± 14, 350 ± 8, 270 ± 8, 230 ± 14, 190 ± 8, and 150 ± 8 mW/cm^2, respectively. The irradiance was measured seven consecutive times at the center of the exit window using a radiometer incorporated in the LCU (Optilux 501, Kerr, Orange, CA, USA) for each irradiation distance. Following polymerization each specimen was removed from the mould, checked for surface imperfections and stored in a light-proof container containing 50 ml of deionised water prior to storage in a climate-controlled chamber maintained at 37 ± 1 °C at 55% relative humidity for 23 h.

2.2. *In vitro wear resistance*

The *in vitro* wear resistance was carried out using the OHSU oral wear simulator [20]. The disc-shaped specimens were mounted in a two part cold-setting acrylic resin (Varidur, Beuhler, Lake Bluff, IL, USA) to produce cylinders (25.0 ± 0.1 mm diameter and 10.0 ± 0.1 mm height) compatible with the chambers of the wear-testing apparatus. The mounted specimens were wet ground using water as the lubricant on a Beta grinder-polisher machine (Beuhler, Lake Bluff, IL, USA) with P600 and P1200 silicon carbide (SiC) abrasive paper at a force of 10 N per specimen for 30 s on each grade of SiC to provide a reproducible surface roughness conductive to wear testing [15]. Each of the four specimens was secured into an individual wear chamber of the wear simulator and a food-like slurry (1.0 g of ground poppy seeds (Holland & Barrett, Burton-upon-Trent, UK), 0.5 g of PMMA beads (Special Tray, Dentsply DeTrey, Kanstanz, Germany) and 5 ml of distilled water) was added to each chamber [13]. The antagonist consisted of steatite spheres (10.0 ± 0.1 mm diameter) which

Please cite this article in press as: Bhamra GS, Fleming GJP. Influence of halogen irradiance on short- and long-term wear resistance of resin-based composite materials. Dent Mater (2008), doi:10.1016/j.dental.2008.06.007

Table 1 – The formulation of the resin-based composite materials used in the current study

Material	Filler			Resin
	Type	Particle size (μm)	vol.%	
Z100™	Zirconia and silica	0.01–3.5	66	Bis-GMA and TEGDMA
Filtek™ Z250	Zirconia and silica	0.01–3.5	60	Bis-GMA, UDMA, Bis-EMA, and TEGDMA
Filtek™ P60	Zirconia and silica	0.01–3.5	61	Bis-GMA, UDMA, Bis-EMA, and TEGDMA
Filtek™ Supreme XT	Zirconia and silica	0.6–1.4	59.5	Bis-GMA, UDMA, Bis-EMA, and TEGDMA

were repeatedly driven along a 7 mm path at 20 N to stimulate abrasion wear and a 90 N force applied at the end of the 7 mm path to simulate attrition wear [15,23,24]. The forces applied in abrasion and attrition were calibrated using a custom-made made jig (Proto-tech, Portland, OR, USA) comprising a 500 N load cell that replaced the testing chamber to ensure consistent conditions throughout the study.

2.3. *Short-term in vitro wear resistance*

Four specimens of each RBC irradiated at output intensities varying from 650 ± 14 to 150 ± 8 mW/cm^2 were subjected to 50,000 wear cycles at a frequency of 1 Hz which was equivalent to 6 months wear in the oral environment [15]. The tear drop wear facet produced on the surface of each specimen was analyzed using a non-contact optical profilometer (Talysurf CLI 2000, Taylor-Hobson Precision, Leicester, England) with a 3 mm range chromatic length aberration gauge with a resolution of 0.1 μm (z-direction) scanning at 2 mm/s. Longitudinal traces were taken at 4 μm intervals (x-direction) across the wear facet with a measurement recorded at 40 μm intervals (y-direction) generating a three-dimensional (3D) profile (Fig. 1) using the TalyMap analysis software package (Talysurf CLI 2000, Taylor-Hobson Precision, Leicester, England). Ten traces were performed across standards with a step height of 1.0 mm to determine the accuracy and precision of the wear depth measurements. The accuracy was calculated as the mean error from the true value, whilst the precision was quantified as the standard deviation of the errors measured. The accuracy and precision for a step size of 1.0 mm were 1.51 and 0.54 μm, respectively for ten measurements. The mean total volumetric wear and mean maximum wear depth measurements were determined using the non-worn areas around the wear facet as a reference in line with the procedure outlined by Dowling and Fleming [29].

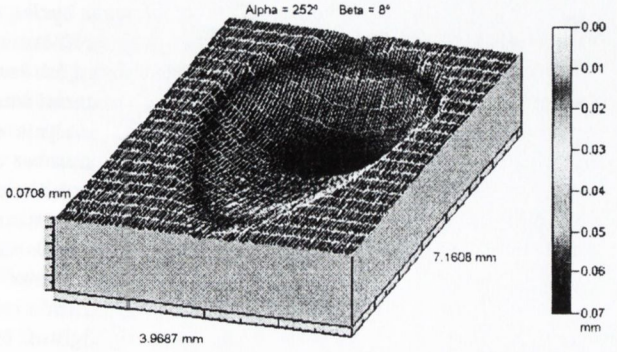

Fig. 1 – A three-dimensional representation of the total wear facet for the 7 mm sliding path produced from the wear regime employed using the OHSU oral wear simulator.

2.4. *Long-term in vitro wear resistance*

The RBCs prepared at irradiances of 650 ± 14, 350 ± 8, and 150 ± 8 mW/cm^2 were subjected to extended wear regimes. Following analysis of the wear facets after 50,000 wear cycles at 1 Hz using the non-contact optical profilometer, the samples were aligned into the individual wear chambers and a fresh food-like slurry was added. A further 100,000 wear cycles at 1 Hz were performed and analysis of the wear facets (after 150,000 wear cycles) was performed using the non-contact optical profilometer prior to realignment of the samples into the individual wear chambers. A fresh food-like slurry was added. An additional 150,000 wear cycles at 1 Hz were performed and analysis of the wear facets (after 300,000 wear cycles) with the profilometer was undertaken prior to realignment of the samples into the individual wear chambers with a fresh food-like slurry. A final 200,000 wear cycles at 1 Hz were performed and the final analysis of the wear facets (after 500,000 wear cycles) with the profilometer was undertaken.

One-, two-, and three-way analyses of variance (ANOVA) were made in software (SPSS, V 12.0.1, Chicago, IL, USA) using a critical significance level of $P = 0.05$, guided as necessary by Tukeys correction in multiple partial analyses of the mean total volumetric wear and mean maximum wear depth measurements.

3. Results

3.1. *Short-term wear resistance*

The summary of the results of the short-term wear resistance tests is given in Table 2 and Figs. 2 and 3. The analysis of variance (on the raw data) was analyzed using a one-way (material) and two-way (irradiance × material) ANOVA for analysis of both the mean total volumetric wear and the mean total wear depth at irradiances varying from 650 ± 14 to 150 ± 8 mW/cm^2. The one-way ANOVA for the mean total volumetric wear of Z100™ (R^2 value = 0.243; F value = 1.101; $P = 0.394$), Filtek™ Z250 (R^2 value = 0.386; F value = 2.157; $P = 0.076$), Filtek™ P60 (R^2 value = 0.280; F value = 1.330; $P = 0.279$) and Filtek™ Supreme XT (R^2 value = 0.213; F value = 0.926; $P = 0.504$) and the mean total wear depth of Z100™ (R^2 value = 0.384; F value = 2.134; $P = 0.079$), Filtek™ Z250 (R^2 value = 0.130; F value = 0.512; $P = 0.816$), Filtek™ P60 (R^2 value = 0.403; F value = 2.315; $P = 0.059$) and Filtek™ Supreme XT (R^2 value = 0.224; F value = 0.990; $P = 0.462$) identified no significant differences for each RBC material at the irradiances investigated. The two-way ANOVA for the mean total volumetric wear identified a significant interaction for material (R^2 value = 0.455; F value = 14.740; $P < 0.001$), a non-

Please cite this article in press as: Bhamra GS, Fleming GJP. Influence of halogen irradiance on short- and long-term wear resistance of resin-based composite materials. Dent Mater (2008), doi:10.1016/j.dental.2008.06.007

Table 2 – *In vitro* wear resistance for (a) Z100™, (b) Filtek™ Z250, (c) Filtek™ P60, and (d) Filtek™ Supreme XT irradiated at distances from 0 to 15 mm using a QTH handheld LCU with varying irradiances

Irradiance (mW/cm²)	Mean volumetric wear (mm³)				Mean wear depth (mm)			
	Z100	Z250	P60	Supreme	Z100	Z250	P60	Supreme
650	0.03 (0.01)	0.05 (0.01)	0.12 (0.02)	0.06 (0.02)	0.05 (0.01)	0.06 (0.01)	0.08 (0.01)	0.07 (0.04)
530	0.02 (0.01)	0.07 (0.01)	0.12 (0.03)	0.05 (0.03)	0.04 (0.01)	0.06 (0.01)	0.09 (0.00)	0.06 (0.01)
420	0.05 (0.02)	0.05 (0.02)	0.06 (0.04)	0.06 (0.03)	0.06 (0.02)	0.06 (0.02)	0.06 (0.02)	0.07 (0.02)
350	0.03 (0.01)	0.05 (0.01)	0.05 (0.00)	0.04 (0.02)	0.05 (0.00)	0.07 (0.01)	0.07 (0.01)	0.06 (0.01)
270	0.04 (0.01)	0.04 (0.02)	0.07 (0.03)	0.03 (0.02)	0.05 (0.02)	0.07 (0.02)	0.07 (0.03)	0.07 (0.02)
230	0.04 (0.02)	0.04 (0.01)	0.06 (0.03)	0.05 (0.02)	0.05 (0.01)	0.07 (0.00)	0.06 (0.02)	0.05 (0.01)
190	0.04 (0.02)	0.06 (0.01)	0.05 (0.02)	0.02 (0.00)	0.05 (0.01)	0.06 (0.01)	0.06 (0.02)	0.05 (0.01)
150	0.03 (0.01)	0.07 (0.01)	0.12 (0.05)	0.04 (0.02)	0.06 (0.02)	0.07 (0.02)	0.04 (0.01)	0.05 (0.01)

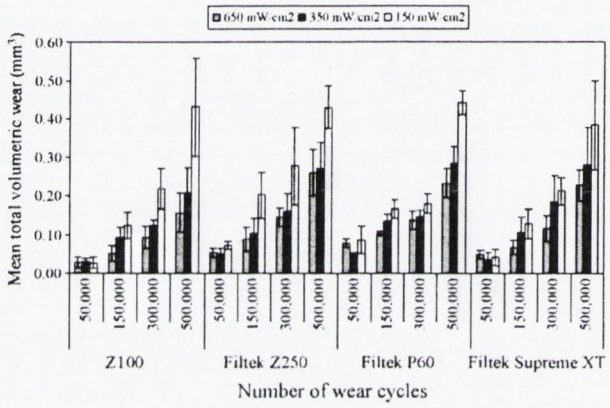

Fig. 2 – The mean total volumetric wear at 50,000, 150,000, 300,000, and 500,000 wear cycles for Z100™, Filtek™ Z250, Filtek™ P60, and Filtek™ Supreme XT irradiated at distances of 0, 7, and 15 mm using a QTH handheld LCU at irradiances of 650 ± 14, 350 ± 8, and 150 ± 8 mW/cm², respectively.

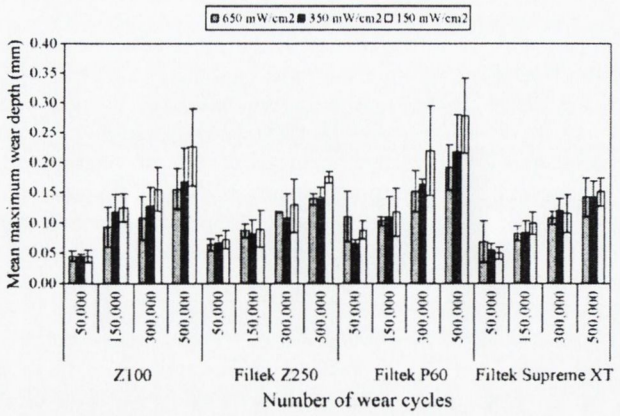

Fig. 3 – The mean maximum wear depth at 50,000, 150,000, 300,000, and 500,000 wear cycles for Z100™, Filtek™ Z250, Filtek™ P60, and Filtek™ Supreme XT irradiated at distances of 0, 7, and 15 mm using a QTH handheld LCU at irradiances of 650 ± 14, 350 ± 8, and 150 ± 8 mW/cm², respectively.

significant interaction for irradiance (F value = 1.188; P = 0.317) and a non-significant interaction for irradiance × material (F value = 1.310; P = 0.188). However, the two-way ANOVA for the mean total wear depth identified a significant interaction for material (R^2 value = 0.462; F value = 11.512; P < 0.001), a non-significant interaction for irradiance (F value = 1.276; P = 0.270) and a significant interaction for irradiance × material (F value = 1.850; P = 0.024) for the short-term wear resistance.

3.2. *Long-term wear resistance*

For the long-term wear resistance, a three-way ANOVA (irradiance × material × number of wear cycles) identified significant differences in the mean total volumetric wear and the mean maximum wear depth when irradiance (P < 0.001), RBC material (P < 0.001) and number of wear cycles (P < 0.001) were considered. The three two-way ANOVAs for the mean total volumetric wear were analyzed: irradiance × RBC material (F value = 1.979; P = 0.072), RBC material × number of wear cycles (F value = 1.266; P = 0.261) and irradiance × number of wear cycles (P < 0.001). Therefore, the two-way ANOVAs for irradiance × number of wear cycles were considered for each RBC material. The resultant analysis of the mean total volumetric wear (Fig. 1) of Z100™ (P < 0.001), Filtek™ Z250 (P < 0.001), Filtek™ P60 (P < 0.001), and Filtek™ Supreme XT (P < 0.001) identified significant differences irradiated at varying irradiances and tested for an increasing number of wear cycles. The three two-way ANOVAs for the mean maximum wear depth were analyzed in terms of: irradiance × RBC material (F value = 1.489; P = 0.186), RBC material × number of wear cycles (P < 0.001) and irradiance × number of wear cycles (F value = 3.124; P = 0.007). Therefore, the two-way ANOVAs for irradiance × number of wear cycles were considered for each RBC material and number of wear cycles × RBC material were considered for each irradiance. The resultant analysis of the mean maximum wear depth for irradiance × number of wear cycles identified a significant interaction for irradiance of Z100™ (R^2 = 0.749; F = 5.095; P = 0.011) and no significant interactions for Filtek™ Z250 (R^2 = 0.751; F = 2.672; P = 0.083), Filtek™ P60 (R^2 = 0.756; F = 2.029; P = 0.087), and Filtek™ Supreme XT (R^2 = 0.731; F = 0.004; P = 0.996). A significant interaction for the number of wear cycles was highlighted for Z100™ (P < 0.001) although no significant interactions were highlighted for Filtek™ Z250 (P < 0.001), Filtek™ P60 (P < 0.001) and Filtek™ Supreme XT (P < 0.001). The analysis of the mean

Please cite this article in press as: Bhamra GS, Fleming GJP. Influence of halogen irradiance on short- and long-term wear resistance of resin-based composite materials. Dent Mater (2008), doi:10.1016/j.dental.2008.06.007

maximum wear depth for the number of wear cycles × RBC material identified a significant interaction for the number of wear cycles of ($P < 0.001$) for the three irradiances investigated (650, 350, and 150 mW/cm^2) For RBC material no significant interactions at 350 mW/cm^2 ($R^2 = 0.829$; $F = 2.723$; $P = 0.055$) was observed, however, significant interactions at 650 mW/cm^2 ($P < 0.001$) and 150 mW/cm^2 ($R^2 = 0.910$; $F = 4.253$; $P = 0.010$) were highlighted.

It was noted that the mean total volumetric wear loss at the three irradiances investigated (650, 350, and 150 mW/cm^2) for the number of wear cycles was linear ($R^2 > 0.95$) for Z100™, Filtek™ Z250, and Filtek™ Supreme XT with Filtek™ P60 having R^2-values of 0.959, 0.911, and 0.816 for irradiances of 650, 350, and 150 mW/cm^2, respectively. Similarly, the mean maximum wear depth at the three irradiances investigated (650, 350, and 150 mW/cm^2) for the number of wear cycles was linear ($R^2 > 0.95$) for Filtek™ Z250 and Filtek™ Supreme XT with Filtek™ P60 having R^2-values of 0.8469, 0.999, and 0.982, respectively, and Z100™ having R^2-values of 0.966, 0.915, and 0.976, respectively, for irradiances of 650, 350, and 150 mW/cm^2.

4. Discussion

The *in vivo* wear of RBC restorations was previously assessed by either direct observation at regular intervals [30] or by indirect assessment of tooth replicas [31]. The major shortcomings of the indices [30] was that numerous patient visits were necessary which was time consuming, expensive and required the same clinical observers to be present on each patient visit. Indirect assessment of tooth replicas immediately after placement and at subsequent visits was difficult as impression and stone materials were susceptible to dimensional instability on setting thus influencing the dimensional accuracy of the tooth replicas given the wear rates involved. Attempts have been made over the years to mimic the masticatory processes that occur in the oral environment by the development of devices that simulate wear of restorative materials. As a result *in vitro* wear simulators were developed to assess the wear resistance of dental materials prior to placement in the mouth to provide an initial screening to potential restorative materials which would avert the need for expensive and time consuming clinical trials on substandard materials.

In 1996 the developers of the OHSU oral wear simulator reported that both abrasion and attrition wear produced by the action of an enamel antagonist could be quantified [15]. The tear drop wear facets were analyzed using a diamond-tipped profilometer by making 10 equally spaced traces perpendicular to the wear facet length. By "profilometric and visual examination" of the wear traces the abrasion region was determined to be 40–60% of the wear facet trace and the attrition region was 80–90% of the wear facet trace based on the average wear depth [15]. However, the reproducibility of results between different test centers was limited and a comparison of the mean wear depth measurements for abrasive wear (20 N) and attrition wear (70–90 N) identified differences of 33–56% and 31–78%, respectively, for three RBC materials [17] suggesting difficulties with using mean wear depth measurements for data reporting. Interestingly, more recently when questioning the "need for *in vitro* wear simulating devices" Ferracane concluded wear-testing methodologies and data reporting (depth, area or volume) needed to be standardized [19]. Archard [33] suggested that material removed due to the interaction of contacting surfaces was more accurately described in terms of volume loss. DeLong [20] reinforced Archard's findings and suggested the determination of the mean total volumetric wear of the wear facet was a more accurate parameter for evaluating material loss due to wear as the wear volume was a measure of the work done to remove material, implying that the wear volume was a material property independent of occlusal factors [20]. More interestingly recent reviews appear to be more concerned with the confidence in the accuracy and precision of results presented from *in vitro* wear simulation [20] so that the technique employed to quantify the wear facet are reported [19].

4.1. *Short-term wear resistance*

4.1.1. *The influence of irradiation distance*

In the current study the wear data analyzed for the four RBCs tested at 50,000 cycles (at scanning resolutions in the *x*-, *y*- and *z*-directions were 4, 40 and 0.1 μm) demonstrated that reducing halogen LCU irradiance (increasing the irradiation distance) resulted in no significant difference in the mean total volumetric wear and mean maximum wear depth. The constant mean total volumetric wear and mean maximum wear depth (Table 2) showed clearly that the top surface was adequately cured within the range of intensities employed, presumably due to the maximum conversion of C=C double bonds to C–C single bonds for the top surface. In the dental literature, Halverson et al. [33] showed that with low irradiances and short exposure times nearly maximum conversion could be achieved at the irradiated surface, such that a 10 s exposure with an irradiance of 200 mW/cm^2 would be sufficient to achieve 90% of the maximum conversion. Therefore, it is not surprising that no significant differences in mean total volumetric wear and mean maximum wear depth between irradiances of 650 ± 14 and 150 ± 8 mW/cm^2 were evident, although differences were identified between RBC materials. However, the effects of irradiance × material (two-way ANOVA) does require further consideration. No significant difference in the mean total volumetric wear were identified although significant differences in the mean total wear depth was identified to be for the short-term wear resistance. Therefore, the first hypothesis that exacerbated wear rates for the RBCs investigated would be evident following irradiation at increased distances was rejected for the mean total volumetric wear and accepted for the mean maximum wear depth. It is suggested that in line with the findings of Archard [32] and DeLong [20] the determination of the mean total volumetric wear was a more accurate parameter for evaluating material loss due to wear since difficulties with the mean maximum wear depth measurements for data reporting are routinely encountered in the dental literature [17,20]. Therefore, in line with the recommendations of Ferracane [19] data reporting needs to be standardized and in the opinion of the authors volume rather than depth or area should be the preferred parameter for evaluating material loss due to wear following *in vitro* wear simulation of RBCs.

Please cite this article in press as: Bhamra GS, Fleming GJP. Influence of halogen irradiance on short- and long-term wear resistance of resin-based composite materials. Dent Mater (2008), doi:10.1016/j.dental.2008.06.007

4.2. *Long-term wear resistance*

4.2.1. *The influence of increased number of wear cycles*

The long-term wear data investigated highlighted at varying QTH LCU irradiances increasing the number of cycles significantly increased the mean total volumetric wear for each RBC material but not the mean maximum wear depth. The increased number of ploughing actions of the antagonist on the RBC results in increased friction which would be expected to play a major role in the wear process [34]. Increasing the number of wear cycles results in a significant increase in the mean total volumetric wear observed over time which is exacerbated at reduced halogen LCU irradiances. Interestingly the mean maximum wear depth observed with increasing number of wear cycles was manifested as a non-significant increase in the mean maximum wear depth observed over time with varying halogen LCU irradiances. Therefore, the second hypothesis that exacerbated wear rates for the RBCs investigated would be evident following an increased number of wear cycles was accepted for the mean total volumetric wear and rejected for the mean maximum wear depth. It is suggested that this result further emphasizes the arguments of DeLong—for the employment of volume [20], and Ferracane—for standardized data reporting [19], for evaluating material loss due to wear following *in vitro* wear simulation of RBCs. Previously in the dental literature when long-term wear studies with increasing number of cycles were considered often the slurry was not changed [35,36] so that the abrasiveness of the slurry increased with removal of RBC filler particles which exacerbated the wear phenomenon. In the current study, the wear media was changed to prevent this phenomenon occurring to more accurately reflect the clinical situation. In addition, the degree of conversion within an RBC material is reduced depending upon the influence of shade, monomeric reactivity, refractive index mismatch, light scattering and absorption [37]. Reducing the LCU output intensity has the effect of further reducing the degree of conversion at varying depths from the LCU such that it becomes easier to remove material as the wear depth is increased following an increased number of cycles. As a result, the proposed hypothesis that exacerbated wear rates would be evident following long-term wear with RBCs irradiated under non-optimized conditions was accepted.

4.2.2. *Monomeric constituents*

In general no significant differences occurred between the methacrylate RBCs which contained similar monomeric resin constituents (Filtek™ Z250, Filtek™ P60 and Filtek™ Supreme XT) and filler loadings compared with Z100™ despite the higher filler volume and elastic modulus of the more brittle Z100™ RBC [15]. This is in agreement with the volume loss data from Palin et al. [34] who determined similar frictional coefficients, wear coefficients and volume loss for the monomeric resin constituents investigated resulting in similar fraction of friction results. However, the results are not in agreement with the study of Söderholm et al. [16] who reported the resin matrix to be the most influential factor influencing wear rate. Therefore, the third hypothesis that exacerbated wear rates for the RBCs investigated would be evident following varying the monomeric constituents was rejected for the mean total volumetric wear and the mean maximum wear depth.

4.2.3. *Varying the filler packing fraction design*

The RBCs (Filtek™ Z250, Filtek™ P60 and Filtek™ Supreme XT) contained the same monomeric constituents with similar filler loadings 59.5–61 vol.% (although different packing fraction designs). Therefore, it would appear that improved wear performance suggested for nano-filled RBCs (Filtek™ Supreme XT) which were proposed to be less prone to filler plucking due to their irregular shape compared with the hybrid RBCs (Filtek™ Z250 and Filtek™ P60) with similar filler loadings may not be entirely correct [38]. Therefore, the fourth hypothesis that exacerbated wear rates for the RBCs investigated would be evident following varying packing fraction designs was rejected for the mean total volumetric wear and for the mean maximum wear depth.

5. Conclusion

The current study has identified that short-term mean total volumetric wear assessment of RBCs may not provide valuable information on RBC clinical performance and that long-term wear testing is needed. The irradiance while not having an impact on the short-term mean total volumetric wear resistance is important in long-term wear resistance assessment. As a result, it is imperative that GDPs are aware of the clinical implications that poor maintenance of LCUs can have on RBC performance. The study also confirms the findings of DeLong [20]—that the employment of volume for evaluating material loss due to wear, and Ferracane—for standardized data reporting [19], are required following the *in vitro* wear simulation of RBCs.

REFERENCES

[1] Bennett AW, Watts DC. Performance of two blue light emitting-diode dental light curing units with distance and irradiation-time. Dent Mater 2004;20:72–9.
[2] Stahl F, Ashworth SH, Jandt KD, Mills RW. Light-emitting diode (LED) polymerisation of dental composites: flexural properties polymerisation potential. Biomaterials 2000;21:1379–85.
[3] Mills RW, Jandt KD, Ashworth SH. Dental composite depth of cure with halogen and blue light emitting diode technology. Br Dent J 1999;8:388–91.
[4] Pollock BF, Lewis AL. Visible light resin-curing generators: a comparison. Gen Dent 1991;29:488–93.
[5] Rueggeberg FA, Caughman WF, Comer RW. The effect of autoclaving on energy transmission through light-curing tips. J Am Dent Assoc 1996;127:1183–7.
[6] Barghi N, Berry T, Hatton C. Evaluating intensity output of curing lights in private dental offices. J Am Dent Assoc 1994;25:992–6.
[7] Martin FE. A survey of the efficiency of visible light curing units. J Dent 1998;26:239–43.
[8] Pilo R, Oelgiesser D, Cardash HS. A survey of output intensity and potential for depth of cure among light-curing units in clinical use. J Dent 1999;27:235–41.
[9] El-Mowafy O, El-Badrawy W, Lewis DW, Shokati B, Kermallli J, Sloiman O, et al. Intensity of

Please cite this article in press as: Bhamra GS, Fleming GJP. Influence of halogen irradiance on short- and long-term wear resistance of resin-based composite materials. Dent Mater (2008), doi:10.1016/j.dental.2008.06.007

quartz-tungsten-halogen-light-curing units used in private practices in Toronto. J Am Dent Assoc 2005;136: 766–73.
[10] Sakaguchi RL, Berge HX. Reduced light energy density decreases post-gel contraction while maintaining degree of conversion in composites. J Dent 1998;26:695–700.
[11] Sarrett DC. Clinical challenges and the relevance of materials testing for posterior composite restorations. Dent Mater 2005;21:9–20.
[12] DeLong R, Douglas WH. Development of an artificial oral environment for the testing of dental restoratives: bi-axial force and movement control. J Dent Res 1983;62:32–6.
[13] De Gee AJ, Pallav P, Davidson CL. Effect of abrasion medium on wear of stress-bearing composites and amalgam in vitro. J Dent Res 1986;65:654–8.
[14] Leinfelder KF, Beaudreau RW, Mazer RB. An in vitro device for predicting clinical wear. Quintessence Int 1989;20: 755–61.
[15] Condon JR, Ferracane JL. A new multi-mode oral wear simulator. Dent Mater 1996;12:218–26.
[16] Söderholm KJ, Lambrechts P, Sarrett D, Abe Y, Yang MC, Labella R, et al. Clinical wear performance of eight experimental dental composites over three years determined by two measuring methods. Eur J Oral Sci 2001;109:273–81.
[17] Heintze SD. How to qualify and validate wear simulation devices and methods. Dent Mater 2006;22:712–34.
[18] Heinze SD, Zellweger G, Cavalleri A, Ferracane JL. Influence of the antagonist material on the wear of different composites using two different wear simulation methods. Dent Mater 2006;22:166–75.
[19] Ferracane JL. Is the wear of dental composites still a clinical concern? Is there still a need for in vitro wear simulating devices? Dent Mater 2006;22:689–92.
[20] DeLong R. Intra-oral restorative materials wear: rethinking the current approaches: how to measure wear. Dent Mater 2006;22:702–11.
[21] St-Georges AJ, Swift EJ, Thompson JY, Heymann HO. Curing light intensity effects on wear resistance of two resin composites. Oper Dent 2002;27:410–7.
[22] Ramp LC, Broome JC, Ramp MH. Hardness and wear resistance of two resin composites cured with equivalent radiant exposure from a low irradiance LED and QTH light-curing units. Am J Dent 2006;19:31–6.
[23] Condon JR, Ferracane JL. Evaluation of seven commercial composites using new in vitro wear simulator. J Dent Res 2002;81. Special Issue A: A337 Abstr. No. 2683.
[24] Sorensen JA, Pham M. In vitro wear of composite resins processed with various systems. J Dent Res 2002;81. Special Issue A: A324 Abstr No. 2578.
[25] Cook WD. Spectral distributions of dental photopolymerization sources. J Dent Res 1982;61: 1436–8.
[26] Pradhan RD, Melikechi N, Eichmiller F. The effect of irradiation wavelength bandwidth and spot size on the scraping depth and temperature rise in composite exposed to an argon laser or a conventional quartz-tungsten-halogen source. Dent Mater 2002;18:221–6.
[27] Obici AC, Sinhoreti MAC, Frollini E, Sobrinho LC, Consani S. Degree of conversion and knoop hardness of Z250 composite using different photo-activation methods. Polym Test 2005;24:814–8.
[28] Peutzfeltz A, Asmussen E. Resin composite properties and energy density of light cure. J Dent Res 2005;84: 659–62.
[29] Dowling AH, Fleming GJP. The in-vitro wear resistance of a montmorillonite clay reinforced glass-ionomer restorative. J Dent 2006;34:802–10.
[30] Cvar JF, Ryge G. Criteria for the clinical evaluation of dental restorative materials. United States Public Health Service Publication #790-244. San Francisco: US Government Printing Office; 1971.
[31] Leinfelder KF, Taylor DF, Barkmeier WW, Goldberg AJ. Quantitative wear measurement of posterior composite resins. Dent Mater 1986;2:198–201.
[32] Archard JF. Contact and rubbing of flat surfaces. J Appl Phys 1953;24:981–8.
[33] Halvorson RH, Erickson RL, Davidson CL. Energy dependent polymerisation of resin-based composite. Dent Mater 2002;18:463–9.
[34] Palin WM, Fleming GJP, Burke FJT, Marquis PM, Pintado MR, Randall RC, et al. The frictional coefficients and associated wear resistance of novel low-shrink resin-based composites. Dent Mater 2005;21:1111–8.
[35] Hu X, Shortall AC, Marquis PM. Wear of three dental composites under different testing conditions. J Oral Rehabil 2002;29:756–64.
[36] Barkmeier WW, Latta MA, Erikson RL, Wilwerding TM. Wear simulation of resin composites and the relationship to clinical wear. Oper Dent 2008;33:177–82.
[37] Shortall AC, Palin WM, Burtscher P. Refractive index mismatch and monomer reactivity influence composite curing depth. J Dent Res 2008;87:84–8.
[38] Mitra SB, Wu D, Holmes BN. An application of nanotechnology in advanced dental materials. J Am Dent Assoc 2003;134:1382–90.

Please cite this article in press as: Bhamra GS, Fleming GJP. Influence of halogen irradiance on short- and long-term wear resistance of resin-based composite materials. Dent Mater (2008), doi:10.1016/j.dental.2008.06.007